Silver(I) and Other Coin Metal Complexes of N, O, S and P Containing Ligands: Structures and Biological Properties

Thesis presented to the Faculty of Sciences
Institute of Physics
University of Neuchâtel

by
Muhammad ALTAF
MSc. and MPhil.
Quaid-i-Azam University Islamabad, Pakistan

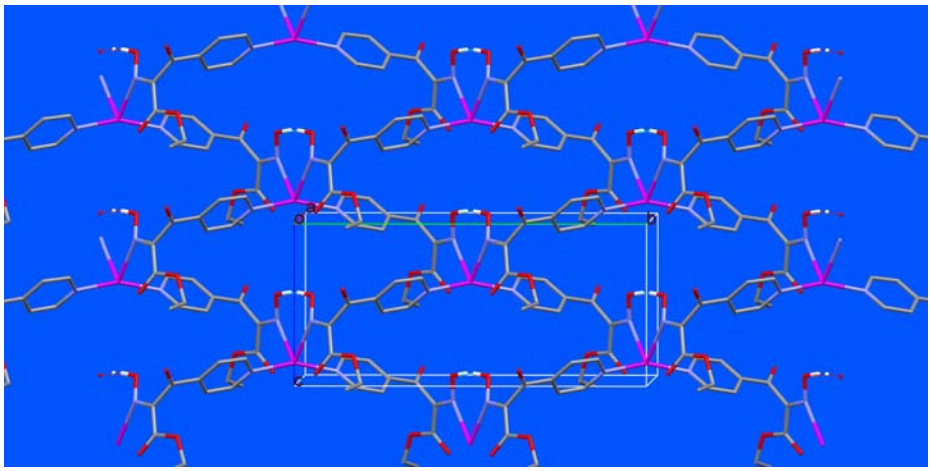

Examined the 27th August 2008
University of Neuchâtel

Université de Neuchâtel

FACULTE DES SCIENCES
Secrétariat-Décanat de la faculté
- Rue Emile-Argand 11
- CP 158
- CH-2009 Neuchâtel

IMPRIMATUR POUR LA THESE

Silver(I) and Other Coin Metal Complexes of N, O, S, and P Containing Ligands : Structures and Biological Properties

Muhammad ALTAF

UNIVERSITE DE NEUCHATEL

FACULTE DES SCIENCES

La Faculté des sciences de l'Université de Neuchâtel,
sur le rapport des membres du jury

Mmes H. Stoeckli-Evans (directrice de thèse),
K.M. Fromm (Université de Fribourg)
et M. R. Neier

autorise l'impression de la présente thèse.

Neuchâtel, le 25 septembre 2008

Le doyen :
F. Kessler

UNIVERSITE DE NEUCHATEL
FACULTE DES SCIENCES
Secrétariat - décanat de la faculté
Rue Emile-Argand 11 - CP 158
CH-2009 Neuchâtel
Felix Kessler

بِسْمِ اللهِ الرَّحْمٰنِ الرَّحِيْمِ

In the name of God, most Gracious, most Compassionate

DEDICATED

TO

MY MOTHER

THE BEACON OF LOVE

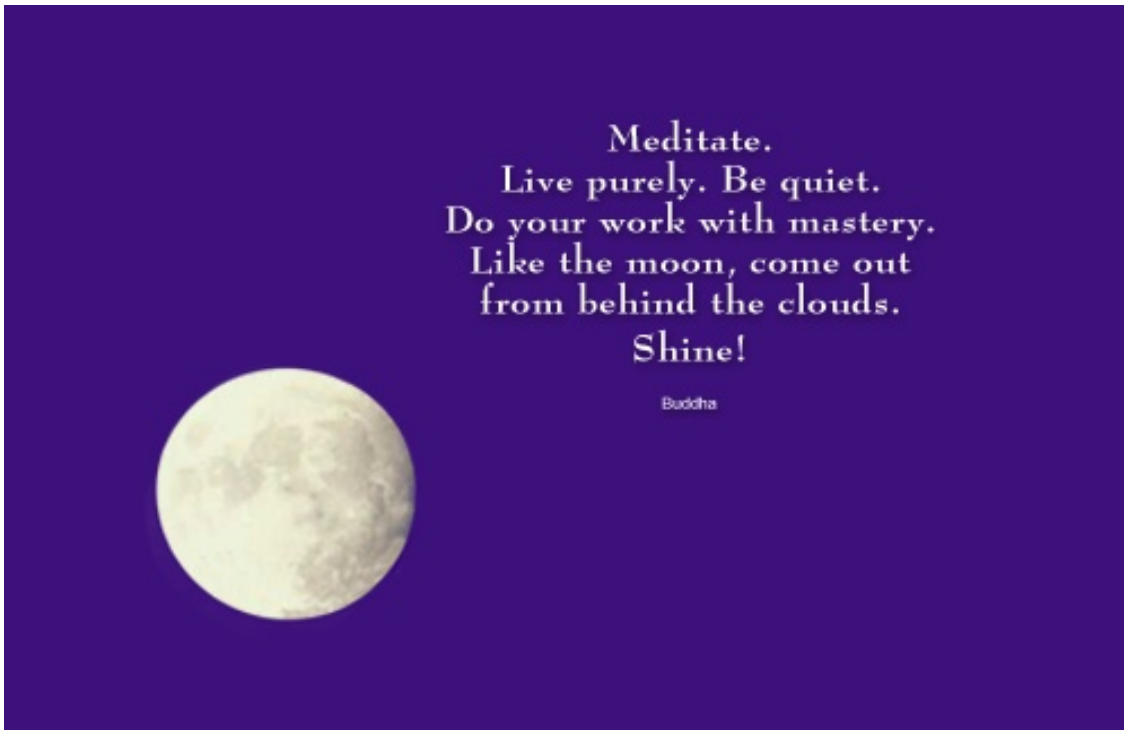
Meditate.
Live purely. Be quiet.
Do your work with mastery.
Like the moon, come out
from behind the clouds.
Shine!
Buddha

Acknowledgements

This work has been carried out from March 2005 to February 2008 in the laboratory of Chemical Crystallography at the University of Neuchâtel under the supervision of Professor Helen Stoeckli-Evans.

I would like to express my deepest gratitude to Professor Helen Stoeckli-Evans for offering me the possibility to work in her group and introducing me to the fascinating field of chemical crystallography. I cordially thank her for the time she generously devoted to me, her enthusiasm and valuable advice. I have no words to pay her the tribute for her kindness, moral and spiritual support during my stay in Switzerland. I would like to say that she is like a mother to me more than a supervisor.

I would like to thank Professor Fritz Stoeckli and Professor Thomas Bürgi (Chimie-Physique) for their kindness and time-to-time moral support.

I am especially indebted to Prof. Saeed Ahmed (University of Engineering and Technology Lahore, Pakistan), Prof. Katharina M. Fromm (University of Fribourg) and Prof. Paul J. Dyson (EPFL Lausanne) for giving me their precious time for useful discussions about the biological aspects of the series of silver(I) compounds.

I would like to thank the members of the jury, Prof. Katharina M. Fromm (University of Fribourg) and Prof. Reinhard Neier (University of Neuchâtel), for accepting to review this work.

I extend my thanks to my friends; Atif Fazal, Faisal Suleman, Sajad, Abdul, Farooq A. Khan and Linda Gysin for their moral support and encouragement. I am also thankful to my group fellows for providing a peaceful and research oriented environment in the laboratory.

The acknowledgements would be definitely incomplete, if I would forget to thank my beloved parents, brothers, sisters, nephew and other family members who always supported me. I can not find the words to express my gratitude to my parents for their generosity, and their financial and moral support, throughout my educational career. My dream to become a doctor would never have come true without their sincere prayers.

Altaf

Silver(I) and Other Coin Metal Complexes of N, O, S and P Containing Ligands: Structures and Biological Properties

Summary *i,ii*

Chapter 1 *1*

Introduction

Chapter 2 *29*

Silver(I)-Phosphine Mixed Ligand Complexes: Synthesis, Crystal Structure, Antimicrobial, Antifungal and Anticancer Activities

Chapter 3 *73*

Role of Hydrogen Bonding in the Construction of One-, Two-, and Three-dimensional Frameworks of Biotin and its Silver(I) complexes

Chapter 4 *107*

Synthesis and Crystal Engineering of Ortho-, Meta-, and Para-Pyridyl Oximes and Silver(I)-Oxime Networks

Chapter 5 *133*

Silver(I)-Phosphine Mixed Ligand Complexes with 4,4′bipyridine: The Synthesis of One- and Two-dimensional Coordination Polymers

Chapter 6 *165*

Coin Metal Tertiary Phosphine Precursors

Part A: Silver(I) tertiary phosphine precursors for mixed ligand Silver(I) tertiary phosphine complexes: Structural and spectroscopic studies *166*

Part B: Copper(I) halide tertiary phosphine complexes and an example of a mixed ligand CuI halide phosphine complex *196*

Part C: Gold(I) halide tertiary phosphine complexes *219*

Chapter 7 *231*

Conclusions and Perspectives

Appendix to Chapter 2 *235*

CV *265*

Posters

Summary

The antimicrobial activity of silver has attracted significant research interest and contributes to an exponentially growing use of this noble metal in commodity products. Research concerning the development of antimicrobial, antifungal and anticancer drugs represents a great challenge for both the academic world and the pharmaceutical industry since the drugs widely used for the treatment of these diseases can be useless due to the emergence of multi-drug resistant strains. Because of this critical situation, an intensive effort has been directed to develop new drugs for fatal diseases like cancer and tuberculosis.

It is well understood that there is direct relationship between the physicochemical properties of the compound and its molecular structure. In order to take advantage of the physicochemical properties of the organic and metal-organic compounds, having the complete knowledge of their molecular structure is very important. X-ray diffraction analysis of single crystals or micro-crystalline compounds is a very useful technique to obtain the true structure of the compound in the solid state.

Chapter 1 gives an Introduction into the biological properties of silver and silver salts. It also includes a discussion of the use of bridging and spacer ligands in the formation of coinage metal complexes, which can be at the origin of the formation of one-, two-, and three-dimensional coordination polymers, and hydrogen bonding. The interaction of metal based drugs with biomolecules is also discussed.

Chapter 2 deals with the synthesis, structural and spectroscopic studies of silver(I)-mixed ligand complexes and their biological properties. This series of silver complexes were tested against *M. tuberculosis* strain, a fungus and a human ovarian cancer cell line, and their minimal inhibitory concentration (MIC) values were determined. The results show that all the complexes of this series are potential candidates for anticancer, antifungal, anti-tuberculosis and antiseptic or disinfectant drugs for patients with fungal, bacterial or cancer diseases.

In chapter 3, we report on the synthesis of biotin (vitamin H) silver(I)-coordination polymers. Due to the different modes of coordination of biotin towards

silver(I) atom, a series of one-, and two-dimensional coordination polymers were obtained and their molecular structures are reported here.

In chapter 4 ortho-, meta-, and para-pyridyloximes were found to be useful flexible ligands for the synthesis and construction of some interesting silver(I)-oxime architectures involving silver-O, -N and -S coordination bonds. The N-H…N, N-H…O, O-H…N and O-H…O hydrogen bonding interactions in the solid state structures of these silver-oxime compounds are also very prominent and result in the formation of one-, and two-dimensional coordination polymeric chains and networks. For example, one compound in particular was found to have a double helix DNA-like structure.

In chapter 5 we report on the syntheses and structural analyses of silver-phosphine mixed ligand complexes with the ligand 4,4′-bipyridine. A series of tertiary and bi-phosphines were used and lead to the formation of one-, and two-dimensional coordination polymers with pseudo-trigonal planar and tetrahedral geometry around the central metal atom.

In chapter 6 the synthesis and molecular structures of the coin metal(I)-phosphine precursors are reported. These silver(I)-, copper(I)-, and gold(I)-phosphine precursors were initially synthesized for the preparation of mixed ligand coin metal complexes (Chapter 2). We have used this precursor successfully for the preparation of silver(I) and copper(I) mixed ligand complexes but all efforts to crystallize the gold(I) mixed ligand complexes have failed until now.

Chapter 7 concerns the Conclusions and Perspectives for future work in this field of research.

Chapter 1:

INTRODUCTION

Silver and silver salts have been recognized and used as antibacterial agents in curative and preventive health care for decades. The application of silver and its salts in the treatment of burn wounds is of interest. The most used reagents have been silver nitrate, silver perchlorate and sulphonamides. In particular, silver sulfadiazine has been used extensively in the treatment of burn wounds. The advances in the wound care management are not only focused on the antimicrobial effects of silver on chronic ulcers, extensive burns and difficult to heal up wounds, but also on the convenience of application, patient comfort and sustained release of silver ions with increased concentration at the wounds surfaces. It has been assumed that the slow release of silver at the area of superficial wounds is responsible for the prevention of infection as well as aiding in the process of healing. This lead to the development of fabrics impregnated with silver (FIS), a new silver technology that has antimicrobial efficacy and provides a protective barrier against infection. In the treatment of burn wounds, a good hydration is recognized as an important factor for wound healing and regeneration of the epithelium.[1-7]

The chemistry of coordination polymers has attracted much attention as they have potentials as functional materials in the field of physi- and chemi-sorption, catalysis, optics and biomedicine. Among the coinage metal polymers, several examples of single and double-stranded helices of silver(I) complexes of heterocyclic ligands that form cluster structures in the solid state are known; the structural analysis of various silver(I) complexes has demonstrated the different coordination behaviour depending upon design, number of suitable donor sites in the ligands used, solvent of crystallization and also the method of crystallization. The single crystal X-ray diffraction studies of silver(I) complexes suggest that the coordination number of silver(I) is usually larger than two in

all cases. In addition the existence of silver(I) ions close to each other in the same molecule (less than 3.5Å) results in d^{10}-d^{10} interactions between two closed shells of silver(I) ions which increases the possibility of the formation of dimers to tetramers, as found in many cases of complicated multi-dimensional systems.[8-15]

In the last decade a large number of reports concerning structural and kinetic features of silver(I)-phosphine complexes have been published. Tertiary phosphine complexes of silver(I), of the type $[AgXL_n]$ (L = tertiary phosphine; n =1-4; X = coordinating or non coordination anion), were first prepared in 1937. These complexes display a diversity of structural types. The structural chemistry of the $[AgXL_n]$ complexes is quite similar to that of the copper(I) analogues.[16-17] Our interest in the coinage metal phosphine complexes is based on their versatile structural chemistry, and in the use of these complexes as precursors for the synthesis and crystal engineering of mixed ligand coinage metal complexes with O, N and S donor ligands. Our interest in the silver(I) complexes with thiosemicarbazide, heterocyclic thione, tertiary phosphines, 4,4′-bipyridine and flexible ligands like bisphosphines etc., stems from our current research on coordination compounds of coinage metals with these ligands, that show an interesting and in some cases unpredictable structural variety, both for the individual ligand and at the overall geometrical level.[18]

The molecular design and structural determination of such coinage metal complexes composed of these same ligands are an intriguing aspect of bio-inorganic, inorganic synthesis and metal-based drug chemistry. The structure-biological activity correlation of coinage metal complexes is also an extremely interesting subject of research.[19]

In many biologically active compounds of silver(I) and gold(I), most of the complexes formed with thiol and nitrogen-containing heterocyclic ligands are difficult to crystallize and believed to be polymeric, unless tertiary phosphine ligands are also employed.[20-25] Recently we found that there is no doubt that tertiary phosphines are quite useful for the crystal engineering of coinage metal complexes and play an important role in the crystallization of coinage metal complexes, but it is also possible to obtain single crystals

of the desired product of coinage metals without a phosphine component. Recently we have used a variety of tertiary phosphines (triphenyl phosphine, tricyclohexyl phosphine, and biphenylcyclohexyl phosphine etc.,) and biphosphines (1,2-bis(diphenyl phosphino) ethane, 1,2-bis(dicyclohexyl phosphino) ethane and 1,2-bis(dicyclohexyl phosphino) propane etc.,) successfully to obtain single crystals of coinage metal complexes with versatile structural, chemical and biological behaviour. In our current studies, the major reason for the use of tertiary phosphine and biphosphine is to obtain light stable pure/mixed ligand coinage metal complexes with versatile structural and potential applications in all fields of life. The major goal was to synthesize light stable silver(I) complexes regardless of their solubility in water. In this regard our attempts were successful, and we managed to synthesize many light stable silver(I) complexes with Ag-N, Ag-O, Ag-S and Ag-P metal cores. The silver(I) complexes with an Ag-O bonding core have shown a wide spectrum of effective antimicrobial activities against bacteria, yeast and moulds.[26-30] It is well understood now that silver(I)-N, silver(I)-S and silver(I)-O bonding complexes are potential bioinorganic materials;[8,31] however, most of them are light sensitive especially in solution and their characterization is not easily performed.

In the current decade an increased interest in the area of N, O and S donor (biologically active) ligand chemistry has been observed. In most of the studies coinage metal complexes of antibiotic–based ligands have demonstrated that metal complexes display greater inhibition of microbial growth than of the metal salts or the free ligands. In some cases, the ligands and the metal salts do not show any inhibition of microbial growth.[32]

Gold was reported as a healing agent as early as 2500 BC in China. Since then the application of gold has been extended mainly due to the implementation of chrysotherapy in the 1930's. Gold compounds have been employed in the search for new drugs in various areas of medicinal chemistry, principally as anti-arthritics and anti-cancer agents.[33-35]

There is a considerable interest in the coordination chemistry of gold(I) complexes with biological and pharmacological activities. In the bioinorganic chemistry of gold(I)

complexes, there have been reported various studies related to their antiarthritic, antitumor, anti HIV and antimicrobial activities.[26,36-40] The molecular design of such gold(I) complexes is an intriguing aspect of bioinorganic chemistry of metal based drugs. The antimicrobial tests of two-coordinate AuSP and AuNP complexes such as [Au(L)(PPh_3)] (HL = 2-mercaptoproionic acid, 6-mercaptonicotinic acid, 2-mercaptonicotinic acid, D-penicillamine, D,L-penicillamine, 2-mercaptobenzoic acid, 3-mercaptobenzoic acid, 4-mercaptobenzoic acid, imidazole, pyrazole, 1,2,3-triazole, 1,2,4-triazole and tetrazole) have been shown selective and to have effective activity against two Gram-positive bacteria (Bacillus subtilis, Staphylococcus aureus) and as having modest activity against one or two yeasts (for example, Candidae albicans).[33-40] In the last couple of years gold(I) complexes with AuSP, AuNP, AuPP and AuSS cores have been studied as antimicrobial agents by many groups.[41-43] Gold(I) phosphine complexes are well known to catalyse aldol type reactions of isocyanides with potential industrial applications. Such complexes are also well known to act as chemotherapeutic agents with antitumor and antiarthritic activities.[44-46] In contrast with the gold(I) phosphine complexes, silver(I) phosphine complexes with Ag-P bonds have shown no activity against bacteria, yeast or moulds. Silver(I) complexes with imidazole and triazole ligands, based on the coordination of the donor atoms to the Ag(I) centre, have shown promising antimicrobial activities. Whereas their PPh_3 derivatives have shown poor antimicrobial activities.[43,47-50]

In the past few decades considerable effort has been devoted to the search for new chemotherapeutic agents with preferential anticancer activity. However, although there have been important developments in the field of anticancer chemotherapy, no breakthrough has been achieved in the search for better anticancer agents since the introduction of cis-diaminedichloro-platinium(II) (cisplatin) into clinical use. In the last few years research has increasingly focused on the potential of gold(III) complexes as anticancer drug candidates, because gold(III) has the same isoelectronic configuration (d^8) and structural characteristics as Pt(II).[51-53]

Another high-lighted topic in the coordination chemistry of coinage metal(I) atoms is concerned with helicity; coordination polymers of silver(I) and copper(I) with N-heterocyclic ligands to their tertiary phosphine derivatives has resulted in the formation of monomers, oligomers and helical polymers. Double helical polymers involving gold(I) complexes have been synthesized with different nitrogen and sulphur donor ligands and shown to have antiarthritic properties. In gold(I) polymers metal–metal (d^{10}-d^{10}) interactions between the two close shell cations have been observed. This aurophilic interaction is of great interest for scientists interested in luminescence, fluorescence, phosphorescence and chemical properties of gold(I).

The advantages of the polymeric-based antibacterial agents over conventional antibacterial agents composed of low molecular-weight compounds, includes them being non volatile, chemically stable and they do not easily permeate human or animal skin. So polymeric based antibacterial compounds can reduce the loss associated with volatilization, photolytic decomposition and transportation. On the other hand metal ions and metal complexes that have biological activity are being used and studied as biological agents.[114-116] For this reason investigating the antimicrobial and therapeutic activities of monomers, dimers and polymer metal complexes, including the single and double stranded helices, represents a new, developing direction in the field of pharmaceutical, medicinal and bioinorganic chemistry.

Coinage metal ions along with some other metal ions (Fe, Pt, Mg, Zn etc.,) are well known for their broad spectrum antimicrobial activities against bacterial and fungal agents together with their lack of cross-resistance with antibiotics.[54-57]

The study of polynuclear metal complexes is one of the most active areas in coordination chemistry. These compounds constitute common ground for two areas of current interest; first molecular magnetism and second metal sites in biology.[58]

A search of the literature revealed that transition metals complexes of established drugs are gaining much biological significance. For example, thiosemicarbazide derivatives are

known for their antibacterial, antineuroplastic and antitubercular properties. Particularly thiacetazone, a well known tuberculostat, inhibits the enzyme neuraminidase in a non-competitive manner with respect to the substrate sialic acid. The inhibition of the enzyme involves the competition for the Ca^{2+} binding site by the thiacetazone. The synthesis of Cu(I) complexes with thiosemicarbazide derivatives and their extensive use as biologically important compounds is well described in literature.[59-63] Similarly, quinolones are a group of synthetic antimicrobial agents now in clinical use for over thirty years, and ciprofloxacin is one of the most widely used representatives. The interaction of quinolones and metal ions has been thoroughly studied especially due to their interesting biological and chemical properties. Metal ions play a key role in the actions of some synthetic and natural antibiotics and are involved in the specific interactions of these molecules with proteins, nucleic acids and other biomolecules. It is known that the magnesium-quinolone complexes interact with DNA and impairs its function, hence quinolones are also described as metalloantibiotics.[64-67] Copper-quinolone complex interactions have been studied in detailed by Drevensek et al. [68] Copper has been found causative for the treatment of several diseases. The field of copper metabolism and the role of copper in medicine are both moving forward on several broad fronts.

The unique property of the ligand plays an important role for the overall properties of the metal complex. Dioxotetraaza macrocycles are able to coordinate divalent metal cations, such as Cu^{2+} and Ni^{2+} by displacing the amide protons. The resulting complexes are of considerable interest as functional catalysts, biological models for metalloproteins, in oxygen uptake and nuclear medicine. The structural features of neutral copper complexes of this type of ligand with versatile and unique radiophysical properties of copper radio isotopes leads to their potential usefulness in diagnostic and /or therapeutic applications.[70-73] Among several copper radio nuclides, the longest-lived ^{67}Cu is of interest for its medium energy β-emissions and its γ-rays that permit imaging of radioactivity distribution during therapy.[74] Our interest in the copper-based complexes and coordination polymers is based on the broad spectrum of their usage in medicinal, electrical and other fields of practical life.

The current interest in the metal-based antibacterial drugs is based on the increasing incidence of bacterial drug resistance. This fact dictates the scientific search for an improvement of the existing antimicrobial drugs and development of new ones.

1.1. Coinage metal complexes of bridging and spacer ligands

Ligands that can serve as bridges between metal centres and that also contain a delocalized π system have received considerable attention for decades. Binuclear and multinuclear metal complexes, comprising two or more metal centres bridged by multi dentate ligands can exhibit metal-metal interactions, such as energy and electron transfer, magnetic coupling, and inter valence transfer.[1] The construction of extended solids from molecular building blocks is of great interest due to the advantages it offers for the design of new materials. The use of spacer ligands in the assembly of extended networks is an attractive synthetic approach and the resulting metal-ligand bond formation provides a very convenient means of linking components into infinite networks. Inorganic chemistry, in particular coordination chemistry is replete with examples of easily accessible potential building blocks with a range of simple geometries and connectivities.[75-78]

The preparation of extended networks using inorganic coordination polymers has become an area of increasing study in the recent years. One of the reasons that this interest has arisen is the simplicity of the synthetic procedure used to construct these multi-dimensional materials. Ultimately this may lead to the development of materials with tuneable properties; including structures with host guest properties similar to those observed in zeolites and compounds with interesting catalytic, electronic or magnetic properties. The high degree of design arises from the coupling of the well understood coordination properties of individual metal ions and highly developed ligand synthesis with new areas of supramolecular chemistry and crystal engineering.[79-85] Coordination

chemistry allows the possibility to rationally design and prepare supramolecular architectures through non-covalent interactions, in which it is crucial to meet both geometric as well as energetic considerations. In the last couple of years, a lot of supramolecular assemblies have been achieved by carefully selecting building blocks and organic ligands containing appropriate functional groups; through supramolecular interactions (hydrogen bonding, π-π interactions etc.,).[86-88] The achievements to date familiarize us with three generation categories, called first, second, and third generation or 1D-, 2D-, & 3D-porous coordination polymers. Porous coordination polymers have attracted attention due to scientific interest in the creation of nanometre-sized spaces and finding of novel phenomena, as well as commercial interest in their application in separation, storage and heterogeneous catalysis.[89-91] Our current interest in the coordination chemistry of coinage metal complexes, either monomers, dimers or infinite one-, two- and three-dimensional (1-, 2- and 3-D) polymers, is based on their versatile properties and interdisciplinary studies. In our recent studies, coordination behaviour of the bridging and spacer ligands with coinage metals have revealed that coordination polymers bridged by thiosemicarbazide, 2-(propan-2-ylidene)hydrazinecarbothioamide, 2-mercapto thiazoline, 4,4′-bipyridyl pyridine, ethylene bis(diphenylphosphine) etc., include examples of one-(1D), two-(2D) and three-dimensional(3D) networks. Chemotherapeutic, electromagnetic, heterogeneous catalysis, host-guest relationships, and in particular the geometrical environment of the metal ions and the dimensionality of the polymeric structures seem to be influenced by the mode of coordination of the ligands used. Several coordination and bonding modes have been observed for bridging and spacer ligands during our current studies and that of other groups.[75-91] The ligands, anions, solvent of crystallization play an important role to determine the structure and geometry around the metal ion. The presence of intermolecular, intramolecular, hydrogen bonding, metal-metal and π-π interactions also offer the possibility to form coordination polymers of variable architectures.

1.2. One-, Two-, and Three-dimensional coordination polymers

The crystal engineering of coordination polymers is presently a large and growing area of research. Materials produced in this area have potential applications in fields as diverse as molecule-based magnetism, non-linear optics and heterogeneous catalysis.[92]
The role of ionic bonds, coordination bonds and hydrogen bonds in crystal engineering is currently of great interest due to their use in constructing one-, two-, and three-dimensional polymers.[93]

1.2.1 One-dimensional coordination polymers

Many researchers have synthesized and structurally characterized numerous one-dimensional polymers with different structural architectures and topologies. The bridging and spacer ligands are quite useful to construct one-dimensional structural motifs.

1.2.1.1 Linear chain structures

Such structural feature has been observed in $\{[Ag\ (4,4'\text{-bipy})](X)\}_n$ ($X = ClO_4^-$, BF_4^- and NO_3^- etc.,).[94-97] In this one-dimensional polymeric chain structure silver(I) ions are linked by 4,4′-bipy groups, Fig. **1**. A search in the Cambridge Structural Database revealed that several linear chain structures with 4,4'-bipy ligand have been reported.

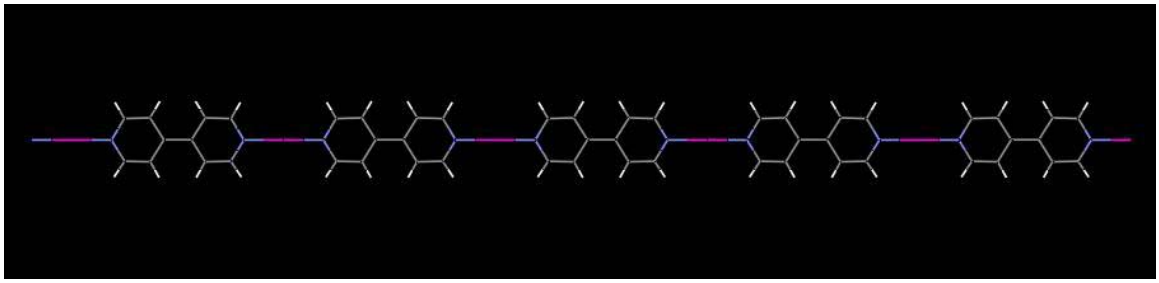

Figure 1. Linear-chain structure found in $\{[Ag(4,4'\text{-bipy})](X)\}_n$. (Anions have not been included for clarity.)

1.2.1.2 Zigzag chain structures

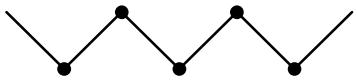

A zigzag polymeric chain structure has been described for the compound $[Cu_2(\mu\text{-}4,4'\text{-bpp})\ (OAc)_4]_n$.[98] In this structure, two individual $[Cu_2\ (OAc)_4]$ fragments are bridged by 4,4'-bpp (= 2,2'-bis(4-pyridylmethyleneoxy)-1,1'-biphenylene) ligands, Fig. **2**. Each Cu(II) centre is coordinated by five donor atoms, four oxygen atoms of the two acetate and one nitrogen atom of the 4,4'-bpp ligand, occupying the vertexes of the pyramid, whereas four oxygen atoms of the acetate counter ions form the basal plan and the axial site is occupied by one nitrogen donor atom from the bridging 4,4'-bpp ligand. The pyridyl rings of the ligand are slightly twisted with respect to one another to meet the requirements for this structural topology.

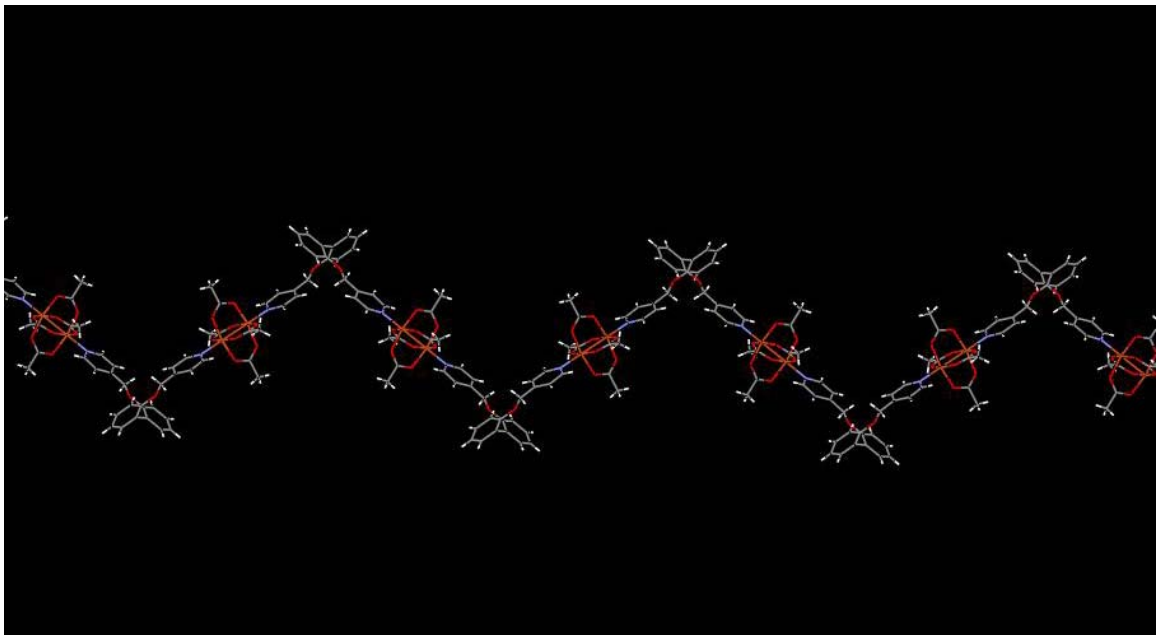

Figure 2. Zigzag chain structure found in complex $[Cu_2(\mu\text{-}4,4'\text{-bpp})\ (OAc)_4]_n$.

1.2.1.3 Ladder chain structures

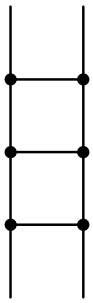

The one-dimensional polymer $[Ag(OAc)(4\text{-bppz})]_n$[99] (where 4-bppz= 2,5-di(pyridin-4-yl)pyrazine) belongs to this class of coordination polymers. The molecule has a centre of symmetry. In this structure, two adjacent Ag(I) ions are bridged by two acetate anions to build a ladder type polymer, Fig. **3**.

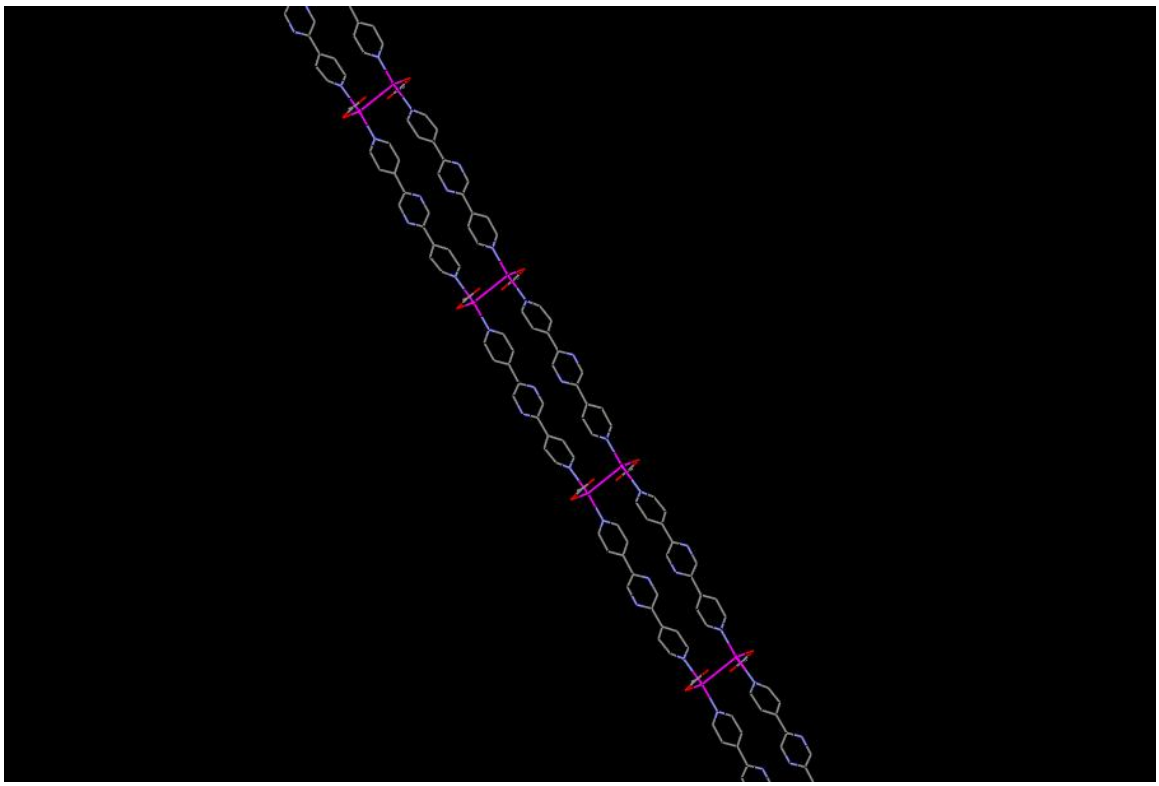

Figure 3. Ladder chain structure found in $[Ag(OAc)(4\text{-bppz})]_n$ complex.

1.2.1.4 Stair-step chain structures

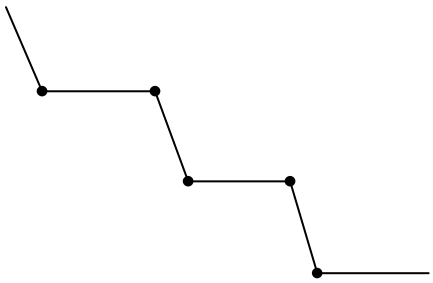

Metal coordination polymers with linear spacer ligands having stair-step chain polymeric structures have been exploited by many research workers. Specially silver(I) and copper(I) ions have been extensively used in inorganic crystal engineering using self-assembly of tailored building blocks. In our recent work, we have synthesized and structurally characterized numerous stair-step chain polymers by using tertiary phosphine and spacer ligands with silver(I) and copper(I) salts. Silver(I) complex $[Ag_2(4,4'\text{-bipy})(PPh_3)_2(NO_3)_2]_n$ belongs to this class of fascinating one-dimensional coordination polymers. In this polymeric compound two $[Ag(PPh_3)(NO_3)]$ units are bridged by a 4,4'-bipy ligand, Fig. **4**. These types of bridging and spacer ligand molecules play an important role to form this type of topology.[100]

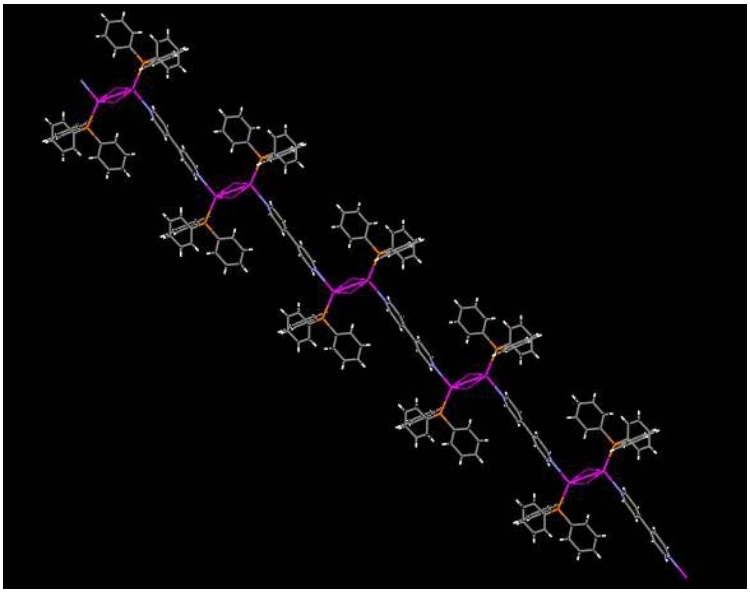

Figure 4. Stair-step chain structure found in $[Ag_2(4, 4'\text{-bipy})(PPh_3)_2(NO_3)_2]_n$ complex.

$[Ag_2I_2(4,4'\text{-bipy})(PPh_3)_2]_n$, $[Cu_2I_2(4,4'\text{-bipy})(PPh_3)_2]_n$ and $[CuCl_2(4,4'\text{-bipy})(PPh_3)_2]_n$ etc., are other examples of this type of polymeric chain structures.[100-103]

1.2.1.5 Helical chain structures

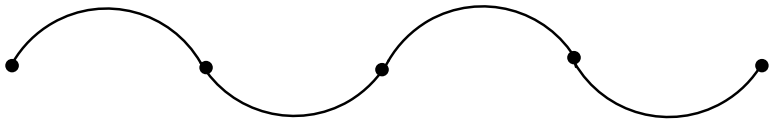

Wang[104] reported the synthesis and structure of the helical complex, $\{[Cu(HL)(H_2O)](NO_3)\}_n$ (HL = 3,6-bis(2-Pyridyl)pyrazine-2-,5-dicarboxylic acid). Here the flexible ligand binds with two metal ions in an asymmetric manner, so forming a helix.

Nomiya et al. has reported the synthesis and X-ray characterization of helical chain polymers. Silver(I) complex $[Ag(tetz)(PPh_3)_2]_n$ for example, has a single helical chain structure as shown in Fig. **5**. The geometry of the Ag(I) atom is described as distorted tetrahedral. The helix consists of $Ag(PPh_3)_2$ units bridged by tetrazolate anions. The metal centre is coordinated by two PPh_3 and two tetrazolate anions.[47]

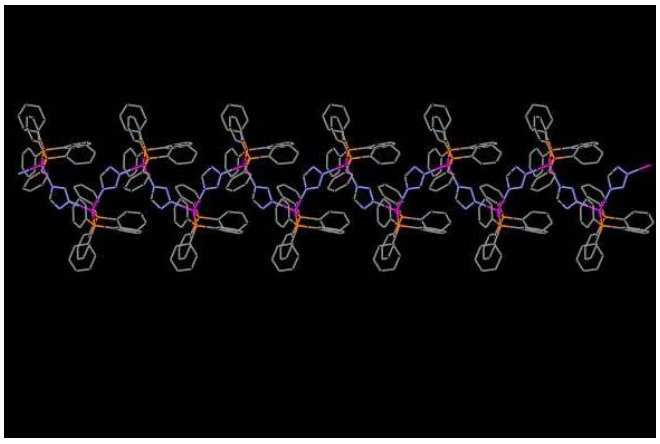

Figure 5. Helical chain structure found in $\{[Ag(tetz)](PPh_3)_2]\}_n$ complex.

1.2.2 Two-dimensional coordination polymers

The synthesis and characterization of infinite two- and three –dimensional networks has been an area of rapid growth recently. The motivation behind much of this activity has been provided by the prospect of generating, by deliberate design, a wide range of purpose-built materials with predetermined structures and useful properties, for example electronic, magnetic, optical and catalytic. The structure types commonly observed for the two-dimensional coordination polymers formed by bridging and spacer ligands are:

1.2.2.1 Square grids

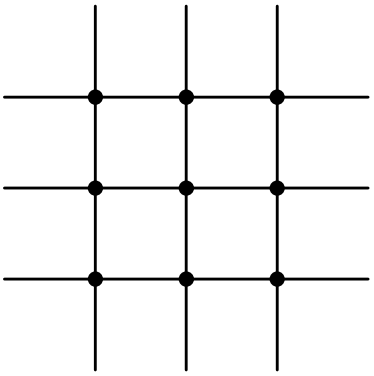

This structural architecture has been found in $\{[Cu_2(4,4'\text{-bipy})(H_2O)_2](SiF_6)_2\}_n$, a coordination polymer complex.[105] In this molecule, the Cu^{II} atom has an elongated octahedral environment with four nitrogen atoms of 4,4'-bipy ligands in the equatorial plane and two oxygen atoms of H_2O molecules in the axial sites, Fig. **6**. The Cu^{II} centres are bridged by 4,4'-bipy ligands to form a 2-D sheet having square grids.

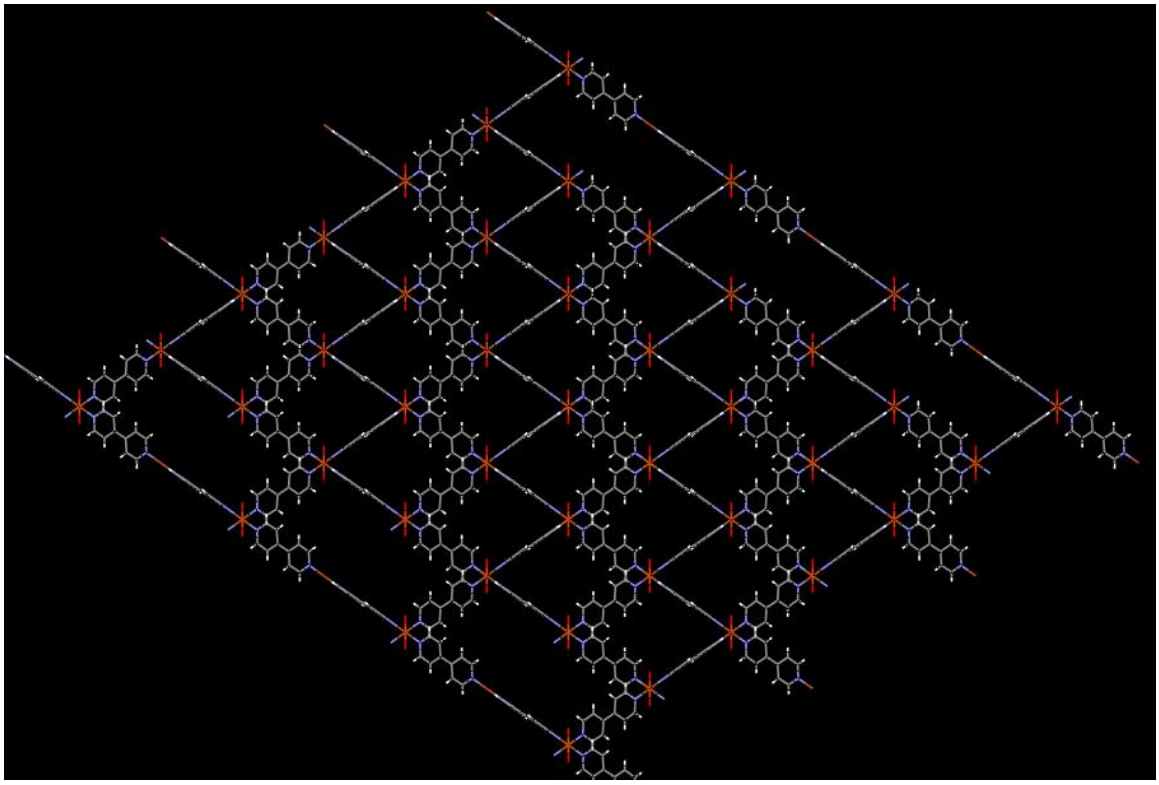

Figure 6. Square grid 2-D network is found in $\{[Cu_2(4,4'\text{-bipy})(H_2O)_2](SiF_6)_2\}_n$ complex.

1.2.2.2 Honey comb grids

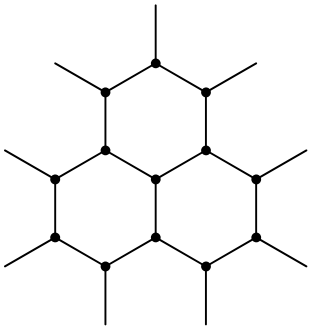

The structure of the complex $\{[Ag_2(pyz)_3](BF_4)_2\}_n$[106] (pyz= pyrazine) is made up of cationic two dimensional layers, consisting of $[Ag(pyz)_3]^+$ units forming hexagons, Fig. **7**. An unusual structural feature of this 2-D polymer is the folding into a chair conformation of the six-member $Ag_6(pyz)_6$ rings.

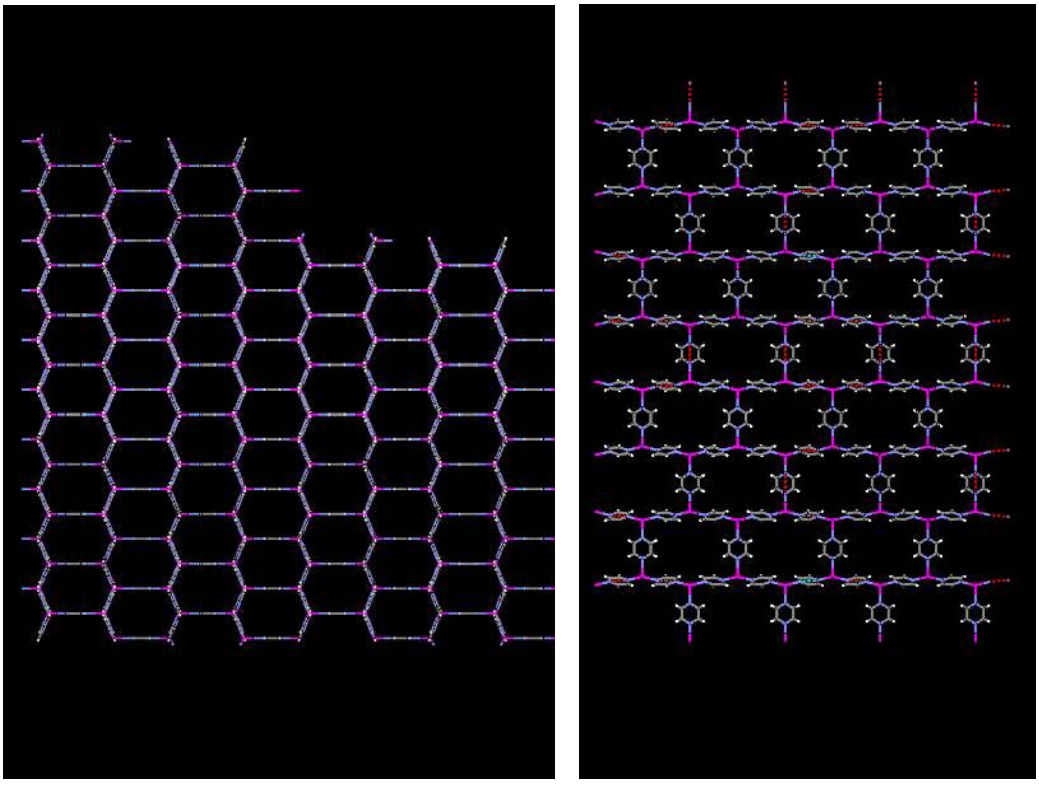

Figure 7. $[Ag_6(pyz)_6]$ unit builds up 2-D honey comb grids of $\{[Ag_2(pyz)_3](BF_4)_2\}_n$ complex.

1.2.3 Three-dimensional coordination polymers

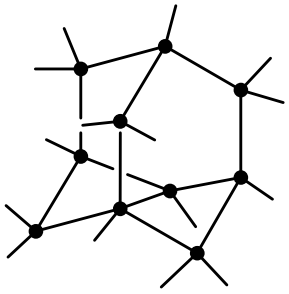

The major challenge in the field of crystal engineering is to pay attention on a functional view of architectures, which could be associated with dynamic aspect of frameworks. Porous materials are often much more dynamic than generally believed, and especially hydrogen bonded networks. It is well known that a wide range of spacer ligands

particularly 2,4,6-tris(2-pyridyl)-1,3,5-triazine (tpt) and its polymorphic forms have been used extensively by many researchers to construct 3-D porous net works,[107-110] those are suitable for host-guest interactions and selective separation of different organic molecules. Recently, 3-D silver(I) coordination polymers and their structures have been reported by Zhou et al.[109] $\{[Ag(tpt)]X\}_n$ ($X = ClO_4^-$, PF_6^-, BF_4^-) belongs to this class of three-dimensional coordination polymers, Fig. **8**. The geometrical environment around the silver(I) ion in these complexes is tetrahedral and each tpt ligand coordinates with three silver(I) ions. The copper(I) complex $\{[Cu_3(tpt)_4](ClO_4)_3\}_n$[110] is another example of a three-dimensional polymer with this type of spacer ligand and with large cavities.

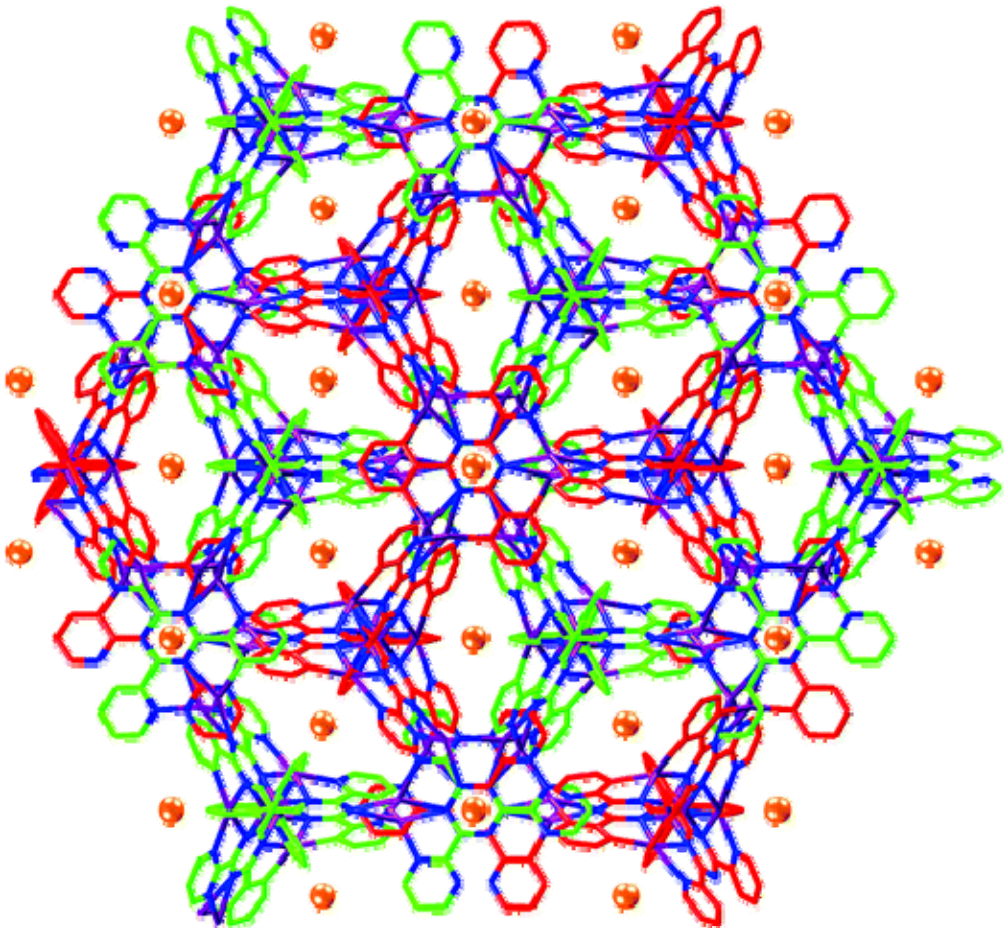

Figure 8. A 3-D network is found in complex $\{[Ag(tpt)]X\}_n$ ($X = ClO_4^-$, PF_6^-, BF_4^-). The golden spheres represent the anion ClO_4^-, BF_4^-, or PF_6^-. Hydrogen atoms are omitted for clarity [see Fig. **1**. in ref. 109].

1.3. Hydrogen bonding and other non-covalent interactions in coordination polymers

The role of coordination bonds and hydrogen bonds in crystal engineering is currently of great interest due to their use in constructing two- and three-dimensional polymers with special properties, such as electrical conductivity, magnetism, host-guest chemistry and catalysis.[58,74-75,93] The design and construction of metal-organic coordination polymers has attracted intense interest not only for their potential applications as new functional materials but also for their fascinating structural and super-structural diversity. Crystal engineering of metal-organic networks via self-assembly of ligand "spacers" and metal "nodes" has attracted considerable interest because of structural diversity in chemistry and material science. The path from molecular to supramolecular systems depends on the nature of its constituents and on the interaction between them. Among these interactions, non-covalent motifs such as metal-ligand coordination, hydrogen bonding, and π-π stacking, have been used for the generation of a wide variety of such super-structures.[124-127] The role of hydrogen bonding interactions is very significant in the construction of supramolecular architectures and by choosing the suitable ligands built from binding subunits of different types to offer hydrogen bonding could result 1-, 2-, and 3-dimensional polymers. In many previous examples, solvent molecules, anion templates or both have been found to produce a dramatic effect on the extended structure of the network.

1.4. Mechanism of interaction of metal based drugs with biomolecules

The complex cis-$[Pt(NH_3)_2Cl_2]$ (cisplatin) is the most well known anticancer drug. Anticancer drugs can cause complete regression of different types of cancer in the early stages. Cisplatin has been used as an anticancer and antitumour agent for decades. The anticancer activity of the complex is due to inhibition of DNA synthesis in the cancer

cell. Displacement of the chloride ligands by nitrogen donors of the two purines in the DNA chain forms a cross linking. Alkylating agents such as the nitrogen mustards are thought to form similar cross-links, but in this case, between bases on different DNA chains. The distance between the chlorides on the Pt(II) complexes is ca. 3.3 Å and on the nitrogen mustards ca. 8.0 Å, fit perfectly for the formation of intra- and inter-strand bridges.[111] Despite the success of cisplatin as an anticancer agent, its clinical use has been limited due to acquired and intrinsic resistance of cancer cells to the drug, and its high toxicity to some normal cells.[112] Hence, there exists an immense interest to improve the design of metallodrugs, having reduced toxicity and a high spectrum of activity, especially drugs that would show activity against the cell lines resistant to cisplatin. A group of complexes that are particularly relevant in this regard are phosphine complexes of group 11 metal ions.[113]

In bioinorganic chemistry the silver(I) ion has long been known as having inhibitory and bactericidal effects and several possible mechanisms of antimicrobial activities for inhibition by aqueous silver(I) ion have been proposed: (i) interference with electron transport, (ii) interaction with the cell membrane, (iii) binding to DNA, and (iv) interaction with the thiol group in vital enzymes to deactivate them.[117]

The first interaction between a metal-based drug and bacteria is at the cell wall level. The basis for this interaction is the strong attraction for positively charged compounds such as cations. Antibacterial drugs having a positive charge would possess one of the important characteristics. If the compound can form a coordination bond or interact electrostatically with the cell wall, it is very probable that the compound will show biocidal activity. Biocidal activity of the metal-based drugs also depends on the size of the compound and in particular the macromolecular dimensions of the polymer type drug. A compound having a size (500 to 2500 nm for gram positive bacterium) comparable to the holes of the cell walls of the biomolecules is considered as a good antibacterial agent. The compound having an appropriate size could easily pass through the cell wall and interact with the cell membrane, producing changes that could finally cause the death of bacteria. It is also possible that these compounds may interact with an important part of the

biomolecule such as DNA and proteins, avoiding replication of the bacteria. However, another probable mechanism is the interaction with teichoic acid at the cell wall, which contains phosphate bridges (negative charges) that could interact electrostatically with the positive charges of the polycations. This would permit the polymeric metal-based drugs to stay close to the bacteria cell, blocking the ion exchange channels, inhibiting growth, and causing the cell death. It is well understood now that the high antibacterial activity of silver(I) complexes and coordination polymers is due to the Ag^{+} ions.[114-116]

Ag^{+}, Cu^{2+}, Fe^{3+} ions are well known for their broad-spectrum antimicrobial activity against bacterial and fungal agents together with their lack of cross-resistance with antibiotics.[51,118-119] The antimicrobial activity of silver has been known for a long time and is attributable to the silver cation Ag^{+}, which binds strongly to electron donor groups (Sulphur, Oxygen, and Nitrogen) present in biomolecules. Although silver has already been employed in medical devices, the research interest in this field is still considerable and mainly focused on the development of innovative methods to incorporate silver into polymeric substrates.[54] Different techniques have been used to incorporate Ag^{+} ions into polymers. Most of these techniques have been discarded due to their draw backs. A high polymer/silver ion affinity is obtained by synthesis of a polymer possessing an anion, like a carboxylate, which can coordinate Ag^{+} ions. Moreover, antimicrobial metallic polymers possess mechanical properties, suitable for the development of medical devices without any risk of loss of antimicrobial activity. Silver(I) complexes having Ag(I)-N and Ag(I)-O bonds exhibit effective and a wide spectrum of antimicrobial activities. Generally, Ag(I)-S complexes have been shown to have a narrower spectrum of antimicrobial activity than Ag(I)-N and Ag(I)-O complexes. Most of the Ag(I)-P complexes investigated so far have shown very poor antimicrobial activity. The effective antimicrobial activities of Ag(I)-N and Ag(I)-O bonding complexes could be due to the weak silver(I)-O/N bonds, which are easily replaced with biomolecules especially those having thiol groups. In short, these results suggest that one of the key factors determining the antimicrobial effects of silver(I) complexes is the nature of the atom coordinated to Ag^{+} and its bonding properties, rather than the solubility, charge, chirality, or degree of polymerization of the silver(I) complexes.[8]

It has long been recognized that Au^{I} complexes can provide sustained relief from rheumatoid arthritis and other autoimmune disorders.[47,49] In a bimolecular setting, Au^{I} interacts with cysteine and other thiol groups, especially those with low pKa values such as the activated thiols in enzyme active sites. These biomolecule-gold(I) adducts, formed upon injection or ingestion of the drugs by facile ligand replacement reactions, are believed to mediate the therapeutic effects of the metal ion.[120]

The earliest fungicides used on plants were sulphur and inorganic copper compounds and the later still find agriculture use.[111] Several copper-based metallodrugs are in use for the treatment of different diseases, for example antimicrobial action of aminoglycosides (Ami) is based on their interaction with ribosomal RNA and also with the cytoplasmic membrane. Aminoglycosides (Ami) also have severe toxic side-effects on kidney and the inner ear. Copper(II) complexes of aminoglycosides cleave DNA and RNA by interacting with the biomolecules. The processes of DNA and RNA oxidation clearly demonstrate that copper(II)-Ami is a potentially dangerous genotoxic agent. Copper(II)-coordinated Ami retains the ability to bind to nucleic acids and cleave phosphodiester bonds, which causes the cell death.[121-123]

1.5 The objectives of this work

The objectives of this work were firstly to explore the possibility of forming silver(I)-phosphine mixed ligand complexes and to study their biological properties and structural characteristics. Secondly to explore the synthesis and structural properties of silver-biotin complexes with pre-design helical chain architectures. Thirdly to study the role of hydrogen bonding interactions in the construction of one-, two-, and three-dimensional frameworks of biotin and ortho-, meta-, and para-pyridyl oximes and their silver(I)-complexes. Finally to study the role of the bridging ligand 4,4'-bipyridine to form coordination polymers with silver(I)-phosphine precursors. We are looking forward positively to study the biological activity of rest of the three series of silver(I)-coordination polymers as early as possible.

References

1. Melaiye, A.; Sun, Z.; Hindi, K.; Milsted, A.; Ely. D.; Reneker, D. H.; Tessier, C. A.; Youngs, W. J. *J. Am. Chem. Soc.* 127, 2285 (2005)
2. Melaiye, A.; Simpson, R. S.; Milsted, A.; Pingitore, F.; Wesdemiotis, C.; Tessier, C. A.; Youngs, W. J. *J. Med. Chem.* 47, 973 (2004)
3. Falanga, V.; *Wound Rep. Reg.* 8, 347 (2000)
4. Lansdown, A. B. G. *J. Wounds Care.* 2, 125 (2002)
5. Klasen, H. J. *J. Burns.* 26, 131 (2000)
6. Atiyeh, B. S.; Ioannovich, J.; Magliacani, G.; Masellis, M.; Costagliola, M.; Dham, R.; Al-Musa, K. A. *J. Burns Wounds Care.* 2, 18: 1 (2003)
7. Fuller, F. W.; Parrish, M.; Nance, F. C. *J. Burns. Care Rehabil.*15, 213 (1994)
8. Kasuga, N. C.; Sugie, A.; Nomiya, K. *J. Chem. Soc. Dalton Trans.* 3732 (2004)
9. Karagiannidis, P.; Aslanidis, P. *Inorganica Chimica acta.* 172, 247 (1990)
10. Catalano, V. J.; Etogo, A. O.; *J. Organomet. Chem.* 690, 6041 (2005)
11. Kitagawa, S.; Kitaura, R.; Noro, S. *Angew. Chem. Int. Ed.* 43, 2334 (2004)
12. Nomiya, K.; Takahashi, S.; Noguchi, R.; Nemoto, S.; Takayama, T.; Oda, M. *Inorg. Chem.* 39, 3301 (2000)
13. Reger, D. L.; Semeniuc, R. F.; Rassolov, V.; Smith, M. D. *Inorg. Chem.* 43, 537 (2004)
14. Erxleben, A. *Inorg. Chem.* 40, 2928 (2001)
15. Adachi, K.; Kaizaki, S.; Yamada, K.; Kitagawa, S.; Kawata, S. *Chem. Lett.* 648 (2004)
16. Bowmaker, G. A.; Effendy.; Hana, J. V.; Healy, P. C.; Sketon, B. W.; White, A. H. *J. Chem. Soc. Dalton Trans.* 1387 (1993)
17. Mann, F. G.; Wells, A. F.; Purdie, D. *J. Chem. Soc.* 1828 (1937)
18. Aslanidis, P.; Karagiannidis, P.; Akrivos, P. D.; Krebs. B.; Läge, M. *Inorganica Chimica acta.* 254, 277 (1997)
19. Crespo, O.; Brusko, V. V.; Gimeno, M. C.; Tornil, M. L.; Laguna, A.; Zabirov, N. G.

Eur. J. Chem. Soc. 423 (2004)

20. Nomiya, K.; Tsuda, K.; Kasuga, N. C. *J. Chem. Soc. Dalton Trans.* 1653 (1998)

21. Shaw, C. F.; Schmitz, G.; Thomson, H. O.; Witkiewicz, P. *J. Inorg. Biochem.* 10, 317 (1979)
22. Nomiya, K.; Kondoh, Y.; Onoue, K.; Kasuga, N. C.; Nagano, H.; Oda, M.; Sudoh, T.; Sakuma, S. *J. Inorg. Biochem.* 58, 255 (1995)
23. Nomiya, K.; Yokoyama, H.; Nagano, H.; Oda, M.; Sakuma, S. *J. Inorg. Biochem.* 60, 289 (1995)
24. Clement, J. L.; Jarrett, P. S. *J. Inorg. Biochem.* 51, 105 (1993)
25. Cookson, P. D.; Tieknik, E. R. T. *J. Chem. Soc. Dalton Trans.* 259 (1993)
26. Noguchi, R.; Hara, A.; Sugie, A.; Nomiya, K. *Inorg. Chem. Commun.* 9, 355 (2006)
27. Nomiya, K.; Takahashi, S.; Noguchi, R.; Takayama, H.; Oda, M. *Inorg. Chem.* 39, 3301 (2000)
28. Nomiya, K.; Takahashi, S.; Noguchi, R. *J. Chem. Soc. Dalton Trans.* 4369 (2000)
29. Nomiya, K.; Takahashi, S.; Noguchi, R. *J. Chem. Soc. Dalton Trans.*1343 (2000)
30. Nomiya, K.; Yokoyama, H. *J. Chem. Soc. Dalton Trans.* 2483 (2002)
31. Kasuga, N. C.; Yamamoto, R.; Hara, A.; Amano, A.; Nomiya, K. *Inorganica Chimica acta.* 359, 4412 (2006)
32. Creaven, B. S.; Egan, D. A.; Kavanagh, K.; McCann, M.; Mahon, M.; Noble, A.; Thati, B.; Walsh, M. *Polyhedron.* 24, 949 (2005)
33. Howe, B. P. *Metal Based Drugs.* 4, 273 (1997)
34. Kean, W. F.; Lock, C. J. L.; Howard-Lock, H. *Inflammopharmacology.*1, 103 (1991)
35. Grootveld, M.; Blake, D. R.; Sahinoglu, T.; Claxson, A. W. D.; Mapp, M.; Steven, C.; Allen, R. E.; Furst, A. *Free Radical Res. Comm.* 10, 199 (1990)
36. Shaw III, C. F. *Chem. Rev.* 99, 2589 (1999)
37. Mckeage, M. J.; Papathanasiou, P.; Salem. G.; Sjaarda, A.; Swiegers, G. F.; Waring, P.; Wild, S.B. *Metal-Based Drugs.* 5, 217 (1998)
38. Barnard, P. J.; Baker, M. V.; Berners-Prince, S. J.; Day, D. A. *J. Inorg. Biochem.* 98, 1642 (2004)
39. Messori, L.; Marcon, G. *Met. Ions Biol. Syst.* 42, 385 (2004)

40. Elsome, A. M.; Hamilton-Miller, J. M. T.; Brumfitt, W.; Noble, W. C. *J. Antimicrob. Chemother.* 37, 911 (1996)
41. Özdemir, I.; Denizci, A.; Öztürk, H. T.; Cetinkaya, B. *Appl. Organometal. Chem.* 18, 318 (2004)
42. Berners-Price, S. J.; Johnson, R. K.; Giovenella, A. J.; Fauctte, L. F.; Mirabelli, C. K.; Sadler, P. J. *J. Inorg. Biochem.* 33, 285 (1988)
43. Nmiya, K.; Noguchi, R.; Oda, M. *Inorganica Chimica Acta.* 298, 24 (2000)
44. Tong, Y.-Y.; Fraústo da Silva, J. J. R.; Pombeiro, A. J. L.; Wagner,G.; Herrmann, R. *J. Organomet. Chem*. 552, 17 (1998)
45. Ahmad, S.; Isab, A. A.; Ali, S.; Al-Arfaj, A. R. *Polyhedron.* 25, 1633 (2006)
46. Best, S. L.; Sadler, P. J. *Gold Bull.* 29, 87 (1996)
47. Nomiya, K.; Tsuda, K.; Sudoh, T.; Oda, M. *J. Inorg. Biochem.* 68, 39 (1997)
48. Nomiya, K.; Noguchi, R.; Ohsawa, K.; Tsuda, K.; Oda, M. *J. Inorg. Biochem*. 78, 263 (2000)
49. Nmiya, K.; Yamamoto, S.; Noguchi, R.; Yokoyama, H.; Kasuga, N. C.; Ohyama, K.; Kato, C. *J. Inorg. Biochem.* 95, 208 (2003)
50. Tsyba, I.; Mui, B. B.-K.; Bau, R.; Noguchi, R.; Nomiya, K. *Inorg. Chem.* 42, 8028 (2003)
51. Wang, Y.; He, Q.-Y.; Che, C.-M.; Chiu, J.-F. *Proteomics.* 6, 131 (2006)
52. Kovarik, J.; Svec, F., Thurzo, V. *Neoplasma.* 19, 569 (1972)
53. Lipman, A. J., Helson, C.; Helson, L.; Krakoff, I. H. *Cancer Chemother. Rep.* 57, 191 (1973)
54. Francolini, I.; Ruggeri, V.; Martinelli, A.; D'Ilario, L.; Piozzi, A. *Macromol. Rapid Commun.* 27, 233 (2006)
55. Donlan, R. M. Emerg. *Infect. Dis.* 7, 277 (2001)
56. Kovacevich, D. S.; Papke, L. F. *Nutr. Clin. Pract.* 14, 95 (2003)
57. Stoodley, P.; Sauer, K.; Davies, D. G.; Costerton, J. W. *Ann. Rev. Microbiol.* 56, 187 (2002)
58. Das, M.; Shivashankar, S. A. *Appl. Organometal. Chem.*21, 15 (2007)
59. Frederic, A.F.; Blanz, E. J. *J. Med. Chem.* 9, 585 (1966)
60. Campbell, M. J. M. *Coord. Chem. Rev.* 15, 279 (1975)

61. Khazi, I. M.; Koti, R. S.; Chadha, M. V.; Mahajanshetti, C. S.; Gadad, A. K. *Arzeim.-Forsch./ Drug Res.* 55, 107 (2005)
62. Khazi, I. M.; Mahajanshetti, C. S.; Gadad, A. K.; Tarnalli, A. D. *Arzeim.-Forsch./ Drug Res.* 46, 949 (1996)
63. Wu, J. C.; Peet, G. W.; Coutts, S. J.; Eckner, R. J.; Griffin, J. A.; Fraina, P. R. *Biochemistry.* 34, 7154 (1995)
64. Ming, L.-J. *Med.Res. Rev.*23, 697 (2003)
65. Brewer, G. J. *Curr. Opin. Chem. Biol.* 7, 207 (2003)
66. Vaidyanthan, V. G.; Nair, B.U. *J. Inorg. Biochem*. 93, 271 (2003)
67. Pratveil, G.; Bernadou, J.; Meunier, B. *Angew. Chem. Int. Ed. Engl.* 34, 746 (1995)
68. Drevens'ek, P.; Turel, I.; Ulrih, N. P. *J. Inorg. Biochem*. 96, 407 (2003)
69. Drevens'ek, P.; Zupancic´, T.; Pihlar, B.; Jerala, R.; Kolitsch, U.; Plaper, A.; Turel, I. *J. Inorg. Biochem*. 99, 432 (2005)
70. Fabbrizzi, L.; Kaden, T. A.; Perotti, A.; Seghi, B.; Siegfried, L. *Inorg. Chem.* 25, 321 (1986)
71. Machida, R.; Kimura, E.; Kodama, M. *Inorg. Chem.* 22, 2055 (1983)
72. Smith, S.A. *J. Inorg. Biochem*.98, 1874 (2004)
73. Novak-Hofer, I.; Zimmermann, K.; Maecke, H.; Amstutz, H. P.; Carrel, F.; Schubiger, P. *J. Nucl. Med.* 38, 536 (1997)
74. Antunes, P.; Delgado, R.; Drew, M. G. B.; Félix, V.; Maecke, H. *Inorg. Chem.* 46, 3144 (2007)
75. Matsumoto, K.; Harada, Y.; Yamada, N.; Kurata, H.; Kawase, T.; Oda, M. *Crystal Growth & Design.* 6, 1083, (2006)
76. Eddaoudi, M.; Moler, D. B.; Li, H.; Chen, B.; Reineke, T. M.; Keeffe, M. O.; Yaghi, O. M. *Acc. Chem. Res.* 34, 319 (2001)
77. Robson, R. *J. Chem. Soc. Dalton Trans.* 3735 (2000)
78. Hoskins, B. F.; Robson, R. *J. Am. Chem. Soc.*112, 1546 (1990)
79. Blake, A. J.; Champness, N. R.; Crew, M.; Parsons, S. *New. J. Chem.* 13, (1999)
80. Blake, A. J.; Baum, G.; Champness, N. R.; Chung, S. S. M.; Cooke, P. A.; Fenske, D.; Khlobystov, A. N.; Lemenovskii, D. A.; Li, W.-S.; Schröder, M. *J. Chem. Soc. Dalton Trans.* 4285 (2000)

81. Yaghi, O. M.; Li, H. *J. Am. Chem. Soc.*118, 295 (1996)

82. Bowmaker, G. A.; Effendy.; Lim, K. C.; Skelton, B. W.; Sukarianingsih, D.; White, A. H. *Inorganica Chimica acta.* 358, 4342 (2005)
83. Janiak, C. *Angew. Chem. Int. Ed. Engl.* 36, 1431 (1997)
84. Tong, M.-L.; Chen, X.-M.; Ng, S. W. *Inorganic Chemistry Communcations.* 436 (2000)
85. Bosch, E.; Barnes, C. L. *Inorg. Chem.* 40, 3097 (2001)
86. Dong, Y. B.; Smith, M. D.; Layland, R.C.; zur Loye, H.-C. *J. Chem. Soc. Dalton Trans.* 775 (2000)
87. Juan, C. M. R.; Lee, B. *Coord. Chem. Rev.* 183, 43 (1999)
88. Sun, D.; Cao, R.; Sun, Y.; Bi, W.; Li, X.; Wang, Y.; Shi, Q.; Li, X. *Inorg. Chem.* 42, 7512 (2003)
89. Kitagawa, S.; Kitaura, R.; Noro, S.-I. *Angew. Chem. Int. Ed.* 43, 2334 (2004)
90. Kitagawa, S.; Kondo, M. *Bull. Chem. Soc. Jpn.* 71, 1739 (1998)
91. Uemura, K.; Matsuda, R.; Kitagawa, S. *Journal of Solid State Chemistry.* 178, 2420 (2005)
92. Abrahams, B. F.; Batten, S. R.; Hoskins, B. F.; Robson, R. *Inorg. Chem.* 42, 2654 (2003)
93. Ma, J.-F.; Liu, J.-F.; Xing, Y.; Jia, H.-Q.; Lin, Y.-H. *J. Chem. Soc. Dalton Trans.* 2403 (2000)
94. Wang, L.-S.; Zhang, J.-F.; Yang, S.-P. *Acta Crystallogr., Sect.E: Struct. Rep. Online,* 60**,** m1484 (2004)
95. Bi, W.; Sun, D.; Cao, R.; Hong, M. *Acta Crystallogr., Sect.E: Struct. Rep. Online,* 58, m324 (2002)
96. Kokunov, Y. V., Khmelevskaya, L. V.; Gorbunova, Y. E.; Mikhailov, Y. N. *Zh .Neorg. Khim. (Russ.) (Russ.J.Inorg.Chem.),* 48, 1452 (2003)
97. Kokunov, Y. V., Khmelevskaya, L. V.; Gorbunova, Y. E. *Zh .Neorg. Khim. (Russ.) (Russ.J.Inorg.Chem.),* 49, 1089 (2004)
98. Gong, Y.-Q.; Wang, R.-H.; Zhou, Y.-F.; Lin, Z.-Z.; Hong, M.-C. *Journal of Molecular Structure*, 751, 121 (2005)

99. Vallat, O.; Neels, A.; Stoeckli-Evans, H. *Journal of Crystallography,* 33, 39 (2003)
100. Sampanthar, J. T.; Vittal, J. J. *Crystal Engineering,* 3, 117 (2000)
101. Marsh, R. E. *Acta Crystallogr.,Sect. B: Struct. Sci.* 61, 359 (2005)
102. Li, R.-Z.; Li, D.; Huang, X.-C.; Qi, Z.-Y.; Chen, X.-M. *Inorg. Chem. Commun.* 6, 1017 (2003)
103. Lu, J.; Crisci, G.; Niu, T.; Jacobson, A. J. *Inorg. Chem.*36, 514 (1997)
104. Wang, Y. Ph. D. Thesis, Université de Neuchatel, 1996
105. Noro, S.-I.; Kitaura, R.; Kondo, M.; Kitagawa, S.; Ishii, T.; Matsuzaka, H.; Yamashita, M. *J. Am. Chem. Soc.* 124, 2568 (2002)
106. Carlucci, L.; Ciani, G.; Proserpio, D. M.; Sironi, A. *J. Am. Chem. Soc.* 117, 4562 (1995)
107. Batten, S. R.; Robson, R. *Angew. Chem. Int. Ed.* 37, 1494 (1998)
108. Ohmori, O.; Kawano, M.; Fujita, M. *Angew. Chem. Int. Ed.* 44, 1962 (2005)
109. Zhou, X.-P.; Zhang, X.; Lin, S.-H.; Li, D. *Crystal Growth & Design.* 7, 485 (2007)
110. Abrahams, B. F.; Batten, S. R.; Hamit, S.; Hoskins, B.F.; Robson, R. *Angew. Chem. Int. Ed. Engl.* 35, 1690 (1996)
111. Hay, R. W. *Bio-Inorganic chemistry.* 1991
112. Sadler, P. J.; Guo, Z. *Pure Appl. Chem.* 70, 863 (1998)
113. Sanghamitra, N. J.; Phatak, P.; Das, S.; Samuelson, A. G.; Somasundaram, K. *J. Med. Chem.* 48, 977 (2005)
114. Rivas, B. L.; Pereira, E. D.; Mondaca, M. A.; Rivas, R. J.; Saavedra, M. A. *J. Appl. Polym. Sci.* 87, 452 (2003)
115. Nandi, M. M.; Ray, R.; Chuadury, J. *Industrial J. Chem Section A: Inorganic.* 27, 687 (1998)
116. Rivas, B. L.; Pereira, E. D. *J. Appl. Polym. Sci.* 80, 2578 (2001)
117. Russell, A. D.; Hugo, W. B. *Prog. Med. Chem.* 31, 351 (1994)
118. Guggenbichler, J. P.; Boswald, M.; Lugauer, S.; Krall, T. *Infection.* 27, S16 (1999)
119. Petering, H. G. *Pharmacol. Ther.* 1, 127 (1976)
120. Larabee, J. L.; Hocker, J. R.; Hanas, J. S. *Chem. Res. Toxicol.* 18, 1943 (2005)
121. Sreedhara, A.; Patwardhan, A.; Cowan, J. A. *Chem. Commun.* 1147 (1999)

122. Sreedhara, A.; Cowan, J. A. *Chem. Commun.* 1737 (1998)

123. Szczepanik, W.; Kaczmarek, P.; Jez'owska-Bojczuk, M. *Bioinorganic Chemistry and Applications.* 2, 55 (2004)

124. Holiday, B. J.; Mirkin, C. A. *Angew. Chem.* 113, 2076 (2001)

125. Desirajau, G. R. Acc. Chem. Rev. 35, 565 (2002)

126. Janiak, C. *J. Chem. Soc., Dalton Trans.* 3885 (2000)

127. Blondeau, P.; Van der Lee, A.; Barboiu, M. Inorg. Chem. 44, 5649 (2005)

Chapter 2:

Silver(I) Phosphine Mixed Ligand Complexes: Synthesis, Crystal structures, Antimicrobial, Antifungal and Anticancer Activities

Introduction

Elemental silver and silver salts have been used for centuries as antimicrobial agents in curative and preventive health care.[1-3] However, the use of silver metal and its salts as antimicrobial agents declined sharply in the middle of the last century upon the introduction of antibiotics. Amongst the few silver(I) compounds commonly prescribed today for their topical anti-bacterial effects are sulfadiazine for the treatment of burns and a dilute solution of $AgNO_3$, which is used prophylactically for bacterial infections and conjunctivitis in infants.[4-6] With the ever increasing problem of microbe resistance to current antimicrobial agents, particularly antibiotics, there is an urgent demand for new classes of compounds that will efficiently inhibit the growth of pathogenic micro-organisms. There is currently tremendous interest in silver(I) complexes with biological therapeutic activities. In bioinorganic chemistry of silver(I) complexes, there have been reported various studies of silver(I) complexes related to antimicrobial, antiviral, and antitumour activities.[7-12] Molecular design of such silver(I) complexes is an intriguing aspect of the bioinorganic chemistry, inorganic chemistry and synthetic chemistry of metal-based drugs.[13-17] Medicinally and pharmaceutically active silver(I) compounds of sulphur and nitrogen containing donor ligands are harder to crystallize and are believed to be polymeric.[18-20]

In bioinorganic chemistry the silver(I) ion has long been known as having inhibitory and antibacterial effects and several possible mechanisms of antimicrobial activities for inhibition by aqueous silver(I) ions have been proposed: (i) interference with electron transport; (ii) interaction with the cell membrane; (iii) binding to DNA; and (iv) interaction with the thiol group in the vital enzymes to inactivate them.[21-22]

Tuberculosis (TB) remains a public health issue at the beginning of 21st century. TB causes nearly 3 million deaths annually world wide. The estimated 8.8 million of new cases corresponds to 52,000 deaths per weak or more than 7,000 deaths each day. In the developing countries TB is a leading cause of morbidity and mortality. Co-infection with human immunodeficiency virus (HIV) has been responsible for changes in the TB epidemiologic situation and also the emergence of multi-drug resistant strains.[23-25] Due to

this critical situation, an intense effort has been directed to develop new drugs for TB therapy.

In order to investigate the structural relationship of silver(I) complexes with antimicrobial activities in aqueous media, silver(I)-N, silver(I)-S, and silver(I)-P bonding complexes have been prepared and tested against selected bacteria.[26-30] Silver(I)-N, silver(I)-S, and silver(I)-P bonds exhibited an effective and wide spectrum of antibacterial activities, as shown here in our recent studies. In general antimicrobial effects of silver(I) complexes are related to the nature of the atoms coordinated to the Ag^+ ion and its bonding properties, rather than the solubility, charge, chirality, or degree of polymerization of silver(I) complexes. Silver(I) complexes having only silver(I)-N and silver(I)-O bonds show potential antimicrobial activities against many micro-organisms, most of them are light sensitive especially in solution and their characterization is not easily performed. To avoid this problem we have prepared a series of mixed ligand silver(I) complexes, with tertiary phosphines, thiosemicarbazide (**L1**), 2-(propan-2-ylidene)hydrazinecarbothioamide (**L2**), and 2-mercaptothiazoline (**L3**) as ligands.

Here we report the synthesis of ten silver(I) complexes, all are light stable and show promising potential antibacterial, antifungal and anticancer activities. These silver(I) complexes with 1:1:2, 1:1:1 and 1:2:1 (Ag:phospine:ligand) compositions $[Ag_2(P1)_2(L1)_4].(NO_3)_2.H_2O$ (**1**), $[Ag_2(P1)_2(L2)_4].(NO_3)_2$ (**2**), $[Ag(P2)(L2)_2].NO_3$ (**3**), $[Ag(P2)(L1)_2].PF_6$ (**4**), $\{[Ag(P3)_2(L3)]_2(NO_3)\}.NO_3$ (**5**), $[Ag_2(P2)_2(L2)_2].(PF_6)_2$ (**6**), $[Ag_2(P4)_2(L3)_2].(ClO_4)_2$ **(7**), $[Ag(P5)_2(L3)(Br)]$ (**8**), $[Ag_2(P1)_2(L3)_2].(NO_3)_2$ (**9**), and $[Ag(P4)_2(L3)].NO_3$ (**10**) were prepared from a series of silver(I) salts [$AgNO_3$, $AgClO_4$, $AgPF_6$ and AgBr], tertiary phosphines [triphenyl phosphine-**P1,** tricyclohexyl phosphine-**P2**, phenyldicyclohexyl phosphine-**P3**, diphenylcyclohexyl phosphine-**P4**, diphenyl(p-tolyl) phosphine-**P5**], and the ligands thiosemicarbazide (**L1**), 2-(propan-2-ylidene)hydrazine carbothioamide (**L2**), and 2-mercaptothaizoline (**L3**).

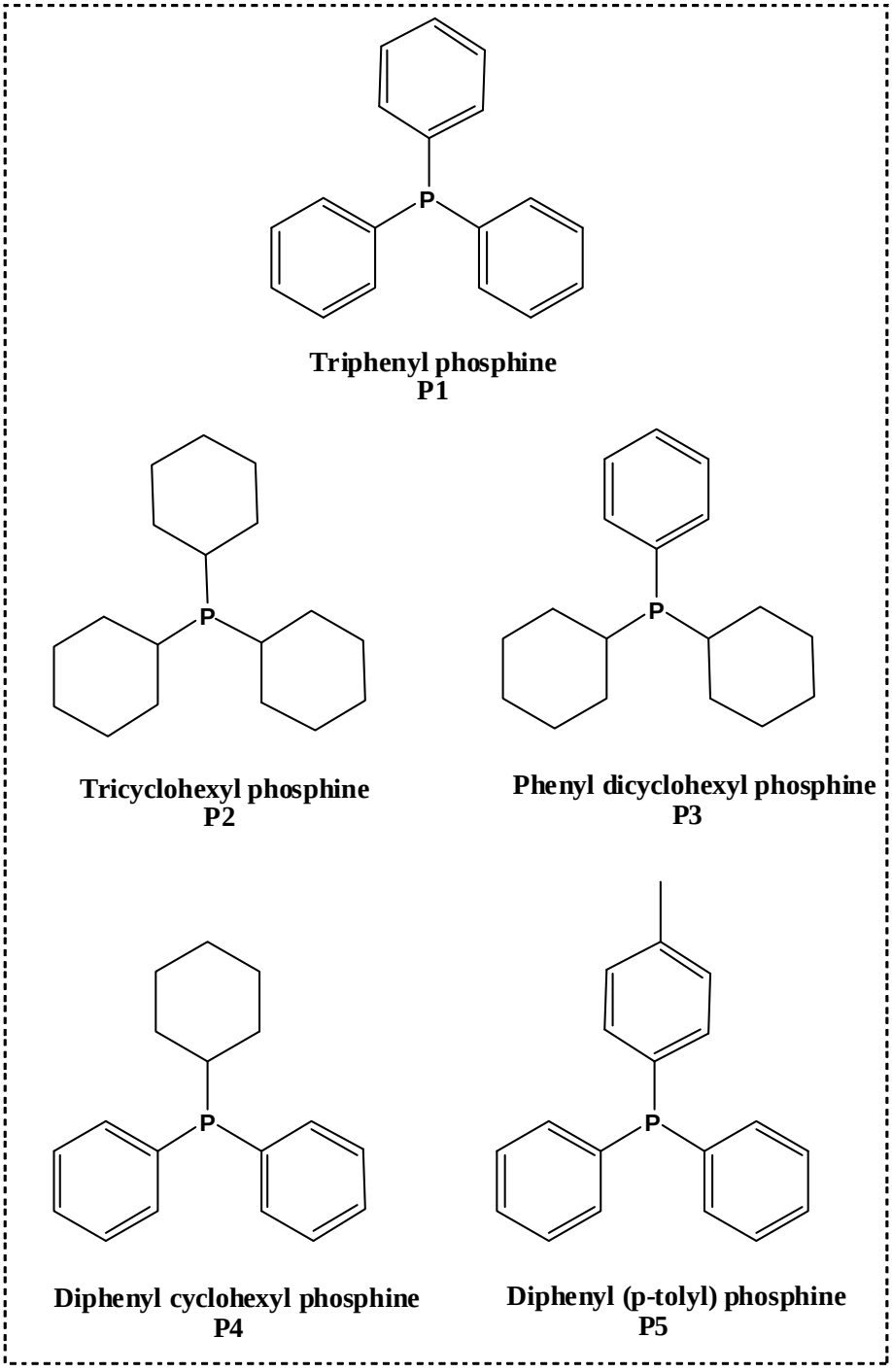
Triphenyl phosphine
P1
Tricyclohexyl phosphine
P2
Phenyl dicyclohexyl phosphine
P3
Diphenyl cyclohexyl phosphine
P4
Diphenyl (p-tolyl) phosphine
P5

Scheme 1

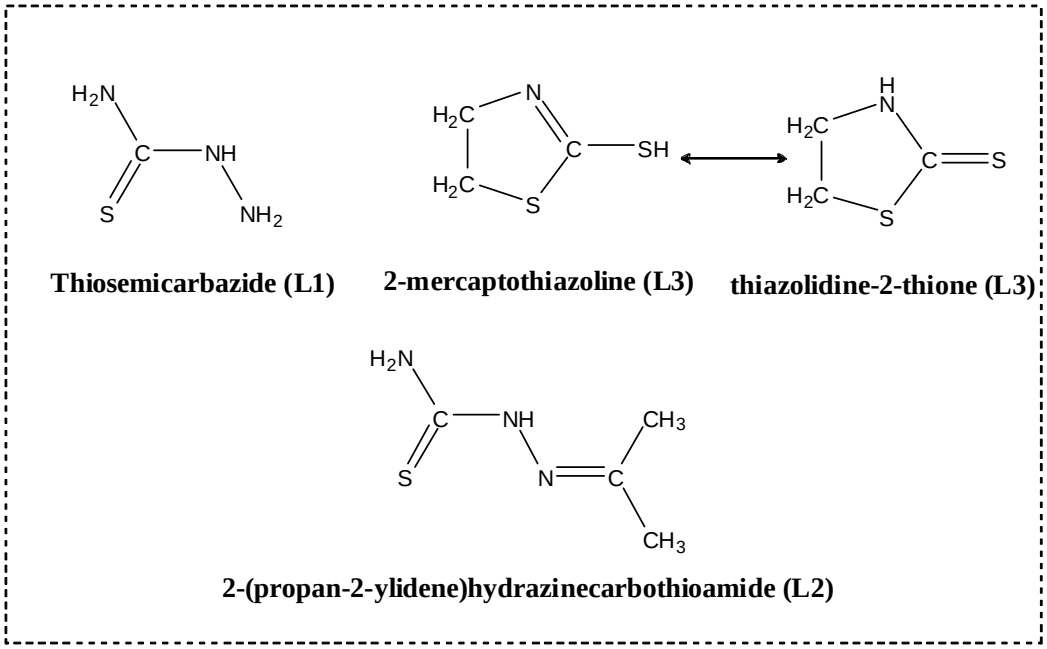

Scheme 2

They were characterized by elemental analysis, FTIR, and NMR spectroscopy. Antimicrobial, anti-fungal, anti-cancer, and anti-tuberculosis activities of these well characterized silver(I) complexes were evaluated by minimum inhibitory concentration (MIC: µg/mL) in aqueous suspension system and comparisons were made.

Experimental Section

Chloroform, dichloroform, methanol, acetonitrile, acetone, $AgNO_3$, $AgClO_4$, $AgPF_6$, AgBr, triphenyl phosphine, tricylohexyl phosphine, phenyldicyclohexyl phosphine, diphenylcyclohexyl phosphine, diphenyl(p-tolyl) phosphine, and 2-mercaptothiazoline, thiosemicarbazide were purchased from ACROS and Aldrich. Microanalysis was done by Mr. D. Mooser (Ecole d'ingénieurs de Fribourg, Filière de chimie). The IR spectra were recorded as KBr pellets on a PerkinElmer Spectrum One FTIR instrument. ^{1}H, ^{13}C, and ^{31}P NMR spectra were recorded on Bruker AMX 400 MHz using CD_2Cl_2-d_2, DMSO-d_6, and CD_3OD-d_4 as solvent. The TMS was used as the internal standard.

Warning: Perchlorate salts are dangerous and should only be used in minimum quantities. Under the conditions used we encountered no problems.

Synthesis of $[Ag_2(P1)_2(L1)_4].(NO_3)_2.H_2O$ (1) :

$AgNO_3$ 0.017 g (0.1 mmol) was dissolved in mixture of acetonitrile/methanol (2:3) (20 ml) and **L1** 0.018 g (0.2 mmol) was added and was stirred mechanically for 1h at 50ºC. The reaction mixture was further treated with triphenyl phosphine (**P1**) 0.028 g (0.1 mmol) in 5 ml chloroform and stirring was continued for another 30 min. The second step results in solubilisation of the precipitates obtained in the first step. The colourless solution obtained was filtered to avoid any impurity and kept undisturbed for crystallization by slow evaporation at room temperature. After three days colourless block like crystals were obtained. A suitable crystal was chosen for X-ray diffraction analysis. Yield (0.054g) 88.37%. Anal. Calc.: C, 38.50; H, 4.17; N, 15.72; Found: C, 38.37; H, 4.13; N, 15.75. IR cm^{-1}: 3477(m), 3413(m), 3040(s), 1633(s), 1633(s), 1434(s), 1359(s), 1156(m), 1093(s), 997(ms), 827(m), 751(m), 695(s). ^1H NMR (400 MHz, CD_3OD-d_4): δ 7.3-7.5 (m, 5H, C_6H_5 of PPh_3), 7.9 (s, 1H, NH). ^{13}C NMR (400 MHz, CD_3OD-d_4): δ 180.43 (C=S), 130-140 (C_6H_5 of triphenyl phosphine). ^{31}P NMR (400 MHz, CD_3OD-d_4): δ 10.34 ppm (a sharp singlet for PPh_3).

Synthesis of $[Ag_2(P1)_2(L3)_4].(NO_3)_2$ (2):

The synthesis of silver(I) complex **2** was carried out by following the same procedure as described for complex **1**. Here 2-mecaptothiazoline (**L3**) was used instead of thiosemicarbazide (**L1**). Suitable crystals for X-ray diffraction studies were obtained by slow evaporation of the solvent of reaction at room temperature. The crystalline product was collected by filtration and air dried. Yield (0.056 g) 93.16%. Anal. Calc.: C, 42.95; H, 3.72; N, 6.26; Found: C, 42.85; H, 3.68; N, 6.31. IR cm^{-1}: 3472(m), 3411(m), 3031(s), 1640(s), 1619(s), 1445(s), 1370(s), 1148(m), 1082(s), 977(ms), 831(m), 744(m), 683(s). ^1H NMR (400 MHz, DMSO-d_6): δ 7.5 (m, 5H, Ph_3P), 3.97 (t, 2H, S-CH_2-CH_2), 3.53 (t, 2H, HN-CH_2-CH_2), 10.60 (s, NH). ^{13}C NMR (400 MHz, DMSO-d_6): δ 200.0 (C=S), 53.40 (S-CH2), 34.45 (N-CH2), 129.20 (C-P), 130-135 (5 peaks for phenyl group of triphenyl phosphine). ^{31}P NMR (400 MHz, DMSO-d_6): δ 10 ppm (single sharp peak).

Synthesis of $[Ag(P2)(L3)_2].(NO_3)$ (3):

$AgNO_3$, tricyclohexyl phosphine (**P2**), and 2-mercaptothiazoline (**L3**) in 1:1:2 molar ratio were used for the synthesis of complex **3** by following the same procedure as described for the synthesis of complexes **1** and **2**. The colourless block like crystals obtained were collected by filtration and air dried. A suitable crystal was used for single crystal X-ray diffraction studies. Yield (0.055 g) 88.85%. Anal. Calc.: C, 41.81; H, 6.24; N, 6.09; Found: C, 41.72; H, 6.29; N, 5.94. IR cm^{-1}: 3551(w), 3478(m), 3417(m), 3107(s), 2922(s), 2846(s), 1729(w), 1637(m), 1616(s), 1526(s) 1463(s), 1383(s), 1198(m), 1042(s), 928(ms), 851(m), 787(m), 651(s), 581(ms). ^{1}H NMR (400 MHz, CD_3OD-d_4): δ 1-2.5 (m, 11H, Cy_3P), 4.18 (t, 2H, S-CH_2-CH_2), 3.72 (t, 2H, HN-CH_2-CH_2). ^{13}C NMR (400 MHz, CD_3OD-d_4): δ 201.60 (C=S), 52.92 (S-CH2), 34.12 (N-CH2), 32.30 (C-P), 25-31 (8 overlapped peaks for CH_2 carbons of cyclohexyl group of tricyclohexyl phosphine). ^{31}P NMR (400 MHz, CD_3OD-d_4): δ 35-45 ppm (several broad resonances showing the possible existence of different species in solution).

Synthesis of $[Ag(P2)(L1)_2].PF_6$ (4):

$AgPF_6$ 0.025 g (0.1 mmol) was dissolved in acteonitrile (15 ml) and tricyclohexyl phosphine (**P2**) in (10 ml) chloroform was added. The reaction mixture was stirred continuously mechanically for 30 min at 30ºC. The clear solution obtained was further treated with thiosemicarbazide (**L1**) 0.018 g (0.2 mmol) in (10 ml) methanol. The reaction mixture was stirred for another 30 min at 50ºC. The colourless clear solution obtained was filtered to avoid any impurity and kept at room temperature for slow evaporation. After a couple of days block like crystals were obtained. A suitable crystal was used for X-ray diffraction studies. Yield (0.061 g) 85.67%. Anal. Calc.: C, 33.54; H, 6.00; N, 11.73; Found: C, 33.57; H, 6.11; N, 11.66. IR cm^{-1}: 3465(m), 3412(m), 3117(s), 2925(s), 2849(s), 1637(s), 1612(s), 1456(s), 1373(s), 1115(m), 1076(s), 981(ms), 812(m), 745(m), 697(s), 505(m). ^{1}H NMR (400 MHz, CD_3OD-d_4): δ 1-2 (m, 11H, cyclohexyl of tricyclohexyl phosphine), 8.58 (s, 1H, NH), 7.80, 8.90 (s, 2H, NH_2). ^{13}C NMR (400 MHz, CD_3OD-d_4): δ 179.72 (C=S), 25-35 (peaks for carbons of cyclohexyl group), while C-P peak is observed at the most down field position. ^{31}P NMR (400 MHz, CD_3OD-d_4): An intense peak at 56.45 ppm, which is 50 ppm down field compared to uncomplexed

tricyclohexyl phosphine (8 ppm). Another less intense peak is observed at 63.2 ppm, which is probably due to the formation of a silver(I) phosphine complex like $[Ag(Cy_3P)_2]^+$ in solution. A broad peak at 40 ppm suggests the equilibration between different species formed in the solution.

Synthesis of $\{[Ag(P3)_2(L2)]_2(NO_3)\}.NO_3$ (5):

$AgNO_3$, dicyclohexylphenyl phosphine (**P3**), and thiosemicarbazide (**L1**) in 1:2:1 stiochiometric molar ratio were used for the synthesis of complex **5** by following the same procedure as described for the synthesis of complexes **1**, **2** and **3**. After slow evaporation of the solvent of reaction a transparent glassy product sticking with the glass of the evaporation dish was obtained unexpectedly. To get suitable crystal for X-ray diffraction studies several attempts were made by using different solvents and combinations of solvents for re-crystallization. While using acetone and acetontrile (1:1) for crystallization of the product in situ transformation of **L1** to **L2** took place. Colourless block crystals obtained were collected and weighed. A suitable crystal was chosen for crystallographic studies. Yield (0.078 g) 92.13%. Anal. Calc.: C, 56.51; H, 7.41; N, 6.59; Found: C, 56.43; H, 7.48; N, 6.64. IR cm^{-1}: 3512(w), 3470(m), 3419(m), 3122(s), 2925(s), 2847(s), 1637(s), 1606(s),1541(m), 1466(s), 1376(s), 1125(m), 1098(s), 975(ms), 812(m), 754(m), 688(s), 515(m). ^1H NMR (400 MHz, CD_2Cl_2-d_2): δ 1-2.5 (m, 11H, Cyclohexyl of dicyclohexylphenyl phosphine), 7-8 (m, 5H, Ph of dicyclohexylphenyl phosphine), 1.96 and 2.03 (s, 3H, N=C-$(CH_3)_2$), 8.98 (s, 2H, NH_2), 11.62 (s, 1H, NH). ^{13}C NMR (400 MHz, CD_2Cl_2-d_2): δ 178.19 (C=S), 152.94 (C=N), 129.20 (C-P of phenyl group), 25-34 (8 peaks instead of four peaks for the carbons of the cyclohexyl group), 18-20 (methyl group bonded to the immine carbon). ^{31}P NMR (400 MHz, CD_2Cl_2-d_2): δ 21.52 ppm (a sharp single peak).

Synthesis of $[Ag_2(P2)_2(L3)_2].(PF_6)_2$ (6):

$AgPF_6$, tricyclohexyl phosphine (**P2**), and 2-mercaptothiazoline (**L3**) in 1:1:1 stoichiometric ratio were used to get silver(I) complex **6** by following the same procedure as described for the synthesis of complex **4**. The clear solution obtained was filtered to

avoid any impurity and kept undisturbed for crystallization by slow evaporation at room temperature. After 4 days colourless block crystals were obtained. A suitable crystal was chosen for X-ray diffraction studies. Yield (0.049 g) 79.03%. Anal. Calc.: C, 38.62; H, 5.82; N, 2.14; Found: C, 38.55; H, 5.81; N, 2.17. IR cm^{-1}: 3517(w), 3460(m), 3417(m), 3125(s), 2925(s), 2843(s), 1633(s), 1615(s),1544(m), 1454(s), 1368(s), 1135(m), 1091(s), 984(ms), 813(m), 759(m), 676(s), 525(m). ^{1}H NMR (400 MHz, CD_3OD-d_4): δ 1-2.5 (m, 11H, cyclohexyl of tricyclohexyl phosphine), 4.18 (t, 2H, S-CH_2-CH_2), 3.72 (t, 2H, HN-CH_2-CH_2), 7.6 (s, 1H, NH). ^{13}C NMR (400 MHz, CD_3OD-d_4): δ 201.55 (C=S), 53.81 (S-CH_2), 34.71 (N-CH_2), 32.08 (C-P), 25-35 (8 peaks for carbons of cyclohexyl group). ^{31}P NMR (400 MHz, CD_3OD-d_4): Several broad resonances are observed in the region of 35-45 ppm, showing the possibility of the existence of different species in solution.

Synthesis of $[Ag_2(P4)_2(L2)_2].(ClO_4)_2$ (7):

$AgClO_4$, diphenylcyclohexyl phosphine (**P4**), and thiosemicarbazide (**L1**) in 1:1:1 stiochiometric molar ratio were used for the synthesis of complex **7** by following the same procedure as described for the synthesis of complex **1-3** but 5ml acetone was used at the start of reaction during the process of stirring for in situ synthesis of ligand **L2**. The clear solution obtained was filtered to avoid any impurity and kept undisturbed for crystallization by slow evaporation at room temperature. After 4 days colourless block crystals were obtained. A suitable crystal was chosen for X-ray diffraction studies. Yield (0.057 g) 93.92%. Anal. Calc.: C, 43.50; H, 4.94; N, 6.92; Found: C, 43.57; H, 5.03; N, 6.98. IR cm^{-1}: 3517(w), 3472(m), 3416(m), 3127(s), 2928(s), 2841(s), 1633(s), 1605(s),1543(m), 1456(s), 1374(s), 1128(m), 1088(s), 979(ms), 810(m), 764(m), 677(s), 505(m). ^{1}H NMR (400 MHz, DMSO-d_6): δ 1-3 (m, 11H, cyclohexyl group of diphenycyclohexyl phosphine), 7-8 (m, 5H, phenyl group of diphenylcyclohexyl phosphine), 1.8-2 (s, 3H, $(CH_3)_2$-C=N), 8.5 (s, NH), 11.0 (s, NH_2). ^{13}C NMR (400 MHz, DMSO-d_6): δ 25-35 (8 peaks for cyclohexyl carbons of diphenylcyclohexyl phosphine), 129-135 (5 peaks for phenyl group of diphenylcyclohexyl phosphine), 131.88 and 34.37 (C-P for phenyl and cyclohexyl carbon bonded to phosphorous respectively), 179.45 and 175.10 (C=S), 159.90 and 157.39 (C=N), 18-20 (N=C-$(CH_3)_2$). ^{31}P NMR (400 MHz, DMSO-d_6): 33.33 ppm, for the presence of Ph_2CyP moiety in the complex, while another

broad band is detected at 21.41 ppm, which indicates some kind of exchange process is occurring in solution.

Synthesis of $[Ag(P5)_2(L2)(Br)]$ (8):

A mixture of AgBr 0.018g (0.1 mmol), diphenyl(p-tolyl) phosphine (**P5**) 0.028 g (0.1 mmol) and thiosemicarbazide (**L1**) 0.018 g (0.2 mmol) in 20 ml of acetone/methanol (1:1) was refluxed with continuous mechanical stirring for overnight at 70ºC. The light yellow transparent solution obtained was filtered to avoid any impurity in the crystallization dish and 3ml distilled water was also added as solvent of crystallization. After few days huge amount of colourless block crystals were obtained in the solvent. Again in situ transformation of **L1** to **L2** took place. The crystalline product was collected by filtration and air dried. A suitable crystal was chosen for single crystal X-ray studies. Yield (0.078 g) 89.31%. Anal. Calc.: C, 57.82; H, 4.93; N, 4.81; Found: C, 57.82; H, 4.93; N, 4.81. IR cm^{-1}: 3531(w), 3479(m), 3413(m), 3119(s), 2926(s), 2842(s), 1633(s), 1608(s),1546(m), 1456(s), 1384(s), 1148(m), 1058(s), 989(ms), 819(m), 767(m), 666(s), 521(m). ^1H NMR (400 MHz, DMSO-d_6): δ 7.1-7.5 (m, phosphine protons), 8.34 (s, 2H, NH_2), 10.13 (s, 1H, NH), 1.8-2.0 (s, 3H, N=C-$(CH_3)_2$). ^{13}C NMR (400 MHz, DMSO-d_6): δ 177.70 (C=S), 154.15 (N=C), 25.90 and 18.97 (N=C$(CH_3)_2$), 21.97 (CH_3-resonance of p-tolyl), 124-141 (signals for aromatic and phenyl groups carbon), 134.35 and 130.25 (C-P resonances of phenyl and p-tolyl groups). ^{31}P NMR (400 MHz, DMSO-d_6): δ 2.40 ppm (a sharp single peak).

Synthesis of $[Ag_2(P1)_2(L2)_2].(NO_3)_2$ (9):

The synthesis of silver(I) complex **9** was done by simply dissolving complex **1** in acetone/methanol (1:2) by gentle heating. The in situ condensation reaction took place in the presence of acetone and **L1** was converted to **L2**. The clear solution obtained was filtered and kept undisturbed for re-crystallization at room temperature. After few days block type colourless crystals were obtained. A suitable crystal was chosen for X-ray diffraction analysis. Yield (0.038 g) 67.63%. Anal. Calc.: C, 46.86; H, 4.26; N, 9.94; Found: C, 46.78; H, 4.19; N, 9.89. IR cm^{-1}: 3472(m), 3411(m), 3031(s), 1640(s), 1603(s),

1435(s), 1362(s), 1141(m), 1085(s), 967(ms), 832(m), 745(m), 683(s), 501(m). ^{1}H NMR (400 MHz, DMSO-d_6): δ 7-8 (m, 5H, phenyl group of triphenyl phosphine), 1.8-2 (d, 3H, $(CH_3)_2$-C=N), 8.2 (s, NH), 10.2 (s, NH_2), 10.45 (s, H_2O). ^{13}C NMR (400 MHz, DMSO-d_6): δ 129-135 (5 peaks for phenyl group of diphenylcyclohexyl phosphine), 131.88 (C-P), 176.79 (C=S), 155.35 (C=N), 18-20 (N=C-$(CH_3)_2$). ^{31}P NMR (400 MHz, DMSO-d_6): 8.12 ppm (a sharp single peak).

Synthesis of $[Ag(P4)_2(L2)].NO_3$ (10)

$AgNO_3$, diphenylcyclohexyl phosphine (**P4**), and thiosemicarbazide (**L1**) in 1:2:1 stiochiometric molar ratio were used for the synthesis of complex **10** by following the same procedure as described for the synthesis of complex **8**. Suitable crystals for X-ray diffraction analysis were obtained by slow evaporation of the solvent of reaction at room temperature. Again in situ condensation reaction took place in the presence of acetone and **L1** was converted to **L2.** The crystalline product was collected by filtration and air dried. Yield (0.067 g) 82.21%. Anal. Calc.: C, 57.29; H, 6.08; N, 6.68; Found: C, 57.21; H, 6.03; N, 6.69. IR cm^{-1}: 3519(w), 3476(m), 3419(m), 3122(s), 2925(s), 2846(s), 1633(s), 1605(s),1547(m), 1446(s), 1378(s), 1138(m), 1085(s), 982(ms), 813(m), 764(m), 676(s), 501(m). ^{1}H NMR (400 MHz, DMSO-d_6): δ 1-3 (m, 11H, cyclohexyl group of diphenycyclohexyl phosphine), 7-8 (m, 5H, phenyl group of diphenylcyclohexyl phosphine), 1.8-2 (s, 3H, $(CH_3)_2$-C=N), 8.7 (s, NH), 11.2 (s, NH_2). ^{13}C NMR (400 MHz, DMSO-d_6): δ 25-35 (8 peaks for cyclohexyl carbons of diphenylcyclohexyl phosphine), 128-134 (5 peaks for phenyl group of diphenylcyclohexyl phosphine), 130.90 and 36.47 (C-P for phenyl and cyclohexyl carbon bonded to phosphorous respectively), 181.60 and 178.30 (C=S), 162.70 and 159.46 (C=N), 18-20 (N=C-$(CH_3)_2$). ^{31}P NMR (400 MHz, DMSO-d_6): 34.45 ppm, for the presence of Ph_2CyP moiety in the complex, while another broad band is detected at 22.35 ppm which indicates some kind of exchange process is occurring in the solution.

X-ray Crystallography.

The intensity data were collected at 173K on either, a one circle (ϕ scans)[1], or a two circle (ω and ϕ scans)[2] Stoe Image Plate Diffraction System, using MoKα graphite

monochromated radiation. The structures were solved by Direct methods using the program SHELXS-97[3]. The refinement and all further calculations were carried out using SHELXL-97[3]. The H-atoms were either located from Fourier difference maps and freely refined or included in calculated positions and treated as riding atoms using SHELXL default parameters. The non-H atoms were refined anisotropically, using weighted full-matrix least-squares on F^2. In most cases multi-scan absorption corrections were applied using the MULscanABS routine in PLATON[4]. A summary of crystal data and refinement details for compounds **1-10** are given in Table 1, and selected bond lengths and angles are listed in Table 2. Details of the hydrogen bonding are given in Table 3.

1) Stoe and Cie (2000) IPDS-I Bedienungshandbuch. Stoe and Cie GmbH, Darmstadt, Germany.

2) Stoe and Cie. (2006) *X-Area V1.35 and X-RED32 V1.31 Software*. Stoe and Cie GmbH, Darmstadt, Germany.

3) G. M. Sheldrick (2008). Acta Crystallgr. A64, 112-122.

4) A. L. Spek (2003). J. Appl. Cryst. 36, 7-13

Results and Discussions

Ten silver(I) complexes with 1:1:2, 1:1:1 and 1:2:1 (Ag:phospine:ligand) compositions $[Ag_2(P1)_2(L1)_4].(NO_3)_2.H_2O$ (**1**), $[Ag_2(P1)_2(L3)_4].(NO_3)_2$ (**2**), $[Ag(P2)(L3)_2].NO_3$ (**3**), $[Ag(P2)(L1)_2].PF_6$ (**4**), $\{[Ag(P3)_2(L2)]_2(NO_3)\}.NO_3$ **(5)**, $[Ag_2(P2)_2(L3)_2].(PF_6)_2$ (**6**), $[Ag_2(P4)_2(L2)_2].(ClO_4)_2$ **(7)**, $[Ag(P5)_2(L2)(Br)]$ (**8**), $[Ag_2(P1)_2(L2)_2].(NO_3)_2$ (**9**), and $[Ag(P4)_2(L2)].NO_3$ (**10**):

For the definitions of the phospine ligands **P1–P5** see **Scheme 1**, for the ligands **L1–L3** see **Scheme 2.**

Table 1. Summary of crystallographic data and refinement details for complexes **1-10**.

{ [a] $R1 = \Sigma||F_O| - |F_C||/\Sigma|F_O|$. [b] $wR2 = [\Sigma w(F_O^2 - F_C^2)^2/\Sigma wF_O^4]^{1/2}$ }

	1	**2**	**3**
Formula	$C_{40}H_{52}Ag_2N_{14}O_7P_2S_4$	$C_{48}H_{50}Ag_2N_6O_6P_2S_8$	$C_{24}H_{43}AgN_3O_3PS_4$
Formula weight	1246.60	1341.18	688.73
Crystal system	Monoclinic	Monoclinic	Monoclinic
Space group	P 2_1/c	P 2_1/c	P 2_1/c
a,Å	9.2126(5)	9.3390(5)	8.7768(6)
b,Å	15.2611(11)	14.5894(7)	36.003(3)
c,Å	17.9972(9)	19.4323(11)	9.7321(6)
α,deg	90	90	90
β,deg	94.993(4)	95.794(4)	95.439(5)
γ,deg	90	90	90
V, Å^3	2520.7(3)	2634.1(2)	3061.4(4)
Z	2	2	4
$D_{calcd,}$ g cm^{-3}	1.643	1.691	1.494
μ, mm^{-1}	1.068	1.176	1.014
R1,[a] [$I > 2\sigma(I)$]	0.0286	0.0367	0.0284
wR2,[b] [$I > 2\sigma(I)$]	0.0742	0.0824	0.0545
GOF	1.042	1.038	1.000

Table 1 cont'd

	4	**5**	**6**
Formula	$C_{20}H_{43}AgF_6N_6P_2S_2$	$C_{80}H_{126}Ag_2N_8O_6P_4S_2$	$C_{42}H_{74}Ag_2F_{12}N2P_4S_4$
Formula weight	715.55	1699.45	1302.93
Crystal system	Monoclinic	Triclinic	Triclinic
Space group	P 2_1	P -1	P -1
a,Å	8.7316(8)	11.7464(18)	8.5777(9)
b,Å	38.147(3)	12.922(2)	12.6937(13)
c,Å	9.6416(9)	15.895(3)	13.9993(13)
α,deg	90	68.857(12)	66.757(7)
β,deg	113.736(7)	69.997(12)	71.507(7)
γ,deg	90	88.422(13)	85.275(8)
V, Å^3	2939.8(4)	2101.8(6)	1326.6(2)
Z	4	1	1
$D_{calcd,}$ g cm^{-3}	1.617	1.343	1.633
μ, mm^{-1}	0.997	0.646	1.091
R1,[a] [$I > 2\sigma(I)$]	0.0547	0.038	0.0731
wR2,[b][$I > 2\sigma(I)$]	0.1309	0.649	0.1938
GOF	0.969	0.881	1.014

Table 1 cont'd

	7	**8**
Formula	$C_{44}H_{60}Ag_2Cl_2N_6O_8P_2S_2$	$C_{42}H_{43}AgBrN_3P_2S$
Formula weight	1213.70	871.57
Crystal system	Triclinic	Triclinic
Space group	P -1	P -1
a,Å	9.9431(9)	10.915(4)
b,Å	12.3088(12)	13.292(7)
c,Å	12.5035(12)	16.129(6)
α,deg	74.074(7)	69.53(3)
β,deg	69.365(7)	80.45(3)
γ,deg	65.626(7)	66.16(4)
V, $Å^3$	1289.4(2)	2004.4(15)
Z	1	2
$D_{calcd,}$ g cm^{-3}	1.563	1.444
μ, mm^{-1}	1.061	1.664
R1,[a] [$I > 2\sigma(I)$]	0.0614	0.0498
wR2,[b] [$I > 2\sigma(I)$]	0.1502	0.0903
GOF	0.924	0.681

Table 1 cont'd

	9	**10**
Formula	$C_{44}H_{48}Ag_2N_8O_6P_2S_2$	$C_{40}H_{51}AgN_4O_3P_2S$
Formula weight	1126.72	837.72
Crystal system	Triclinic	Triclinic
Space group	P -1	P -1
a,Å	9.8495(6)	11.6412(10)
b,Å	11.8208(7)	12.6009(11)
c,Å	12.5180(7)	13.9573(12)
α,deg	72.480(5)	98.163(7)
β,deg	68.290(4)	97.029(7)
γ,deg	66.644(4)	91.435(7)
V, Å^3	1222.59(12)	2009.5(3)
Z	1	2
$D_{calcd,}$ g cm^{-3}	1.530	1.384
μ, mm^{-1}	1.005	0.675
R1,[a] [$I > 2\sigma(I)$]	0.0222	0.0441
wR2,[b] [$I > 2\sigma(I)$]	0.054	0.1145
GOF	1.028	0.981

$[Ag_2(P1)_2(L1)_4].(NO_3)_2.H_2O$ (1):

The molecular structure of silver(I) complex **1** is depicted in Fig. **1a**. Complex **1** is a centrosymmetric dimer molecule with $[Ag(P1)(L1)_2]^+$ units bridged by thiosemicarbazide ligand molecules, as shown in the Fig. **1a**. The crystallographic environment around the silver(I) atom is pseudo-tetrahedral. The central metal atom is surrounded by three S donor atoms of the thiosemicarbzide (**L1**) ligand molecules, (one mono-coordinated and two bridging ligands) and one P atom of the triphenyl phosphine (**P1**) ligand molecule.

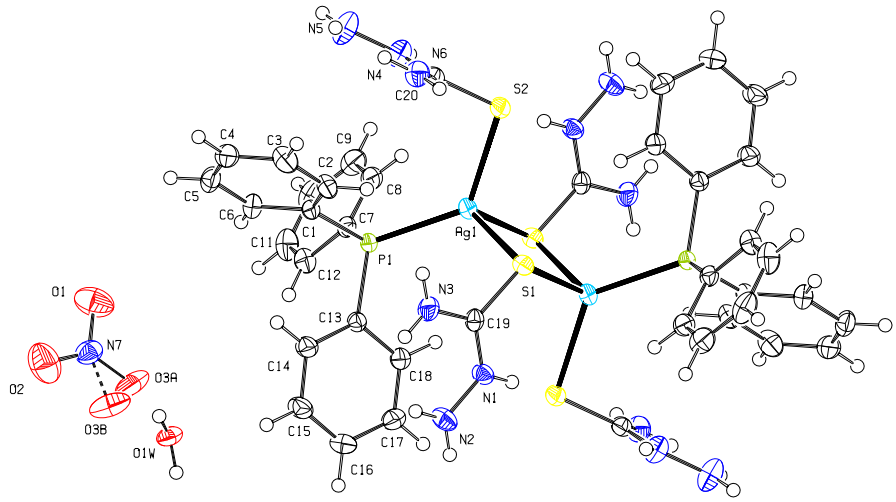

Figure 1a. A view of the molecular structure of compound **1** with complete atom labelling scheme and displacement ellipsoids drawn at the 50% probability level (only one disordered anion and one water molecule of crystallization are shown).

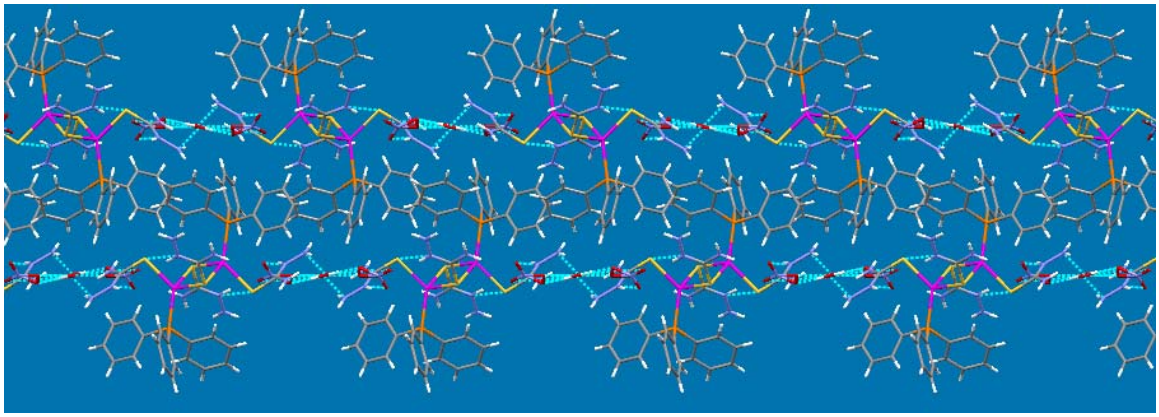

Figure 1b. View of the hydrogen bonded polymeric chain complex **1** along a-axis. The dotted blue lines show intra- and inter-molecular hydrogen bonding interactions.

The S-Ag-S bond angles are 93.56(2), 101.26(2), and 108.60(2)º. Whereas the S-Ag-P bond angles are 105.95(2), 115.79(2) and 128.43(2)º. The Ag-S bond length distances vary from 2.5403(6) to 2.6683(5) Å, whereas the Ag-P bond length is 2.4276(4) Å. In this dimer complex molecule Ag…Ag distance is 3.3566(4) Å, which is greater than the Ag-Ag distance of 2.88 Å present in metallic silver. The presence of nitrate counter ions, water lattice molecules and thiosemicarbazide(**L1**) ligand containing -NH and -NH_2

groups facilitate hydrogen bonds formation in the solid state of complex **1**. These weak inter- and intra-molecular hydrogen bond interactions result two-dimensional polymeric chain structure of complex **1** as shown in the Fig. **1b**.

$[Ag_2(P1)_2(L3)_4].(NO_3)_2$ (2):

The single crystal structure of silver(I) complex **2** is shown in Fig. **2a** and exists as a centrosymmetric dimer molecule as complex **1**. The geometrical environment around the Ag(I) atom is pseudo-tetrahedral, again similar to complex **1**.

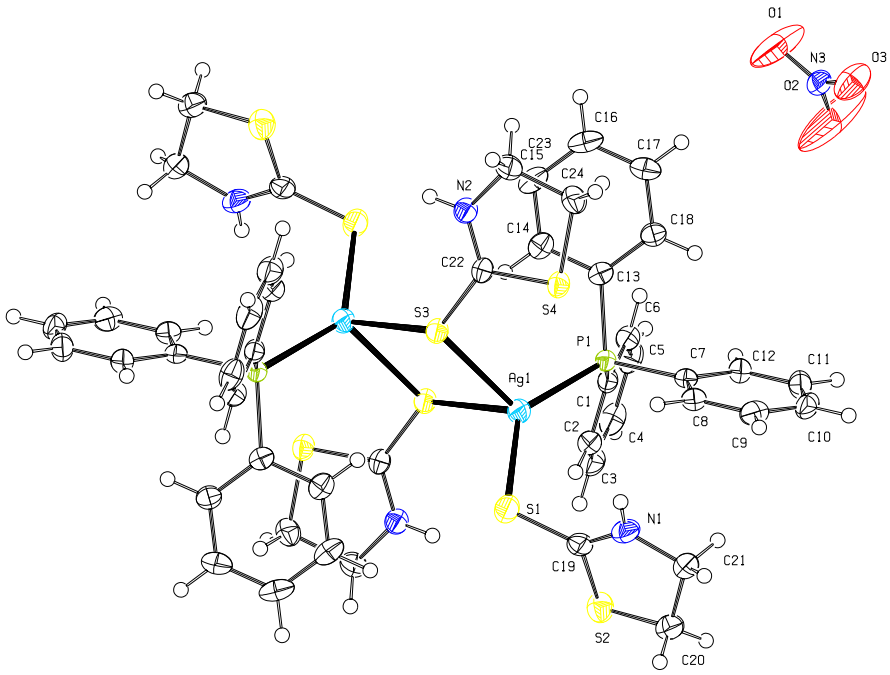

Figure 2a. A view of the molecular structure of compound **2** with complete atom labelling scheme and displacement ellipsoids drawn at the 50% probability level (only one anion is shown).

The Ag(I) atom in the complex **2** is surrounded by three S donor atom from **L3** (thiazolidine-2-thione) ligand and one P donor atom of the triphenyl phosphine (**P1**) ligand molecules. The Ag-S bond distances range from 2.4813(10) to 2.8049(9) Å. Whereas, the Ag-P bond length is 2.4268(8) Å. The bond angles around the silver(I) atom for S-Ag-S vary from 78.52(3) to 112.94º. Whereas, S-Ag-P bond angles range from

97.31(3) to 135.80(3)º. The counter ion (NO_3^-) does not show coordination with the metal centre like, complex **1**. The nitrate ion and ligand **L3** play prominent role in hydrogen bond formation in the solid state structure of complex **2** and result one-dimensional hydrogen bonded polymeric chain structure of complex **2** as shown in the Fig. **2b**.

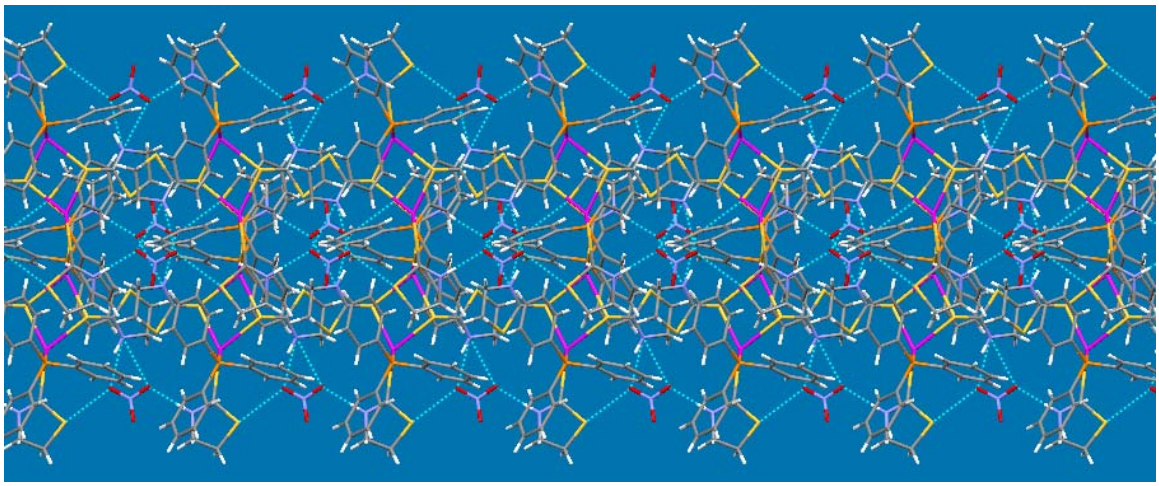

Figure 2b. View of hydrogen bonded polymeric structure of complex **2** along *c* axis. The dotted blue lines show the inter-molecular hydrogen bonding interactions.

[Ag(P2)(L3)$_2$].(NO_3) (3):

The molecular structure of silver(I) complex **3** is shown in Fig. **3a**, with complete atom labelling scheme. The crystal structure of complex **6** does not exists in the dimer form like complexes **1** and **2**. The geometry around Ag(I) atom in complex **3** is distorted trigonal planar. The S-Ag-P bond angles are 109.83(2) and 120.75(3)º and bond angle S-Ag-S is 123.70(2)º. These bond angle values show considerable deviation from the ideal trigonal planar angle of 120º. The Ag-S bond distances vary between 2.5405(8) and 2.5540(8) Å, and bond distance Ag-P is 2.4228(7) Å. The counter ion (NO_3^-) does not show any coordination to the metal centre like complex **1** and **2**. The counter ion and ligand molecule, as in complex **2,** play a major role in non-covalent bond (hydrogen bond) formation and result in the formation of a one-dimensional polymeric chain structure.

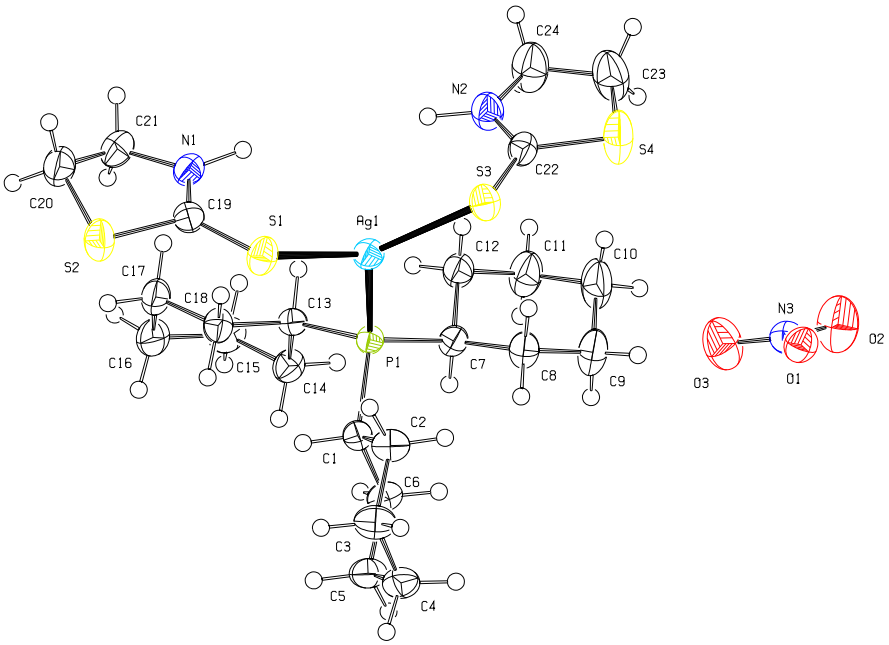

Figure 3a. View of the molecular structure of **3** with complete atom labelling scheme and displacement ellipsoids drawn at the 50% probability level.

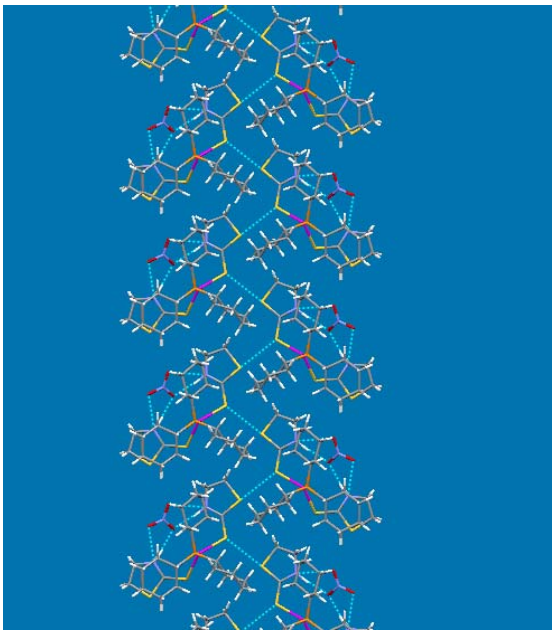

Figure 3b. View of the hydrogen bonded polymeric chain structure of complex **3**.

$[Ag(P2)(L1)_2].PF_6$ (4):

The view of the molecular structure of complex **4** is shown in Fig. **4**, with complete atom labelling scheme. The single crystal structure consists of two independent molecules per asymmetric unit (molecules **1** and **2**) with the same geometrical environments around the silver(I) atoms but slightly different bond lengths and bond angles. The geometry around each silver(I) atom is triangular planar and the central metal atom is surrounded by two S donor atoms of **L1** two ligand molecules and one P donor atom of tricyclohexyl phosphine (**P2**). The Ag-S bond lengths for molecule **1** (around Ag1) and molecule **2** (around Ag2) are 2.471(2) & 2.517(2) and 2.509(2) & 2.530(3) Å, respectively. The Ag-P bond distances are 2.3997(18) and 2.3857(18) Å for molecule **1** and molecule **2**, respectively. The S-Ag-S bond angles around atom Ag1 and Ag2 are 115.96(4) and 103.48(4)º, and for the S-Ag-P bond angle values are 112.15(7) & 131.32(7) and 124.72(6) & 131.68(7)º, respectively. These bond angle values again show considerable deviation from the ideal triangular planar angle of 120º. The presence of PF_6^- anions in complex **4** results in quenching of intermolecular and intramolecular hydrogen bond formation and no polymeric chain structure is observed here. Hence the presence of hydrogen bond interactions in complexes **1-3** is attributed to the presence of nitrate counter ions in these complexes.

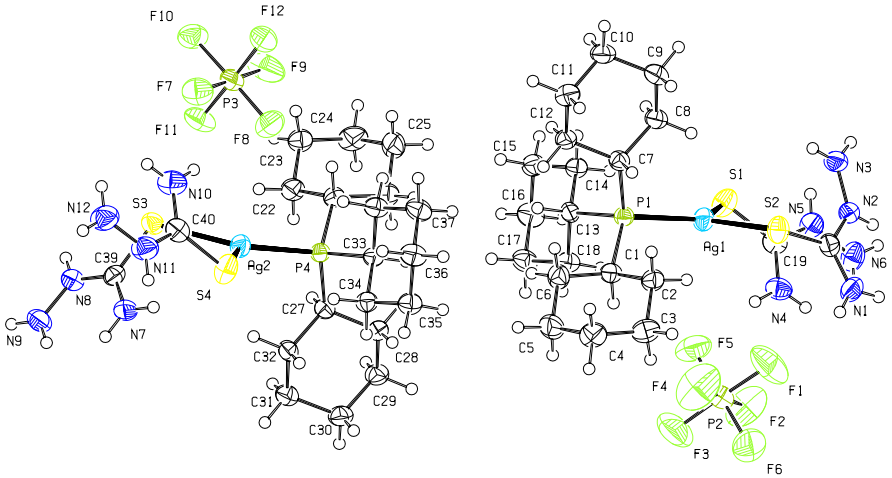

Molecule 2 (Ag2) **Molecule 1 (Ag1)**

Figure 4. Ortep view of the molecular structure of complex **4** with complete atom labelling scheme and displacement ellipsoids drawn at the 50% probability level.

$[Ag(P3)_2(L2)]_2(NO_3)\}.NO_3$ (5):

The molecular structure of complex **5** is depicted in Fig. **5a**. Complex **5** exists as a centrosymmetric dimer and the environment around each silver(I) atom is pseudo-tetrahedral. Complex **5** is different than the other dimer complexes **1** and **2**. Here there are two fragments of the dimer molecule bridged by one of the two disordered nitrate anions, unlike the situation in complexes **1** and **2**. The silver(I) atom is coordinated with two tertiary phosphine (**P3**) monodentate ligand molecules and one **L2** ligand molecule. One cyclohexyl ring of one of the tertiary phosphine ligand is also disordered. The presence of the nitrate anions and ligand **L2** facilitate hydrogen bond formation in the solid state and result in the formation of a one-dimensional polymeric undulating chain structure. The Ag-S bond distance is 2.600(1) Å, the Ag-P bond distances are 2.4501(11) and 2.4365(11) Å, and the Ag-O bond distances are 2.589(6) and 2.652(8) Å (Table **2**).

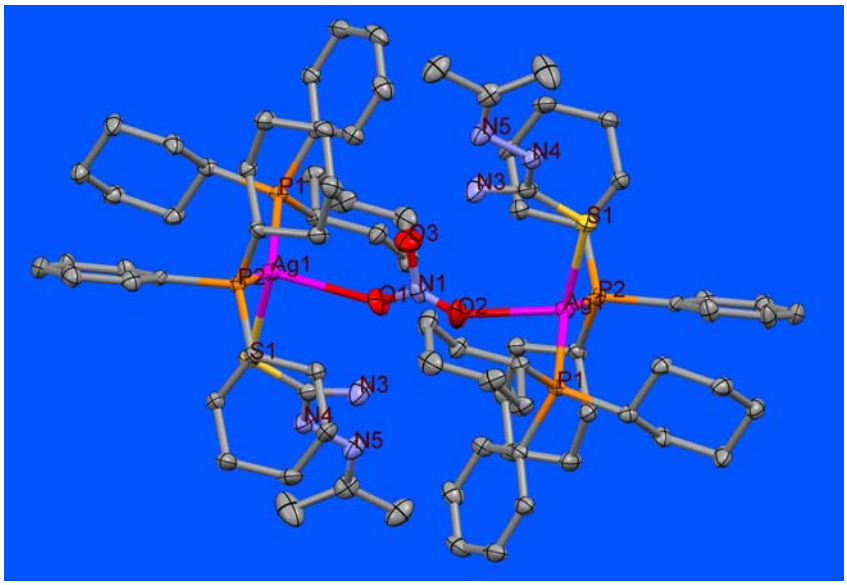

Figure 5a. A view of the molecular structure of complex **5** (the second disordered nitrate anion and the hydrogen atoms have been omitted for the clarity) with partial atom labelling scheme and displacement ellipsoids drawn at the 50% probability level.

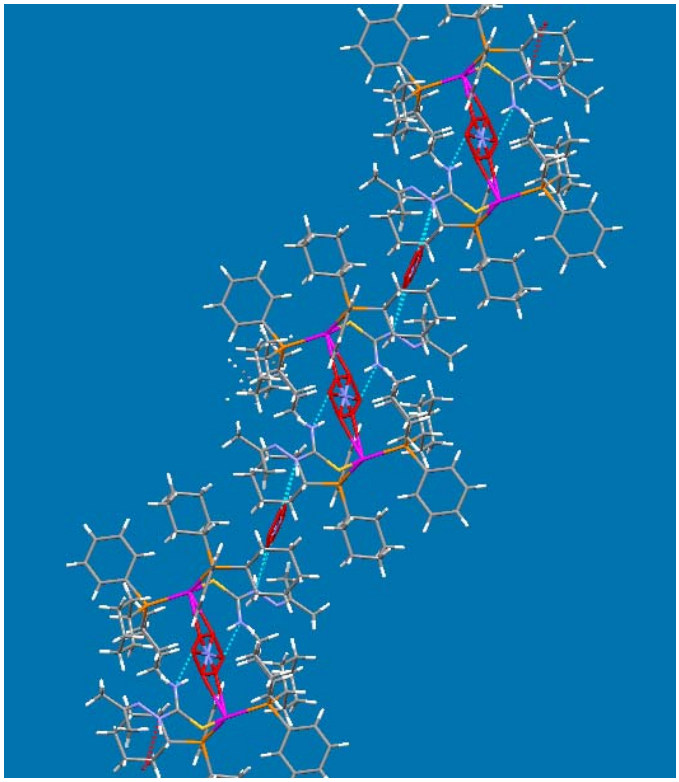

Figure 5b. A view of the hydrogen bonded polymeric chain structure of complex **5**.

The P-Ag-S bond angles are 100.71(4) and 113.96(4)º and bond angle P1-Ag-P2 is 137.93(4)º. Whereas, the O-Ag-S, and P-Ag-O bond angles values range from 91.31(16)–114.8(2)º, and 88.8(2)–101.63(15)º, respectively. These bond angles values provide extra evidence of pseudo-tetrahedral geometry around the silver(I) ions in complex **5**. However, they show considerable deviation from the ideal tetrahedral angle of 109.5º.

$[Ag_2(P2)_2(L3)_2].(PF_6)_2$ (6):

The molecular structure of silver(I) complex **6** is depicted in Fig. **6**, with complete atom labelling Scheme. The silver(I) complex **6** exists in dimer form like complexes **1** and **2**. The crystallographic environment around silver(I) atom in complex **6** is triangular planar unlike to complexes **1** and **2**. The crystallographic C_2 symmetry is present in complex **6** and each silver(I) atom in the dimer molecule has same geometry and other geometric parameters. Each silver(I) atom is coordinated with two **L3** (thiazolidine-2-thione) ligand molecules and one phosphine (P2) molecule. Both **L3** (thiazolidine-2-thione) ligand molecules act as bridging ligands in this silver(I) complex **6.** The Ag-P bond length is

2.3725(11) Å and the Ag-S bond distances are 2.4421(12) and 2.8526(13) Å. Whereas, the bond angles Ag-S-Ag is 97.93(4) º and S-Ag-S is 82.07(4)º, and the S-Ag-P are 121.63(4) and 155.36(4)º. These bond angles values show much deviation from the ideal triangular planar angle of 120º and confirm the presence of a distorted triangular planar geometry around the silver(I) ions in this dimer complex molecule. Moreover, no classical hydrogen bonding forces are observed in complex **6** unlike complexes **1-3** and **5**. The absence of hydrogen bonding interactions in complex **6** is due to PF_6^- counter ion.

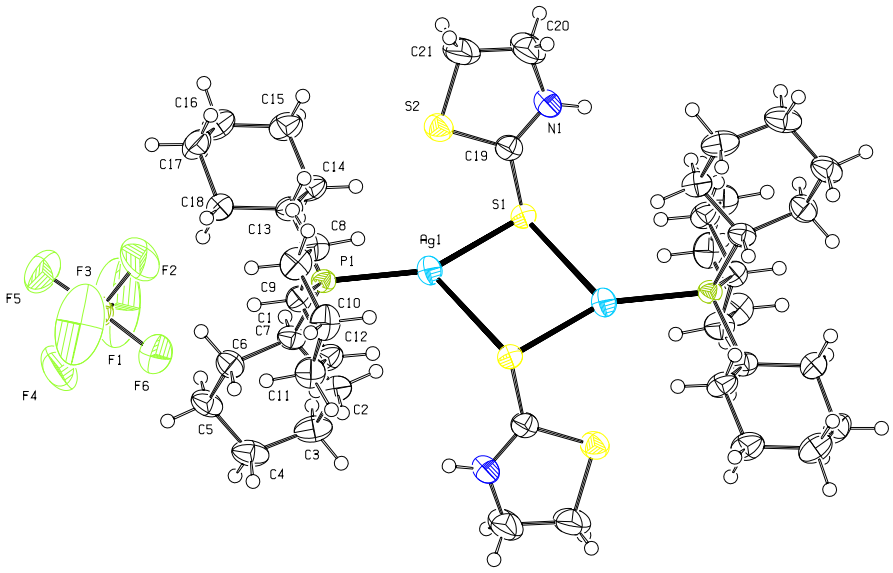

Figure 6. Aview of the molecular structure of dimer complex **6** with complete atom labelling scheme and displacement ellipsoids drawn at the 50% probability level (only one anion is shown).

$[Ag_2(P4)_2(L2)_2].(ClO_4)_2$ (7):

The view of the molecular structure of silver(I) complex **7** is depicted in Fig. **7a**, with complete atom labelling Scheme. Complex **7** also exists in the dimer form in the solid state like complexes **1**, **2, 5** and **9**. The crystallographic C_2 symmetry is also present complex **4** as in complexes **1**, **2**, **5** and **9**. The geometry around each silver(I) atom in this dimer molecule of complex **7** is distorted tetrahedral and each Ag(I) atom is surrounded by two S and one N and one P donor atoms from three ligand molecules. The **L2** ligand molecule coordinates with the silver(I) atom through S and N donor atoms, acts as a bidentate bridging ligand. The presence of ClO_4^- counter ions facilitate the hydrogen

bond formation in complex **7** like complexes **1**-**3** and **5**. These inter- and intra-molecular weak bond forces result the one-dimensional polymeric chain structure of complex **7** as shown in the Fig. **7b**.

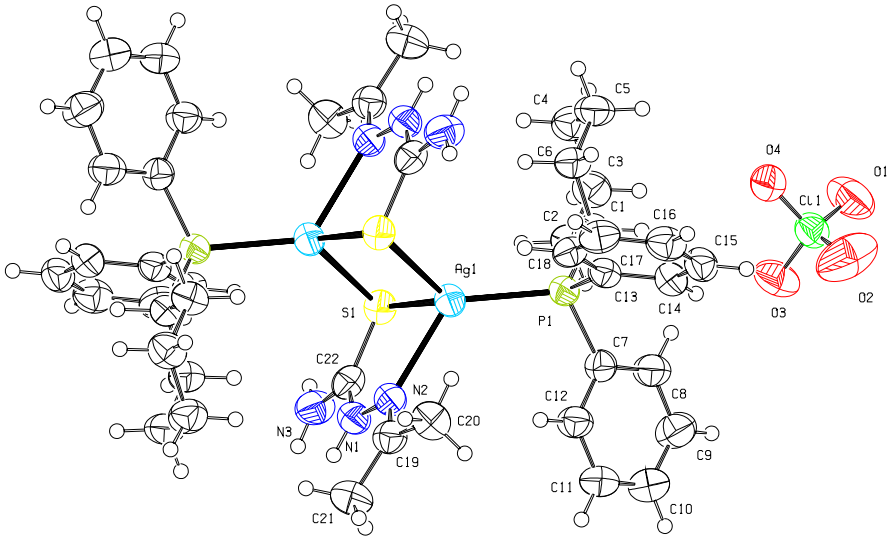

Figure 7a. A view of the molecular structure of compound **7** with complete atom labelling scheme and displacement ellipsoids drawn at the 50% probability level (only one anion is shown).

In complex **7**, the Ag-S, Ag-N, and Ag-P bond distances are 2.5766(13), 2.6792(16), 2.419(4), and 2.3850(14) Å, respectively. The S-Ag-S and S-Ag-P bond angles are 104.65(5), and 123.91(5) and 120.62(4)º respectively. Whereas, the N-Ag-P and S-Ag-N bond angles are 125.75(12), and 75.73(11) and 95.62(13)º respectively. In this dimer molecule of complex **7**, the Ag-Ag distance is 3.2133(6) Å. The Ag-Ag distance in complex **7** is less than complex **1** and greater than free silver metal.

In the crystal structure of complex **7**; symmetry related molecules are linked via N-H…O hydrogen bonds involving the perchlorate anions.

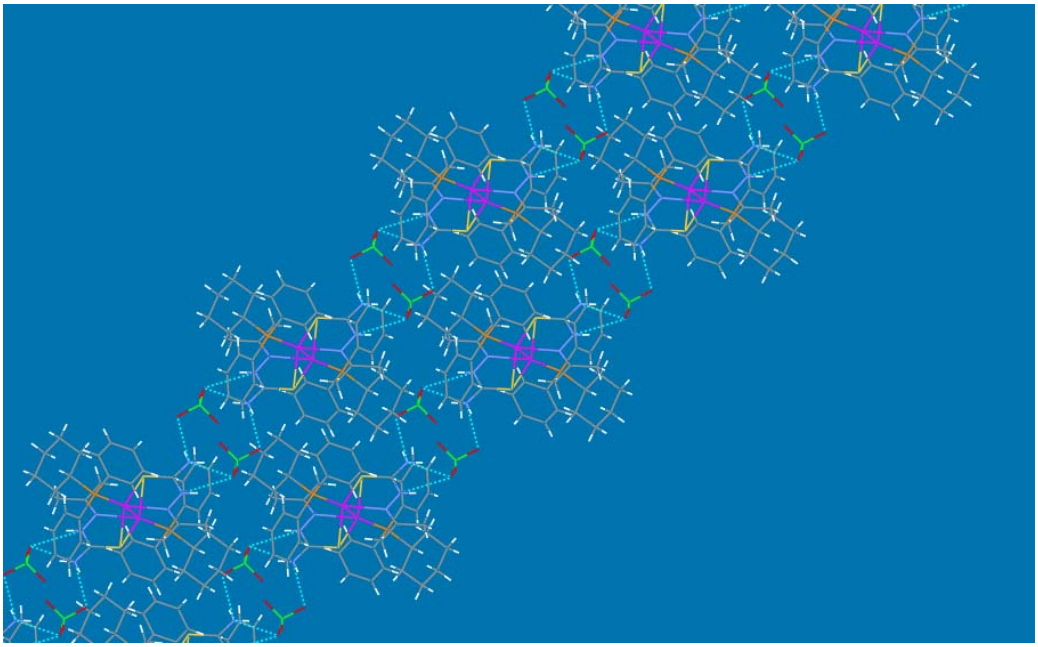

Figure 7b. Pattern showing hydrogen bonded polymeric chain structure of **7** and with blue dotted lines for hydrogen bonds.

[Ag(P5)$_2$(L2)(Br)] (8):

The molecular structure of silver(I) complex **8** is shown in Fig. **8a**. The complex molecule exists in a monomer form, like complexes **4** and **10**. The geometrical environment around the silver(I) centre is pseudo tetrahedral as that found in complexes **1**, **2, 7** and **9**. In complex **8**, silver(I) atom is coordinated with two P donor atoms of tertiary phosphine ligand molecules, one S donor atom of ligand **L2** and one Br atom acting as a counter ion. The Ag-S and Ag-Br bond distances are 2.580(3) and 2.663(2) Å, respectively, and the Ag-P bond distances are 2.496(3) and 2.473(3) Å. The P-Ag-P and Br-Ag-S bond angles are 120.61(12) and 108.47(10)º. The S-Ag-P bond angles are 102.07(11) and 109.30(11)º, and the Br-Ag-P bond angles are 104.76(10) and 111.24(10)º. These bond angles values show considerable deviations from the ideal tetrahedral angle of 109.5º.

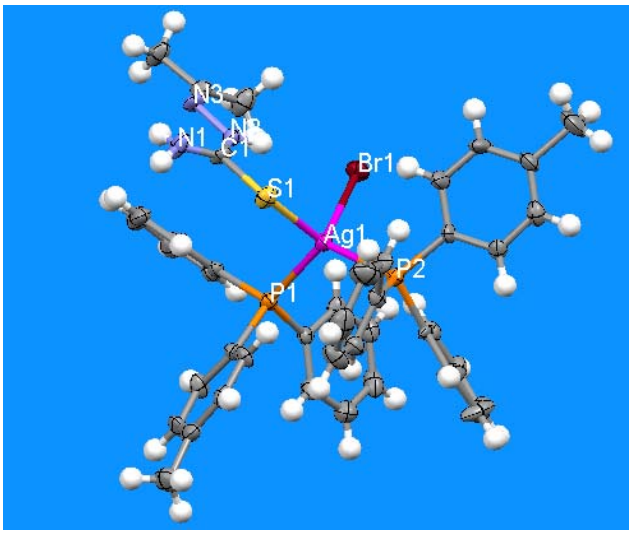

Figure 8a. View of the molecular structure of complex **8**.

In the crystal structure of complex **8** N-H…S hydrogen bonding leads to the formation of centrosymmetric dimers (see Fig. **8b** and Table **3**).

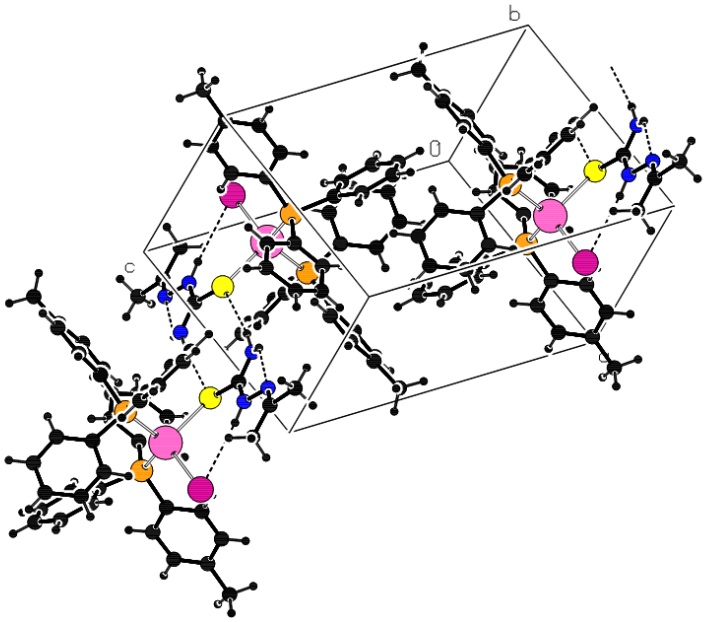

Figure 8b. Panel is showing the presence of the intramolecular N-H…N and N-H…Br hydrogen bonds and the intermolecular N-H…S hydrogen bonding interaction in complex **8**.

$[Ag_2(P1)_2(L2)_2].(NO_3)_2$ (9):

The molecular structure of silver(I) complex **9** is shown in Fig. **9a**. The geometry around the Ag(I) atom in this dimer complex is pseudo-tetrahedral. Each silver(I) atom is coordinated with two S, one N and one P donor atom. Here ligand **L2** is acting as a bidentate bridging ligand, as in complex **7**.

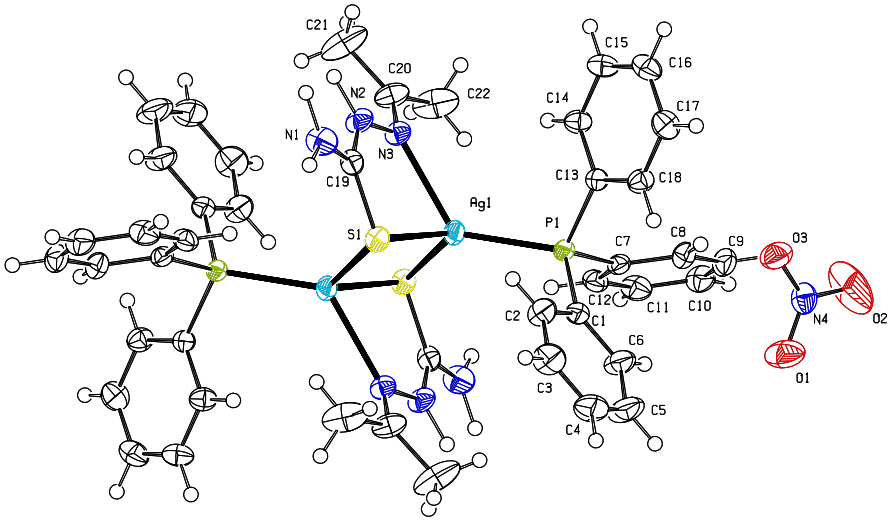

Figure 9a. A view of the molecular structure of complex **9** with complete atom labelling scheme and displacement ellipsoids drawn at the 50% probability level (only one anion is shown).

In complex **9**, the Ag-S / Ag-N / Ag-P bond lengths are 2.6226(4) and 2.6431(4) / 2.4158(13) / 2.3946(4) Å, respectively. The S-Ag-S bond angle is 112.137(10)º and the S-Ag-P bond angles are 116.476(14) and 119.044(13)º. Whereas, the N-Ag-P bond angle is 127.80(3)º and the S-Ag-N bond angles are the S-Ag-N bond angles are 75.08(3) and 98.11(3)º. These bond angle values around Ag(I) atom again show considerable deviation from the ideal tetrahedral angle of 109.5º. The presence of an oxy counter ion facilitates hydrogen bonding interactions in complex **9,** as in complexes **1-3, 5** and **7**. These weak inter- and intra-molecular hydrogen bonds result in the formation of one-dimensional polymeric chain structure (Fig. **9b**).

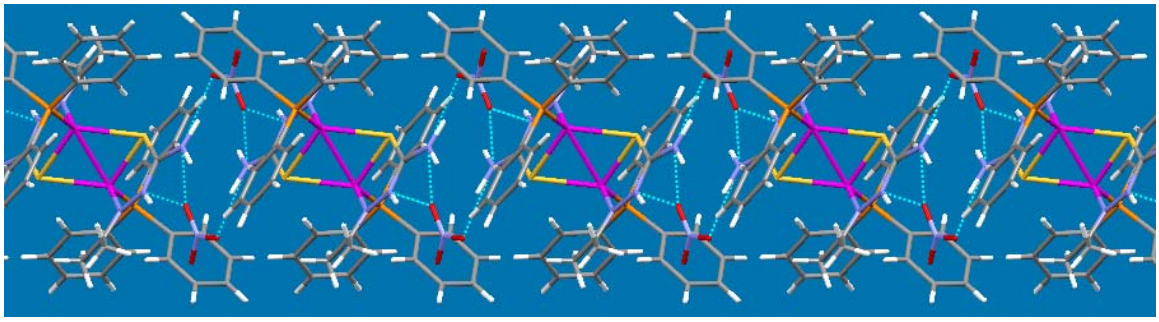

Figure 9b. A view of the hydrogen bonded one-dimensional polymeric network of complex **9**.

[Ag(P4)$_2$(L2)].NO$_3$ (10):

The molecular structure of silver(I) complex **10** is depicted in Fig. **10a**. Complex **10** exists in a monomer form unlike the other silver(I) complexes containing nitrate as counter ion. The crystallographic environment around the Ag(I) atom is distorted tetrahedral. The central metal atom is coordinated with two P, one N and one S donor atoms of the three ligand molecules.

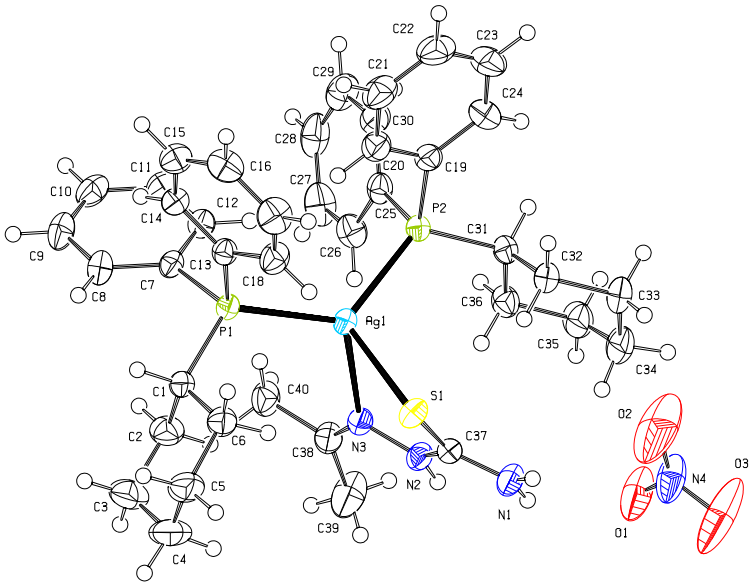

Figure 10a. A view of the molecular structure of compound **10** with complete atom labelling scheme and displacement ellipsoids drawn at the 50% probability level.

The Ag-S / Ag-N / Ag-P bond lengths are 2.5591(6) / 2.560(2) / 2.4581(7) and 2.4881(7) Å, respectively. The P-Ag-S bond angles are 114.50(2) and 112.66(2)º and the P-Ag-P bond angle is 124.77(2)º. Whereas the N-Ag-S bond angle is 72.69(5)º, the N-Ag-P bond angles are 114.06(5) and 105.98(5)º. These bond angles values around the silver(I) atom show considerable deviation from the ideal tetrahedral angle of 109.5º as in the previous structures.

The presence of the NO_3^- counter ion and ligand **L2** facilitates short range N-H…O hydrogen bond formation. In the solid state structure, this type of hydrogen bonding interactions result in eight membered rings in this dimer-like complex (Fig **10b**), instead of the formation of a polymeric chain structure.

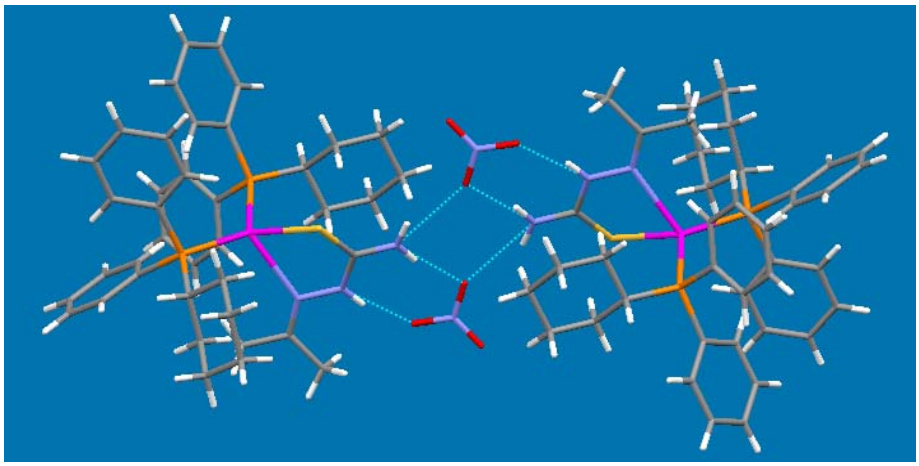

Figure 10b. A view of the dimer like complex **10** with NH…O hydrogen bonding interactions (dotted blue lines).

Intermediate Conclusions – structural features of complexes **1–10**.

The complexes can be grouped into monomers and dimers. Amongst the monomers there are those that involve one phosphine and two **L** ligands, and others that involve two phosphines and one or two **L** ligands. In general the dimers involve two phosphines and four **L** ligands or two phosphines and two **L** ligands.

In the crystal structures of all but one of the complexes N-H…O, N-H…N, N-H…S and even N-H…F hydrogen bonding plays an important role in the formation of 1D- and 2D-polymer chains and networks.

Table 2. Selected bond distances (Å) and bond angles (°) in complexes **1**-**10**.

(1)	
Ag1 -S1 2.6683(5)	S1 -Ag1 -S2 93.56(2)
Ag1 -S2 2.5403(6)	S1 -Ag1 -P1 115.79(2)
Ag1 -P1 2.4276(4)	S1 -Ag1 -S1_a 101.26(2)
Ag1 -S1_a 2.6228(5)	S2 -Ag1 -P1 128.43(2)
	S1_a -Ag1 -S2 108.60(2)
Symmetry operation: a) -x,-y,-z	S1_a -Ag1 -P1 105.95(2)
	Ag1 -S1 -Ag1_a 78.74(1)

(2)	
Ag1 -S1 2.4813(10)	S1 -Ag1 -S3 102.70(3)
Ag1 -S3 2.6395(9)	S1 -Ag1 -P1 135.80(3)
Ag1 -P1 2.4268(8)	S1 -Ag1 -S3_a 112.94(3)
Ag1 -S3_a 2.8049(9)	S3 -Ag1 -P1 114.76(3)
	S3 -Ag1 -S3_a 78.52(3)
Symmetry operation: a) -x,-y,-z	S3_a -Ag1 -P1 97.31(3)
	Ag1 -S3 -Ag1_a 101.48(3)

(3)	
Ag1 -S1 2.5540(8)	S1 -Ag1 -S3 109.83(2)
Ag1 -S3 2.5405(8)	S1 -Ag1 -P1 120.75(3)
Ag1 -P1 2.4228(7)	S3 -Ag1 -P1 123.70(2)

(4)					
Ag1	-S1	2.471(2)	S1	-Ag1	-S2	115.93(7)
Ag1	-S2	2.517(2)	S1	-Ag1	-P1	131.32(7)
Ag1	-P1	2.3997(18)	S2	-Ag1	-P1	112.15(7)
Ag2	-S4	2.530(3)	S4	-Ag2	-P4	124.72(6)
Ag2	-P4	2.3857(18)	S3	-Ag2	-P4	131.68(7)
Ag2	-S3	2.509(2)	S3	-Ag2	-S4	103.44(6)

(5)					
Ag1	-S1	2.5994(13)	S1	-Ag1	-P1	100.71(4)
Ag1	-P1	2.4501(11)	S1	-Ag1	-P2	113.95(4)
Ag1	-P2	2.4365(11)	S1	-Ag1	-O2_a	114.8(2)
Ag1	-O2_a	2.652(8)	S1	-Ag1	-O1_c	91.31(16)
Ag1	-O1_c	2.589(6)	P1	-Ag1	-P2	137.93(4)
			P1	-Ag1	-O2_a	97.9(2)
Symmetry operations:			P1	-Ag1	-O1_c	100.60(16)
a) -1+x,y,z					
c) 1-x,-y,1-z			P2	-Ag1	-O2_a	88.8(2)
			P2	-Ag1	-O1_c	101.63(15)

(6)					
Ag1	-S1	2.4431(12)	S1	-Ag1	-P1	155.36(4)
Ag1	-P1	2.3725(11)	S1	-Ag1	-S1_a	82.07(4)
Ag1	-S1_a	2.8526(13)	S1_a	-Ag1	-P1	121.63(4)
Symmetry operations:			Ag1	-S1	-Ag1_a	97.93(4)
a) 1-x,-y,1-z					

(7)	
Ag1 -S1 2.5766(13)	S1 -Ag1 -P1 123.91(5)
Ag1 -P1 2.3850(14)	S1 -Ag1 -N2 75.73(11)
Ag1 -N2 2.419(4)	S1 -Ag1 -S1_a 104.65(5)
Ag1 -S1_a 2.6792(16)	P1 -Ag1 -N2 125.75(12)
	S1_a -Ag1 -P1 120.62(4)
Symmetry operations a) 1-x,1-y,1-z	S1_a -Ag1 -N2 95.62(13)

(8)	
Ag1 -Br1 2.663(2)	Br1 -Ag1 -S1 108.47(10)
Ag1 -S1 2.580(3)	Br1 -Ag1 -P1 104.76(10)
Ag1 -P1 2.496(3)	Br1 -Ag1 -P2 111.24(10)
Ag1 -P2 2.473(3)	S1 -Ag1 -P1 109.30(11)
	S1 -Ag1 -P2 102.07(11)
	P1 -Ag1 -P2 120.61(12)

(9)	
Ag1 -S1 2.6226(4)	S1 -Ag1 -P1 116.48(1)
Ag1 -P1 2.3946(4)	S1 -Ag1 -N3 75.08(3)
Ag1 -N3 2.4159(13)	S1 -Ag1 -S1_a 112.14(1)
Ag1 -Ag1_a 2.9394(2)	P1 -Ag1 -N3 127.81(4)
Ag1 -S1_a 2.6431(5)	S1_a -Ag1 -P1 119.04(1) S1_a -Ag1 -N3 98.11(4)
Symmetry operations: a) 1-x,1-y,1-z	Ag1 -S1 -Ag1_a 67.86(1)

(10)	
Ag1 -S1 2.5591(6)	S1 -Ag1 -P1 114.50(2)
Ag1 -P1 2.4581(7)	S1 -Ag1 -P2 112.66(2)
Ag1 -P2 2.4881(7)	S1 -Ag1 -N3 72.69(5)

Ag1 -N3 2.560(2)	P1 -Ag1 -P2 124.77(2) P1 -Ag1 -N3 114.06(5) P2 -Ag1 -N3 105.98(5)

****

Table 3. Hydrogen bonding in complexes **1**–**10**

D-H….A	D-H(Å)	H…A(Å)	D…A(Å)	D-H…A(º)	Sym op
(1)					
N1 -- H1A .. S2	0.86	2.56	3.3371(19)	152	3_555
N2 -- H2B .. N3	0.86	2.36	2.658(3)	101	.
N3 -- H3A .. N2	0.86	2.32	2.658(3)	104	.
N3 -- H3B .. O1	0.86	2.32	3.159(3)	165	4_554
N4 -- H4A .. O2	0.86	2.19	3.044(3)	172	4_454
N5 -- H5B .. N6	0.86	2.35	2.646(3)	101	.
N6 -- H6A .. N5	0.86	2.30	2.646(3)	105	.
N6 -- H6A .. O1W	0.86	2.31	2.963(4)	133	4_554
N6 -- H6B .. O1	0.86	2.43	3.068(3)	131	4_554
Symmetry operations: a =[3555.00] = -x,-y,-z b =[4554.00] = x,1/2-y,-1/2+z h =[4454.00] = -1+x,1/2-y,-1/2+z					

(2)					
N1 -- H1A .. O1	0.88	2.54	3.180(5)	130	4_554
N1 -- H1A .. O2	0.88	1.85	2.733(6)	177	4_554
N2 -- H2A .. O3	0.88	1.99	2.827(4)	159	2_645
C2 -- H2 .. O3	0.95	2.57	3.405(5)	146	4_454
Symmetry operations: b =[4554.00] = x,1/2-y,-1/2+z d =[4454.00] = -1+x,1/2-y,-1/2+z					

h =[2645.00] = 1-x,-1/2+y,1/2-z

(3)

N2	-- H2A	.. O1	1.08	1.80	2.883(3)	176	1_554
N2	-- H2A	.. O2	1.08	2.41	3.056(4)	117	1_554
N1	-- H1A	.. O1	1.08	1.79	2.865(3)	170	1_554
N1	-- H1A	.. O3	1.08	2.46	3.049(3)	113	1_554

Symmetry operation:
a =[1554.00] = x,y,-1+z

(4)

N1	-- H1M	.. F1	0.88(4)	2.20(5)	2.978(10)	147(7)	.
N1	-- H1N	.. F11	0.88(8)	2.15(8)	3.022(11)	176(8)	2_646
N2	-- H2N	.. S3	0.87(6)	2.40(7)	3.224(7)	157(7)	2_646
N3	-- H3M	.. S1	0.88(6)	2.87(7)	3.683(7)	155(7)	.
N3	-- H3N	.. S2	0.87(7)	2.69(8)	3.071(7)	108(7)	.
N3	-- H3N	.. F2	0.87(7)	2.45(8)	3.098(12)	132(7)	1_554
N4	-- H4M	.. F5	0.87(7)	2.32(6)	3.170(10)	165(5)	.
N4	-- H4N	.. N6	0.88(6)	2.29(6)	2.589(11)	100(4)	.
N4	-- H4N	.. F10	0.88(6)	2.51(6)	3.283(9)	147(7)	2_646
N5	-- H5N	.. F3	0.87(5)	2.54(7)	3.235(13)	138(7)	1_454
N6	-- H6M	.. F6	0.88(5)	2.29(5)	3.113(11)	155(5)	1_454
N6	-- H6N	.. F11	0.88(6)	2.41(6)	3.275(9)	168(6)	2_646
N7	-- H7M	.. S4	0.88(7)	2.69(7)	3.529(8)	161(6)	.
N8	-- H8N	.. N3	0.87(6)	2.32(6)	3.190(9)	173(5)	2_656
N9	-- H9M	.. F4	0.89(4)	2.48(6)	3.225(11)	142(5)	2_757
N10	-- H10M	.. F7	0.88(6)	2.40(7)	2.871(9)	114(5)	.
N11	-- H11N	.. F9	0.88(4)	2.10(4)	2.944(9)	161(8)	1_656
N11	-- H11N	.. F12	0.88(4)	2.45(7)	3.163(10)	139(7)	1_656
N12	-- H12M	.. S3	0.88(6)	2.85(6)	3.574(10)	141(8)	1_655

N12 -- H12N .. N10	0.87(7)	2.20(8)	2.639(12)	112(8)	.

Symmetry operations:
a =[1655.00] = 1+x,y,z
c =[2646.00] = 1-x,-1/2+y,1-z
f =[1554.00] = x,y,-1+z
g =[1454.00] = -1+x,y,-1+z
q =[2656.00] = 1-x,1/2+y,1-z
s =[2757.00] = 2-x,1/2+y,2-z
r =[1656.00] = 1+x,y,1+z

(5)

N3 -- H3AN .. N5	0.88	2.22	2.599(5)	105	.
N3 -- H3BN .. O3	0.88	2.04	2.782(8)	142	1_455
N3 -- H3BN .. O1	0.88	1.95	2.766(8)	154	2_656
N4 -- H4AN .. O5	0.88	2.38	2.763(9)	107	.
N4 -- H4AN .. O6	0.88	2.12	2.860(6)	142	.

Symmetry operations:
a =[1455.00] = -1+x,y,z
c =[2656.00] = 1-x,-y,1-z

(6)

C9 -- H9B .. F5	0.99	2.53	3.504(12)	169	.
C21 -- H21A .. F12	0.99	2.30	3.206(15)	152	2_566

Symmetry operation:
c =[2556.00] = -x,-y,1-z

(7)

N3 -- H3NA .. O3	0.82(7)	2.21(8)	2.993(8)	162(8)	2_566
N1 -- H1N .. O4	0.92(6)	2.09(6)	2.957(5)	157(6)	1_556
N3 -- H3NB .. O1	0.86(7)	2.55(8)	3.242(8)	138(7)	1_556
N3 -- H3NB .. O4	0.86(7)	2.27(7)	3.033(7)	148(7)	1_556

Symmetry operations:
b =[1556.00] = x,y,1+z
c =[2566.00] = -x,1-y,1-z

(8)

N1 -- H1M .. S1	0.85(8)	2.63(7)	3.461(13)	167(9)	2_657

```
N1   -- H1N  .. N3     0.87(8)    2.01(10)  2.563(16)   120(9)     .

N2   -- H2N  .. Br1    0.88(7)    2.84(7)   3.709(10)   173(9)     .

Symmetry operation:
b =[  2657.00 ]  = 1-x,-y,2-z
```

(9)

```
N1   -- H1A  .. O1       1.08     2.40    3.102(2)   121   2_566

N1   -- H1A  .. O3       1.08     1.83    2.881(2)   164   2_566

N1   -- H1B  .. O1       1.08     1.93    2.907(2)   148   1_556

N2   -- H2A  .. O1       1.08     1.92     .885(2)   147   1_556

Symmetry operations:
b =[  1556.00 ]  = x,y,1+z
c =[  2566.00 ]  = -x,1-y,1-z
```

(10)

```
N2   -- H2A  .. O3      0.86     2.02   2.859(5)     166   2_556

N1   -- H1A  .. O1      0.86     1.98   2.824(4)     168   2_556

N1   -- H1B  .. O1      0.86     2.16   2.842(4)     136     .

Symmetry operation:
b =[  2566.00 ]  = -x,1-y,1-z
```

****

Biological Activity

Anti-tubercular activities of silver(I) complexes 1-10

The MIC values of the ten silver(I) complexes against *M. tuberculosis* (ATCC 27294) are shown in Table **4**. The MIC values were determined by using micro dilution plates and Alamar Blue as a vital dye, according to the methodology of Franzblau et al.[31] The

bacterial suspension used was prepared by adjusting its turbidity by the McFarland No. 1 scale, and further dilution (1:25 v/v) in the culture medium 7H9. Two fold serial dilutions of the silver complexes and isoniazid (isonicotinyl hydrazine) ranged from 1.00 to 100 μg/mL and 0.50 to 0.015 μg/mL, respectively. Isoniazid is a standard antituberculous drug and it was used to confirm that the complexes were active against *M. tuberculosis* or not. A control was run without bacterial *inoculum* in the medium to confirm that there is no reaction of the complexes themselves with the Alamar Blue. The maintenance of a blue colour in the wells was considered to reflect a lack of bacterial growth and the development of a pink colour was interpreted as a contrary. Thus MIC is considered as the minimum concentration able to inhibit the change of colour from blue to pink.

Table 4. MIC of the silver complexes **1-10**

Compound	MW	Ag (%)	*M. tuberculosis* MIC (μg/mL) [μM]
1	623.44	17.30	(10) [4]
2	670.55	16.08	(15) [6]
3	688.69	15.66	(10) [1]
4	1431.07	15.07	(10) [1]
5	849.81	12.69	(12) [5]
6	652.45	16.53	(7) [8]
7	606.84	17.77	(12) [5]
8	871.57	12.37	(12) [5]
9	837.72	12.87	(10) [1]
10	563.35	19.14	N/A

Commercial silver(I)-sulfadiazine (SSD) was also tested against *M. tuberculosis* and showed a MIC value of 7.8 μg/mL. Complex **6** showed a MIC value of 7.0 μg/mL. The MIC values of complexes **1**, **3**, **4** and **9** are similar and in the same way complexes **5**, **7** and **8** also show the same MIC values against *M. tuberculosis*. The MIC values for complex **2** (15 μg/mL) are considerably different than all other silver(I) complexes. The

MIC values of complex **6** are comparable with silver(I)-sulfadiazine (SSD) and show that it is more efficient against *M. tuberculosis* than SSD. The nine silver(I) complexes and SSD are less effective against *M. tuberculosis* than isoniazid which showed a MIC value of 0.030 μg/mL and are much more effective than pirazinamide (MIC value of 25 μg/mL).[32] The MIC value for silver nitrate solution against *M. tuberculosis* is 12 μg/mL.[27] These values demonstrate that complexes **1**, **3**, **4** and **9** are more effective than silver nitrate. So all the silver complexes described here show a good reactivity against *M. tuberculosis* except complex **2**. Isoniazide and pirazinamide are used extensively for tuberculosis treatment.[33]

Antimicrobial and antifungal activities of silver(I) complexes 1-10
(see Appendix Part 1)

Antimicrobial and antifungal activities of free ligands and three- and four-coordinate silver(I)-Phosphine complexes of AgS_3P, AgS_2P, AgS_2NP, $AgSNP_2$, AgS_2P, $AgBrSP_2$, and $AgOSP_2$ cores are listed in detailed (Appendix; supplementary material for chapter **2**) as estimated by minimum inhibitory concentration (MIC; μg/mL) and inhibition growth sensitivity. Antimicrobial activity of silver has been known for a long time and is attributable to the silver cation Ag^+, which binds strongly to electron donor groups (sulphur, oxygen and nitrogen) present in biological molecules. All silver-complexes with different cores **1-10** have shown selective and effective activities against four gram-negative and one gram-positive bacteria. Complexes **8** and **10** show weak activities against all strains of gram-negative bacteria and moderate activities against gram-positive bacterium. It is well known that the structural difference between gram-positive and gram-negative bacteria is the cell wall. Hence, it is possible to conclude that the different bactericidal actions of these compounds can be explained by this fact.

The first interaction between a compound and the bacterium is at the cell wall level. The basis for this interaction is the strong attraction on positively charged compounds such as polycations. If the compounds can form bond complexes or interact electrostatically with the cell wall, it is very probable the compound will possess biocidal activity. The anterior phenomenon occurs most easily with gram-positive bacteria, which is attributed to the

cell wall of these microorganisms being constituted basically of a network of peptidoglycan whose holes are not efficient barriers for the solutes of determined size. The normal size of bacteria varies between 500 to 3000 nm. In our recent studies; the size of the compounds is in the range of peptidoglycan network holes. The compound can pass through the membrane and interact with the cell membrane, producing changes that would finally cause the death of the bacteria. It is also possible that these compounds achieved cytoplasm bonding with important part such as DNA and proteins avoiding the replication of the bacteria.

Antifungal studies of the silver(I)-complexes and the free ligands are given in the appendix (supplementary material for chapter **2**). Four silver(I)-complexes **3, 4, 5** and **6** showed the best antifungal activities, while complexes **1**, **2**, **7**, **9** and **10** show moderate activity, and complex **8** shows little or no activity. Antifungal activity can be correlated with the presence of same geometry (trigonal planar) and same metallic cores (AgS_2P) in case of complexes **3**, **4** and **6**. The complex **5** has pseudotetrahedral geometry and AgS_2OP metal core. The presence of Ag-Br (very strong) ionic bond in complex **8** is the reason for its poor antifungal activity.

Antimicrobial and antifungal studies of this series of silver(I)-complexes with the same or different metal cores and structures, it is likely that the magnitude of the intensity of the antibacterial activity is correlated to the availability of the Ag^+ ion and ligand exchange reactions. A fast rate of ligand exchange or the easy availability of Ag^+ ions has the tendency to show more intensive activities.

Anticancer activity of silver(I)-complexes 1-10 (see Appendix Part 2)

Anti-tumour activities of silver(I)-phosphine complexes of sulphur and nitrogen containing ligands **L1-L3** with different metal cores and geometrical environment around central metal atoms have been studied in detail against KGN cancer cell line (see Appendix; supplementary material for chapter **2**: part 2). In vitro biological experiments, these silver-complexes are active against KGN cancer line. Whereas cytotoxicity of free the ligands **L1** and **L3** on the same cell line was not observed at concentrations up to 50

μg/mL. This indicates the important impact of coordination of these inactive ligands to the silver(I) ions. These results show that two compounds **7** and **2** kill 50% of the ovarian cancer cells in ten hours with a concentration of 70 and 200 ng/mL, respectively. Compound **7** is the best with an IC50 (50% inhibitory concentration) of 70 ng/mL (115 nM) while compound **2** has an IC50 of 200 ng/mL (330 nM).

In contrast to platinum only a few silver(I) complexes have been tested for anticancer activity. Our preliminary results indicate that silver phosphine mixed-ligand complexes can reduce the growth of cancer cells at a low concentration, and perhaps merit further attention for in vivo anticancer tests.

Conclusions

Mixed ligand silver-complexes of a variety of tertiary phosphines and thiourea and thione type ligands were prepared and structurally and spectroscopically characterized. The structural and elemental analysis revealed that complexes **1**, **2**, **3, 6,** **7** and **9** exist in the dimer form with the thio-ligand acting as a bridging ligand, except in case of complex **5** where the nitrate counter ion acts as a bridging ligand. The complexes **1**, **2**, **7** and **9** are isomorphous and the geometry around the silver(I) centre is pseudotetrahedral. In complex **6** the geometry around the silver(I) atom is trigonal planar. Complexes **8** and **10** are slightly different from the other complexes with the geometry around the silver(I) atom being distorted tetrahedral and they exist in the monomer form, like complex **4**. The elemental analysis, ^{1}H, ^{13}C, and ^{31}P NMR, IR spectroscopic analyses are consistent with the single crystal X-ray analyses. The presence of intramolecular and intermolecular N-H…N, N-H…O, N-H…S and N-H…F hydrogen bonding interactions enhance the symmetry and result in the formation of one- and two-dimensional hydrogen bonded polymeric chain structures for many of this series of silver(I) complexes.

Antimycobacterial, antifungal and anticancer activities of these silver(I) mixed ligand complexes were investigated. Silver(I) complexes are well known for their broad

spectrum antimicrobial activity against bacterial and fungal agents, together with their lack of cross-resistance with antibiotics. In this perspective this series of compounds are highly interesting since their MIC values are at the μg/mL level. Compounds **1-10** showed marked activities against several strains of gram-negative bacteria and one strain of gram-positive bacterium. They also have antifungal activity and show good anticancer activity in vitro. These antibacterial, antifungal and anticancer studies merit more attention and further in vivo studies.

In this article, various structural and mechanistic aspects of silver-complexes have been presented, although the exact mechanism of these silver-complexes is not completely understood. The biological activity of silver(I)-complexes is highly dependent on the nature and type of donor atom coordinated with the metal centre. In our recent studies all complexes show quite high selectivity for a particular strain.

References

1. Melaiye, A.; Sun, Z.; Hindi, K.; Milsted, A.; Ely, D.; Reneker, H. A.; Tessier, C. A.; Youngs, W. J. *J. Am. Chem. Soc.* **2005**, 127, 2285-2291.
2. Klasen, H. J. *J. Burns* **2000**, 26, 131-138.
3. Landsdown, A. B. G. *J. Wounds Care* **2002**, 2, 125-130.
4. Rowan, R.; Tallon, T.; Sheahan, A. M.; Curran, R.; McCann, M.; Kavanagh, K.; Devereux, M.; McKee, V. *Polyhedron*. **2006**, 25, 1771-1778.
5. Hamilton-Miller, J. M. T.; Shah, H. *Int. J. Antimicrob. Agent*. **1996**, 7, 97.
6. Melaiye, A.; Simons, R. S.; Milsted, A.; Pingitore, F.; Wesdemiotis, C.; Tessier, C. A.; Youngs, W. J. *J. Med. Chem.* **2004**, 47, 973-977.
7. Noguchi, R.; Hara, A.; Sugie, A.; Nomiya, K. *Inorganic Chemistry Commun.* **2006**, 9, 355.
8. McKeage, M. J. ; Papathanasiou, P. ; Salem, G. ; Sjaarda, A. ; Swiegers, G. F. ; Waring, P. ; Wild, S. B. *Metal-Based Drugs*. **1998**, 5, 217.
9. Barnard, P. J.; Bakar, M. V.; Berner-Prince, S. J.; Day, D. A. *J. Inorg. Biochem.* **2004**, 98, 1642.

10. Messori, L.; Marcon, G. *Met. Ions Biol. Syst*. 2004, 42, 385.

11. Fricker, S. P. *Gold Bull*. **1996**, 29, 53.

12. Elsome, A. M.; Hamilton-Miller, J. M. T.; Brumfitt, W.; Noble, W. C. *J. Antimicrob. Chemother*. **1996**, 37, 911.

13. Nomiya, K.; Noguchi, R.; Oda, M. *Inorg. Chim. Acta*. **2000**, 298, 24-32.

14. Nomiya, K.; Noguchi, R.; Ohsawa, K. ; Tsuda, K. *J. Chem. Soc., Dalton Trans*. **1998**, 1401.

15. Nomiya, K.; Tsuda, K.; Kasuga, N. C. *J. Chem. Soc., Dalton Trans*. **1998**, 1653.

16. Nomiya, K.; Tsuda, K.; Tanabe, Y.; Nagano, H. *J. Inorg. Biochem*. **1998**, 69, 9.

17. Nomiya, K.; Tsuda, K.; Sudoh, T. Oda, M. *J. Inorg. Biochem*. **1997**, 68, 39.

18. Kasuga, N. C.; Yamamoto, R.; Hara, A.; Amano, A.; Nomiya, K. *Inorg. Chim. Acta*. **2006**, 359, 4412-4416.

19. Kasuga, N. C.; Sugie, A.; Nomiya, K. *Dalton Trans*. **2004**, 3732-3740.

20. Nomiya, K. ; Takahashi, S. ; Noguchi, R. *J. Chem. Soc., Dalton Trans*. **2000**, 2091-2097.

21. Feng, Q. L. ; Wu, J. ; Chen, G. Q.; Cui, F. Z. ; Kim, T. N. ; Kim, J. O. *J. Biomed. Mater. Res*., **2000**, 52, 662.

22. Clement, J. L.; Jarrett, P. S. *Metal-based drugs*. **1994**, 1, 467.

23. Cuin, A.; Massabni, A. C.; Leite, C. Q. F. ; Sato, D. N. ; Neves, A. ; Szpoganicz, B. ; Silva, M. S. ; Bortoluzzi, A. J. *J. Inorg. Biochem*. **2007**, 101, 291-296.

24. Ratan, A.; Kalia, A.; Ahmad, N. *Emerg. Infect. Dis*. **1998**, 4, 195-209.

25. *World Health Organization Bulletin*. **1992**, 70, 17-21.

26. Klasen, H. J. *J. Burns* **2000**, 26, 117-130.

27. Nomiya, K.; Yokoyama, H. *J. Chem. Soc., Dalton Trans*. **2002**, 12, 2483-2490.

28. McFarlane, W. ; Akrivos, P. D. ; Aslanidis, P. ; Karagiannidis, P. ; Hatzisymeon, C. ; Numan, M. ; Kokkou, S. *Inorg. Chim. Acta*. **1998**, 281, 121-125.

29. Orvig, C. ; Abrams, M. *J. Chem. Rev*. **1999**, 99, 2201-2203.

30. Nomiya, K.; Kondoh, Y.; Onoue, K.; Kasuga, N. C.; Nagano, H.; Oda, M.; Sudoh, T.; Sakuma, S. *J. Inorg. Biochem*. **1995**, 58, 255-267.

31. Franzblau, S. G.; Witzig, R. S.; McLaughlin, J. C.; Torres, P.; Madico, G.; Hernandez, A.; Degnan, M. T.; Cook, M. B.; Quenzer, V. K.; Ferguson, R. M.; Gilman, R. H. J. Clin. Microbiol. **1998**, 36, 362-366.

32. Kent, P. T.; Kubica, C. Public Health Mycobacteriology: A Guide for the Level-III Laboratory, Centers for Disease Control and Prevention, Atlanta, GA, **1985**.

33. Castelo, F. A.; Kritiski, A. L.; Barreto, A. W. J. Bras. Pneumol. 2004, 30, S24-S37.

Chapter 3:

Role of Hydrogen Bonding in the Construction of One-, Two-, and Three-dimensional Frameworks of Biotin and its Silver(I) Complexes

Introduction

Biotin, also known as vitamin H or B_7, is an essential coenzyme that has biological activity only when covalently attached at the active site of biotin carboxylases, a class of important enzymes for fatty acid biosynthesis, gluconeogenesis, and propionate catabolism (Knowles et al., 1998, Bagautdinov et al., 2005, Goodwin et al., 1998). Vitamin H also acts as a coenzyme for a number of enzymatic processes catalyzing the fixation and transfer of carbon dioxide. In this process, the carboxylate group of biotin is amide linked with the amino group of the lysine residue in the active site of the respective enzyme and a N1′-carboxybiotinyl intermediate is formed (Moss and Lane., 1971). There are a number of different biotin dependent carboxylases, all of which require metal ions such as Mg^{2+}, Mn^{2+}, Co^{2+}, Zn^{2+}, or Cu^{2+} for carboxylation of biotin with HCO_3^- and adenosine triphosphate (Moss and Lane., 1971, Wood and Zwolinski., 1976). The exact role of these tightly bound metal ions is not well understood (Greisser et al., 1973, Sigel et al., 1969).

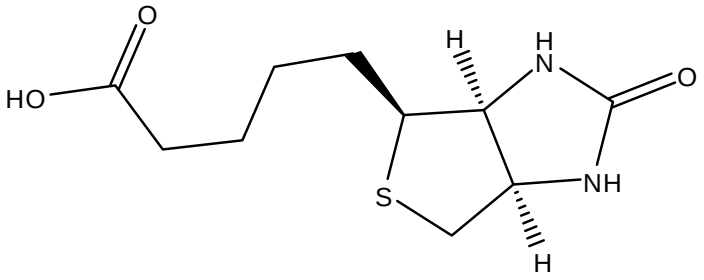

Biotin

Our interest in coordination polymers of biotin and in the mode of action of the biotin-dependent enzyme as well as our own interest in the formation of silver(I)-biotin coordination polymers, ultimately led to the determination of a number of single crystal structures. From the structure of biotin it is evident that this molecule has three possible binding sites for metal ions: the carboxylate, the urea, and the thioether group. The tetrahydrothiophene ring has an envelope conformation with sulphur atom at the flap and directed towards the same side as urea ring (Lett et al., 1966, DeTitta et al., 1976, DeTitta

et al., 1980). The coordination tendency of the urea moiety is very week, while that of the thioether sulphur seems slightly more pronounced; in fact the corresponding thioether complexes with Pd^{2+} & Pt^{2+} are very stable. The most fascinating aspect of this thioether coordination is that there are indications that it occurs in a stereoselective manner (Sigel et al., 1969, Greisser et al., 1970, Greisser et al., 1973 and Hadjiliandis and Pneumatikakis, 1979).

Over the past two decades, the design and construction of metal organic one-, two-, and three-dimensional coordination polymers has attracted intense interest not only for their potential applications as a new functional materials but also for their fascinating structural and super structural architectures. The crystal engineering of metal organic network via the self assembly of ligand ‘‘spacer’’ and metal ‘‘nodes’’ has attracted considerable interest because of structural diversity in chemistry or material sciences (Leininger et al., 2000, Siedel et al., 2002, Desiraju et al., 2002, and Archer et al., 2001).

Our interest in the silver(I) coordination polymers with biotin stems from our current research on synthesis & crystal engineering of coordination compounds of coinage metals with biological & potential applications and structural diversity. In this article we describe, single crystal structures of biotin and some new silver(I) coordination polymers. The latter are built up through the combination of silver-coordination and anion–hydrogen bonding interactions. The self assembly of the discrete unit of the $\{[Ag_2(biotin)_2(NO_3)_2].H_2O\}_n$ (**1**), $\{[Ag(biotin)].(SbF_6)\}_n$ (**2**), $\{[Ag_3(biotin)_3].(PF_6)_3\}_n$ (**3**), $\{[Ag(biotin^-)].3H_2O\}_n$ (**4**) and $[Ag_2(biotin)_2(ClO_4)_2]_n$ (**5**) complexes in crystalline form relies on the use of counter ions for the silver(I) cation, solvent of crystallization, and the presence of lattice solvent molecules.

Experimental

Synthesis

The synthesis of complex **1** was carried out by dissolving an equimolar amount (0.1mmol) of biotin and silver nitrate in methanol/water (4:1) 20 ml at room temperature

by continuous stirring for ½ hour. The clear solution obtained was filtered to avoid any impurity and kept undisturbed for crystallization by slow evaporation. After five days colourless rod like crystals were obtained. The synthesis of complexes **2** and **3** was carried out by following the same procedure as described for complex **1** by using $AgPF_6$ and $AgSbF_6$ respectively, and biotin in 1: 2 molar ratio with respect to the silver(I) salts. The synthesis of complex **4** was carried out by using silver acetate and biotin in an equimolar ratio and five drops of aqueous ammonia solution, following the same procedure as described for complex **1**. The synthesis of complex **5** was done by following the same procedure described for complex **1,** using silver perchlorate.

Warning: Perchlorate salts are dangerous and should only be used in minimum quantities. Under the conditions used we encountered no problems.

X-ray Crystallography.

The intensity data were collected at 173K on either, a one circle (ϕ scans)[1], or a two circle (ϕ and ω scans)[2] Stoe Image Plate Diffraction System, using MoKα graphite monochromated radiation. The structures were solved by Direct methods using the program SHELXS-97[3]. The refinement and all further calculations were carried out using SHELXL-97[3]. The H-atoms were either located from Fourier difference maps and freely refined or included in calculated positions and treated as riding atoms using SHELXL default parameters. The non-H atoms were refined anisotropically, using weighted full-matrix least-squares on F^2. Absorption correction was applied using either MULscanAbs or the DELrefABS routines in PLATON[4]. A summary of the crystal data and refinement details are given in Table **1**, and selected bond lengths and angles are listed in Table 2. Details of the hydrogen bonding are given in Table 3.

1) Stoe & Cie (2000) IPDS-I Bedienungshandbuch. Stoe & Cie GmbH, Darmstadt, Germany.

2) Stoe & Cie. (2006) *X-Area V1.35 & X-RED32 V1.31 Software*. Stoe & Cie GmbH, Darmstadt, Germany.

3) G. M. Sheldrick (2008). Acta Crystallgr. A64, 112-122.

4) A. L. Spek (2003). J.Appl.Cryst. 36, 7-13

Table 1. Summary of crystal data and structure refinement details for **biotin** and complexes **1-5.**

$\{^{a}$ **R1** $= \Sigma||F_o| - |F_c||/\Sigma|F_o|.$ ^{b} **wR2** $= [\Sigma w(F_o^2 - F_c^2)^2/\Sigma wF_o^4]^{1/2}\}$

Biotin	
Chemical formula	$C_{10}H_{16}N_2O_3S$
M_r	244.31
Cell setting, space group	Orthorhombic, $P2_12_12_1$
Temperature (K)	173 (2)
a, b, c (Å)	5.1955 (6), 10.3017 (17), 20.943 (2)
α, β, γ (°)	90, 90, 90
V (Å^3)	1120.9 (2)
Z	4
D_x (Mg m^{-3})	1.448
Radiation type	Mo $K\alpha$
μ (mm^{-1})	0.28
Crystal form, colour	Rod, colourless
Crystal size (mm)	0.50 × 0.13 × 0.13 mm
Diffractometer	STOE IPDS-2 diffractometer
Data collection method	phi + ω rotation scans
Absorption correction	none
R_{int}	0.053
θ_{max} (°)	25.6
Refinement on	F^2
$R[F^2 > 2\sigma(F^2)]$, $wR(F^2)$, S	0.035, 0.091, 0.97
No. of reflections	2102
No. of parameters	152
H-atom treatment	H atoms treated by a mixture of independent and constrained refinement
Weighting scheme	$w = 1/[\sigma^2(F_o^2) + (0.0622P)^2]$ where $P = (F_o^2 + 2F_c^2)/3$
$(\Delta/\sigma)_{max}$	0.001
$\Delta\rho_{max}$, $\Delta\rho_{min}$ (e Å^{-3})	0.20, −0.24
Extinction method	none
Absolute structure	Flack H D (1983), Acta Cryst. A39, 876-881
Flack parameter	−0.03 (10)

1	
Chemical formula	$C_{20}H_{32}Ag_2N_4O_6S_2{\cdot}2(NO_3){\cdot}H_2O$
M_r	846.39
Cell setting, space group	Monoclinic, *C*2
Temperature (K)	173 (2)
a, *b*, *c* (Å)	21.8568 (12), 8.0321 (4), 16.8886 (9)
α, β, γ (°)	90, 99.337 (4), 90
V (Å^3)	2925.6 (3)
Z	4
D_x (Mg m^{-3})	1.922
Radiation type	Mo *K*α
μ (mm^{-1})	1.55
Crystal form, colour	Block, colourless
Crystal size (mm)	0.29 × 0.27 × 0.22 mm
Diffractometer	STOE IPDS-2 diffractometer
Data collection method	phi + ω rotation scans
Absorption correction	refdelF DELrefABS in PLATON (Spek, 2003)
T_{min}, T_{max}	0.271, 0.722
R_{int}	0.035
θ_{max} (°)	29.3
Refinement on	F^2
$R[F^2 > 2\sigma(F^2)]$, $wR(F^2)$, *S*	0.021, 0.048, 1.01
No. of reflections	7863
No. of parameters	409
H-atom treatment	H atoms treated by a mixture of independent and constrained refinement
Weighting scheme	$w = 1/[\sigma^2(F_o^2) + (0.0273P)^2]$ where $P = (F_o^2 + 2F_c^2)/3$
$(\Delta/\sigma)_{max}$	0.006
$\Delta\rho_{max}$, $\Delta\rho_{min}$ (e Å^{-3})	0.50, −0.66
Extinction method	none
Absolute structure	Flack H D (1983), Acta Cryst. A39, 876-881
Flack parameter	−0.015(2)

2	
Chemical formula	$C_{20}H_{32}AgN_4O_6S_2{\cdot}F_6Sb$
M_r	832.24
Cell setting, space group	Monoclinic, $P2_1$
Temperature (K)	173 (2)
a, b, c (Å)	9.6902 (11), 14.6452 (12), 9.8604 (12)
α, β, γ (°)	90, 91.167 (10), 90
V (Å^3)	1399.0 (3)
Z	2
D_x (Mg m^{-3})	1.976
Radiation type	Mo $K\alpha$
μ (mm^{-1})	1.90
Crystal form, colour	Block, colourless
Crystal size (mm)	0.35 × 0.15 × 0.09 mm
Diffractometer	STOE IPDS-2 diffractometer
Data collection method	phi + ω rotation scans
Absorption correction	multi-scan MULscanABS (Spek, 2003)
T_{min}, T_{max}	0.909, 1.107
R_{int}	0.023
θ_{max} (°)	26.8
Refinement on	F^2
$R[F^2 > 2\sigma(F^2)]$, $wR(F^2)$, S	0.026, 0.064, 1.04
No. of reflections	5915
No. of parameters	376
H-atom treatment	H atoms treated by a mixture of independent and constrained refinement
Weighting scheme	$w = 1/[\sigma^2(F_o^2) + (0.0413P)^2 + 0.3541P]$ where $P = (F_o^2 + 2F_c^2)/3$
$(\Delta/\sigma)_{max}$	0.002
$\Delta\rho_{max}$, $\Delta\rho_{min}$ (e Å^{-3})	0.77, −0.56
Extinction method	SHELXL
Extinction coefficient	0.0010 (3)
Absolute structure	Flack H D (1983), Acta Cryst. A39, 876-881
Flack parameter	0.0010(3)

3	
Chemical formula	$C_{60}H_{96}Ag_3N_{12}O_{18}S_6 \cdot 3(F_6P)$
M_r	2224.37
Cell setting, space group	Monoclinic, $P2_1$
Temperature (K)	173 (2)
a, b, c (Å)	15.1130 (7), 9.6028 (3), 28.6670 (13)
α, β, γ (°)	90, 90.946 (4), 90
V (Å^3)	4159.8 (3)
Z	2
D_x (Mg m^{-3})	1.776
Radiation type	Mo $K\alpha$
μ (mm^{-1})	1.02
Crystal form, colour	Rod, colourless
Crystal size (mm)	0.37 × 0.25 × 0.24 mm
Diffractometer	STOE IPDS-2 diffractometer
Data collection method	phi + ω rotation scans
Absorption correction	multi-scan MULscanABS in PLATON (Spek, 2003)
T_{min}, T_{max}	0.718, 0.818
R_{int}	0.038
θ_{max} (°)	25.6
Refinement on	F^2
$R[F^2 > 2\sigma(F^2)]$, $wR(F^2)$, S	0.044, 0.109, 1.03
No. of reflections	14703
No. of parameters	1123
H-atom treatment	H atoms treated by a mixture of independent and constrained refinement
Weighting scheme	$w = 1/[\sigma^2(F_o^2) + (0.0556P)^2 + 7.6945P]$ where $P = (F_o^2 + 2F_c^2)/3$
$(\Delta/\sigma)_{max}$	0.011
$\Delta\rho_{max}$, $\Delta\rho_{min}$ (e Å^{-3})	1.53, −0.76
Extinction method	none
Absolute structure	Flack H D (1983), Acta Cryst. A39, 876-881
Flack parameter	0.02(2)

4	
Chemical formula	$C_{10}H_{14}AgN_2O_3S{\cdot}3(H_2O)$
M_r	404.21
Cell setting, space group	Monoclinic, $P2_1$
Temperature (K)	173 (2)
a, b, c (Å)	8.7869 (8), 8.2847 (10), 9.8588 (10)
α, β, γ (°)	90, 95.718 (8), 90
V (Å^3)	714.12 (13)
Z	2
D_x (Mg m^{-3})	1.880
Radiation type	Mo $K\alpha$
μ (mm^{-1})	1.58
Crystal form, colour	Plate, colourless
Crystal size (mm)	0.40 × 0.40 × 0.15 mm
Diffractometer	STOE IPDS-2 diffractometer
Data collection method	Phi + ω rotation scans
Absorption correction	multi-scan MULscanABS in PLATON (Spek, 2003)
T_{min}, T_{max}	0.574, 0.810
R_{int}	0.024
θ_{max} (°)	29.2
Refinement on	F^2
$R[F^2 > 2\sigma(F^2)]$, $wR(F^2)$, S	0.023, 0.062, 1.07
No. of reflections	3832
No. of parameters	197
H-atom treatment	H atoms treated by a mixture of independent and constrained refinement
Weighting scheme	$w = 1/[\sigma^2(F_o^2) + (0.0384P)^2 + 0.3546P]$ where $P = (F_o^2 + 2F_c^2)/3$
$(\Delta/\sigma)_{max}$	0.001
$\Delta\rho_{max}$, $\Delta\rho_{min}$ (e Å^{-3})	0.42, −0.64
Extinction method	SHELXL
Extinction coefficient	0.0130 (13)
Absolute structure	Flack H D (1983), Acta Cryst. A39, 876-881
Flack parameter	0.00(2)

5	
Chemical formula	$C_{20}H_{30}Ag_2N_4O_6S_2 \cdot 2(ClO_4)$
Mr	901.24
Cell setting, space group	Triclinic, P1
Temperature (K)	173 (2)
a, b, c (Å)	8.1827 (18), 9.658 (2), 11.431 (3)
α, β, γ (°)	93.54 (2), 109.77 (2), 113.009 (17)
V (Å3)	762.6 (3)
Z	1
Dx (Mg m−3)	1.962
Radiation type	Mo Kα
μ (mm−1)	1.67
Crystal form, colour	Colourless , Block
Crystal size (mm)	0.40 x 0.35 x 0.30 mm
Diffractometer	STOE IPDS-2 diffractometer
Data collection method	phi & ω scans
Absorption correction	none
Rint	0.0000
θmax (°)	25.2
Refinement on	F2
R[F2 > 2σ(F2)], wR(F2), S	0.121, 0.316, 1.25
No. of reflections	4361
No. of parameters	392
H-atom treatment	H-atom parameters constrained
Weighting scheme	w = 1/[σ2(Fo2) + (0.2P)2] where P = (Fo2 + 2Fc2)/3
(Δ/σ)max	0.002
Δρmax, Δρmin (e Å−3)	2.79, −2.18
Extinction method	none
Absolute structure	Flack H D (1983), Acta Cryst. A39, 876-881
Flack parameter	0.09(12)

Table 2. Selected bond lengths (Å) and bond angles (˚) for **Biotin** and complexes **1-5**

Bond lengths (Å)		Bond angles (˚)	
Biotin			
S(1)-C(9)	1.812(3)	C(9)-S(1)-C(6)	88.87(11)
S(1)-C(6)	1.824(2)	C(10)-N(1)-C(8)	112.9(2)
O(1)-C(1)	1.322(3)	C(10)-N(2)-C(7)	112.59(19)
O(1)-H(1O)	0.8400	O(2)-C(1)-O(1)	122.6(2)
O(2)-C(1)	1.210(3)	O(2)-C(1)-C(2)	124.6(2)
O(3)-C(10)	1.246(3)	O(1)-C(1)-C(2)	112.8(2)
N(1)-C(10)	1.346(3)	N(2)-C(7)-C(6)	113.26(18)
N(1)-C(8)	1.450(3)	N(2)-C(7)-C(8)	102.72(17)
1			
Ag(1)-O(1)	2.4531(16)	O(1)-Ag(1)-S(2)	96.81(4)
Ag(1)-S(2)	2.4698(5)	O(1)-Ag(1)-S(1)	112.33(4)
Ag(1)-S(1)	2.4851(5)	S(2)-Ag(1)-S(1)	149.076(18)
Ag(1)-O(12)#1	2.5229(17)	O(1)-Ag(1)-O(12)#1	92.83(6)
Ag(2)-O(4)	2.3960(16)	S(2)-Ag(1)-O(12)#1	99.87(4)
Ag(2)-S(1)	2.4399(5)	S(1)-Ag(1)-O(12)#1	89.16(4)
Ag(2)-S(2)#1	2.4639(5)	O(4)-Ag(2)-S(1)	105.38(4)
Ag(2)-O(9)#1	2.5288(16)	O(4)-Ag(2)-S(2)#1	109.37(5)
Symmetry operations		S(1)-Ag(2)-S(2)#1	143.621(17)
#1 x, y-1, z		O(4)-Ag(2)-O(9)#1	89.18(6)
		S(1)-Ag(2)-O(9)#1	98.64(4)
		S(2)#1-Ag(2)-O(9)#1	92.36(4)
2			
Ag(1)-S(2)	2.4192(10)	S(2)-Ag(1)-O(2)#1	113.97(9)
Ag(1)-O(2)#1	2.440(3)	S(2)-Ag(1)-S(1)	157.22(3)
Ag(1)-S(1)	2.4496(10)	O(2)#1-Ag(1)-S(1)	88.77(9)
Symmetry operations			

#1 x, y, z+1			
3			
Ag(1)-S(1)	2.4232(16)	S(1)-Ag(1)-S(2)	151.54(6)
Ag(1)-S(2)	2.4524(16)	S(1)-Ag(1)-O(16)	124.92(15)
Ag(1)-O(16)	2.518(5)	S(2)-Ag(1)-O(16)	80.40(15)
Ag(2)-S(4)	2.4600(17)	S(4)-Ag(2)-S(3)	147.51(6)
Ag(2)-S(3)	2.4656(15)	S(4)-Ag(2)-O(1)	128.67(12)
Ag(2)-O(1)	2.517(4)	S(3)-Ag(2)-O(1)	80.10(12)
Ag(3)-S(6)	2.4271(16)	S(6)-Ag(3)-S(5)	157.56(5)
Ag(3)-S(5)	2.4751(16)	S(6)-Ag(3)-O(7)#1	116.73(13)
Ag(3)-O(7)#1	2.491(4)	S(5)-Ag(3)-O(7)#1	83.88(12)
Symmetry operations			
#1 x, y, z-1			
4			
Ag(1)-O(2)#1	2.301(2)	O(2)#1-Ag(1)-O(3)#2	124.47(10)
Ag(1)-O(3)#2	2.514(2)	O(2)#1-Ag(1)-S(1)#3	118.16(9)
Ag(1)-S(1)#3	2.5147(6)	O(3)#2-Ag(1)-S(1)#3	82.01(5)
Ag(1)-S(1)	2.5646(7)	O(2)#1-Ag(1)-S(1)	101.07(10)
Symmetry operations		O(3)#2-Ag(1)-S(1)	100.67(5)
#1 x, y+1, z		S(1)#3-Ag(1)-S(1)	130.359(13)
#2 x, y, z+1			
#3 -x+2, y+1/2, -z			
5			
Ag(1)-O(8)	2.32(2)	O(8)-Ag(1)-S(2)#1	104.7(5)
Ag(1)-S(2)#1	2.439(6)	O(8)-Ag(1)-S(1)	94.2(6)
Ag(1)-S(1)	2.521(6)	S(2)#1-Ag(1)-S(1)	152.0(2)
Ag(2)-O(5)#2	2.402(18)	O(5)#2-Ag(2)-S(1)	104.4(6)
Ag(2)-S(1)	2.438(7)	O(5)#2-Ag(2)-O(1)	93.1(9)

Ag(2)-O(1)	2.51(3)	S(1)-Ag(2)-O(1)	100.3(6)
Ag(2)-S(2)	2.523(7)	O(5)#2-Ag(2)-S(2)	93.8(6)
Symmetry operations		O(1)-Ag(2)-S(2)	99.8(6)
#1 x+1, y, z			
#2 x-1, y, z			

Table 3. Hydrogen bond distances and bond angles (Å, °) for **Biotin** and complexes **1-5**

Donor-H...Acceptor	D-H	H…A	D…A	D - H...A (°)
Biotin				
N1-H1N…O2[f]	0.85(3)	2.24(2)	3.044(3)	159(3)
N2-H2N…O2[b]	0.86(2)	2.04(2)	2.881(3)	168(2)
O1-H1O…O3[j]	0.84	1.72	2.545(3)	167

Symmetry operations:
f = 1/2-x,1-y,1/2+z
b = 1/2-x,1-y,-1/2+z
j = 1/2+x,3/2-y,-z

Donor-H...Acceptor	D-H	H…A	D…A	D - H...A (°)
1				
O1W-H1WA…O12[b]	0.90(3)	2.10(3)	2.981(2)	166(3)
O2W-H2WA…O9[d]	0.88(3)	2.03(3)	2.884(2)	165(4)
N3-H3N…O4[a]	0.85(2)	2.08(2)	2.897(2)	162(3)
N4-H4N…O2[d]	0.879(19)	2.239(19)	3.025(3)	149(2)
N5-H5N…O5[p]	0.873(19)	2.307(19)	3.104(2)	152(2)
N6-H6N…O1[a]	0.86(2)	2.14(2)	2.975(2)	163(2)
O8-H8O…O11[j]	0.84	1.78	2.608(2)	167
O10-H10O…O7[m]	0.84	1.80	2.620(2)	166

Symmetry operations:
b = x,1+y,z
d = 2-x,y,1-z
a = x,-1+y,z
p = 2-x,-1+y,2-z
j = 1/2+x,1/2+y,1+z
m = -1/2+x,-1/2+y,-1+z

Donor-H...Acceptor	D-H	H…A	D…A	D - H...A (°)
2				
O4-H4O…O3[g]	0.84	1.85	2.646(4)	159
O1-H1O…O6[k]	0.84	1.98	2.674(4)	140
N1-H1N…F1[a]	0.90(3)	2.09(3)	2.967(5	166(4)
N2-H2N…F5[b]	0.87(3)	2.36(3)	3.122(6)	160(4)
N3-H3N…F2[a]	0.88(3)	2.11(4)	2.944(4)	157(4)
N4-H4N…F3[b]	0.85(3)	1.95(3)	2.765(5)	147(5)

Symmetry operations:
g = 1+x,y,z
k = 1+x,y,-1+z
a = x,y,-1+z
b = x,y,1+z

Donor-H...Acceptor	D-H	H…A	D…A	D - H...A (°)
3				
N1-H1N…F17	0.88(5)	2.47(5)	3.211(8)	144(5)
N1-H1N…F18	0.88(5)	2.38(5)	3.231(8)	163(6)
N2-H2N…F4[i]	0.90(5)	2.45(6)	3.222(9)	144(7)
N2-H2N…F6[i]	0.90(5)	2.33(4)	3.100(8)	144(7)
O2-H2O…O12	0.84	1.84	2.672(7)	173
N3-H3N… F13[e]	0.88(5)	2.26(5)	2.960(8)	137(5)
N4-H4N…O14	0.87(3)	2.38(7)	2.978(8)	127(6)
N5-H5N…F12	0.88(4)	2.26(4)	3.119(8)	165(5)
O5-H5O…O9	0.84	1.84	2.655(7)	163
N6-H6N…F16	0.89(3)	2.23(4)	3.051(7)	154(7)
N7-H7N…F7[e]	0.87(4)	2.40(4)	3.138(8)	144(5)
N8-H8N…F14[e]	0.88(4)	2.52(6)	3.359(9)	159(7)
N8-H8N…F15[e]	0.88(4)	2.40(6)	3.169(8)	146(7)
O8-H8O…O18[a]	0.84	1.83	2.644(6)	163
N9-H9N…F1[i]	0.88(4)	2.46(5)	3.210(8)	143(6)
N10-H10N…F10[b]	0.88(3)	2.34(3)	3.179(8)	159(6)

N11-H11N…F3[k]	0.86(5)	2.31(5)	3.076(7)	148(5)
O11-H11O…O15[a]	0.84	1.76	2.578(7)	162
N12-H12N…F8[n]	0.87(5)	2.46(6)	3.252(9)	151(5)
N12-H12N…F9[n]	0.87(5)	2.49(6)	3.082(8)	126(4)
O13-H13O…O6	0.84	1.78	2.606(7)	168
O17-H17O…O3	0.84	1.80	2.630(7)	167

Symmetry operations:
l = 1-x,-1/2+y,1-z
e = x,-1+y,z
a = x,y,-1+z
b = x,y,1+z
k = 1-x,-3/2+y,1-z
n = x,-1+y,1+z

Donor-H...Acceptor	D-H	H…A	D…A	D - H...A (°)
4				
N1-H1N…O1W	0.86(3)	2.11(3)	2.934(4)	163(3)
N2-H2N…O1A[n]	0.90(3)	1.86(3)	2.758(8)	178(4)
N2-H2N…O1B[n]	0.90(3)	2.10(3)	2.962(6)	161(3)

Symmetry operatios:
n = x,1+y,-1+z

Donor-H...Acceptor	D-H	H…A	D…A	D - H...A (°)
5				
N1-H1N…O1[a]	0.88	2.30	3.08(4)	148
N2-H2N…O3[k]	0.88	2.41	3.25(3)	159
N3-H3N…O14	0.88	2.37	3.13(5)	145
N4-H4N…O11[c]	0.88	2.56	3.34(5)	149
O7-H7O…O9[e]	0.84	1.85	2.65(4)	157
O10-H10O…O6[g]	0.85	1.89	2.60(4)	140

Symmetry operations:
a = -1+x,y,z
k = -1+x,-1+y,z
c = 1+x,1+y,z
e = 1+x,2+y,1+z
g = -1+x,-2+y,-1+z

Results and discussions

Biotin

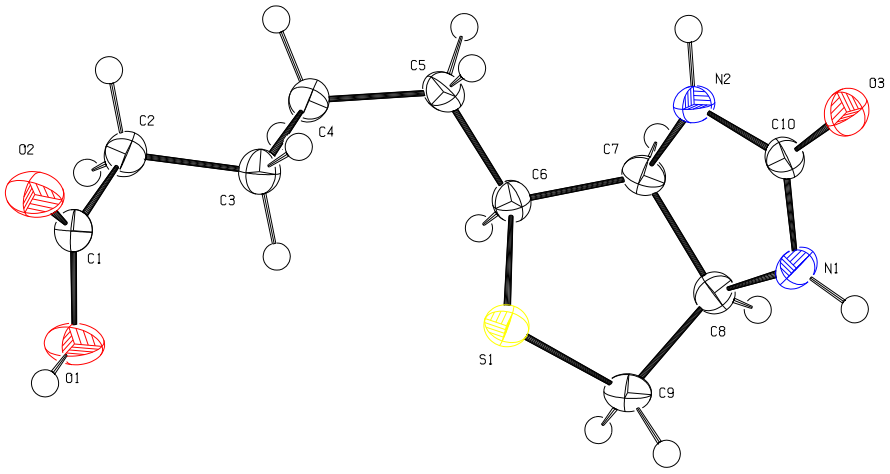

Figure 1a. View of the molecular structure of **biotin** with complete atom labelling Scheme and displacement parameters are shown at 50% probability.

The bond lengths and bond angles observed in the single crystal structure of **biotin** are within the normal range and very close to the previously reported structure of biotin (DeTitta et al., 1976). In the molecular structure of biotin, ureido ring including the carbonyl oxygen is planar. The ureido C=O bond distance is 1.246(3) Å, whereas the HN-C bond distances are 1.346(3) and 1.450(3) Å. The tetrahydrothiophene ring has an envelope conformation with sulphur atom at the flap and directed towards the same side as urea ring. The C9-S & C6-S bond distances are 1.812(3) and 1.824(2) Å respectively. The C-S-C bond angle is 88.87(11)˚. The dihedral angle between the ureido and tetrahydrothiophene rings is 75.02(12)˚. The valeric acid side chain is not extended but folds back on itself. The bond lengths and bond angles found within the chain are comparable with the reported structure (DeTitta et al., 1976).

The most interesting and notable feature of the solid state structure of biotin is the presence of intramolecular and intermolecular hydrogen bonding interactions. These hydrogen bonding interactions result in the formation of three-dimensional hydrogen bonded polymeric network. In the molecular structure of biotin, all potentially available

hydrogen donor atoms are utilized. Three different types of inter-molecular hydrogen bonding and inter-atomic interactions are observed.

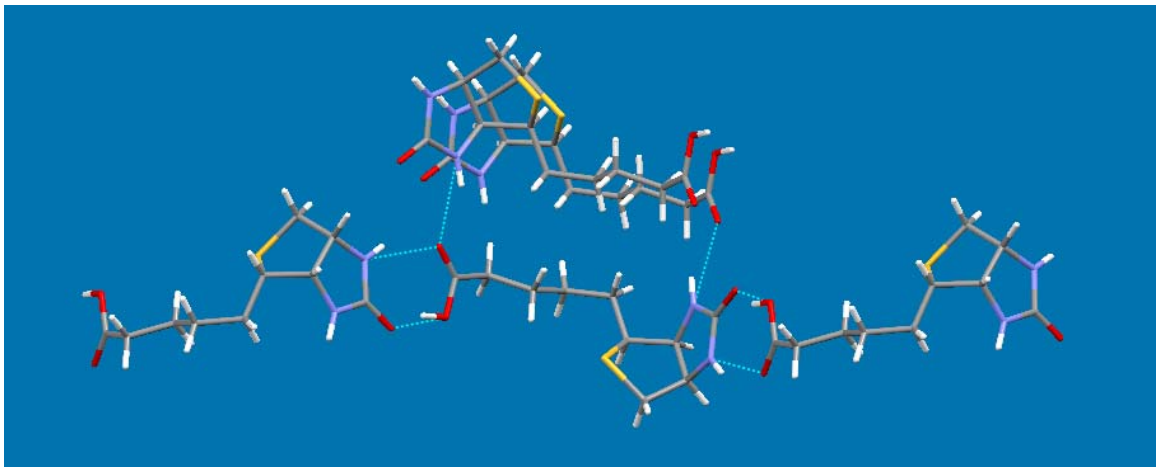

Figure 1b. Pattern of N-H…O, O-H…O hydrogen bonding interactions (blue dotted lines) in the solid state structure of **biotin.**

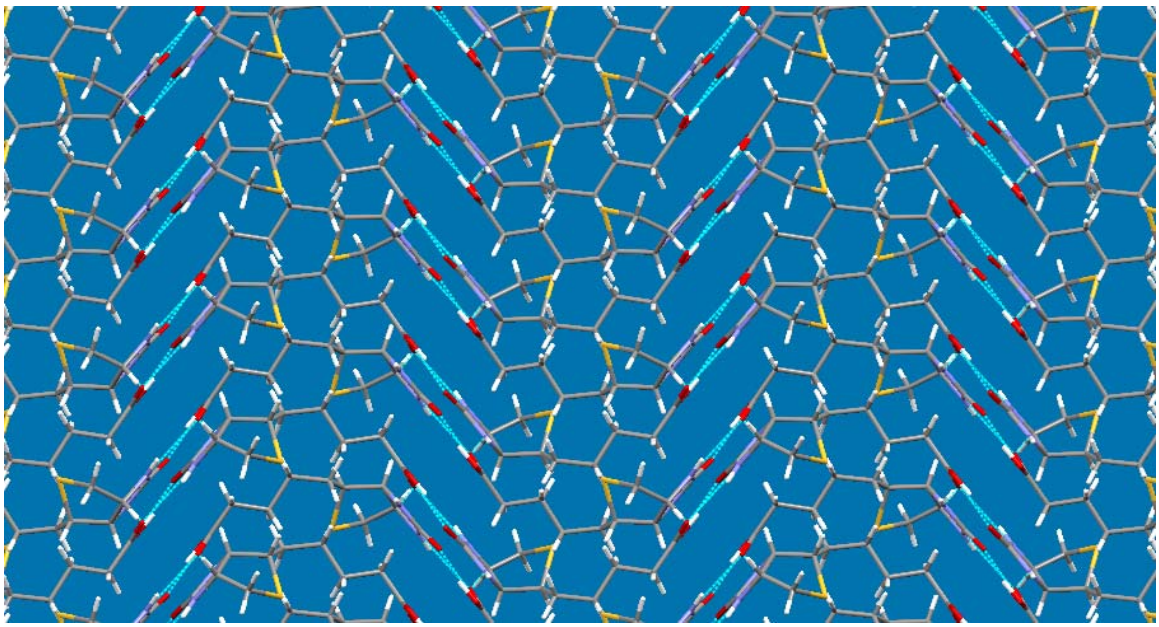

Figure 1c. View along the *b*-axis of the hydrogen bonded polymeric structure of **biotin**.

The O1-H1O...O3, N1-H1N...O2, and N2-H2N...O2 hydrogen bond distances are 1.72, 2.24(2), and 2.04(2) Å and O1-H1O...O3, N1-H1N...O2, and N2-H2N...O2 bond angles are 167, 159(3) and 168(2)˚ respectively. Whereas, the O1...O3, N1...O2, and N2...O2 inter-atomic distances are 2.545(3), 3.044(3), and 2.881(3) Å. The ureido […O=C-N1-

H1…] and carboxylic acid [...H1O1-C1-O2...] form an eight member hydrogen bonded ring, as shown in Fig. **1b**. A view along the *b*-axis of the three-dimensional polymeric structure of **biotin** is shown in Fig. **1c**.

$\{[Ag_2(biotin)_2(NO_3)_2]\cdot H_2O\}_n$ (1)

The molecular structure of the one-dimensional coordination polymer of silver(I)-biotin complex **1** is shown in Fig. **2a**, with complete atom labelling scheme. The molecular structure of complex **1** is a pseudo polymorph of silver(I) complex with chemical composition $\{[Ag(biotin)(NO_3)].0.5H_2O\}_n$ (Katsuyuki and Wolfram Saenger., 1983).

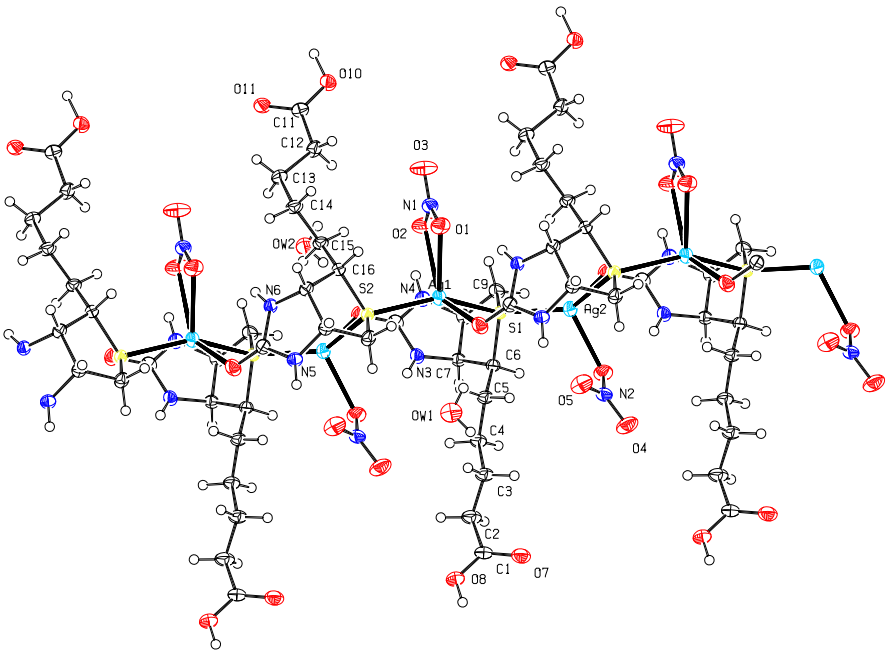

Figure 2a. View of the one-dimensional coordination polymer of complex **1** with complete atom labelling scheme and ellipsoids are shown at 50% probability.

In the single crystal structure of complex **1**, the geometry around silver(I) atoms is pseudo-tetrahedral and each silver(I) atom is coordinated with three different biotin molecules and one nitrate counter ion. The lattice water molecules present in the crystal structure do not show any coordination with the metal centres and play an important role in hydrogen bond formation, as shown in Fig. **2b.** Two out of three biotin molecules, coordinate with the silver(I) atom through the sulphur atom of the tetrathioether group

and one coordinates to the silver(I) atom through a carbonyl oxygen of the ureido group. The Ag-S and Ag-O (ureido) bond distances vary from 2.4399(5) to 2.4851(5) and 2.5229(17) to 2.5288(16) Å respectively; whereas, the Ag-O (nitrate) bond distances range from 2.3960(16) to 2.4531(16) Å. Each sulphur atom bridges two silver(I) atoms and results in an infinite $[\text{-Ag-S-Ag-S-}]_n$ spiral network. S-Ag-S and O-Ag-O bond angles around silver(I) atoms are 149.076(18) & 143.621(17) and 89.18(6) & 92.83(6)˚. Whereas, S-Ag-O bond angle values range from 89.16(4) to 112.33(4)˚. These bond angle values confirm the presence of pseudo-tetrahedral geometry around silver(I) metal centres in complex **1**. Bond angle values observed around the silver(I) metal centres in complex **1**; show considerable deviations from an ideal tetrahedral angle of 109.5˚. Moreover, the Ag-S, Ag-O bond distances and S-Ag-S, O-Ag-O and S-Ag-O bond angles values observed around the two different Ag(I) atoms in the polymeric chain structure of complex **1** are slightly different, as shown in Table **2**. The most notable feature in the single crystal structure of coordination polymer of complex **1** is individual geometry of biotin molecules bonded to the same or different Ag^I atoms. In the coordinated biotin molecules, the ureido rings including the carbonyl oxygens are not planar as found in free biotin molecular structure. The C=O bond distances of the two different biotin molecules coordinated with different Ag^I atoms are shorter than those found in the free ligand molecule. The dihedral angle between the two best planes of the ureido rings and tetrahydrothiophene rings are 74.90(12) and 74.31(12)˚ for two biotin molecules present in the asymmetric unit of complex **1**. The conformation of the valeric acid chain is all-trans except for the carboxylate group, which is almost perpendicular to the planar side chain and is protonated.

The presence of intramolecular and intermolecular hydrogen bonding interactions in the solid state structure is another important feature of complex **1** (Table **3**). The hydrogen bonding forces provide extra stability to this silver(I) complex **1** in the solid state. These hydrogen bonding interactions play important role in the construction of hydrogen bonded three-dimensional topology. In complex **1**, most of the potentially available hydrogen donor atoms are utilized for hydrogen bond formation (Table 3). The presence of water molecules and nitrate anions enhance the hydrogen bond formations. Two types (N-H…O and O-H…O) of intermolecular hydrogen bonding interactions are observed in

the solid state structure of complex **1**. The N6-H6N...O1, N4-H4N...O2, and N3-H3N…O4 hydrogen bond distances are 2.14(2), 2.239(19), and 2.08(2) Å, respectively. Whereas the N6-H6N...O1, N4-H4N...O2, and N3-H3N...O4 bond angles are 163(2), 149(2), and) 152(2)˚.

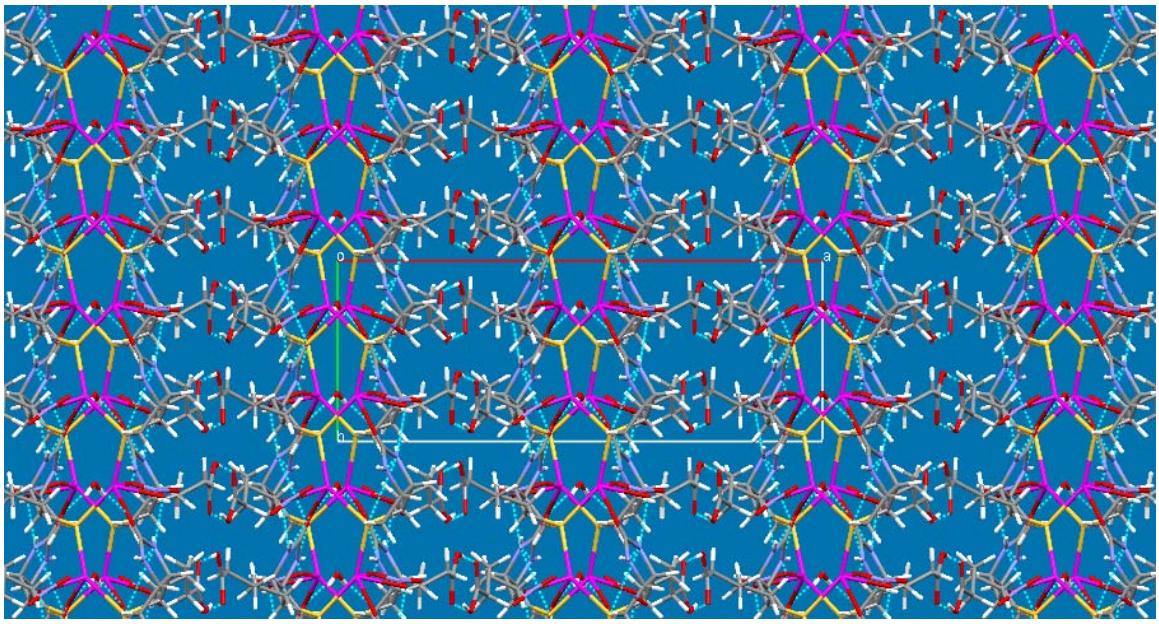

Figure 2b. View along the *c*-axis of the hydrogen bonded (blue dotted lines) three-dimensional polymeric structure of complex **1**.

The N6...O1, N4...O2, and N3...O4 inter-atomic distances are 2.975(2), 3.025(3), and 2.897(2) Å respectively. These hydrogen bond distances, bond angles and inter-atomic distance values show the presence of strong hydrogen bonding forces in the solid state structure of complex **1**. The water of crystallization and valeric acid side chains of the ligand molecules coordinated with silver(I) ions are also involved in hydrogen bond formations in the solid state. The O2W-H2WA...O9 and O1W-HIWA...O12 bond distances are 2.03(3) and 2.10(3) Å. The O2W...O9 and O1W...O11 inter-atomic distances are 2.884(2) and 2.981(2) Å respectively. The O10-H10O...O7 and O8-H8O...O11 hydrogen bond distances are 1.80 and 1.78 Å, whereas O10-H10O...O7 and O8-H8O…O11 bond angles are 166 and 167˚ respectively. The O10...O7 and O8...O11 short inter-atomic distances are 2.620(2) and 2.608(2) Å. These hydrogen bond distances

show the presence of huge and strong hydrogen bonding interactions in silver(I) complex **1** and provide additional stability to polymeric complex in the solid state.

$\{[Ag(biotin)].(SbF_6)\}_n$ (2)

The silver(I) coordination polymer **2** forms one-dimensional polymeric chain architecture as shown in Fig. **3a**, with complete atom labelling scheme. In complex **2**, each silver(I) atom is coordinated with three individual biotin molecules with trigonal planar geometry around each silver(I) atom. Two out of three biotin molecules coordinating to the same silver(I) atom through sulphur donor atom of tetrahydrothiophene group and in one case, carbonyl oxygen of valeric acid side chain group is involved for coordination, unlike to complex **1**, where ureido carbonyl oxygen atom was involved in coordination with silver(I) atom. The Ag-S and Ag-O bond distances are 2.4496(10) & 2.4192(10) and 2.440(3) Å respectively.

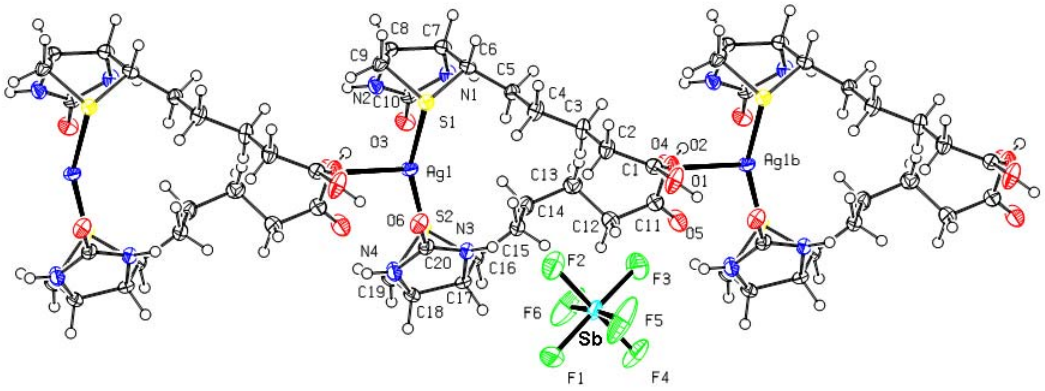

Figure 3a. Ortep view of the molecular structure of complex **2** with complete atom labelling scheme and ellipsoids are shown at 50% probability (only one anion is shown).

The S-Ag-S and S-Ag-O bond angles are 157.22(3) and 88.77(9) & 113.97(9)˚ respectively. These bond angle values around the central metal atom show much deviation from the ideal triangular planar angle of 120˚. The Ag-S bond distances are comparable to those found in complex **1**, whereas, the Ag-O bond distance is much

shorter than complex **1**. The reason for the shorter Ag-O bond distance in complex **2** is attributed to coordination of the Ag^{I} atom with the carbonyl oxygen atom of the biotin molecule. In complex **1**, the Ag(1) atom is coordinated with the ureido carbonyl oxygen and in complex **2** the Ag(1) atom is coordinated with the valeric acid carbonyl oxygen atom as described earlier. The dihedral angles between the two best planes of ureido and tetrathioether rings are 73.9(2) and 75.4(2)˚ for the two different biotin molecules coordinating with the same Ag^{I} atom. The SbF_6^- is a non-coordinating counter ion and does not show any interaction with Ag^{I} atom in complex **2**. The geometry around Sb^{V} atom is distorted octahedral. There are small differences in the individual geometry of the biotin molecules coordinating with atom Ag(1) and the free biotin molecular structure. In one case the ureido ring including the carbonyl oxygen is not as planar as that found in the free ligand molecular structure, but in the second case, the ureido ring is planar and the bond distances are comparable to those in the free biotin molecular structure.

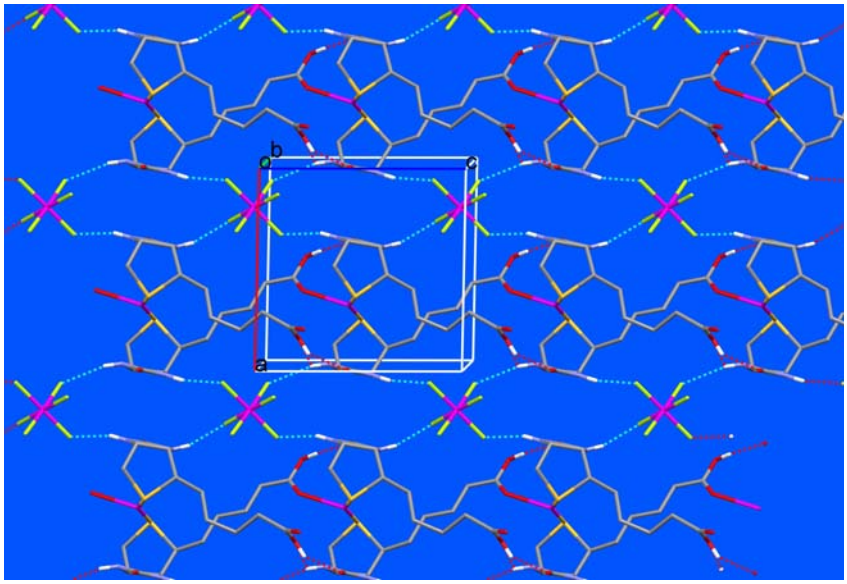

Figure 3b. View down the *b* axis of the two-dimensional network of intermolecular hydrogen bonding interactions (red and blue dotted lines) in complex **2**.

In the solid state structure of complex **2**, intermolecular O-H…O and O-H…N hydrogen bonding interactions are observed like in complex **1** and free **biotin** molecular structures, and most of the potentially available hydrogen donor atoms are utilized for hydrogen bond formation. These hydrogen bonding interactions (Table **3**) result in the formation of

two-dimensional hydrogen bonded polymeric architecture**,** as that found in complex **1**. The N2-H2N...O4, O4-H4O...O3, N1-H1N...F1, and N4-H4N...F3 hydrogen bond distances 2.60(6), 1.85, 2.09(3), and 1.95(3) Å respectively. Whereas, N2-H2N...O4, O4-H4O...O3, N1-H1N...F1, and N4-H4N...F3 hydrogen bond angles are 111(4), 159, 166(4), and 147(5)˚ respectively. The N2...O4, O4...O3, N1...F1, and N4...F3 short inter-atomic distances are 3.014(4), 2.646(4), 2.967(5), and 2.765(5) Å. The hydrogen bond distances, bond angles and inter-atomic short distances show the presence of strong non-covalent bonding forces in solid state structure of complex **2**; these types of non-covalent interactions are very useful for the extra stability of complex in the solid state.

$\{[Ag_3(biotin)_3].(PF_6)_3\}_n$ (3)

The silver(I) complex **3** forms one-dimensional polymeric chain structure as depicted in Fig**. 4a.** There are two different types of geometries observed around the two different silver(I) atoms present in the asymmetric unit. The crystallographic environment around atom Ag1 is distorted trigonal planar and three biotin molecules are coordinated to it, while the geometrical environment around atom Ag2 is distorted tetrahedral and four different biotin molecules are coordinated to it.

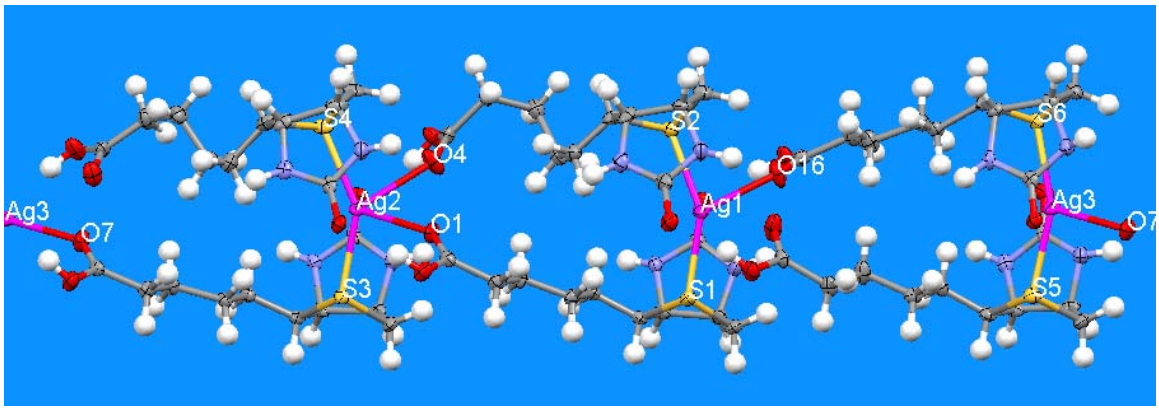

Figure 4a. View of the one-dimensional coordination polymer of complex **3** (counter ions have been removed for clarity).

In case of atom Ag1, two biotin molecules are coordinated through the sulphur atom of the thioether group and other biotin ligand molecule is coordinated through carbonyl oxygen of the valeric acid side chain group. Whereas, in case of atom Ag2, the two out of four biotin molecules are coordinated through sulphur atom of the thioether group and the other two biotin molecules are coordinated through the carbonyl oxygen of the valeric acid side chain. The carbonyl oxygen of the ureido ring does not show any coordination with the central Ag^{I} atoms in complex **3,** unlike in complex **1**. The non-coordinating behaviour of the ureido carbonyl oxygen is similar to that found in complex **2**. The molecular structure of complexes **2** and **3** are isostructural. The Ag-S and Ag-O bond distances vary from 2.4232(16) to 2.4751(16) and 2.491(4) to 2.518(5) Å. The S-Ag-O and S-Ag-S bond angles range from 80.10(12) to 128.67(12) and 147.51(6) & 157.56(5)˚. The individual geometries of biotin molecules coordinated with different Ag(I) atoms in complex **3** are comparable with free biotin molecular structure with minimal differences. The dihedral angle between the best planes of ureido and tetrathioether rings are 73.7(4), 73.6(4), 74.2(3), 73.6(4), 74.3(3), and 74.8(3)˚ for all the six biotin molecules coordinated with different silver(I) atoms in the asymmetric unit cell. In complex **3** a large number of hydrogen bonds are observed. The presence of O-H…O hydrogen bonding interactions result in the formation of a one-dimensional polymeric chain structure, as shown in Fig. **4b**.

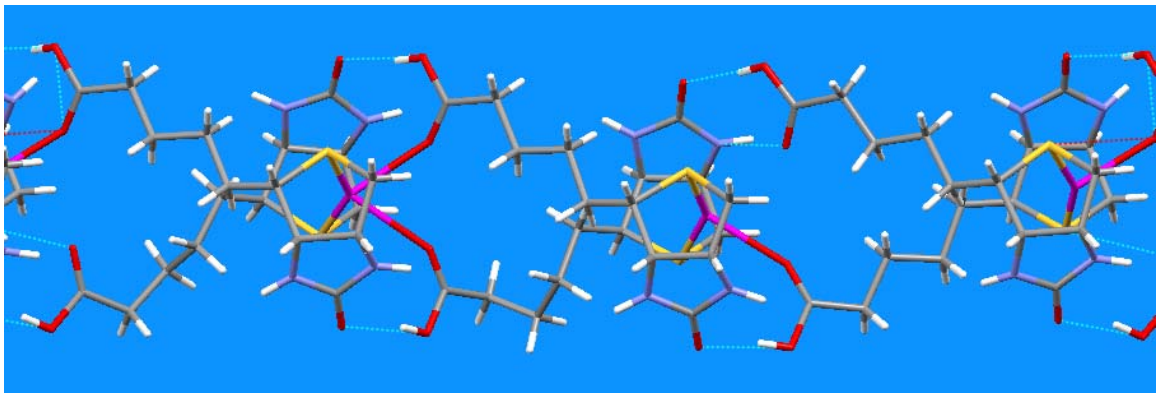

Figure 4b. Panel showing the N-H…O and O-H…O hydrogen bonding interactions (blue dotted lines) in complex **3**.

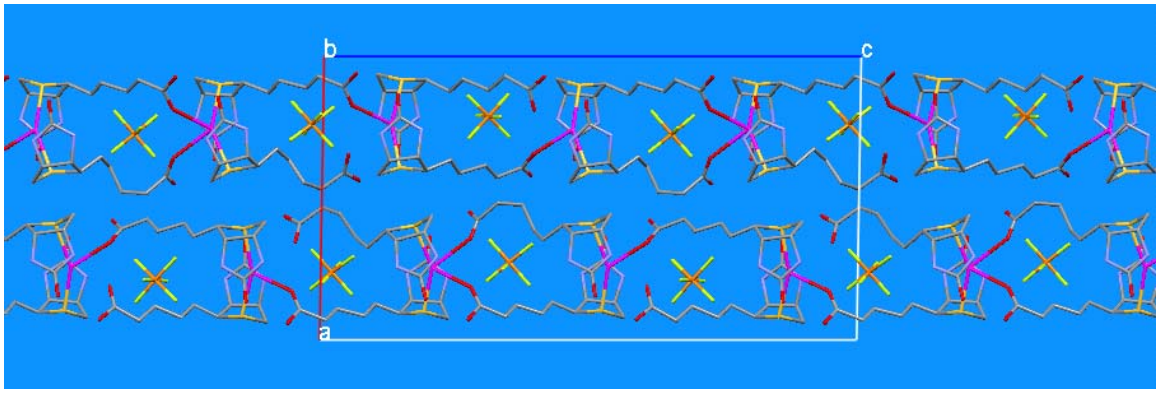

Figure 4c. View of polymeric chain structure of complex **3** along the *b*-axis.

$\{[Ag(biotin^{-})].3H_2O\}_n$ (4)

In the silver(I) coordination compound **4,** the biotin molecule is deprotonated, as shown in Fig. **5a**.

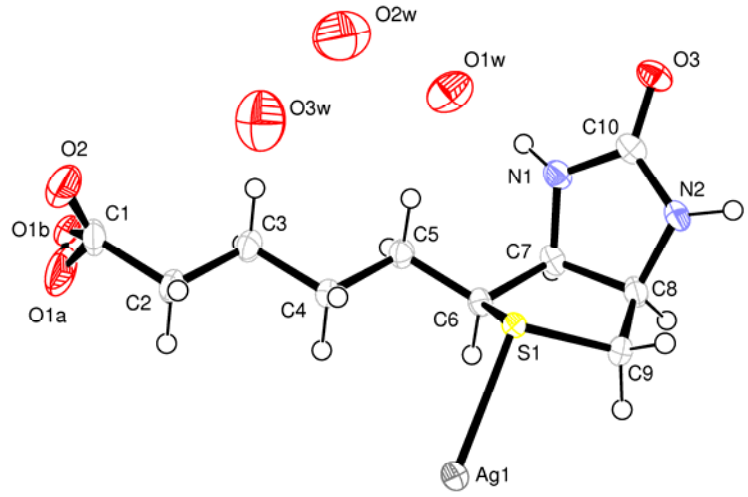

Figure 5a. View of asymmetric unit of compound **4**, with the numbering scheme and the displacement ellipsoids drawn at the 50% probability level.

In complex **4**, the silver(I) ion is coordinated to four biotin molecules. Two out of the three biotin ligand molecules coordinate via the sulphur donor atom of the tetrathioether

rings. The third coordinates via the carbonyl oxygen of the ureido group and the fourth via the carbonyl oxygen of the carboxylate group of the valeric acid side chain (Fig.**5b**).

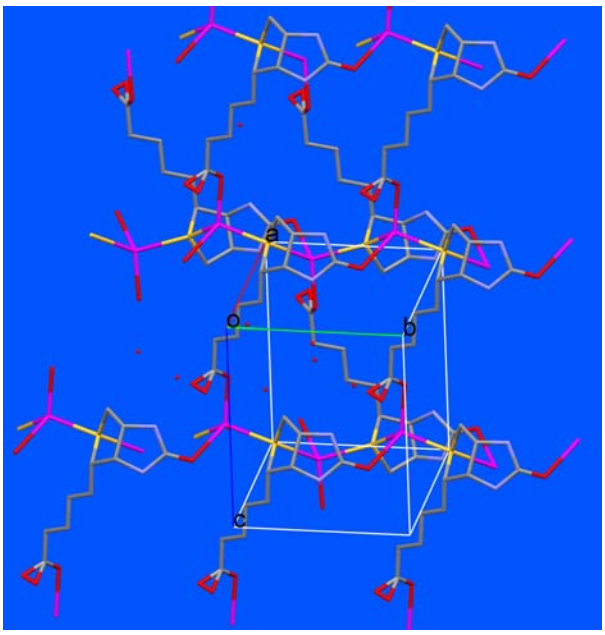

Figure 5b. A view of the two-dimensional polymer network in compound **4.**

The geometrical environment around the silver(I) atom is pseudo-tetrahedral. The Ag-S and Ag-O bond distances are 2.5147(6) & 2.5646(7) and 2.301(2)& 2.514(2) Å respectively. The S-Ag-S and O-Ag-O bond angles are 130.359(13) and 124.47(10)˚. Whereas O-Ag-S bond angles range from 82.01(5) to 118.16(9)˚. The Ag-S-Ag bond angle is 130.05(2)˚. Each sulphur atom bridges two Ag(I) atoms of the polymer framework. The bridging of Ag(I) atoms through sulphur atom is similar as that found in complex **1**. Such type of bridging behaviour of the sulphur atoms of the coordinated biotin molecules is not observed in complexes **2** & **3**. The bicyclic system of the biotin molecule is folded along the C7-C8 bond; the dihedral angle between the best planes of ureido ring and tetrathioether ring is 71.91(15)˚. The dihedral angle found in complex **4** is much smaller than that found in the free ligand molecule. Generally the individual geometry of the biotin molecules coordinating with different silver(I) ions is similar to that in biotin itself, with very small differences.

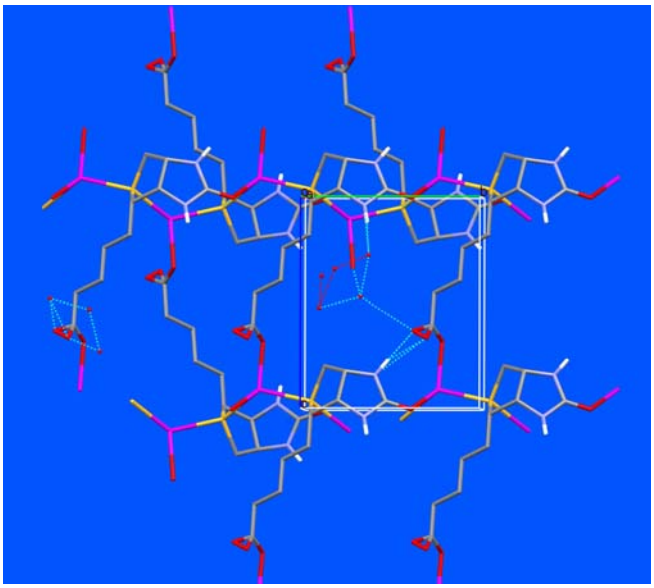

Figure 5c. A view down the *a* axis of the two-dimensional polymer network in compound **4**, showing also the N-H…O hydrogen bonds and the O…O interactions.

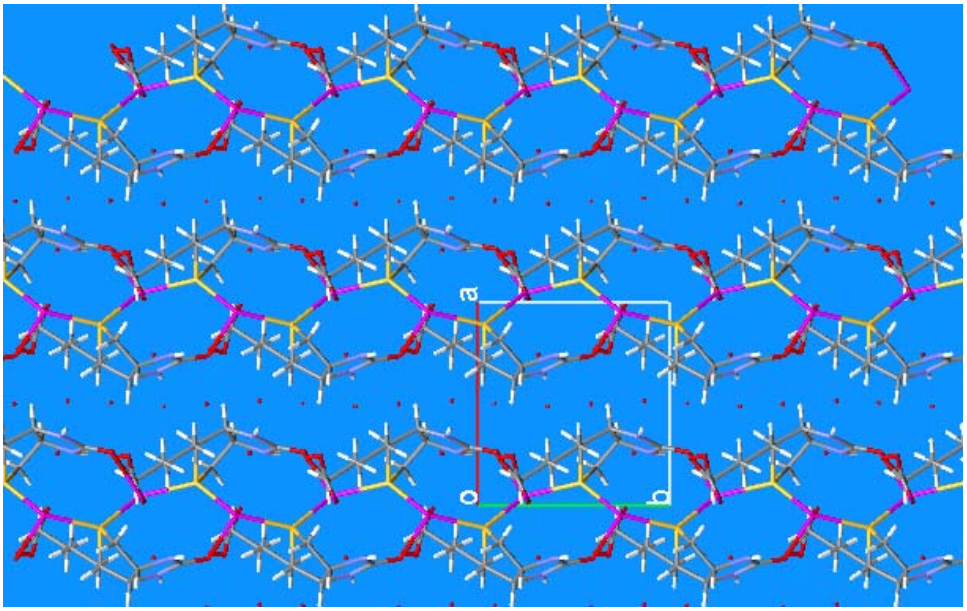

Figure 5d. View down the *c* axis, with the two-dimensional polymer structure of complex **4** lying in the *bc* plane**.** These sheets stack along the *a* axis, separated by the water molecules of crystallization, those link the 2D-sheets to form a 3D structure.

In complex **4** intermolecular hydrogen bonding interactions are observed (see Figs. **5c** and **5d**), and as in complexes **1** & **2** all potentially available hydrogen donor atoms are utilized for hydrogen bond formation. These hydrogen bonds play a major role in the construction of the three-dimensional framework structure of complex **4**.

$[Ag_2(biotin)_2(ClO_4)_2]_n$ (5)

Molecular structure of complex **5** is shown in Fig. **6a**. There are two independent silver(I) atoms and the geometry around each central metal atom is pseudo-tetrahedral with AgS_2O_2 metal core. In complex **5**, each silver(I) atom is coordinated with three individual biotin ligand molecules and biotin acts as bidentate ligand. Each silver(I) atom is coordinated with two sulphur donor atoms of the tetrathioether group and one oxygen donor atom of the ureido group from three biotin molecules as shown in Fig. **6a**. The perchlorate (ClO_4^-) counter ion also shows unusual coordination with central metal atom in complex **5**.

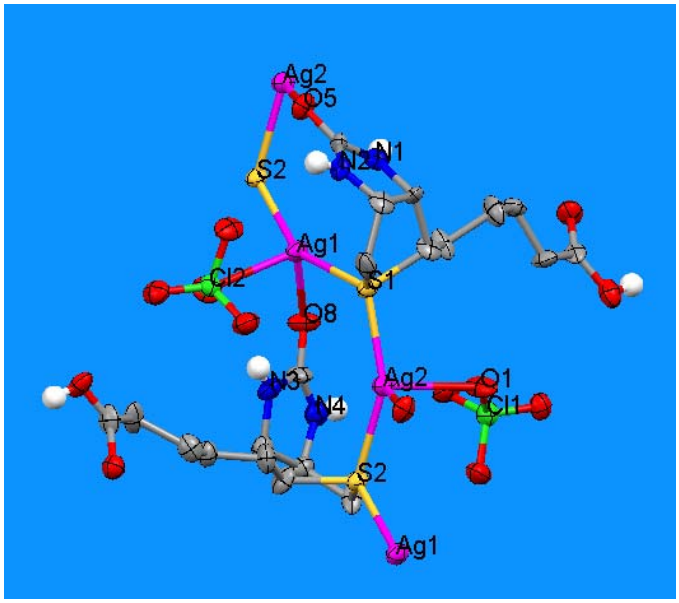

Figure 6a. View of the molecular structure of complex **5** with selected atom labelling scheme and displacement ellipsoids are shown at 50% probability.

The Ag-S bond distances range from 2.438(7) to 2.523(7) Å. The Ag-O bond distances for ureido oxgen atom are 2.32(2) and 2.402(18) Å. Whereas Ag-O bond distance for counter ion oxygen is 2.51(3) Å. The Ag-S and Ag-O bond distances for the biotin donor atoms are comparable with those in complexes **1-4**. The S-Ag-S and O-Ag-O bond angles values are 152.0(2) and 93.1(9)˚ respectively. The S-Ag-O bond angle values range from 94.2(6) to 104.7(5)˚. These bond angles values show considerable deviation from the ideal tetrahedral angle of 109.5˚.

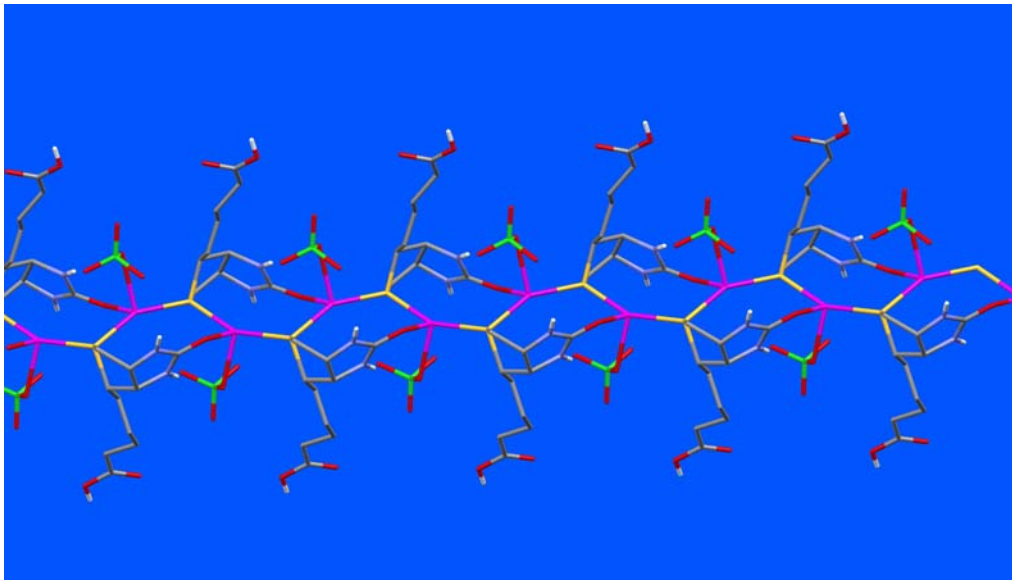

Figure 6b. A view of the one-dimensional polymeric chain structure of complex **5**.

This type of bonding behaviour of biotin leads to the formation of a one dimensional coordination polymer (Fig. **6b**). The presence of O-H…O hydrogen bonding interactions involving the carboxylic acid groups links these chains to form a two-dimensional polymeric structure. These chains are further linked by N-H…O (perchlorate) hydrogen bonds to give finally a three-dimensional network, as shown in Fig. **6c**.

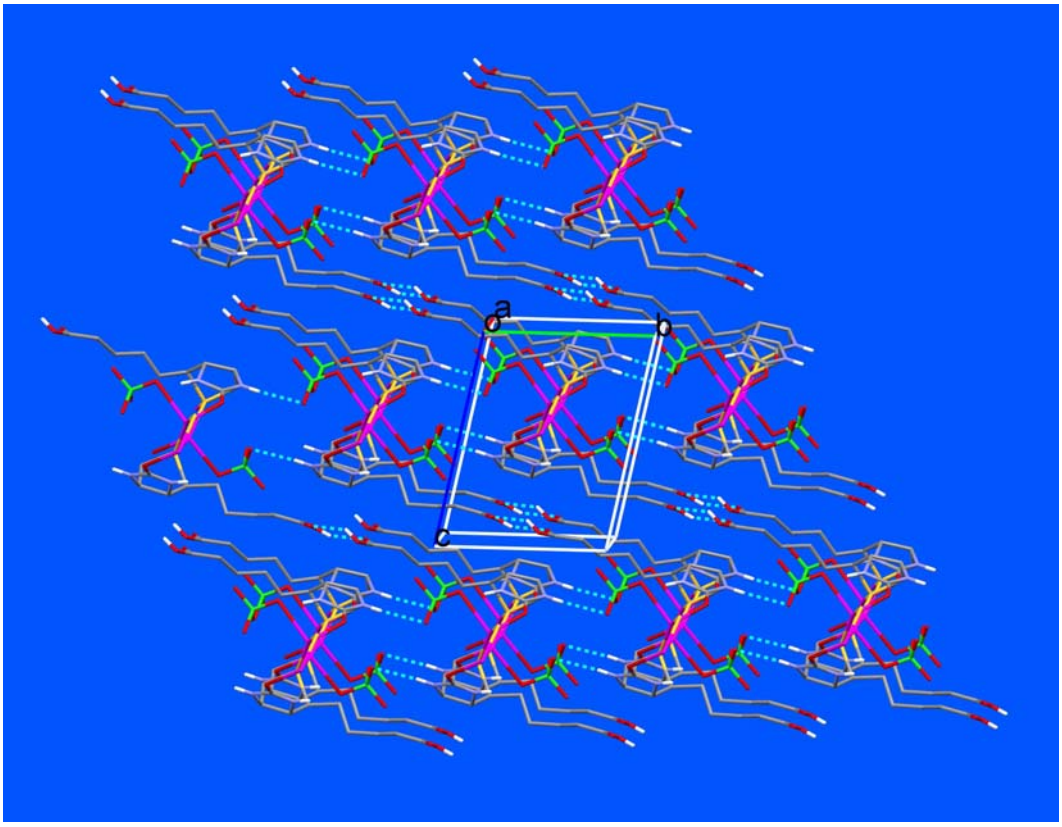

Figure 6c. View down the *a* axis of the hydrogen bonded (blue dotted lines) polymeric 3D structure of complex **5**.

Conclusions

Biotin has been used successfully to design and synthesize new silver(I) one-, two-, and three-dimensional coordination polymers via a combination of coordination bonds, hydrogen bonds. The presence of ureido, tetrathioether, and carboxylic acid groups facilitate coordination and hydrogen bond formation in the solid state of the ligand (biotin) and its silver(I) complexes. In these silver(I) complexes, each silver(I) atom is coordinated with 3 or 4 biotin molecules and the coordination sphere around the silver(I) atom varies from triangular planar to tetrahedral.

In these coordination polymer complexes **1-5**, the silver(I) coordination with sulphur atom of tetrathioether group is not surprising because of the strong tendency of the Ag^{+}

ion to act as a soft acid towards sulphur, and metal binding to carbonyl oxygen of ureido group in complexes **1**, **4** & **5** clearly indicates the nucleophilicity of the latter. In complexes **2** & **3** the carbonyl oxygen of ureido group does not show any coordination to the metal centre and only carbonyl oxygen of the valeric acid side chain group participates in coordination to the central silver(I) ion. This observation indicates that carbonyl oxygen of valeric acid is more nucleophilic than the carbonyl oxygen of the ureido group.

References

Aoki, K. & Saenger, W. (1983). *J. Inorg. Biochem.* **19,** 269-273.

Archer, E. A., Gong, H. & Krische, M. J. (2001). *Tetrahedron.* **57,** 1139-1159.

Bagautdinov, B., Kuroishi, C., Sugahara, M. & Kunishima, N. (2005). *J. Mol. Biol.* **353,** 322-333.

Blondeau, P., Lee, A. & Barboiu, M. (2005). *Inorg. Chem.* **44,** 5649-5653.

Brady, R. N., Ruis, H., McCormick, D. B. & Wright, L. D. (1966). *J. Biol. Chem.* **241,** 4717-4721.

Desiraju, G. R. (2002). *Acc. Chem. Res.* **35,** 565-573.

DeTitta, G. T., Edmonds, J. W., Stallings, W. & Donohue, J. (1976). *J. Am. Chem. Soc.* **98,** 1920-1926.

Fung, C. H., Mildvan, A. S. & Leigh, (1974). *Jr. Biochemistry.* **13,** 1160-1169.

Goodwin, D. A., Meares, C. F. & Osen, M. (1998). *J. Nuclear Medicine.* **39,** 1813-1818.

Griesser, R., Sigel, H., Wright, L. D. & McCormick, D. B. (1973). *Biochemistry.* **12,** 1917-1922.

Hadjiliadis, N. & Pneumatikakis, G. (1979). *J. Inorg. Biochem.* **10,** 215-224.

Inverarity, I. A., Viguier, R. F. H., Cohen, P. & Hulme, A. N. (2007). *Bioconjugate Chem.* **18,** 1593-1603.

Knowles, J. R. (1989*). Annu. Rev. Biochem.* **58,** 195-221.

Leininger, S., Olenyuk, B. & Stang, P. (2000). *Chem. Rev.* **100,** 853-908.

Lett, R. & Marquet, A. (1971). *Tetrahedron Lett.* 2851-2854.

Lo, K. K.-W. & Lau, J. S.-Y. (2007). *Inorg. Chem.* **46,** 700-709.

Lo, K. K.-W. & Lee, T. K.-M. (2007). *Inorg. Chim. Acta.* **360,** 293-302.

Moss, J. & Lane, M. D. (1971). *Advan. Enzymol.* **35,** 321-442.

Northrop, D. B. & Wood, H. G. (1969). *J. Biol. Chem.* **244,** 5801-5807.

Ruis, H., Brady, R. N., McCormick, D. B. & Wright, L. D. (1968). *J. Biol. Chem.* **243,** 547-551.

Scrutton, M. C., Utter, M. F. & Mildvan, A. S. (1966). *J. Biol. Chem.* **241,** 3480-3487.

Seidel, S. R. & Stang, P. J. (2002). *Acc. Chem. Res.* **35,** 972-983.

Sigel, H., McCormick, D. B., Griesser, R., Prijis, B. & Wright. L. D. (1969). *Biochemistry.* **8,** 2687-2695.

Sigel, H. & Scheller, K. H. (1982). *J. Inorg. Biochem.* **16,** 297-310.

Wood, H. G. & Zwolinski, G. K. (1976). *Crit. Rev. Biochem.* **4,** 47-122.

Chapter 4:

Synthesis and Crystal Engineering of Ortho-, Meta-, and Para-Pyridyl Oximes and Silver(I)-Oxime Networks

Introduction

Elemental silver and silver salts have been used for decades as antimicrobial agents in curative and preventive health care.[1-8] The chemistry of coordination polymers has attracted much attention as they have potential as functional materials in the fields of physi- and chemical-sorption, catalysis and optics, for example.[9-11] The silver(I) complexes and coordination polymers having silver(I)-N and silver(I)-O bonds show potential antimicrobial activities against many microorganisms.[12-17] The effective antimicrobial activities of silver(I)-N and silver(I)-O bonding complexes is thought to be due to the weak silver(I)-N/O bonds, which are easily replaced by biomolecules especially those having thiol groups. The rapidly growing area of coordination polymers and polymeric materials based on non-covalent interactions of metal cations with organic ligands, has given rise to a wide variety of fascinating one-, two-, and three-dimensional polymeric structures. The high degree of design arises from the coupling of the well understood coordination properties of the individual metal ions and highly developed ligand syntheses within the newer areas of supramolecular chemistry and crystal engineering.[18-23] In the synthesis of crystalline materials by design, the assembly of molecular units in predefined arrangements is a key goal. Directional inter- and intra-molecular interactions are the primary tools in achieving this goal, and π-π interactions and hydrogen bonding interactions are currently the best among them.[24-25] The controlled self assembly of one-, two-, and three-dimensional polymer species with potential applications has been the subject of our recent interest in research. Normally rigid components (ligand and metal) are most commonly used for rational construction of various molecular architectures. We have adopted a different approach using flexible building blocks in order to gain access to self design architectures and topologies, not easily accessible from more rigid precursors. We have found that oxime derivatives are particularly useful components for the construction of some interesting coordination polymers with physically and potentially useful architectures.

The new organic ligand molecules ortho-, meta-, and para-pyridyloximinoacetoacetates (**L1, L2** and **L3**), prepared previously by Yi Wang of our group, are shown in Scheme **1**.

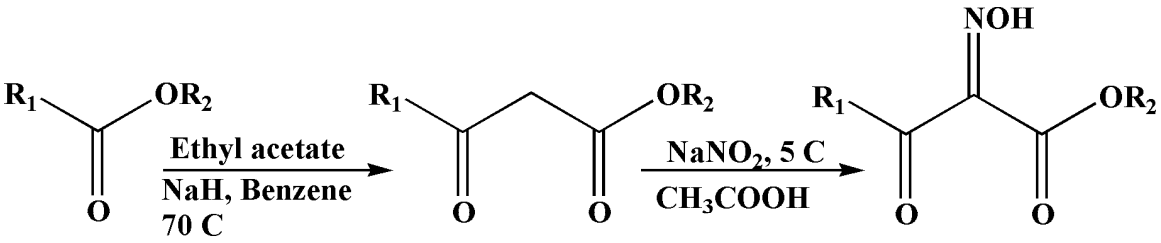

R1 = ortho-, meta-, or para- substituted pyridines
&
R2 = Ethyl or methyl group

Scheme 1. Synthesis of ortho-, meta-, and para- pyridyloximinoacetoacetates

General synthesis of the ligands L1, L2 and L3

To a mechanically stirred solution of 3-oxo-3-(2-pyridyl)-propanoic acid ethyl ester (6.4 g, 0.033 mmol) and glacial acetic acid (4.7 g) was added 6.5 ml aqueous solution of sodium acetate (2.5 g) during a period of one hour, maintaining the temperature of the solution at 5ºC. The solution was stirred for an additional two hours until a large quantity of a white solid had been formed. The temperature of the solution was raised to room temperature on leaving the solution to stand in ambient temperature. The mixture was filtered, well washed with water, and dried to give a white solid in good yield for **L1**.
The synthesis of **L2** & **L3** was carried by following the same procedure as described for **L1**. Methyl nicotinoylacetate and ethyl isonicotinoylacetate were used, instead of 3-oxo-3-(2-pyridyl)-propanoic acid ethyl ester, for the synthesis of **L2** and **L3**, respectively.

Spectroscopic and Elemental analysis:

The ligands 2-Hydroxyimino-3-oxo-3-(2-pyridyl)-propanoic acid ethyl ester (**L1**), 2-Hydroxyimino-3-oxo-3-(3-pyridyl)-propanoic acid methyl ester (**L2**), and 2-

Hydroxyimino-3-oxo-3-(4-pyridyl)-propanoic acid ethyl ester (**L3**) have been fully characterized by NMR and IR spectroscopic data and elemental analysis.

L1: δ_H (200 MHz, CD_3OD) 8.69-8.65(m, 1H, PyH), 8.10-7.98(m, 2H, PyH), 7.68-7.61(m, 1H, PyH), 4.27(q, J = 7.1 Hz, 2H, CH_2), 1.23(t, J = 7.1 Hz, CH_3) ppm; υ_{max} (KBr): 3123, 2998, 2754, 1729, 1691, 1631, 1589, 1471, 1442, 1328, 1272, 1140, 1024, 941, 839, 789 cm^{-1}; Elemtal analysis $C_{10}H_{10}N_2O_4$(222.20) calcd. C 54.05 H 4.54 N 12.61%; found C 53.90 H 4.58 N 12.18%;

L2: δ_H (400 MHz, $CDCL_3$) 15.94(br s, 1H, NOH), 9.63-9.62(m, 1H, PyH), 8.71-8.70(m, 1H, PyH), 8.42-8.40(m, 1H, PyH), 7.65-7.58(m, 1H, PyH), 3.99(s, 3H, CH_3) ppm; υ_{max} (KBr): 3110, 3005, 2497, 1916, 1727, 1687, 1597, 1494, 1474, 1438, 1334, 1260, 1139, 1030, 964, 833, 796, 756 cm^{-1}; Elemtal analysis $C_9H_8N_2O_4$ (208.17) calcd. C 51.93 H 3.87 N 13.46%; found C 51.66 H 3.84 N 13.43%;

L3: δ_H (200 MHz, CD_3OD) 8.84-8.81(m, 2H, PyH), 7.79-7.76(m, 2H, PyH), 4.30(q, J = 7.2 Hz, 2H, CH_2), 1.27(t, J = 7.2 Hz, CH_3) ppm; υ_{max} (KBr): 3079, 2990, 1732, 1651, 1625, 1597, 1555, 1501, 1475, 1445, 1382, 1339, 1203, 1028, 995, 827, 746 cm^{-1}; Elemtal analysis $C_{10}H_{10}N_2O_4$(222.20) calcd. C 54.05 H 4.54 N 12.61%; found C 53.88 H 4.52 N 12.32% (**L3**).

Silver(I) complexes **1-3** were fully characterized by spectroscopic data and elemental analysis.

Complex 1: Reaction of $AgNO_3$ with meta-pyridyl oximinoacetoacetate (**L2**) in ethanol/water gave the corresponding silver(I) complex $[Ag(L2)_2]\ NO_3$ (**1)**.

IR, υ_{max} (KBr): 3073, 2984, 1722, 1631, 1605, 1581, 1485, 1455, 1372, 1319, 1223, 1009, 971, 823, 742 cm^{-1}; Elemtal analysis $C_{18}H_{16}AgN_5O_{11}$(586.23) calcd. C 36.83 H 2.72 N 11.94%; found C 36.88 H 2.69 N 11.93%;

Complex 2: The reaction of **L2** in ethanol with AgX (X= ClO_4^-, BF_4^-, SbF_6^-, PF_6^-, CH_3COO^-) in water gave pale yellow plate like crystals in good yield of the silver(I) complex $[Ag_2(L2^-)_2(L2)_2]$ (**2)**. IR υ_{max} (KBr): 3071, 2986, 1723, 1635, 1606, 1583, 1489, 1445, 1378, 1325, 1228, 1017, 989, 835, 735 cm^{-1}; Elemtal analysis

$C_{36}H_{30}Ag_2N_8O_{16}$(1046.6) calcd. C 41.28 H 2.86 N 10.70%; found C 41.17 H 2.76 N 10.75%;

Complex 3: Following the same procedure as described above for complex **2** a crystalline product was obtained by the reaction of **L3** with $AgNO_3$, and other silver(I) salts containing non-coordinating anions, $[Ag_2(L2^-)_2(L2)_2]$ (**3)**. IR υ_{max} (KBr): 3068, 2987, 1721, 1645, 1608, 1598, 1543, 1512, 1477, 1453, 1386, 1349, 1217, 1017, 982, 835, 743 cm^{-1}; Elemtal analysis $C_{20}H_{19}AgN_4O_8$(551.26) calcd. C 43.53 H 3.45 N 10.15%; found C 43.66 H 3.41 N 10.22%.

X-ray Crystallography.

The intensity data were collected at 173K on either, a one circle (ϕ scans)[1], or a two circle (ϕ and ω scans)[2] Stoe Image Plate Diffraction System, using MoKα graphite monochromated radiation. The structures were solved by Direct methods using the program SHELXS-97[3]. The refinement and all further calculations were carried out using SHELXL-97[3]. The H-atoms were either located from Fourier difference maps and freely refined or included in calculated positions and treated as riding atoms using SHELXL default parameters. The non-H atoms were refined anisotropically, using weighted full-matrix least-squares on F^2. In one case a DIFABS absorption correction was applied using the DELrefABS routine in PLATON[4]. A summary of the crystal data and refinement details for ligands **L1-L3** and compounds **1-3** are given in Table 1, and selected bond lengths and angles are listed in Table 2. Details of the hydrogen bonding are given in Table 3.

1) Stoe & Cie (2000) IPDS-I Bedienungshandbuch. Stoe & Cie GmbH, Darmstadt, Germany.

2) Stoe & Cie. (2006) *X-Area V1.35 & X-RED32 V1.31 Software*. Stoe & Cie GmbH, Darmstadt, Germany.

3) G. M. Sheldrick (2008). Acta Crystallgr. A64, 112-122.

4) A. L. Spek (2003). J.Appl.Cryst. 36, 7-13

Table 1. Summary of crystal data and structure refinement details for ligands **L1-L3** and complexes **1–3**

$\{^{a}$ **R1** $= \Sigma||F_O| - |F_C||/\Sigma|F_O|$. ^{b} **wR2** $= [\Sigma w(F_O^2 - F_C^2)^2/\Sigma wF_O^4]^{1/2}\}$

	L1	**L2**
Formula	$C_{10}H_{10}N_2O_4$	$C_9H_8N_2O_4$
M	222.20	208.17
Wavelength/Å	0.71073	0.71073
Temperature/K	173	173
Crystal symmetry	Monoclinic	Orthorhombic
Space group	C 2/c	P 2_1 2_1 2_1
a,Å	20.7192(19)	5.7247(9)
b,Å	8.1493(4)	9.5387(12)
c,Å	14.3365(13)	17.044(3)
α,deg	90	90
β,deg	118.732(6)	90
γ,deg	90	90
V/ Å^3	2122.6(3)	930.7(2)
Z	8	4
D_c/Mg m^{-3}	1.391	1.486
μ(Mo-Kα)/mm^{-1}	0.109	0.119
F(000)	928	432
Crystal size/mm	0.50 x 0.26 x 0.14	0.40 x 0.30 x 0.08
θ Limits/°	1.62 - 29.59	1.39 – 26.14
Measured reflections	14073	5933
Unique reflections(R_{int})	2859(0.0411)	1729(0.0716)
Observed reflections	2364	1492
Goodness of fit on F^2	1.038	0.966
$R_1(F)$,^{a}[$I > 2\sigma(I)$]	0.0365	0.0391
w$R_2(F^2)$,^{b}[$I > 2\sigma(I)$]	0.0926	0.0956

Table 1 cont,d

	L3	**1**
Formula	$C_{10}H_{10}N_2O_4$	$C_{18}H_{16}AgN_5O_{11}$
M	222.20	586.23
Wavelength/Å	0.71073	0.71073
Temperature/K	173	173
Crystal symmetry	Monoclinic	Monoclinic
Space group	P 2_1/c	C 2/c
a,Å	13.0334(14)	17.8112(10)
b,Å	5.6646(3)	8.4799(6)
c,Å	14.4111(14)	14.9098(8)
α,deg	90	90
β,deg	99.175(8)	100.616(4)
γ,deg	90	90
V/ Å^3	1050.34(16)	2213.4(2)
Z	4	4
D_c/Mg m^{-3}	1.405	1.759
μ(Mo-Kα)/mm^{-1}	0.111	0.982
F(000)	464	1176
Crystal size/mm	0.45 x 0.35 x 0.14	0.40 x 0.10 x 0.10
θ Limits/°	1.80 - 29.58	2.33 - 29.51
Measured reflections	14471	14819
Unique reflections(R_{int})	2837(0.0614)	2989(0.0368)
Observed reflections	2237	2595
Goodness of fit on F^2	1.036	0.678
$R_1(F)$,[a] $[I > 2\sigma(I)]$	0.0399	0.0267
w$R_2(F^2)$,[b] $[I > 2\sigma(I)]$	0.0991	0.0787

Table 1 cont,d

	2	3
Formula	$C_{36}H_{30}Ag_2N_8O_{16}$	$C_{20}H_{19}AgN_4O_8$
M	1046.4	551.26
Wavelength/Å	0.71073	0.71073
Temperature/K	173	173
Crystal symmetry	Orthorhombic	Orthorhombic
Space group *a*,Å	P b c a	F d d 2
a,Å	8.5697(4)	34.376(2)
b,Å	21.4134(7)	16.8249(9)
c,Å	21.3474(8)	7.7317(5)
α,deg	90	90
β,deg	90	90
γ,deg	90	90
V/ $Å^3$	3917.4(3)	4471.8(5)
Z	4	8
D_c/Mg m^{-3}	1.774	1.638
μ(Mo-Kα)/mm^{-1}	1.085	0.955
F(000)	2096	2224
Crystal size/mm	0.30 x 0.30 x 0.09	0.27 x 0.18 x 0.14
θ Limits/°	1.91 - 29.64	2.37 - 29.57
Measured reflections	46616	14969
Unique reflections(R_{int})	5293(0.0403)	2986(0.0338)
Observed reflections	4718	2837
Goodness of fit on F^2	1.043	1.075
$R_1(F)$,[a][$I > 2\sigma(I)$]	0.0225	0.0297
wR_2 (F^2),[b][$I > 2\sigma(I)$]	0.0528	0.0776

Results and Discussion

Suitable single crystals of ligands **L1**, **L2** and **L3** for X-ray diffraction analysis were prepared by recrystallization from solutions in ethanol and a small amount of water. The X-ray crystallographic results are consistent with the elemental analysis results and spectroscopic data. The bond lengths, bond angles in the solid state structures of these organic compounds are similar and no significant differences were observed. However, the carboxylate moiety of ligand **L3** presents a different orientation with respect to the pyridine ring than that found in **L1** or **L2**. The three molecules are T-shaped with respect to the different groups (pyridyl versus the oxime and acetate).

The molecular structure of **L1, L2** and **L3** are shown in Fig. **1** below:

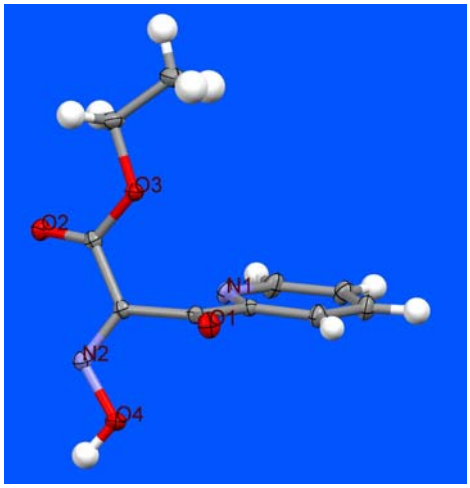

L1

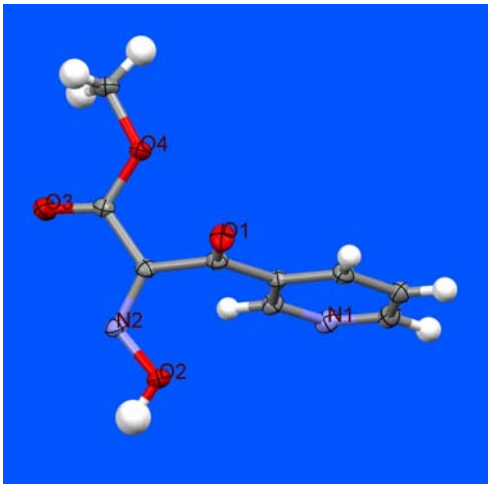

L2

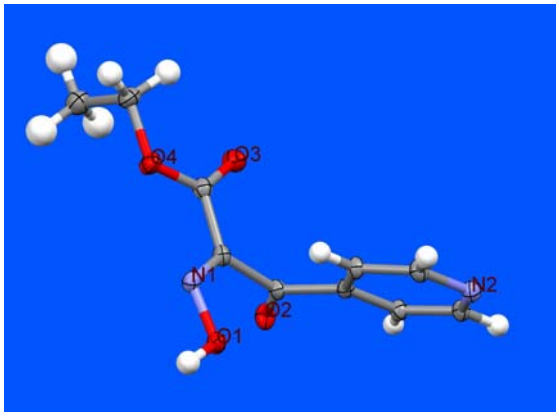

L3

Figure 1. The molecular structures of ligands **L1**, **L2** and **L3**.

Ligand L1

In the solid state the O-H…O intermolecular hydrogen bonding interaction results in the formation of a zigzag polymeric chain, extending in the *b* direction, as shown in Figs. **1a, b** and **c**.

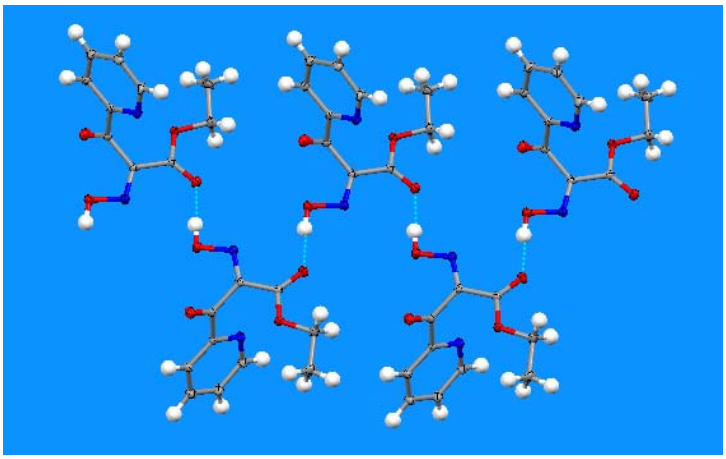

Figure 1a. A view of the O-H…O hydrogen bonding interactions in **L1**.

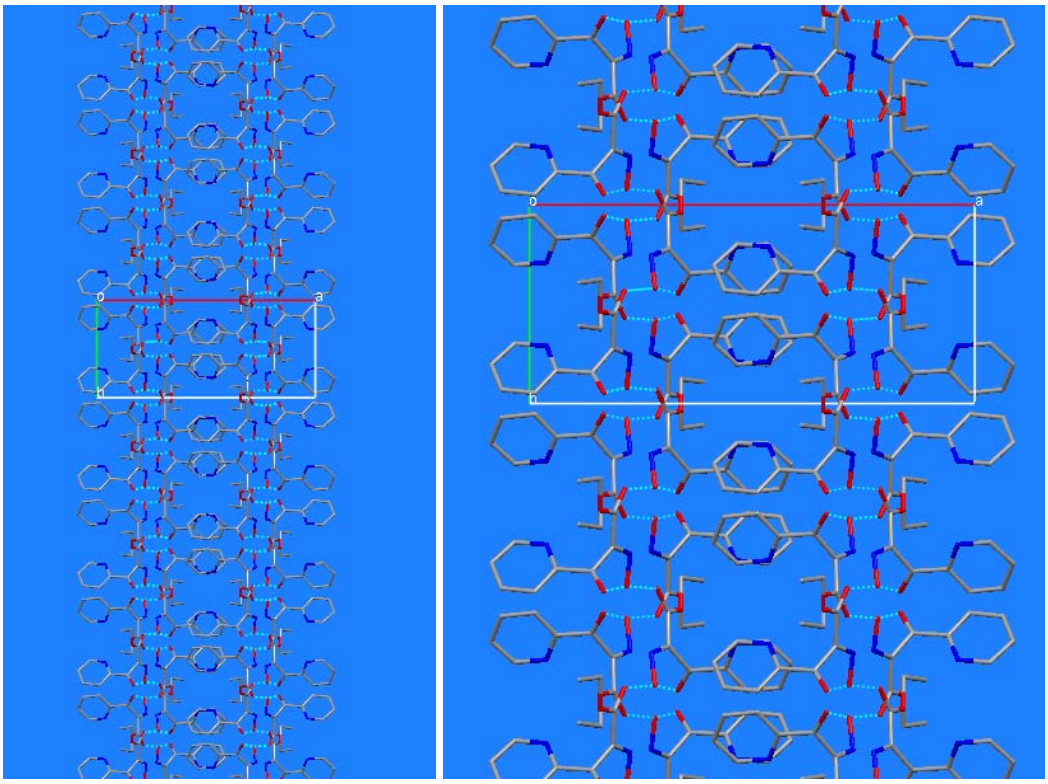

(**1b**) (**1c**)

Figure 1b & 1c. Panel **1b** showing the hydrogen bonded polymeric chain structure of **L1; 1c** is an enlarged view of **1b**.

Ligand L2

The most notable difference between the molecular structure of **L2** and **L1** is the presence of O-H…N hydrogen bonding interactions instead of O-H…O as that found in **L1** (Figs. **2a-c**). These hydrogen bonding interactions result in the formation of single stranded helical DNA-like polymeric structure, as shown in Fig. **2c**.

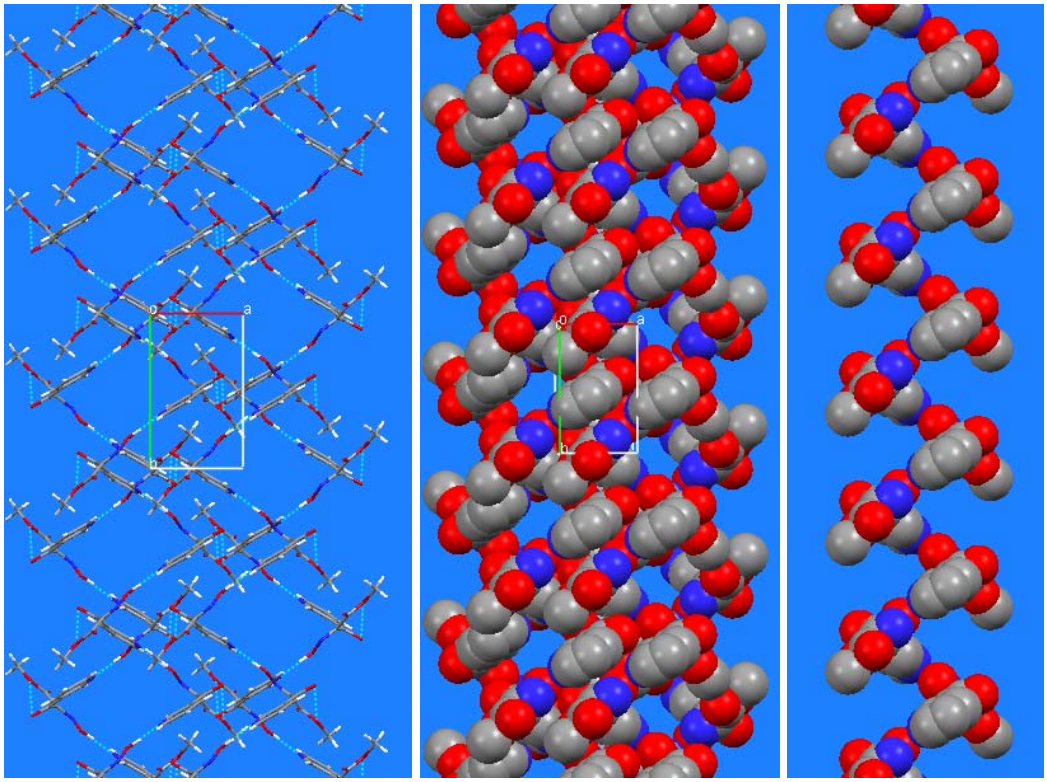

(**2a**) (**2b**) (**2c**)

Figure 2a-c. Panel **2a** showing the packing diagram of hydrogen bonded polymeric chain structure, and **2b** is showing the presence of pores in this one-dimensional polymeric network by space filled diagram; panel **2c** shows that the hydrogen bonding interactions result single stranded DNA like network in the solid state of organic ligand **L2**.

Ligand L3

The molecular structure of **L3** is more similar to **L2** than **L1**. The presence of O-H…N hydrogen bonding (Fig. **3a**) interactions result in the formation of a helical polymeric chain, as also found in **L2**, and as shown in Figs. **3c** and **3d**.

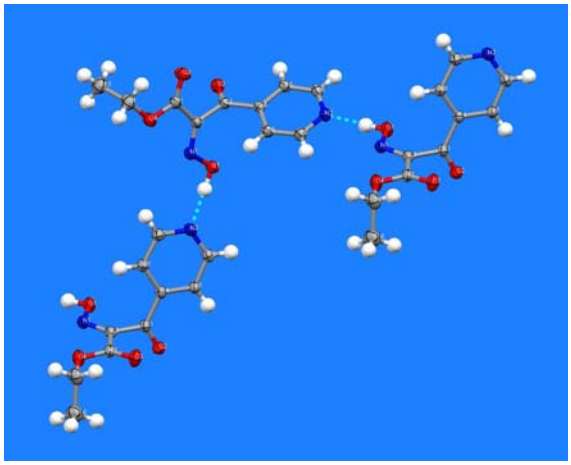

Figure 3a. Representative view of the molecular structure of **L3** with O-H…N hydrogen bonding interactions.

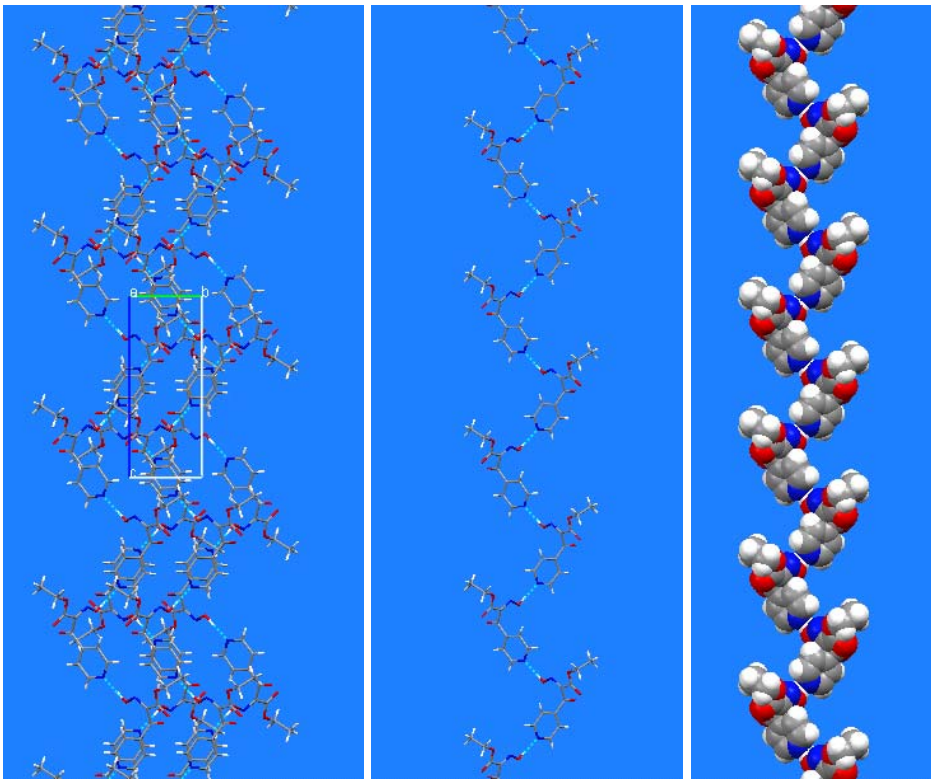

(**3b**) (**3c**) (**3d**)

Figure 3b–3d. Panel **3b** showing the CPK view of the hydrogen bonded polymeric chain structure of **L3** along *a* axis; Whereas, pattern **3c** & **3d** depicts the single stranded helical DNA like structure of the organic molecule of **L3**.

Complex 1

Reaction of $AgNO_3$ with meta-pyridyl oximinoacetoacetate in ethanol/water gave the corresponding silver(I) complex $[Ag(L2)_2].NO_3$ (**1)** containing **L2**; acting as a monodentate ligand. The crystal structure analysis revealed that the molecular structure is consistent with the elemental analysis and spectroscopic data. The prospective views of the molecular structure of compound **1** are shown in Figs. **4a-e**.

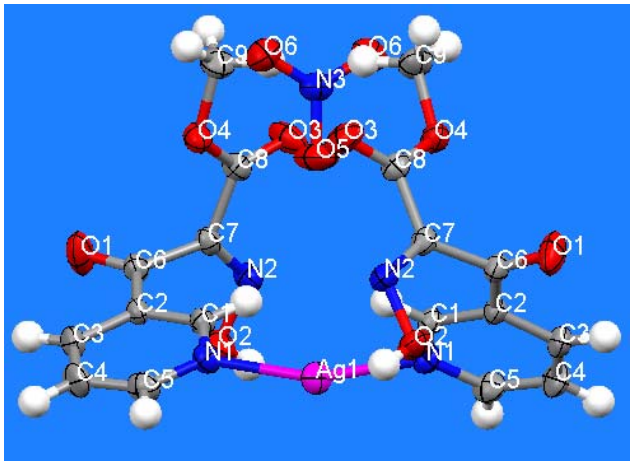

Figure 4a. View of the molecular structure of complex **1** with complete atom labelling Scheme.

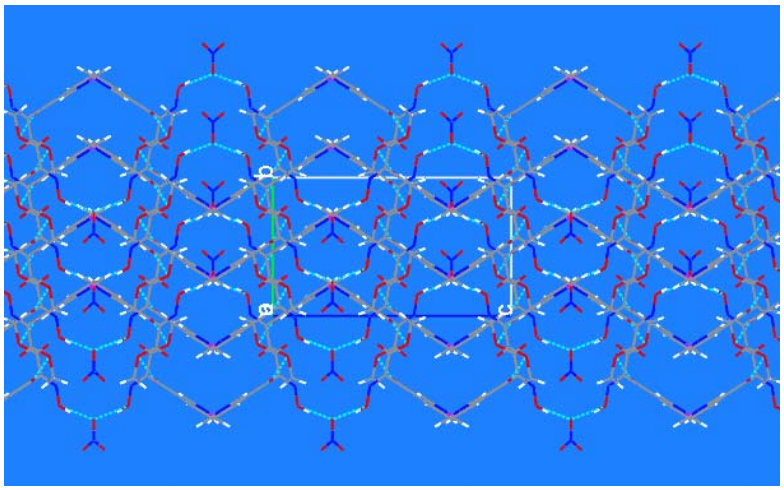

(**4b**)

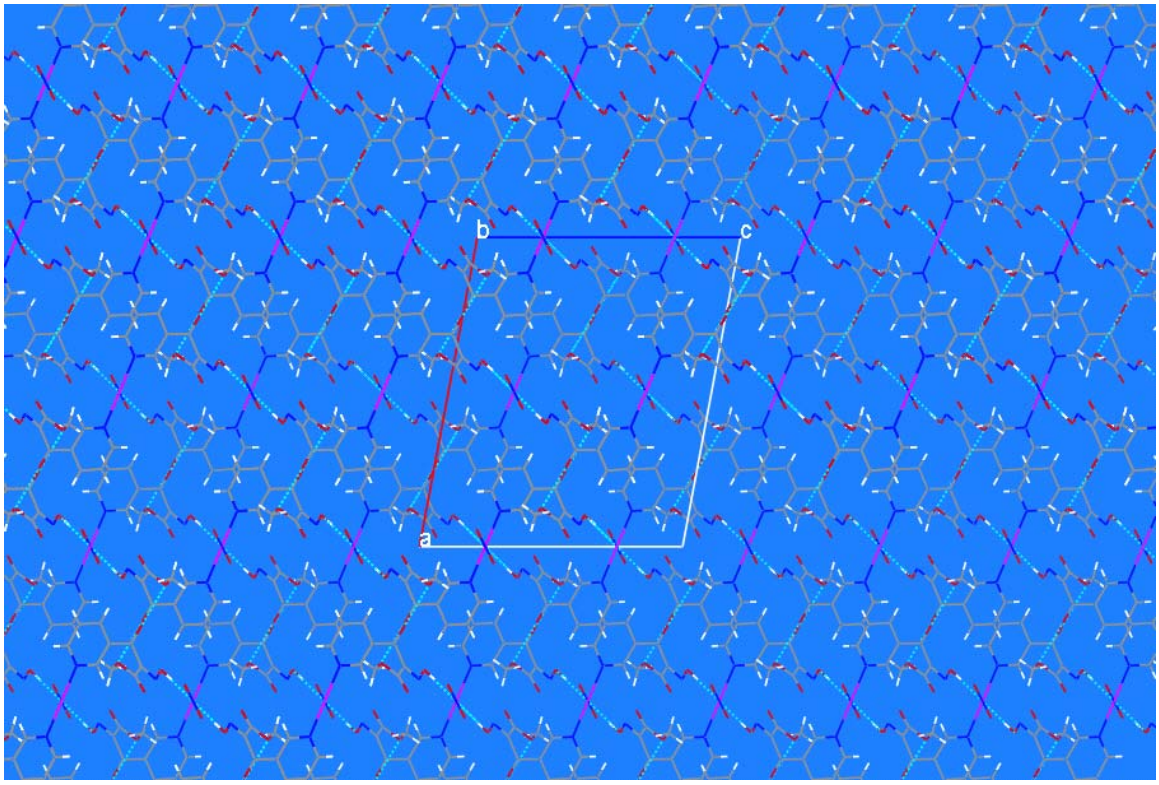

(**4c**)

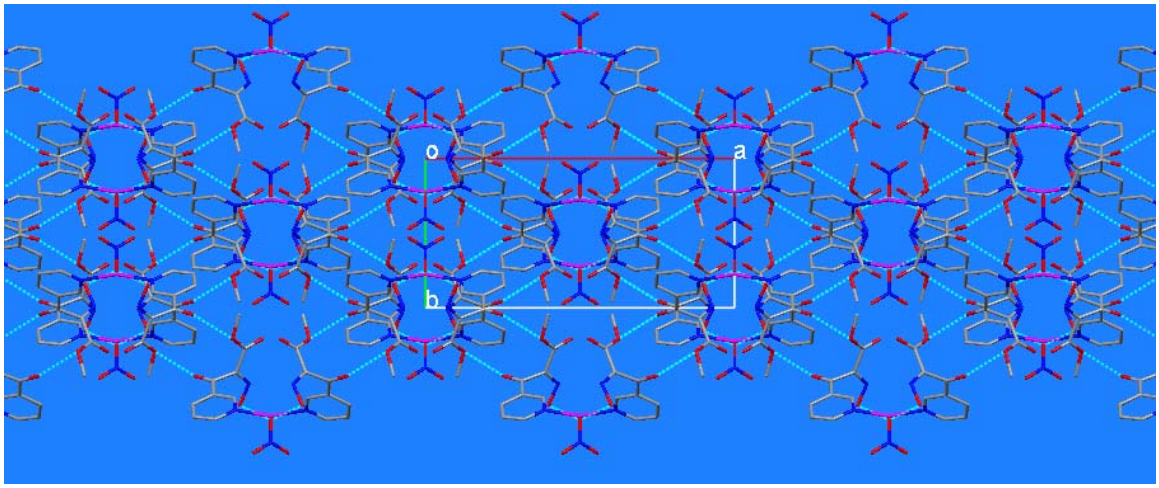

(**4d**)

Figure 4b–4d. Crystal packing views of the two-dimensional hydrogen bonded polymeric structure of complex **1** along the *a*, *b* & *c* axes, respectively.

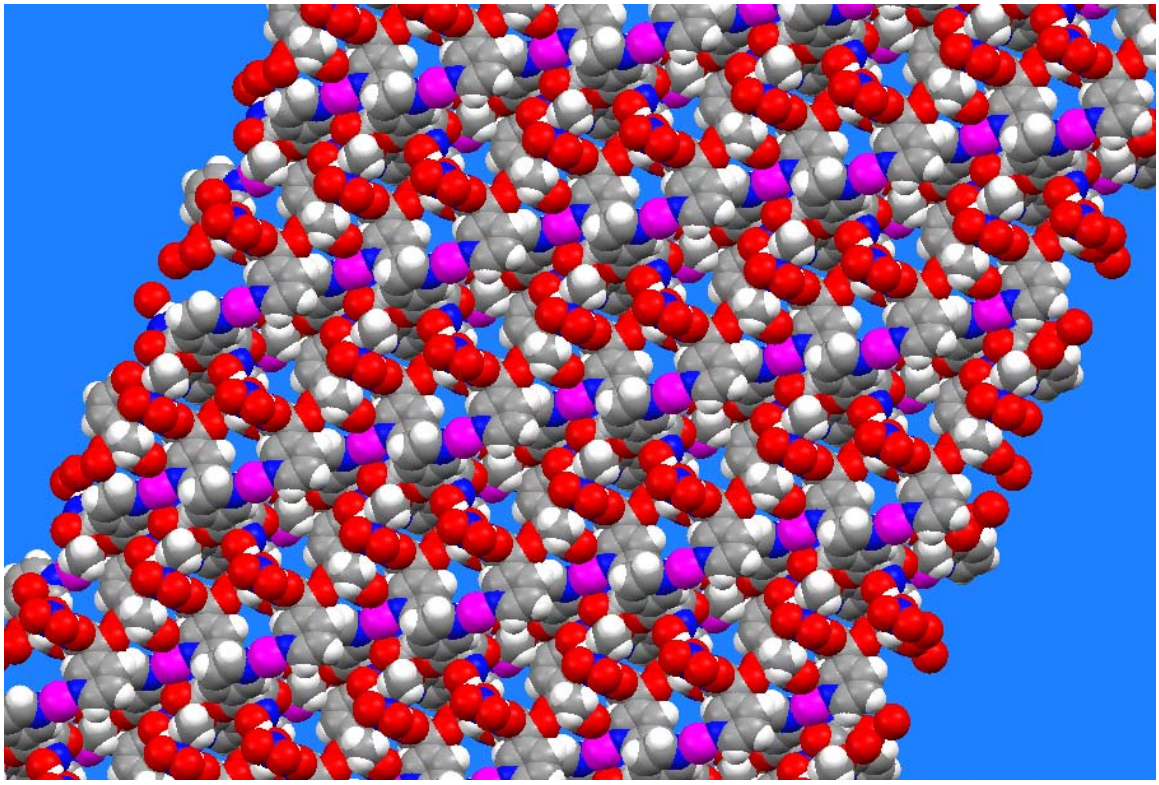

Figure 4e. Panel showing the presence of pores in the two-dimensional coordination polymer network of silver(I) compound **2** by a space filled diagram.

The geometrical environment around silver(I) is linear and the central metal atom in this complex lies on a 2-fold axis. The Ag-N bond distance is 2.2104(17) Å and the N-Ag-N bond angle is 162.06(9)º. The bond angles values show considerable deviation from the ideal linear angle of 180º. The nitrate counter ion is also present on a C_2 symmetry axis and does not show any coordination with the metal centre. The presence of high electronegative atoms (oxygen and nitrogen) in ligand **L2** and the anion results in numerous hydrogen bonding interactions in the solid state structure of compound **1**. Due to O-H…O hydrogen bonding the nitrate ion seems to be trapped between the two **L2** ligand molecules coordinated to the silver(I) atom, as shown in Fig. **4a-b** & **d**. These weak intermolecular interactions result in the formation of a two-dimensional helical hydrogen bonded polymeric chain structure, as shown in the Figs. **4b-4d**.

Table 2. Selected bond lengths and bond angles (Å, º) for **L1**, **L2** & **L3** and complexes **1**, **2** and **3**

Bond lengths (Å)		Bond angles (˚)	
L1			
O(1)-C(6)	1.2096(13)	C(8)-O(3)-C(9)	117.15(8)
O(2)-C(8)	1.2099(12)	C(5)-N(1)-C(1)	116.86(9)
O(3)-C(8)	1.3239(12)	C(7)-N(2)-O(4)	110.65(8)
O(3)-C(9)	1.4582(13)	N(1)-C(1)-C(2)	123.50(11)
O(4)-N(2)	1.3836(12)	N(1)-C(5)-C(4)	123.84(9)
N(1)-C(5)	1.3377(13)	N(1)-C(5)-C(6)	115.63(8)
N(1)-C(1)	1.3395(14)	O(1)-C(6)-C(5)	122.89(9)
L2			
O(1)-C(6)	1.211(2)	C(8)-O(4)-C(9)	116.55(16)
O(2)-N(2)	1.369(2)	C(1)-N(1)-C(5)	117.3(2)
O(2)-H(2O)	0.910(19)	C(7)-N(2)-O(2)	110.47(17)
O(3)-C(8)	1.200(3)	N(1)-C(1)-C(2)	123.6(2)
O(4)-C(8)	1.325(2)	N(2)-C(7)-C(8)	115.87(18)
O(4)-C(9)	1.450(3)	N(2)-C(7)-C(6)	122.76(18)
N(1)-C(1)	1.334(3)	O(4)-C(8)-C(7)	110.16(17)
N(1)-C(5)	1.346(3)		
L3			
O(1)-N(1)	1.3677(13)	C(1)-O(4)-C(9)	116.52(10)
O(2)-C(3)	1.2078(15)	C(2)-N(1)-O(1)	111.33(9)
O(3)-C(1)	1.2070(15)	C(7)-N(2)-C(6)	118.09(10)
O(4)-C(1)	1.3288(14)	O(3)-C(1)-O(4)	125.22(12)
O(4)-C(9)	1.4591(17)	O(3)-C(1)-C(2)	121.04(11)
N(1)-C(2)	1.2865(15)	O(4)-C(1)-C(2)	113.71(10)
N(2)-C(7)	1.3358(16)	N(1)-C(2)-C(1)	120.15(10)

1			
Ag(1)-N(1)	2.2104(17)	N(1)-Ag(1)-N(1)#1	162.06(9)
Symmetry operation;			
#1 -x, y, -z+1/2			
2			
Ag(1)-N(3)	2.2928(12)	N(3)-Ag(1)-N(1)	119.59(4)
Ag(1)-N(1)	2.3240(12)	N(3)-Ag(1)-N(4)	119.60(4)
Ag(1)-N(4)	2.3882(13)	N(1)-Ag(1)-N(4)	119.73(4)
3			
Ag(1)-N(1)	2.212(2)	N(1)-Ag(1)-N(1)#1	159.04(13)
Ag(1)-N(2)#2	2.581(2)	N(1)-Ag(1)-N(2)#2	104.44(8)
Symmetry operations;		N(1)#1-Ag(1)-N(2)#2	92.03(8)
#1 x, y+1/2, z+1/2		N(2)#2-Ag(1)-N(2)#3	76.99(10)
#2 -x, -y, z			
#3 x, y-1/2, z-1/2			

Complex 2

The reaction of **L2** in ethanol with AgX (X= ClO_4^-, BF_4^-, SbF_6^-, PF_6^-, CH_3COO^-) in water gave pale yellow plate like crystals in good yield of silver(I) complex $[Ag_2(L2^-)_2(L2)_2]$ (**2**). For the synthesis of compound **2** systematic variations, including the ratio of the reactants and solvents, did not affect the end product of the reaction. In each attempt deprotonation of one ligand molecule, **$L2^-$,** coordinating with the metal centre was observed. This deprotonated ligand acts as a counter ion and balances the charge on the molecule of complex **2**. So all reactions of different silver(I) salts with non-coordinating anions resulted in the same end product as compound **2**. The ligand **L2** did not show any reaction with silver(I) salts containing coordinating anions like AgI or AgBr, as shown by our recent studies using the same experimental conditions. Complex **2** was characterized by X-ray diffraction analysis, spectroscopic and elemental analysis. The solid state structure is consistent with the elemental analysis and spectroscopic data. The Ag-N bond

distances are 2.2928(12), 2.3240(12), and 2.3882(13) Å, and the Ag-O bond distance is ca. 2.679 Å. In this centrosymmetric dimer like complex molecule, the geometrical environment around the silver(I) metal centre is pseudo trigonal pyramidal. The N-Ag-N bond angles vary from 119.59(4) to 119.72(4)º and the O-Ag-N bond angles range from 65.97 to 109.37º.

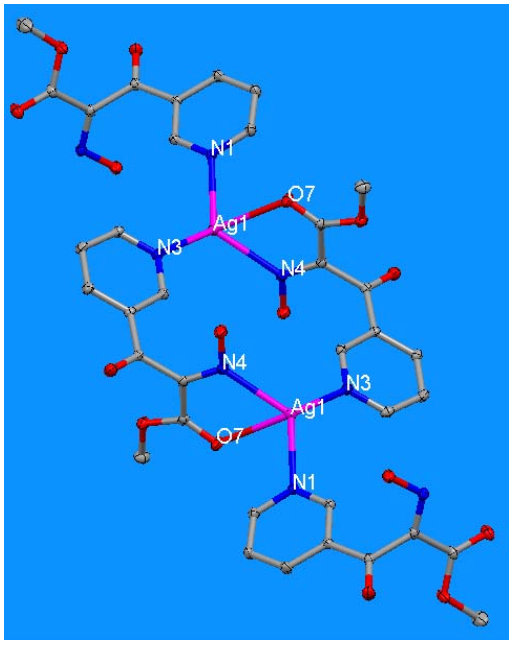

Figure 5a. View of the molecular structure of the centrosymmetric dimer complex molecule **5**.

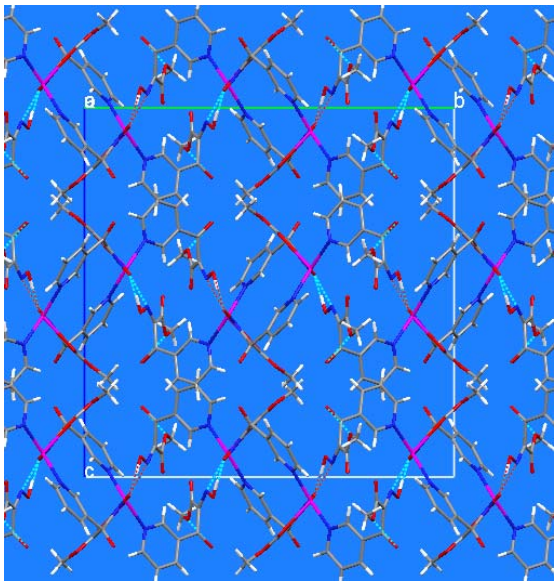

Figure 5b. View along *a* axis of the crystal packing diagram of the hydrogen bonded two-dimensional polymeric framework of compound **2**.

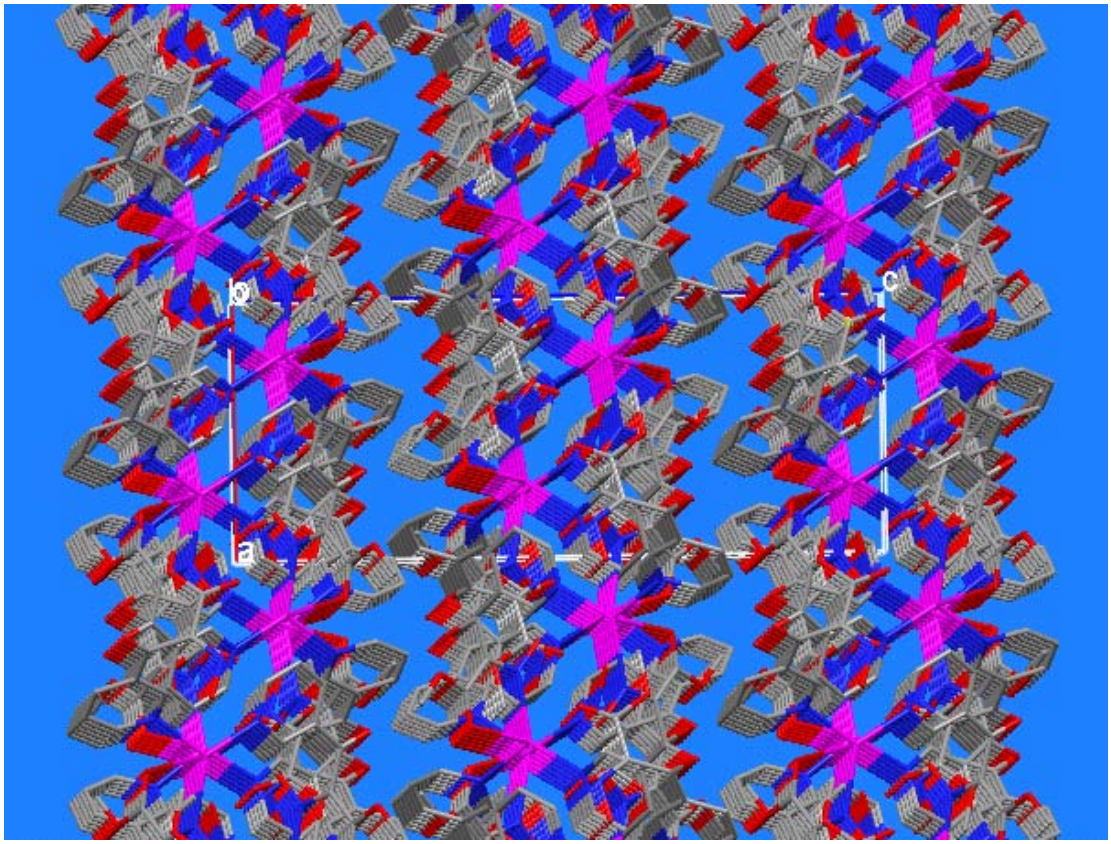

Figure 5c. View along *b* axis of the crystal packing of compound **2**.

In this dimer complex molecule, the Ag...Ag distance is ca. 6.845 Å. The maximum/minimum distances between different parts of caging ligand molecules coordinating with the two metal centres are 10.287 to 4.046 Å. These distances between the metal centres and the ligand molecules result a vacant guest cavity in the complex molecule. The presence of oxygen and nitrogen atoms in the ligand molecules coordinating with silver(I) centre afford numerous intermolecular and intramolecular hydrogen bonding interactions and these non-covalent weak interactions play major role in the construction of two-dimensional multi-layered polymeric networks, as shown in Figs. **5a–5d**.

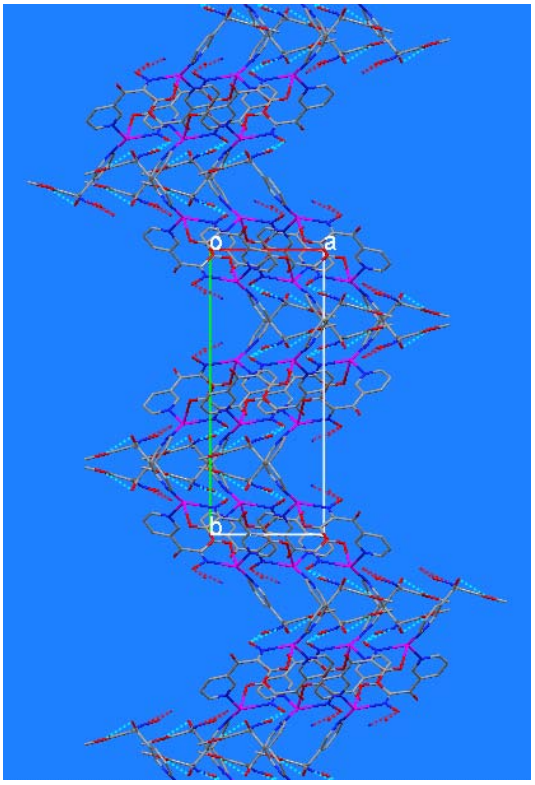

Figure 5d. View along *c* axis of the multi-layered zigzag hydrogen bonded chain structure of complex **2**.

Complex 3

The synthesis of silver(I) complex **3** was carried out following the same procedure as described above for complex **2**. A single crystal product was obtained by the reaction of **L3** with $AgNO_3$, and other silver(I) salts containing non-coordinating anions. The X-ray single crystal measurement revealed that complex **3** is a two-dimensional coordination polymer and crystallizes in the orthorhombic space group F d d 2. The geometrical environment around the silver(I) atoms is distorted tetrahedral, as shown in Fig. **3a**.

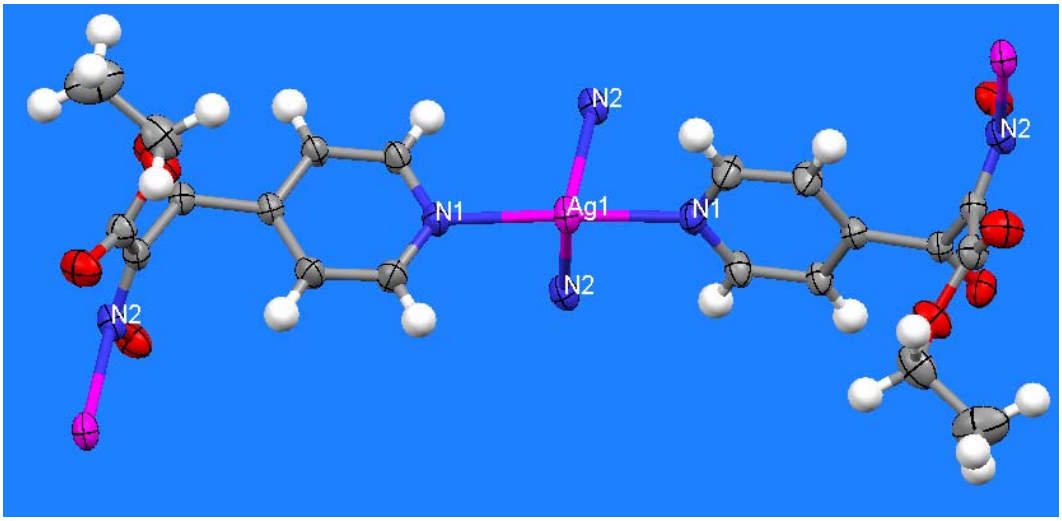

Figure 6a. A view of part of the polymeric chain structure of complex **3**, illustrating the coordination geometry around the silver(I) atom.

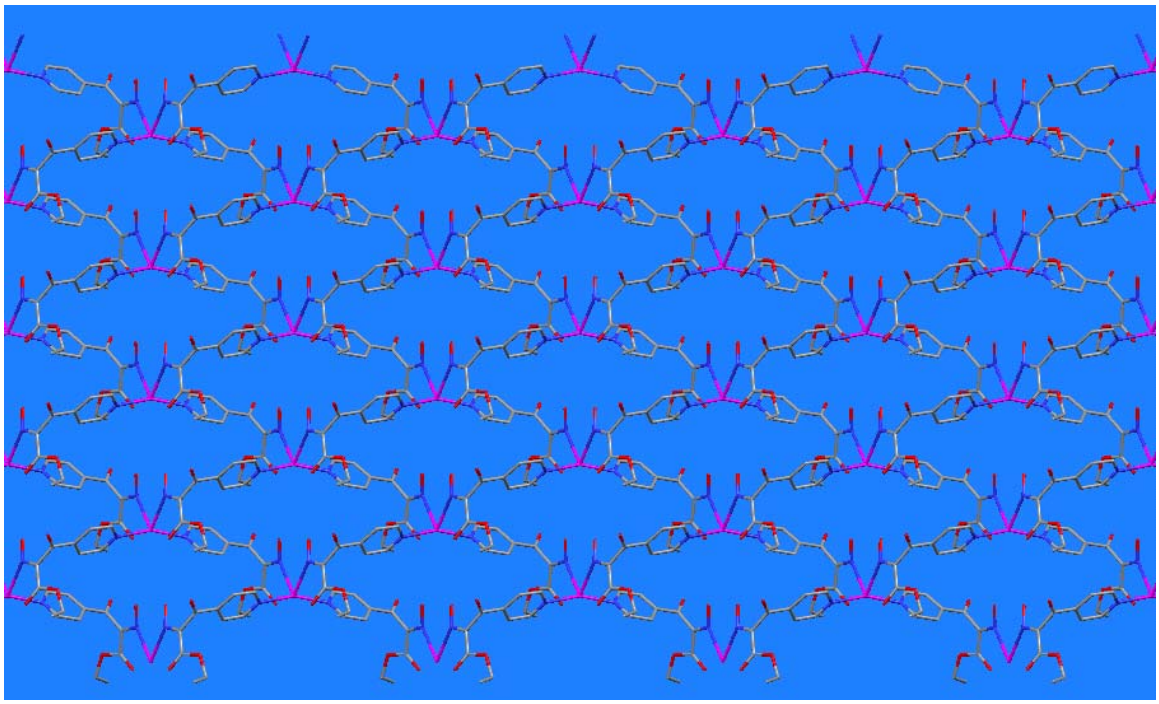

Figure 6b. View along the *a* axis of the 2D-coordination polymer complex **3**.

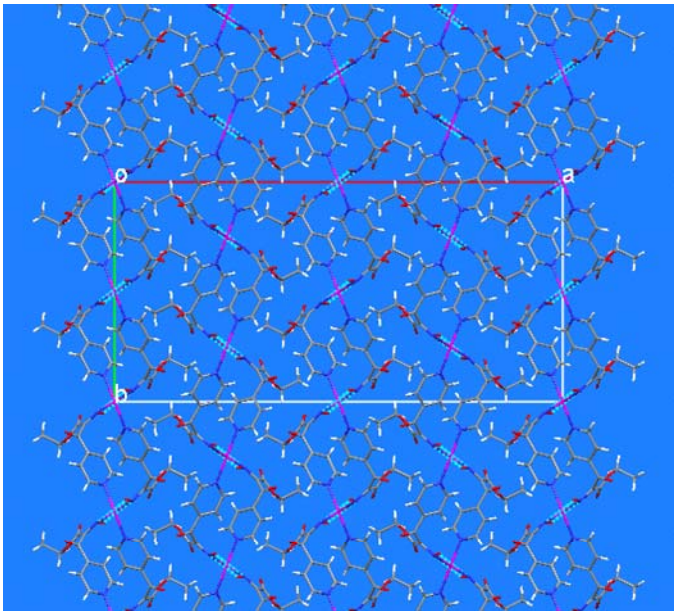

Figure 6c. Crystal packing diagram of polymer complex **3** viewed along the *c* axis.

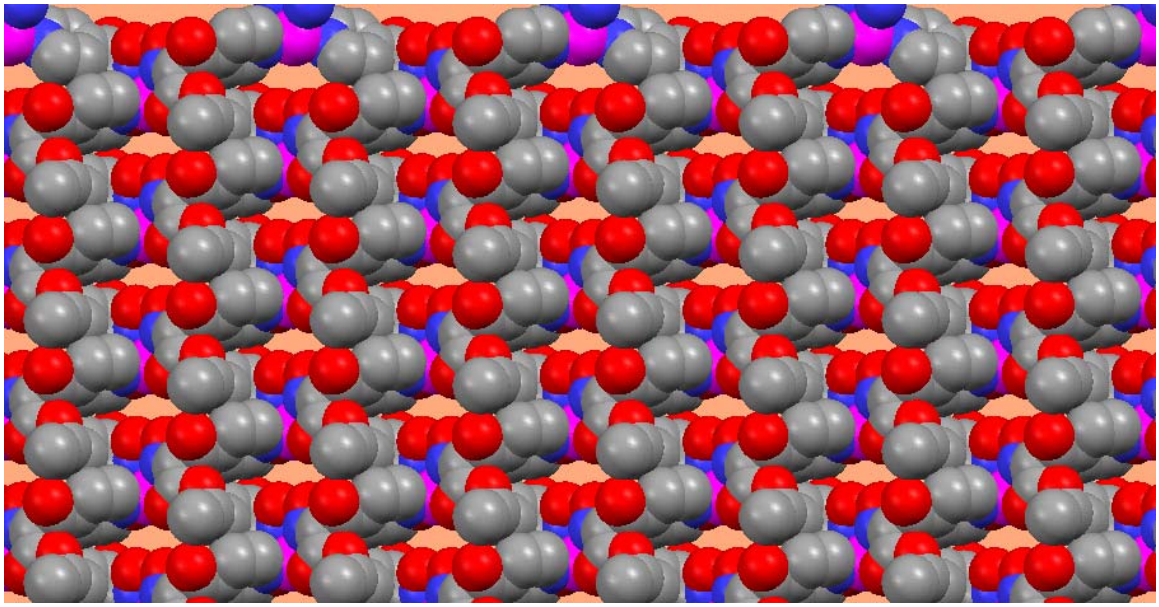

Figure 6d. Panel showing the sieve like holes or channels in the space filled diagram of the two-dimensional polymer complex **3**.

The Ag-N bond distances range from 2.212(2) to 2.581(2) Å and N-Ag-N bond angles vary from 76.99(10) to 159.04(13)º. The most notable feature in this polymeric chain structure is that each ligand molecule is acting as a bidentate ligand and coordinates with two metal centres. Each ligand is 50% deprotonated, and the hydrogen (Proton) atom is

shared by two oxygen atoms of the oxime groups of the two individual ligand **L3** molecules. In this two-dimensional polymeric chain structure, similar to complex **2** and **3**, intramolecular hydrogen bonding interactions are also observed.

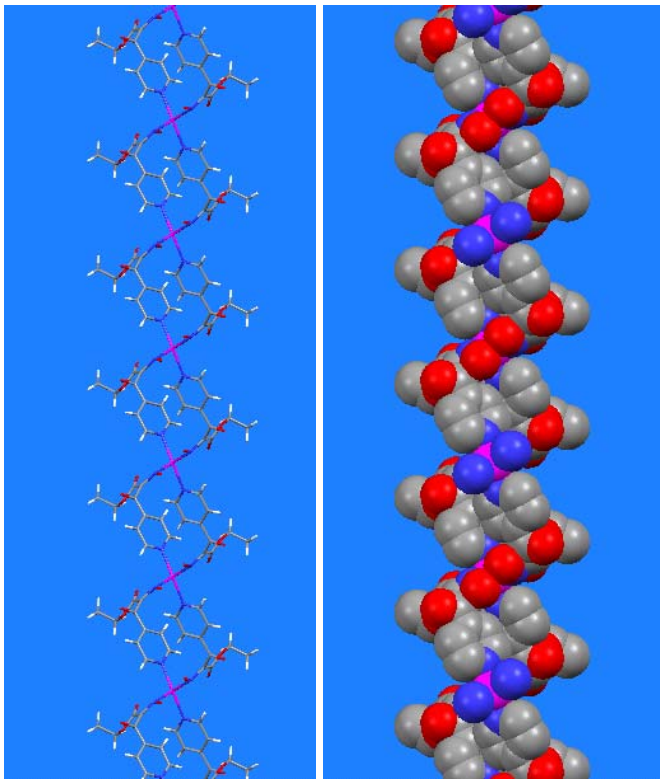

(**6e**) (**6f**)

Figure 6e-6f. A view of the double stranded helical DNA-like structure of coordination polymer complex **3**.

Table 3. Selected hydrogen bond distances and bond angles (Å, º) for **L1 L2** and **L3** and complexes **1**, **2** and **3**

Donor-H...Acceptor	D - H	D…A	H…A	D - H...A(˚)
L1				
O4-H4O…O2^{g}	0.908(19)	1.801(19)	2.7022(11)	171.3(19)
L2				
O2-H2O…N1^{e}	0.91(3)	1.79(3)	2.690(2)	172(3)

L3				
O1-H1O…N2[b]	0.96	1.71	2.6497(14)	166
1				
O2-H2O…O5[e]	0.89	1.80	2.6797(19)	170
O2-H2O…O6[i]	0.89	2.45	3.112(2)	131
2				
O2-H2O…O6[g]	0.91(2)	1.59(2)	2.4968(17)	179(3)
O2-H2O…N4[g]	0.91(2)	2.37(2)	3.1721(17)	148(2)
3				
O2-H2O…O2[k]	0.84	1.62	2.443(3)	164
O2-H2O…N2[k]	0.84	2.43	2.0673(3)	134

Symmetry operations;
g = 1/2-x,-1/2+y,1/2-z
e = 2-x,-1/2+y,1/2-z
b = x,-1/2-y,-1/2+z
e = -x,2-y,-z
i = x,2-y,-1/2+z
g = 1/2+x,1/2-y,-z
k = -x,1-y,z

Conclusions

Simple and systematic reactions of silver(I) salts with two oximinoacetoacetate ligands (**L2** and **L3**) gave helical and porous silver(I) coordination polymers. These coordination polymers could be very useful for the treatment of various pathogenic bacterial and fungal diseases and also for the separation and storage of hydrogen and other gaseous and liquid organic materials.

References

1. I. Tsyba, B. B.-K. Mui, R. Bau, R. Noguchi & K. Nomiya, *Inorg. Chem,* 2003, **42**, 8028.
2. K. Nomiya, K.-I. Onoue, Y. Kondoh, N. C. Kasuga, H. Nagano, M. Oda & S. Sakuma, *Polyhedron,* 1995, **14**, 1359.
3. K. Nomiya, S. Takahashi & R. Noguchi, *J. Chem. Soc., Dalton Trans.,* 2000, 2091. 4.
O. Crespo, V. V. Brusko, M. C. Gimeno, M. L. Tornil, A. Laguna & N. G. Zabirov, *Eur. J. Inorg. Chem,* 2004, 423.
5. A. Melaiye, Z. Sun, K. Hindi, A. Milsted, D. Ely, D. H. Reneker, C. A. Tessier & W. J. Youngs, *J. Am. Chem. Soc,* 2005, **127**, 2285.
6. R. Rowan, T. Tallon, A. M. Sheahan, R. Curran, M. McCann, K. Kavanagh, M. Devereux & V. McKee, *Polyhedron,* 2006, **25**, 1771.
7. J. M. T. Hamilton-Miller & S. Shah, *Int. J. Antimicrob. Agent,* 1996, **7**, 97.
8. H. J. Klasen, *Burns,* 2000, **26**, 131.
9. S. Kitagawa, R. Kitaura & S. Noro, *Angew. Chem. Int. Ed,* 2004, **43**, 2334.
10. C. Janiak, Dalton Trans., 2003, 2781.
11. N. C. Kasuga, A. Sugie & K. Nomiya, *Dalton Trans.,* 2004, 2732.
12. B. S. Creaven, D. A. Egan, K. Kavanagh, M. McCann, M. Mahon, A. Noble, B. Thati & M. Walsh, *Polyhedron,* 2005, **24**, 949.
13. N. C. K asuga, R. Yamamoto, A. Hara, A. Amano & K. Nomiya, *Inorg. Chim. Acta,* 2006, **359**, 4412.
14. K. Nomiya, R. Noguchi & M. Oda, *Inorg. Chim. Acta,* 2000, **298**, 24.
15. R. Noguchi, A. Hara, A. Sugie, K. Nomiya, *Inorg. Chem. Commun,* 2006, **9**, 355.
16. A. Melaiye, R. S. Simons, A. Milsted, F. Pingitore, C. Wesdemiotis, C. A. Tessier & W. J. Youngs, *J. Med. Chem,* 2004, **47**, 973.
17. F. W. Fuller, M. Parrish & F. C. Nanace, *J. Burn. Care Rehabil,* 1994, **15**, 1994.
18. M. Eddaoudi, D. B. Moler, H. Li, B. Chen, T. M. Reineke, M. O'Keeffe & O. M. Yaghi, *Acc. Chem. Res,* 2001, **34**, 319.
19. A. J. Blake, G. Baum, N. R. Champness, S. S. M. Chung, P. A. Cooke, D. Fenske, .A. N. Khlobystov, D. A. Lemenovskii, W.-S. Li & M. Schröder, *J. Chem. Soc.,*

Dalton Trans., 2000, 4285.

20. A. J. Blake, N. R. Champness, M. Crew & S. Parsons, *New. J. Chem.,* 1999, 13.
21. R. Robson, *J. Chem. Soc., Dalton Trans.,* 2000, 3735.
22. O. M. Yaghi & H.Li, *J. Am. Chem. Soc,* 1996, **118**, 295.
23. M.-L. Tong, X.-M. Chen & S. W. Ng, *Inorg. Chem. Commun,* 2000, 436.
24. A. Angeloni & A. G. Orpen, *Chem. Commun.,* 2001, 343.
25. X.-P. Zhou, X. Zhang, S.-H. Lin & D. Li, *Crystal Growth & Design.* 2007, **7**, 485.

Chapter 5:

Silver-Phosphine One- and Two-dimensional Coordination Polymers with the Exo-dentate Spacer Ligand 4,4′-bipyridine

Introduction

The crystal design and synthesis of coordination polymers of transition metals is presently a large and growing area of research.[1-5] Our interest in the preparation of extended networks using inorganic coordination polymer is based on the development of materials with tuneable properties similar to those observed in zeolites[6] and compounds with interesting biological, and electrical properties.

The rapidly growing area of coordination polymers based on metal cations with organic ligands and counter ions, has given rise to a wide variety of fascinating one-, two- and three-dimensional structures.[7] The versatile ligands, those can impose different geometries on the metal ions are of interest for many reasons. These include, selective metal extraction[8], intermolecular aromatic, metal-metal, metal organic ligand and metal anion interactions, electrostatic repulsions, pore size of the porous framework (host guest relationship), catalysis, electrical conductivity, and magnetic properties of the crystal designed.[9-11] The high degree of design arises from the coupling of the well understood coordination properties of the organic ligand, individual metal ions, anions and the solvent of crystallization. The selection of a highly developed ligand within the newer area of supra-molecular chemistry and crystal engineering is most important.[12] Metal-ligand coordination bond formation of 4,4′-bipy provides a very convenient means of linking up components into infinite networks. Inorganic chemistry, in particular coordination chemistry is replete with examples of easily accessible potential building blocks with a range of simple-complex geometries and connectivities.[13] It has been well understood that the existence and use of 4,4′-bipy ligand with the silver(I) salts can result in surprising architectures.[14-17] However information on mixed ligands (tertiary phosphines and 4,4′-bipy) complexes of silver(I) are not yet well explored.[18]

Our interests lie in the study of crystalline materials since the attainment of well defined structures is intimately linked to an understanding the design, synthesis and properties of new materials. Here we report on seven structures of coordination polymers of silver(I) containing the spacer ligand 4,4′-bipy, a tertiary phosphine or biphosphine and an oxy anion. The compounds namely, $[Ag_2(4,4'\text{-bipy})(P1)_2(NO_3)_2]_n$ (**1**), $[Ag_2(4,4'$-

bipy)$(P2)_2(NO_3)_2]_n$ (**2**), $[Ag_2(4,4'\text{-bipy})(P3)_2(NO_3)_2]_n$ (**3**), $[Ag_2(4,4'\text{-bipy})(P4)_2(NO_3)_2]_n$ (**4**), $\{[Ag(4,4'\text{-bipy})(P2)](ClO_4)\}_n$ (**5**), $\{[(CH_3CN)Ag(4,4'\text{-bipy})][Ag(4,4'\text{-bipy})]_3.(ClO_4)_4.5CH_3CN\}_n$ (**6**) and $[Ag_2(4,4'\text{-bipy})(P5)_2(NO_3)_2]_n$ (**7**) [where P1 = Diphenylcyclohexyl phosphine, P2 = Dicyclohexylphenyl phosphine, P3 = Diphenyl(p-tolyl) phosphine, P4 = Tricyclohexyl phosphine, and P5 = 1,2-Bis(diphenyl-phosphino)ethane: Scheme 1], were synthesized and structurally characterized. A number of structures containing silver(I) and 4,4′-bipy have been reported.[1-5] We have chosen tertiary phosphines and biphosphines to explore the affect of these neutral ligands on silver(I) and 4,4′-bipy complexes. A considerable affect on the geometry around the silver(I) metal centre has been observed during our current studies. We report here on how extended silver(I) organic frameworks can be designed, synthesized and fully characterized.

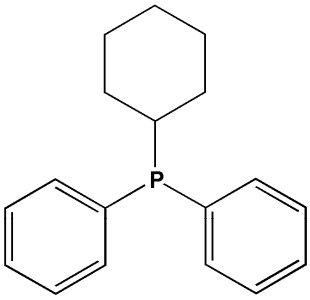

Diphenyl cyclohexyl phosphine
P1

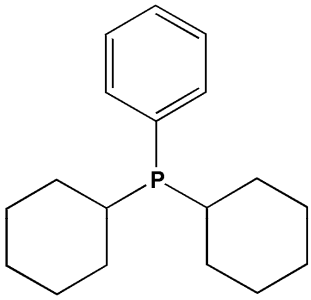

Phenyl dicyclohexyl phosphine
P2

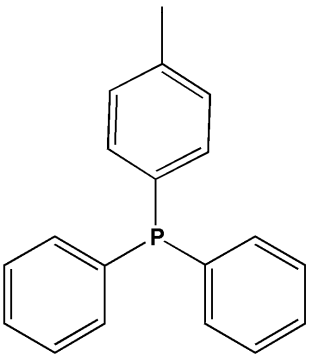

Diphenyl (p-tolyl) phosphine
P3

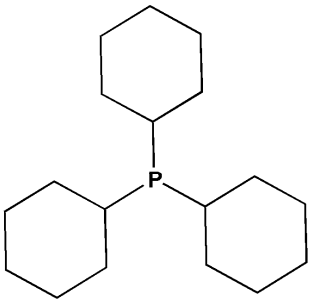

Tricyclohexyl phosphine
P4

Scheme 1

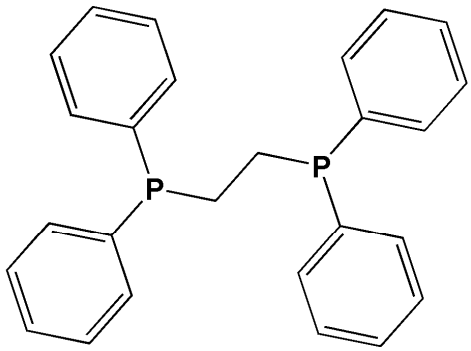

1, 2-Bis(diphenyl-phosphino)ethane
P5

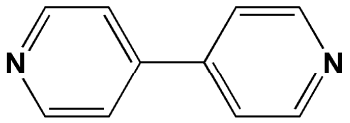

4,4'-bipyridine
= 4,4'-bipy

Scheme 1 cont'd

Experimental

All reactions were carried out under normal conditions at rt. All reactants and solvents were of analytical grade commercial products and were purchased from Aldrich and ACROS. They were used without further purification. Microanalysis was done by Mr. D. Mooser (Ecole d'ingénieurs de Fribourg, Filière de chimie). The IR spectra were recorded as KBr pellets on a Perkin Elmer Spectrum One FTIR instrument.

Warning: Perchlorate salts are dangerous, only a minimum quantity should be used. Under the conditions used we experienced no problems.

Synthesis of $[Ag_2(4,4'\text{-bipy})(P1)_2(NO_3)_2]_n$ (1): This compound was prepared by a procedure similar to that reported by Sampanthanthar and Vittal.[19] A mixture of $AgNO_3$ (0.34 g, 0.2 mmol) and diphenylcyclohexyl phosphine (0.268 g, 0.1 mmol) in 20 ml (acetonitrile/dichloromethane) was stirred for 10 minutes. 0.1 mmol (0.156 g) solution of 4,4′-bipy was prepared in acetonitrile and was added in the above reaction mixture drop wise with continuous stirring until clear solution was obtained. The resultant solution was filtered in an evaporation dish and left undisturbed for crystallization. After few days

colourless rod like crystals were obtained. A suitable crystal was chosen for X-ray diffraction analysis. (Yield: 75.3%). Anal. Calcd for $C_{46}H_{50}Ag_2N_4O_6P_2$: C, 53.45; H, 4.84; N, 5.42: Found: C, 53.15; H, 4.95; N, 5.38: IR (KBr, cm^{-1}): 3065(w), 2926(ms), 2853(m), 1602(s), 1404(s), 1295(s), 1074(ms), 814(m), 694(s).

Synthesis of $[Ag_2(4,4'\text{-bipy})(P2)_2(NO_3)_2]_n$ (2): The synthesis of this complex followed the same procedure as for complex **1**. In this reaction dicyclohexylphenyl phosphine was used instead of diphenylcyclohexyl phosphine. All reactants were used in the same stoichiometric ratio as in the above reaction. After three days rod like colourless crystals were obtained, a suitable crystal was used for X-ray structure determination (Yield: 68.7%). Anal. Calcd for $C_{46}H_{62}Ag_2N_4O_6P_2$: C, 51.78; H, 5.74; N, 5.79: Found: C, 52.83; H, 5.93; N, 5.36: IR (KBr, cm^{-1}): 3052(w), 2928(ms), 2848(m), 1596(s), 1448(s), 1385(s), 1073(ms), 850(m), 699(s).

Synthesis of $[Ag_2(4,4'\text{-bipy})(P3)_2(NO_3)_2]_n$ (3): The synthesis was carried out by following the same procedure as described for complexes **1** & **2**. Biphenyl(p-tolyl) phosphine (0.1 mmol) was used in this reaction. Crystallization was done by slow evaporation at room temperature, with in five days plate like colourless crystals were obtained. A suitable crystal was used for crystallographic analysis (Yield: 78.44%). Anal. Calcd for $C_{48}H_{42}Ag_2N_4O_6P_2$: C, 54.70; H, 4.01; N, 5.22: found C, 54.98; H, 4.01; N, 5.34: IR (KBr, cm^{-1}): 3054(w), 2928(ms), 2844(m), 1605(s), 1436(s), 1380(s), 1035(ms), 845(m), 691(s).

Synthesis of $[Ag_2(4, 4'\text{-bipy})(P4)_2(NO_3)_2]_n$ (4): The synthesis of silver(I) complex **4** was also followed by the same procedure as explained for complex **1-3**. In this reaction tricyclohexyl phosphine was used instead of mixed tertiary phosphines. All reactants were used in the same stoichiometric ratio as in the above reactions. After three days rod like colourless crystals were obtained; a suitable crystal was used for X-ray diffraction analysis (Yield: 77.8%). Anal. Calcd for $C_{52}H_{74}Ag_2N_4O_6P_2$: C, 52.24; H, 7.00; N, 5.29: Found: C, 52.47; H, 6.93; N, 5.28: IR (KBr, cm^{-1}): 2928(ms), 2848(m), 1596(s), 1448(s), 1385(s), 1073(ms), 850(m), 699(s).

Synthesis of $\{[Ag(4,4'\text{-bipy})(P2)](ClO_4)\}_n$ (5):

The synthesis of the silver(I) complex **5** was done according to the reported procedure.[19] A mixture of $AgClO_4$ (0.21 g, 0.1 mmol) and dicyclohexylphenyl phosphine (0.274 g, 0.1 mmol) in 10 ml methanol was stirred for twenty minutes. 4,4′-bipy (0.312 g, 0.2 mmol) was dissolved in 10 ml of CH_2Cl_2 and was added drop wise in the above mixture with continuous mechanical stirring for thirty minutes. The resultant clear solution was filtered in evaporation dish to avoid any impurity. The crystallization was done by slow evaporation method at room temperature; after two days colourless rod like crystals were appeared in the rest of the solvent. The crystals were separated carefully by decanting rest of the solvent and air dried. A suitable crystal was chosen for X-ray diffraction studies (yield: 58.5%). Anal. Calcd for $C_{28}H_{35}AgClN_2O_4P$: C, 53.02; H, 5.74; N, 3.66: Found: C, 52.67; H, 5.48: N, 4.38: IR (KBr, cm^{-1}): 3058(w), 2925(ms), 2851(m), 1603(s), 1415(s), 1384(s), 1095(ms), 810(m), 622(s).

Synthesis of $\{[(CH_3CN)Ag(4,4'\text{-bipy})][Ag(4,4'\text{-bipy})]_3\cdot(ClO_4)_4\cdot 5CH_3CN\}_n$ (6): The unexpected silver(I) complex was obtained as a side product along with some powder during the failed attempt of the synthesis of $\{[Ag(4,4'\text{-bipy})(P3)].(ClO_4)\}_n$. A suitable crystal was used for X-ray diffraction analysis. Many attempts were made to get the single crystal of the major product but all in vain. IR (KBr, cm^{-1}): 3062(w), 2927(s), 2852(m), 2230(w), 1598(s), 1420(s), 1388(s), 1099(ms), 818(m), 633(s).

Synthesis of $\{Ag_2(4,4'\text{-bipy})(P5)_2(NO_3)_2\}_n$ (7): A mixture of $AgNO_3$ (0.34 g, 0.2 mmol) and 1,2-bis(diphenyl-phosphino)ethane (0.398 g, 0.1 mmol) in 10 ml (dichloromethane) was stirred for 10 mins. 0.1 mmol (0.156 g) solution of 4,4′-bipy was prepared in methanol and was added slowly in the reaction mixture with continuous stirring and 5 ml of acteonitrile was added to get the transparent solution. The resultant solution was filtered to avoid any impurity and kept undisturbed at room temperature for crystallization. After seven days colourless rod like crystals were obtained. A suitable crystal was chosen for X-ray diffraction analysis (Yield: 77.8%). Anal. Calcd for

$C_{36}H_{32}Ag_2N_4O_6P_2$: C, 48.30; H, 3.57; N, 6.26: Found: C, 48.28; H, 3.53; N, 6.21: IR (KBr, cm^{-1}): 2928(ms), 2848(m), 1596(s), 1448(s), 1385(s), 1073(ms), 850(m), 699(s).

X-ray Crystallography.

The intensity data were collected at 173K on either, a one circle (ϕ scans)[1], or a two circle (ω and ϕ scans)[2] Stoe Image Plate Diffraction System, using MoKα graphite monochromated radiation. The structures were solved by Direct methods using the program SHELXS-97[3]. The refinement and all further calculations were carried out using SHELXL-97[3]. The H-atoms were either located from Fourier difference maps and freely refined or included in calculated positions and treated as riding atoms using SHELXL default parameters. The non-H atoms were refined anisotropically, using weighted full-matrix least-squares on F^2. In most cases multi-scan absorption corrections were applied using the MULscanABS routine in PLATON[4]. A summary of crystal data and refinement details for compounds **1-7** are given in Table 1, and selected bond lengths and angles are listed in Table 2.

1) Stoe & Cie (2000) IPDS-I Bedienungshandbuch. Stoe & Cie GmbH, Darmstadt, Germany.

2) Stoe & Cie. (2006) *X-Area V1.35 & X-RED32 V1.31 Software*. Stoe & Cie GmbH, Darmstadt, Germany.

3) G. M. Sheldrick (2008). Acta Crystallgr. A64, 112-122.

4) A. L. Spek (2003). J.Appl.Cryst. 36, 7-13

Results and discussions

In order to construct coin metal containing coordination polymer networks by using mixed ligands; well known exo-dentate ligand 4,4′-bipyridine has been used for its versatile coordination ability. silver(I) complexes of exo-bidentate ligands usually result in the formation of one-dimensional polymer chains. The introduction of monodentate tertiary phosphine ligand with an exo-bidentate ligand will provide a new combination of non-covalent interactions into the supra-molecular chemistry of silver(I), which usually prefers a linear geometry with exo-dentate ligands. Here our synthetic approach is to

build one-, and two-dimensional polymer networks containing 4,4′-bipy, tertiary phosphines, bisphosphines and silver(I) salts.

Table 1. Summary of crystal data and structure refinement parameters for complexes **1-7**

{ [a] $\mathbf{R1 = \Sigma||F_O| - |F_C||/\Sigma|F_O|}$; [b] $\mathbf{wR2 = [\Sigma w(F_O^2 - F_C^2)^2/\Sigma wF_O^4]^{1/2}}$ }

	1	**2**
Formula	$C_{46}H_{50}Ag_2N_4O_6P_2$	$C_{46}H_{62}Ag_2N_4O_6P_2$
M	1032.58	1044.68
Wavelength/Å	0.71073	0.71073
Temperature/K	173	173
Crystal symmetry	Triclinic	Triclinic
Space group	P -1	P -1
a/Å	8.746(2)	9.9336(8)
b/Å	10.382(2)	10.1644(7)
c/Å	13.383(3)	13.1582(10)
α/°	69.457(16)	109.321(6)
β/°	73.686(18)	101.523(6)
γ/°	79.293(18)	103.186(6)
V/ Å^3	1086.9(4)	1164.63(15)
Z	1	1
D_c/Mg m^{-3}	1.578	1.490
μ(Mo-Kα)/mm^{-1}	1.028	0.960
F(000)	526	538
Crystal size/mm	0.30 x 0.16 x 0.10	0.45 x 0.27 x 0.20
θ Limits/°	1.67-25.47	1.72 - 29.58
Measured reflections	8018	16959
Unique reflections(R_{int})	3750(0.0327)	6272(0.0669)
Observed reflections	3062	5467
Goodness of fit on F^2	1.049	1.109
$R_1(F)$,[a] [$I > 2\sigma(I)$]	0.0360	0.0548
w$R_2(F^2)$,[b] [$I > 2\sigma(I)$]	0.0825	0.1435

Largest diff.peak, hole/e $Å^{-3}$	0.437, -1.031	0.925, -1.139

Table 1 cont,d

	3	**4**
Formula	$C_{48}H_{42}Ag_2N_4O_6P_2$	$C_{52}H_{74}Ag_2N_4O_6P_2$
M	1048.53	1056.78
Wavelength/Å	0.71073	0.71073
Temperature/K	173	173
Crystal symmetry	Triclinic	Triclinic
Space group	P -1	P -1
a/Å	9.5566(7)	9.6553(9)
b/Å	13.6522(9)	10.6319(18)
c/Å	18.6405(13)	13.6748(16)
α/°	100.038(5)	106.993(10)
β/°	104.666(6)	105.492(10)
γ/°	99.543(6)	104.058(12)
V/ $Å^3$	2259.8(3)	1212.7(3)
Z	2	1
D_c/Mg m^{-3}	1.541	1.430
μ(Mo-Kα)/mm^{-1}	0.990	0.922
F(000)	1060	538
Crystal size/mm	0.40 x 0.40 x 0.12	0.44 x 0.22 x 0.11
θ Limits/°	1.71 - 29.54	2.00 - 26.00
Measured reflections	43501	9648
Unique reflections(R_{int})	12206(0.0903)	4433(0.0725)
Observed reflections	7409	3412
Goodness of fit on F^2	1.018	0.959
$R_1(F)$,[a] $[I > 2\sigma(I)]$	0.0712	0.0446
w$R_2(F^2)$,[b] $[I > 2\sigma(I)]$	0.1854	0.1096
Largest diff.peak, hole/e $Å^{-3}$	0.834, -1.934	0.916, -0.836

Table 1 cont,d

	5	**6**
Formula	$C_{28}H_{35}AgN_2P$, ClO_4	$C_{52}H_{50}Ag_4N_{14}$, $4ClO_4$
M	637.87	1700.34
Wavelength/Å	0.71073	0.71073
Temperature/K	173	173
Crystal symmetry	Monoclinic	Triclinic
Space group	P 2_1	P -1
a/Å	9.3834(11)	10.6135(13)
b/Å	16.9174(14)	11.3989(10)
c/Å	10.0223(12)	26.108(3)
α/°	90	88.824(12)
β/°	109.000(13)	86.678(15)
γ/°	90	78.493(13)
V/ $Å^3$	1504.3(3)	3089.8(6)
Z	2	2
D_c/Mg m^{-3}	1.408	1.828
μ(Mo-Kα)/mm^{-1}	0.846	1.500
F(000)	656	1688
Crystal size/mm	0.30 x 0.27 x 0.15	0.44 x 0.17 x 0.08
θ Limits/°	2.05 - 26.00	2.05 - 25.95
Measured reflections	12022	21317
Unique reflections(R_{int})	5773(0.0507)	10290(0.0439)
Observed reflections	4898	4477
Goodness of fit on F^2	0.940	0.766
$R_1(F)$,[a] $[I > 2\sigma(I)]$	0.0327	0.0443
wR_2 (F^2),[b] $[I > 2\sigma(I)]$	0.0765	0.1086
Largest diff.peak, hole/e $Å^{-3}$	0.595, -0.834	0.775, -0.883

Table 1 cont,d

	7
Formula	$C_{36}H_{32}Ag_2N_4O_6P_2$
M	894.34
Wavelength/Å	0.71073
Temperature/K	173
Crystal symmetry	Triclinic
Space group	P -1
a/Å	10.0565(9)
b/Å	12.9071(13)
c/Å	15.2012(14)
α/°	93.380(8)
β/°	108.508(7)
γ/°	98.108(8)
V/ Å^3	1841.0(3)
Z	2
D_c/Mg m^{-3}	1.613
μ(Mo-Kα)/mm^{-1}	1.200
F(000)	896
Crystal size/mm	0.50 x 0.20 x 0.13
θ Limits/°	1.61 - 26.13
Measured reflections	15513
Unique reflections(R_{int})	6496(0.0868)
Observed reflections	5042
Goodness of fit on F^2	1.033
$R_1(F)$,[a] $[I > 2\sigma(I)]$	0.0746
w$R_2(F^2)$,[b] $[I > 2\sigma(I)]$	0.1937
Largest diff.peak, hole/e Å^{-3}	2.799, -1.410

$[Ag_2(4,4'\text{-bipy})(P1)_2(NO_3)_2]_n$ (1)

A perspective view of the molecular structure of complex **1** is shown in the Fig. **1a**. The exo-dentate ligand (4,4′-bipy) acts as a bridging ligand between $[Ag\ (P2)(NO_3)]_2$ units. 4,4′-bipy bridges silver(I) atoms directly to form a stair-step infinite undulating chain as shown in Fig. **1b**.

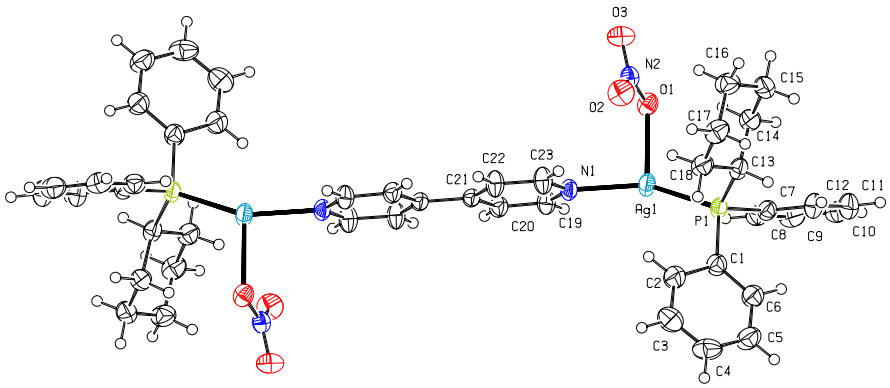

Figure 1a. A view of the asymmetric unit of the molecular structure of compound **1** with complete atom labelling Scheme and displacement ellipsoids are shown at 50% probability.

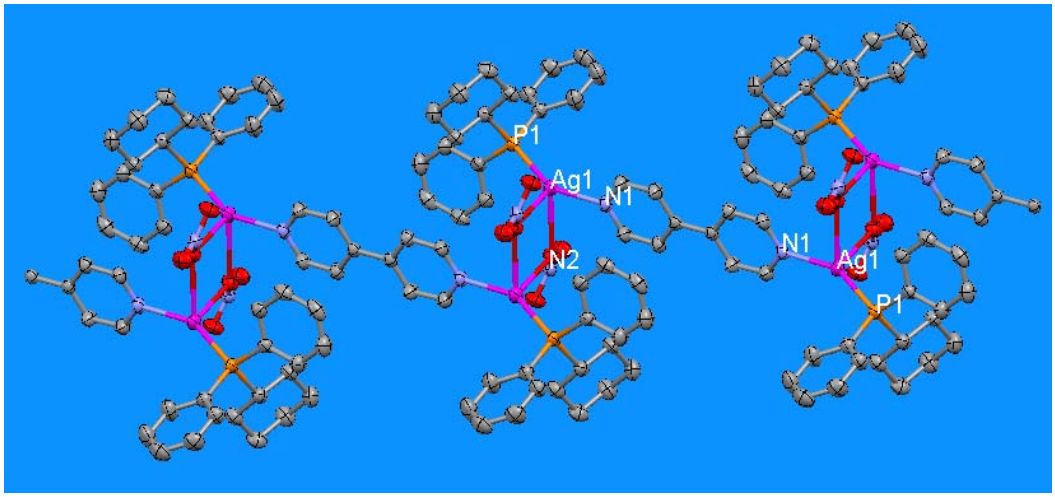

Figure 1b. A view of the bridging behaviour of 4,4′-bipy and NO_3^- in complex **1**.

This structure is isomorphous and isostructural with $[Ag_2(PPh_3)_2(4,4'\text{-bipy})(NO_3)_2]_n$ complex.[19] In the molecular structure of complex **1** the Ag-N bond distance is 2.246(4) Å. The Ag-O-Ag bond angle is ca. 103.91°, which accounts for the long Ag...Ag distance of

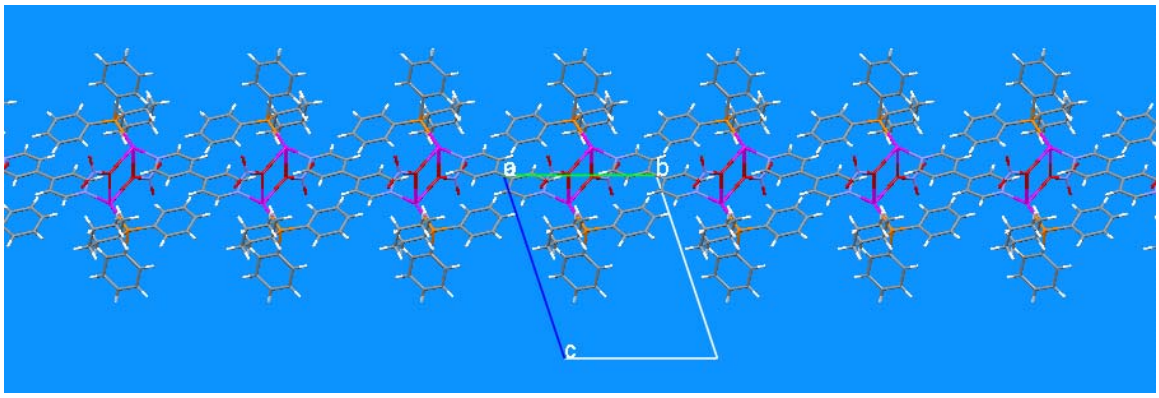

(1c)

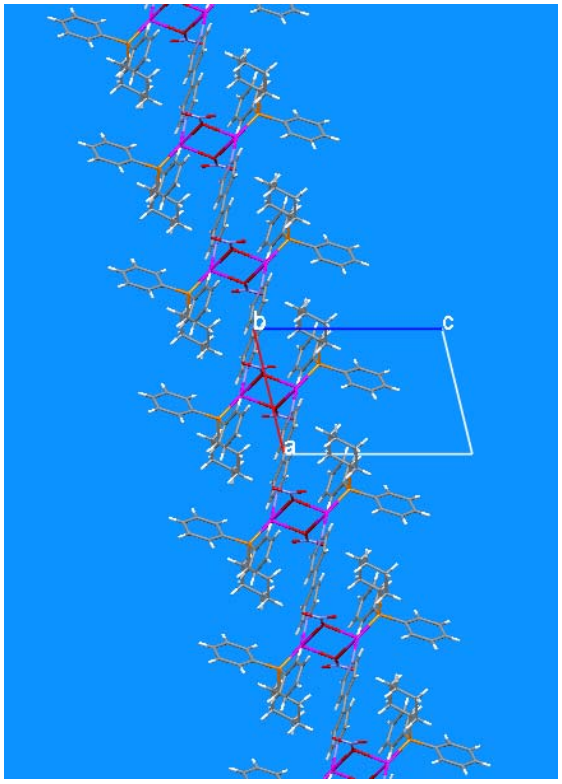

(1d)

Figures 1c & **1d**. Panel **1c** showing the polymeric chain running along *b*-axis and panel **1d** showing the stacking of polymeric chains along *b*-axis.

ca. 4.047 Å, hence there are no d^{10}-d^{10} interactions. The angle range around the Ag(I) atom is 93.28(11)-150.14(10)º. The Ag-P bond distance is 2.3636(12) Å, which is comparable to the Ag-P bond distance in the isomorphous structure of $[Ag_2(PPh_3)_2(4,4'\text{-bipy})(NO_3)_2]_n$ complex.[19] Both pyridyl rings of the 4,4′-bipy ligand are coplanar. The geometry around atom Ag(I) is distorted tetrahedral. Two crystallographic inversion centres are found in this molecule, one in the middle of Ag_2O_2 four membered ring and other at the mid point of the bridging C-C bond in the 4,4′-bipy ligand. The polymeric chains run parallel to the *b*-axis and are stacked up the *c*-axis (Fig **1c**).

$[Ag_2(4,4'\text{-bipy})(P2)_2(NO_3)_2]_n$ (2):

The view of the structure of compound **2** is shown in Fig. **2a**, with the atom labelling Scheme. It is isostructural and isomorphous with complex **1** and 4,4′-bipy is acting as a bridging ligand between $[Ag(P2)(NO_3)]_2$ units and both pyridyl rings of the exo-dentate ligand are coplanar to each other, as found in complex **1**.

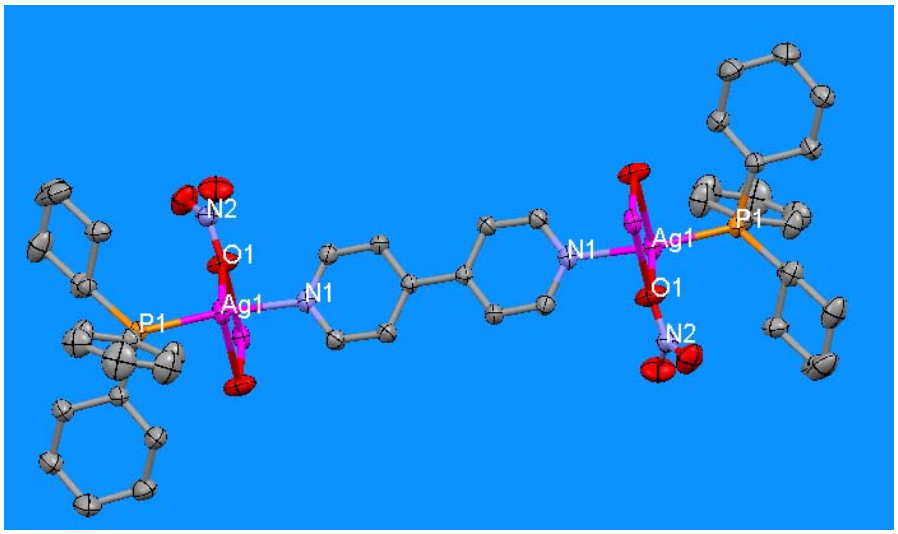

Figure 1a. View of molecular structure of compound **2**.

The Ag-N bond distance is 2.209(4) Å shorter than 2.246(4) Å as found in complex **1**. The Ag-O-Ag bond angle is ca. 101.63º, which is also smaller than that found in the molecular structure of complex **1**. This smaller angle accounts for the shorter Ag...Ag distance of ca. 3.933 Å in the Ag_2O_2 four membered ring. The Ag-P bond distance is

2.3489(10) Å and shorter than that found in complex **1**. However, the Ag-O bond distances are 2.451(4) and 2.620(4) Å. In first case is comparable and in second case is longer than that found in complex **1** [2.454(3) Å]. The molecule structure has two crystallographic inversion centres. 1st in the centre of the Ag_2O_2 four membered ring and 2nd in the middle of the central C-C bond in the 4,4′-bipy ligand, like in complex **1**. The packing diagram of polymeric chain structure of complex **2** is shown in Fig. **2b**. The solid state structure of complex **2** is one-dimensional coordination polymer; containing stair or step like undulating infinite polymeric chain. This polymeric chain run parallel to the *b*-axis and is stacked up the *c*-axis. The geometry around the silver(I) atom is distorted tetrahedral, as found in complex **1**.

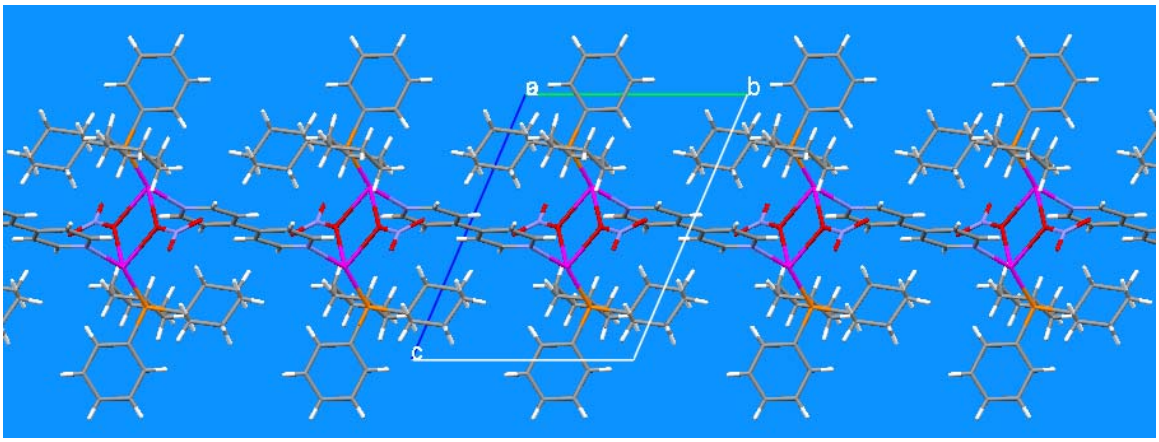

Figure 2b. Panel is showing one-dimensional polymeric chain structure of compound **2** along *a*-axis.

$[Ag_2(4,4'\text{-bipy})(P3)_2(NO_3)_2]_n$ (3):

The molecular structure of complex **3** is depicted in Fig. **3a**; with atom labelling Scheme. The single crystal structure of complex **3** also consists of one-dimensional step-like infinite undulating polymeric chain, as shown in Fig. **3c**.

The structural explanation of this coordination polymer compound requires dividing it in two parts. In first part of the molecule as shown in the Fig. **3a**, one of the oxygen atom of the NO_3^- anion bridges symmetry equivalent Ag(1) atoms with a Ag(1)-O(1A)-Ag(1) bond angle ca. 105.34º, which accounts for the longer Ag(1)...Ag(1) distance of 4.006 Å. This Ag(1)…Ag(1) distance is longer than in compound **2** but comparable with

compound **1.** The bond angles are bigger than those found in complexes **1** and **2**. The geometry around the silver(I) atom Ag(2) is more complicated. The difference in geometry is encountered by the disorder in the bridging counter ion (NO_3^-) involved here. In the second part of the molecular structure of complex **3**, the geometrical environment around silver(I) atom Ag(2) is different than those found in compounds **1** and **2**. The Ag(2)-Ag(2) bond distance is ca. 4.569 Å and Ag(2)-O(4)-Ag(2) bond angle is ca. 148.40º. The Ag(2)…Ag(2) bond distance and Ag-O-Ag bond angle values found in the second part of complex **3** are much longer and bigger than those found in the first part. These bond lengths and bond angles values are also longer and bigger than those found in complexes **1** and **2** as well**.** The Ag-N bond distances are 2.266(5) and 2.211(4) Å. The 4,4′-bipy ligand acts as a bridging ligand but this time the pyridyl rings are not coplanar with a dihedral angle of 9.2(3)º. The Ag-P bond distances are 2.3616(16) and 2.3578(15) Å and are longer than those found in complex **2,** but comparable to those observed in complex **1**. The geometrical environment around the Ag(1) atom is distorted tetrahedral, as in complexes **1** and **2**, while the geometry around atom Ag(2) can be described as distorted trigonal bipyramidal.

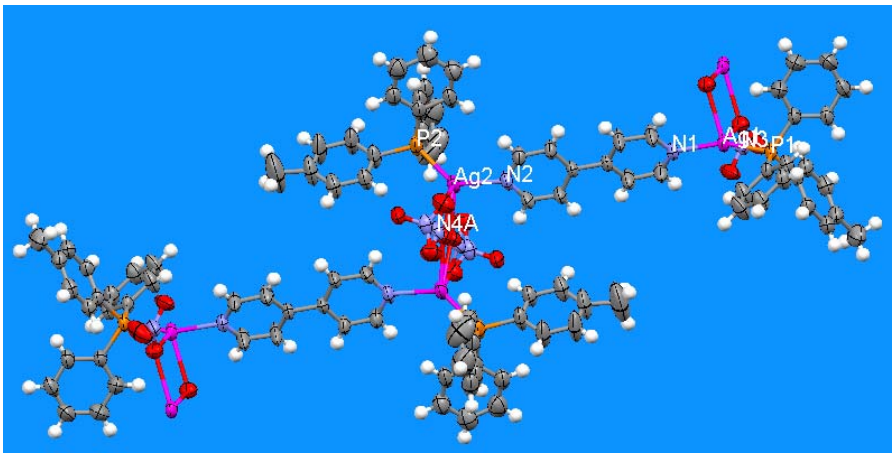

Figure 3a. View of the molecular structure of complex **3** with labelled silver(I), phosphorus and nitrogen atoms.

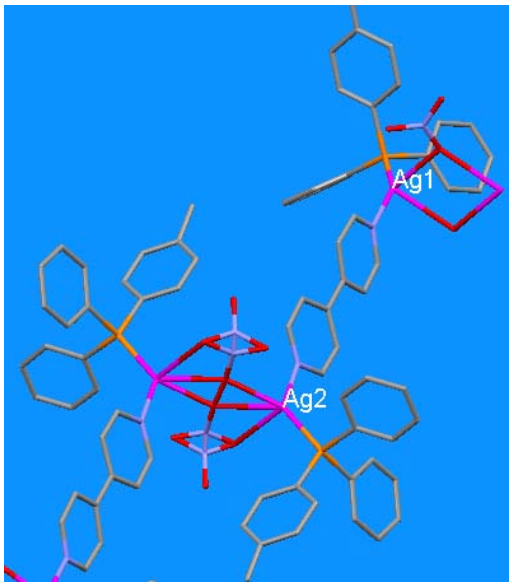

Figure 3b. A view of the geometrical environments around atoms Ag(1) and Ag(2) in complex **3**.

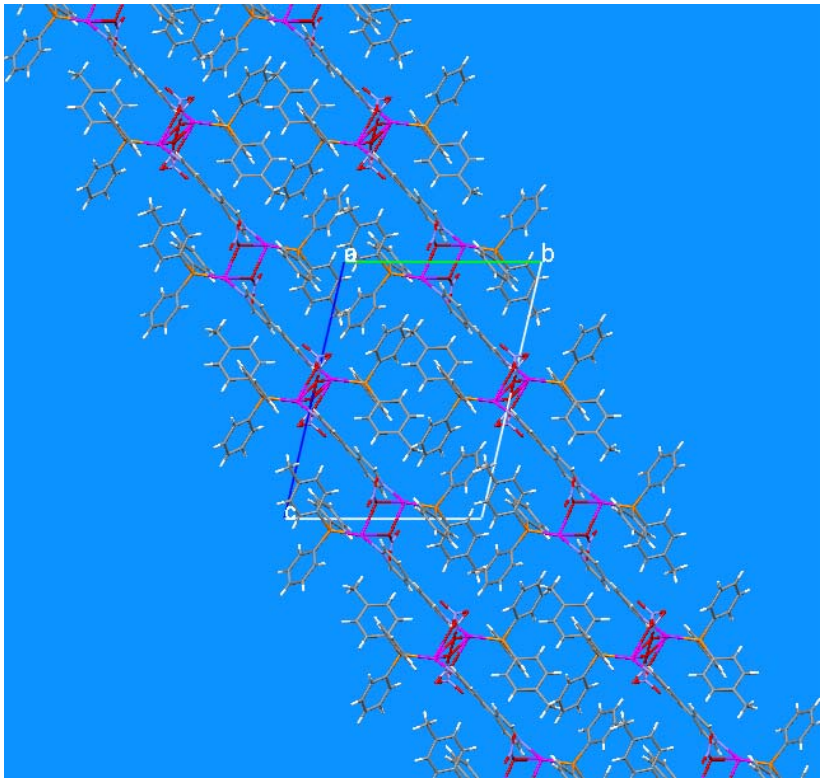

Figure 3c. View along the *a*-axis of the crystal packing in complex **3**.

$[Ag_2(4,4'\text{-bipy})(P4)_2(NO_3)_2]_n$ (4):

The molecular structure of complex **4** is shown in Fig. **4a**. There are two units of $[Ag(P1)(NO_3)]$ and two half molecules of 4,4′-bipy in the asymmetric unit. The single crystal structure of complex **4** is isostructural and isomorphous to complexes **1**, **2** and **3**.

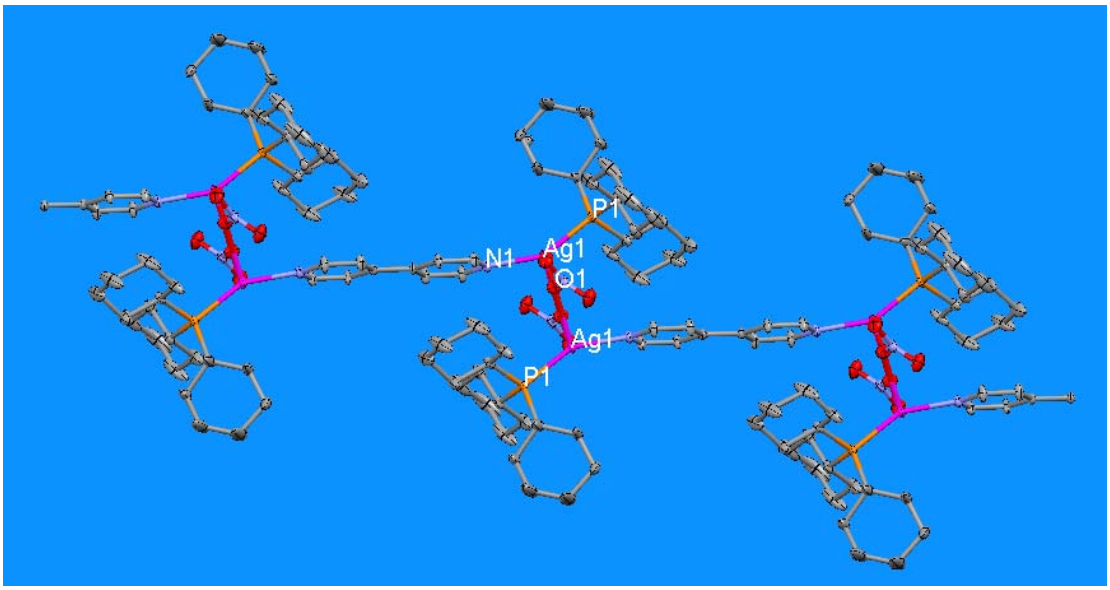

Figure 4a. View of the molecular structure of complex **4** and displacement ellipsoids are drawn at the 30% probability level.

The geometrical environment around the silver(I) atoms is pseudo tetrahedral like complexes **1–3**. The Ag-N and Ag-P bond distances are 2.216(4) and 2.3566(12) Å, respectively, while the Ag-O bond distance is 2.460(4) Å. The Ag-P bond distances are comparable with those found in complexes **1–3**. The Ag-N bond distance is comparable to that found in complex **2,** but shorter than that found in complexes **1** and **3**. The N-Ag-P/ O-Ag-P, and N-Ag-O bond angles are 152.02(10)/ 106.23(9), and 99.66(13) & 82.76(13)º, respectively. These bond angles values show considerable deviation from the ideal tetrahedral angle of 109.5º.

The solid state structure of complex **4** consists of step-like undulating infinite polymeric chain, which run parallel to the *a*-axis and is staked along *b*-axis, as shown in Fig. **4b**. The molecular structure shows two crystallographic inversion centres, one in the middle

of Ag_2O_2 four member ring and other in the middle of central C-C bond in the 4,4′-bipy ligand molecule. The Ag-O-Ag bond angle 98.4º is smaller than that found in complexes **1–3**. The Ag...Ag distance ca. 3.837 Å; therefore does not show any metal–metal interaction.

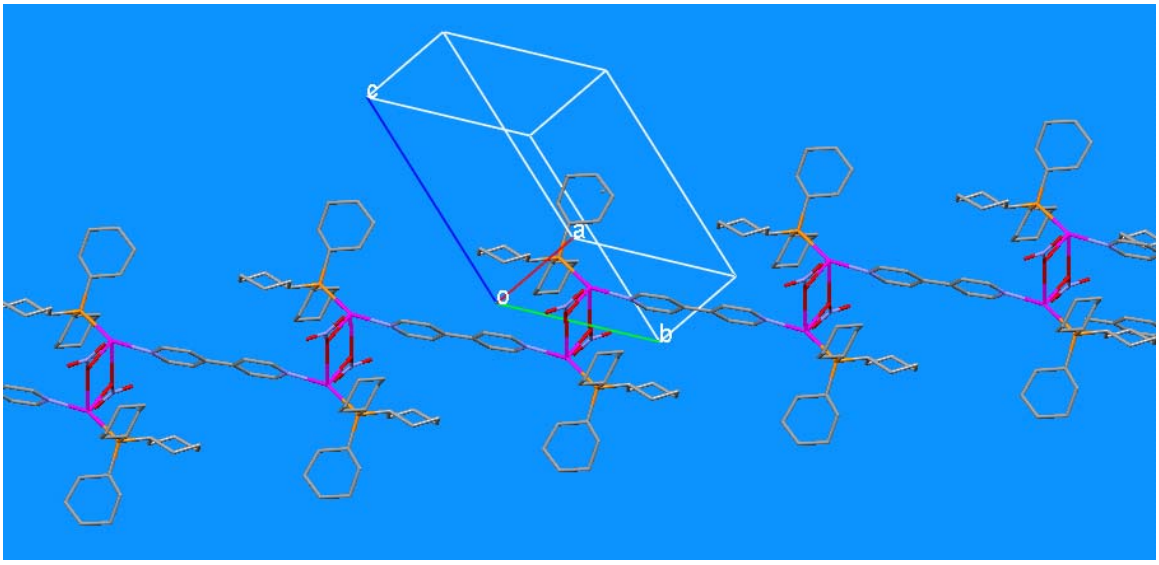

Figure 4b. Panel is showing the polymeric chain structure of complex **4**.

{[Ag(4,4′-bipy)(P2)](ClO_4)}$_n$ (5):

The single crystal structure of the complex **5** is shown in the Fig. **5a**. The crystal structure reveals that replacing the NO_3^- counter ion with a ClO_4^- counter ion results in considerable changes in the final structure of complex **5**. The silver(I) atom is coordinated with two independent 4,4′-bipy molecules and these exo-dentate ligand molecules act as bridging ligand between [Ag(P2)] units to form a one-dimensional polymeric chain structure. This type of bridging behaviour, in the solid state structure of complex **5,** results in a unique zigzag infinite polymeric chain, as shown in Fig. **5b**. In this coordination polymer, the counter ions (ClO_4^-) do not show coordination with the silver(I) atoms. Due to the counter ion effect; prominent changes in geometry around silver(I) atom has been observed. The geometry around the central metal atom is changed from distorted tetrahedral to trigonal planar. The pyridyl rings of the 4,4′-bipy ligand molecules are highly twisted around the central C-C bond with a dihedral angle of 84.0(3)º. This dihedral angle value is much bigger than that found in complexes **1-4**.

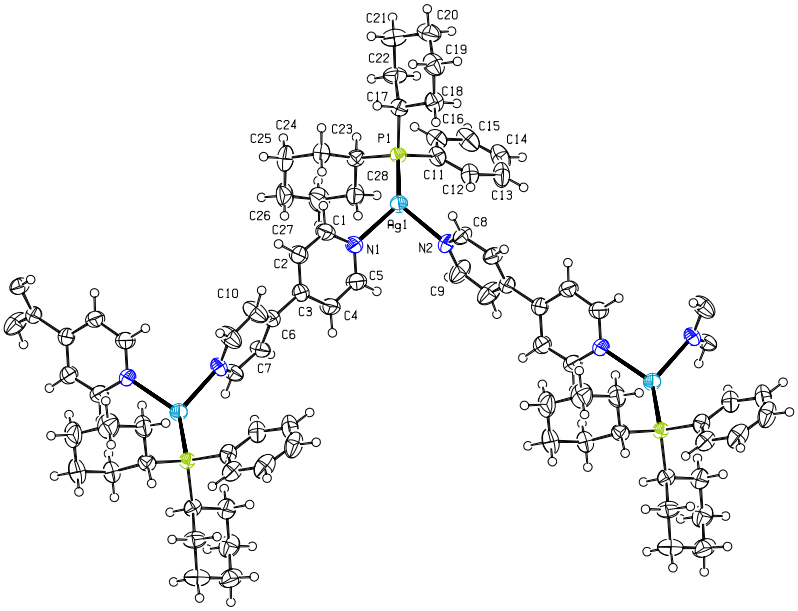

Figure 5a. A view of the molecular structure of complex **5** with complete atom labelling Scheme and displacement ellipsoids drawn at the 50% probability level (anion omitted for clarity).

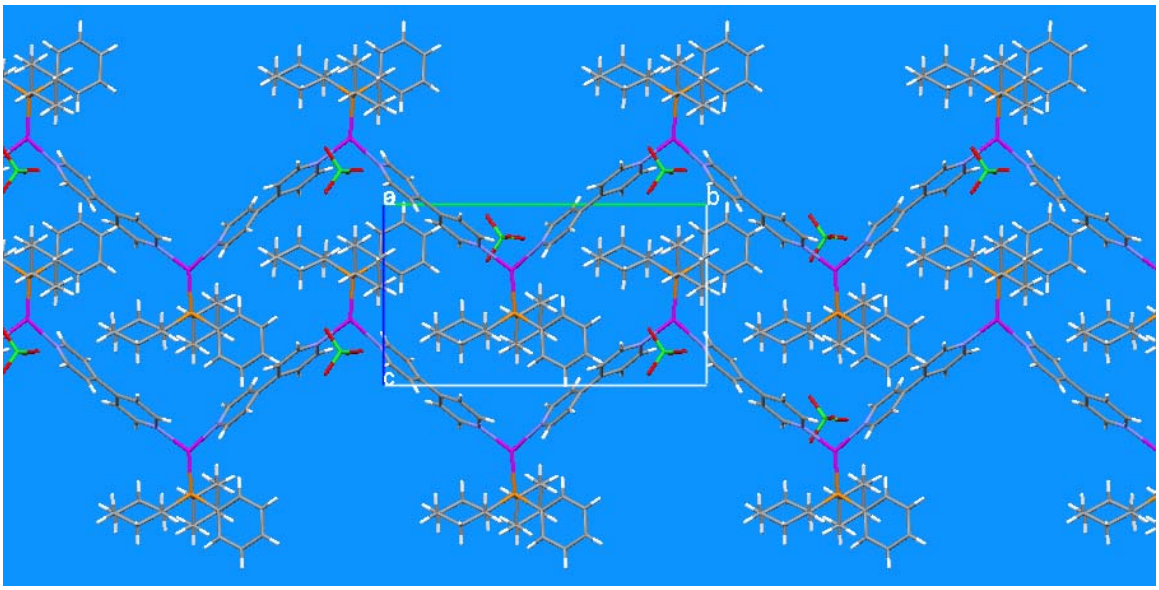

Figure 5b. View along *a*-axis of the crystal packing of complex **5**.

The Ag-N bond distances 2.292(4) and 2.314(4) Å, are longer than those found in complexes **1-3**. The N-Ag-N bond angle is 91.01(12)° and shows that both 4,4′-bipy

ligand molecules are coordinated to the central metal atom at right angle to each other. The N-Ag-P bond angles values are 133.30(12) and 132.21(11)º. The bond angles values around the silver(I) atom are considerably bigger than the ideal trigonal planar angle value of 120º. The Ag-P bond distance is 2.3448(9) Å, which is comparable to that found in complexes **1-4**. The geometry around the silver(I) atom provides additional evidence that coordinating and non-coordinating counter ions can have a pronounced affect on the final geometry of the central metal ion.

{[(CH$_3$CN)Ag(4,4′-bipy)][Ag(4,4′-bipy)]$_3$·(ClO$_4$)$_4$·5CH$_3$CN}$_n$ (6):

The molecular structure of complex **6** is a pseudo polymorph of {[Ag(4,4′-bipy)].ClO$_4$.CH$_3$CN}$_n$,[20] and is shown in Fig. **6a**. There are four independent one dimensional polymeric chains in this multi-layered structure. The geometrical environments around the different silver(I) atoms is linear and distorted trigonal planar, as shown in Fig. **6a**.

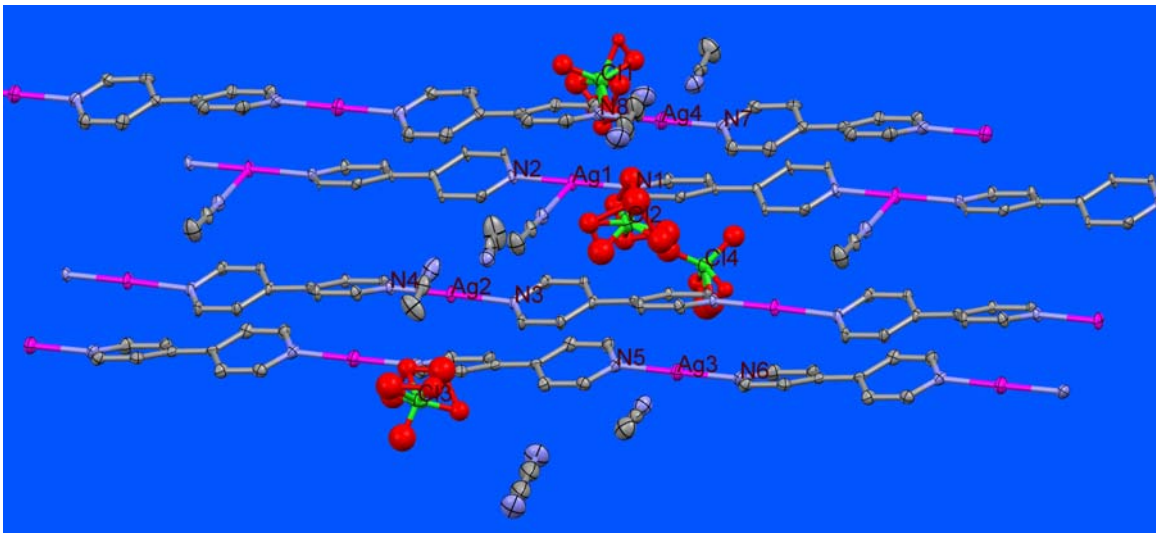

Figure 6a. View of the four independent one-dimensional polymeric chains in the multi-layered structure of complex **6**.

In one chain, the silver(I) atoms are also coordinated with acetonitrile molecules. This coordination mode results in a distorted trigonal planar geometry around atom Ag1.In rest of the chains, the silver(I) atoms do not show any coordination with the acetonitrile lattice

molecules and have linear geometry around them. The Ag-N bond distances range from 2.156(7) to 2.187(6) Å. The N-Ag-N bond angles (with 4,4′-bipy ligand) range from 174.0(4) to 177.2(2)˚ and show deviation from the ideal linear angle of 180º in this multi-layered linear chain structure (Table **2**).

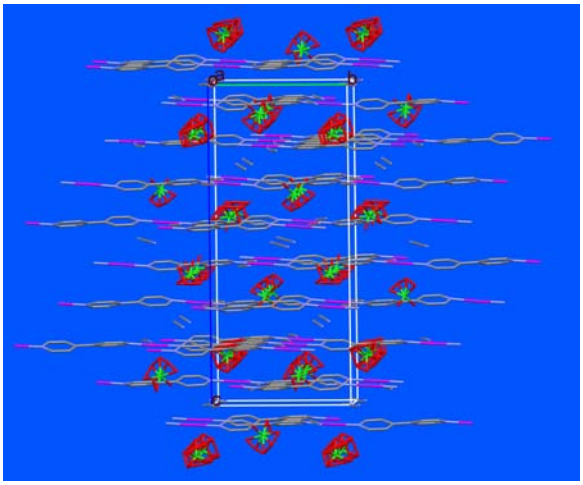

Figure 6b. View along the *a*-axis of the crystal packing of complex **6**.

In the crystal structure of **6** the linear chains stack up the *c*-axis and are separated by perchlorate anions and acetonitrile molecules of crystallization (Figure **6b**).

$[Ag_2(4,4'\text{-bipy})(P5)_2(NO_3)_2]_n$ (7):

The crystal structure of complex **7** is composed of two independent infinite two–dimensional networks which lie parallel to the *ab* plane (Figures **7a** and **7b**). One involves atom Ag1 and is situated at *c* equal to 0 (and 1), while the other involves atom Ag2 and lies at *c* = 0.5, see Figures **7a** and **b**.

The geometrical environment around the silver(I) atoms is pseudo-tetrahedral, similar to that found in complexes **1–4**. The nitrate counter ions act as bridging ligands between the $[Ag_2(P5)(4,4'\text{-bipy})]$ units. Each 1,2-bis(diphenyl-phosphino)ethane (P5) ligand molecule is coordinated with two silver(I) atoms, as are the 4,4′-bipy ligand molecules. The Ag-N bond distances are 2.277(7) and 2.254(7) Å and the Ag-P bond distances are 2.3605(19) and 2.336(2) Å. The Ag-O bond distances range from 2.373(7) to 2.547(7) Å. The

Ag…Ag distances are ca. 3.912 and 4.067 Å, hence no metal-metal interactions are observed here.

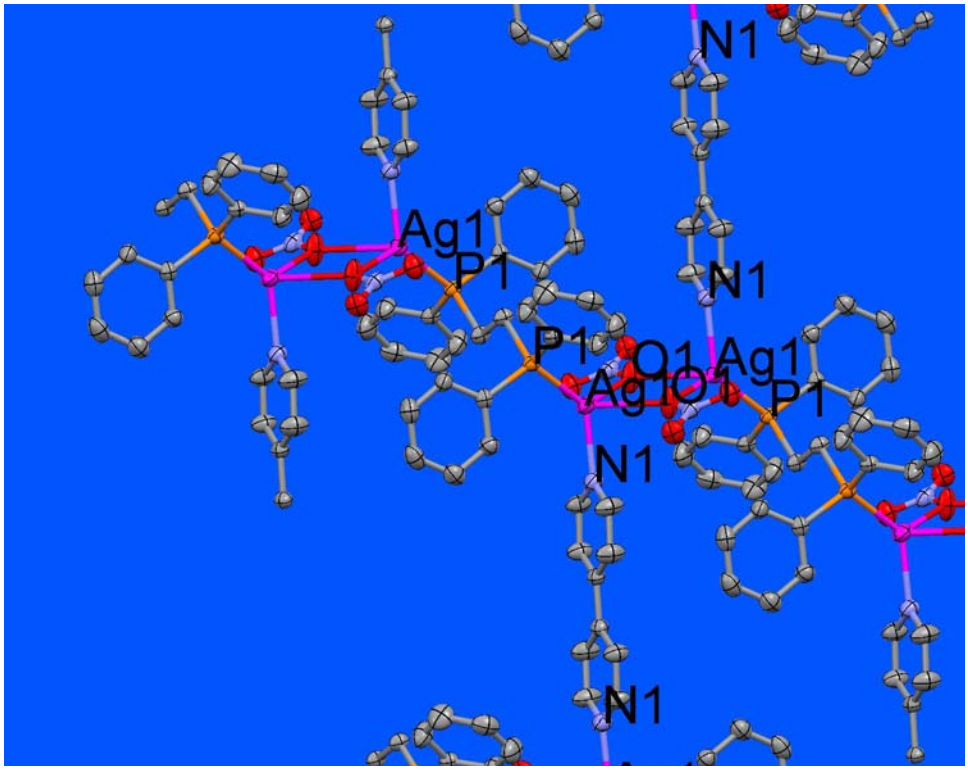

Figure 7a. A view of part of the 2D-network involving atom Ag1.

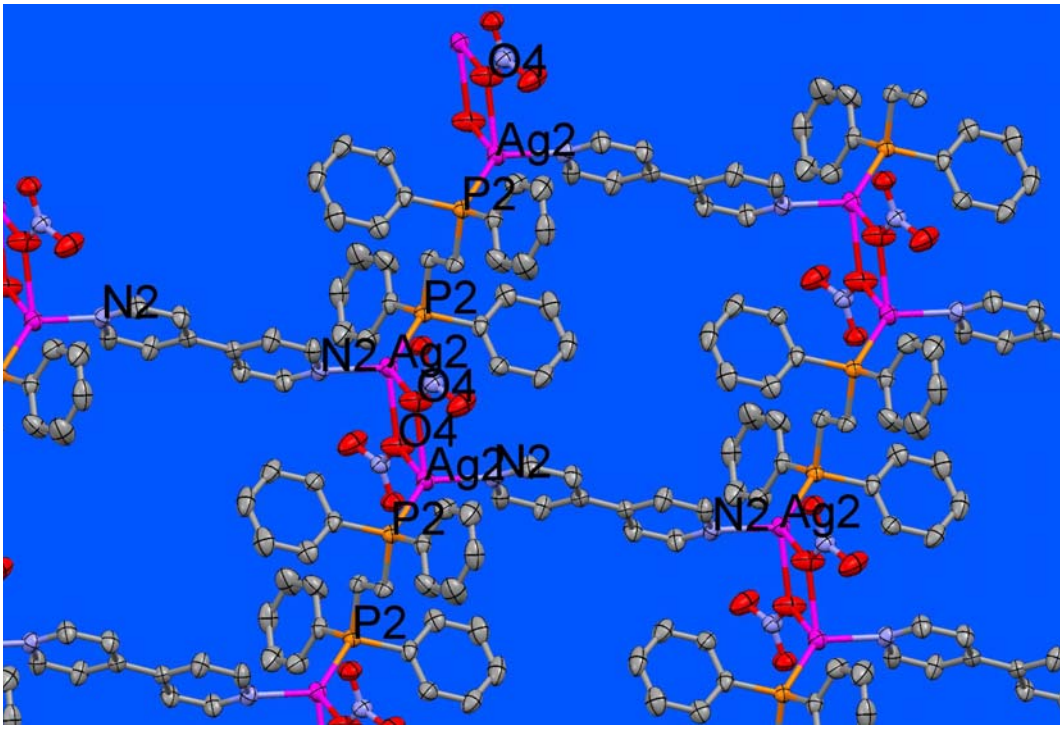

Figure 7b. A view of part of the 2D-network involving atom Ag2.

The P-Ag-N bond angles are 130.37(18) and 131.73(19)º. The O-Ag-P and O-Ag-N bond angles vary from 120.68(15) to 128.17(18) and 86.9(2) to 101.8(2)º respectively. The O-Ag-O and Ag-O-Ag bond angles values are 68.5(2) & 71.6(2)º, and 111.4 & 108.42º respectively. The bond angle values around the silver(I) atoms in complex **7** show a considerable deviation from the ideal tetrahedral angle of 109.5º. In this highly symmetrical complex molecule, both pyridyl rings of the two 4,4′-bipy ligand molecules are coplanar.

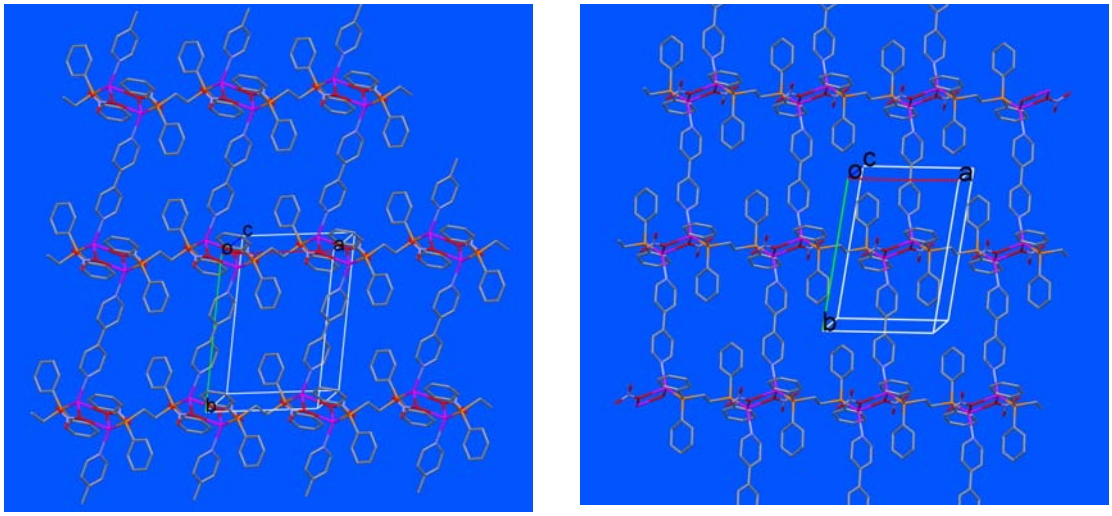

Figure 7c. A view of the two-dimensional networks in complex **7**.
Left: c = 0 (or 1) involving atom Ag1; ***Right***: c = 0.5 involving atom Ag2.

It can be seen from Figs. **7c** that the two networks are slightly differently orientated. The 4,4′-bipy ligands are inclined by a smaller angle to the *a*-axis in the network involving atom Ag1, than is the case for the network involving atom Ag2. The latter network is also shifted by *a*/2 with respect to the network involving atom Ag1.

In Fig. **7d** an AUTO-FIT has been carried out using the routine in the program PLATON (Spek, 2003). The best fit was achieved by inverting the network involving atom Ag2 (red) and fitting it to the network involving atom Ag1 (black).

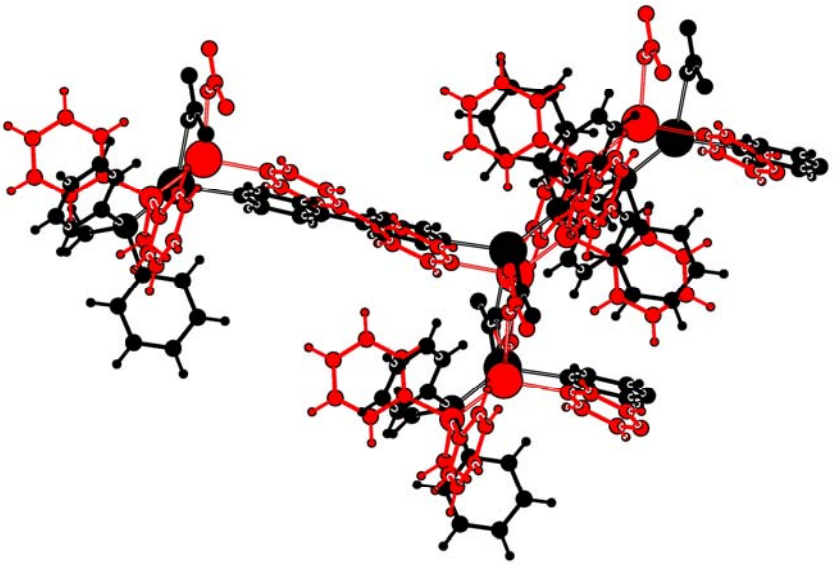

Figure 7d. An AUTO-FIT (PLATON: Spek, 2003) of the inverted form of the network involving atom Ag2 (red) with the network involving atom Ag1 (black)

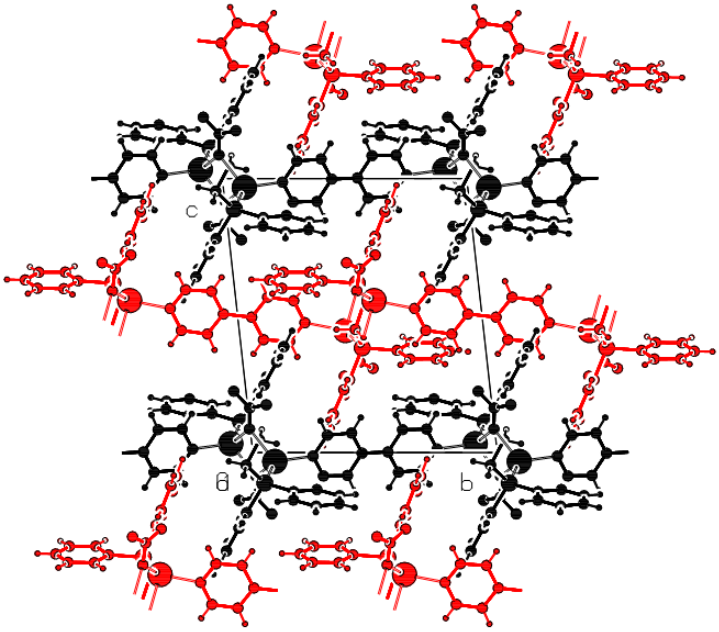

Figure 7f. A view along the *a*-axis of the crystal packing in complex **7**.
The network involving atom Ag2 is in red and that involving atom Ag1 is in black.

Table 2. Selected bond distances (Å) and bond angles (˚) in complexes **1**–**7**.

(**1**)	
Ag1 -P1 2.3637(12)	P1 -Ag1 -O1 112.98(7)
Ag1 -O1 2.454(3)	P1 -Ag1 -N1 150.14(10)
Ag1 -N1 2.246(4)	O1 -Ag1 -N1 93.28(11)

(**2**)	
Ag1 -P1 2.3489(10)	P1 -Ag1 -O1 114.80(10)
Ag1 -O1 2.451(4)	P1 -Ag1 -N1 154.22(10)
Ag1 -N1 2.209(4)	P1 -Ag1 -O1_b 103.37(9)
Ag1 -O1_b 2.620(4)	O1 -Ag1 -N1 89.81(14)
Symmetry operation: b = 2-x,1-y,1-z	O1 -Ag1 -O1_b 78.37(13)
	O1_b -Ag1 -N1 88.39(14)

(**3**)	
Ag1 -P1 2.3616(16)	P1 -Ag1 -O1A 128.5(2)
Ag1 -O1A 2.322(9)	P1 -Ag1 -O2 110.81(13)
Ag1 -O2 2.656(5)	P1 -Ag1 -N1 131.60(13)
Ag1 -N1 2.266(5)	P1 -Ag1 -O1A_a 127.0(2)
Ag1 -O1A_a 2.422(9)	O1A -Ag1 -O2 79.4(2)
Ag2 -P2 2.3578(15)	O1A -Ag1 -N1 96.7(3)
Ag2 -O4 2.461(4)	O1A -Ag1 -O1A_a 31.2(3)
Ag2 -N3 2.211(4)	O2 -Ag1 -N1 91.81(17)
Ag2 -O4_b 2.576(4)	O1A_a -Ag1 -O2 48.5(2)
Symmetry operations: a = -x,2-y,1-z b = 1-x,1-y,-z	O1A_a -Ag1 -N1 100.3(3)
	P2 -Ag2 -O4 105.03(10)

	P2 -Ag2 -N3 151.68(11) P2 -Ag2 -O4_b 114.05(10) O4 -Ag2 -N3 101.06(14) O4 -Ag2 -O4_b 74.65(12) O4_b -Ag2 -N3 83.29(15)

(**4**)	
Ag1 -P1 2.3566(12) Ag1 -O1 2.460(4) Ag1 -N1 2.216(4) Ag1 -O1_a 2.604(4) Symmetry operation: a = -x,1-y,-z	P1 -Ag1 -O1 106.23(9) P1 -Ag1 -N1 152.02(10) P1 -Ag1 -O1_a 111.09(9) O1 -Ag1 -N1 99.66(13) O1 -Ag1 -O1_a 81.53(12) O1_a -Ag1 -N1 82.76(13)

(**5**)	
P1 -Ag1 -N1 133.30(13) P1 -Ag1 -N2 132.21(10) N1 -Ag1 -N2 91.02(15)	P1 -Ag1 -N1 133.30(13) P1 -Ag1 -N2 132.21(10) N1 -Ag1 -N2 91.02(15)

(**6**)	
Ag1 -N1 2.174(6) Ag1 -N9 2.663(9) Ag1 -N2_a 2.161(7) Ag2 -N3 2.187(6)	N1 -Ag1 -N9 92.7(2) N1 -Ag1 -N2_a 174.0(3) N3 -Ag2 -N4_c 177.2(2) N5 -Ag3 -N6_f 178.9(3)

Ag2 -N4_c 2.159(6) Ag3 -N5 2.156(7) Ag3 -N6_f 2.179(7) Ag4 -N8_g 2.175(7) Ag4 -N7 2.169(7) Symmetry operations: a = x,-1+y,z c = x,-1+y,z g = x,-1+y,z f = x,1+y,z	N7 -Ag4 -N8_g 178.2(3)

(7)	
Ag1 -P1 2.3605(19) Ag1 -O1 2.547(7) Ag1 -N1 2.277(7) Ag1 -O1_a 2.373(7) Ag2 -O4_e 2.411(6) Ag2 -P2 2.336(2) Ag2 -O4 2.412(7) Ag2 -N2 2.254(7) Symmetry operations: a = -x,-y,2-z e = 1-x,1-y,1-z	P1 -Ag1 -O1 P1 -Ag1 -N1 P1 -Ag1 -O1_a O1 -Ag1 -N1 O1 -Ag1 -O1_a O1_a -Ag1 -N1 O4_e -Ag2 -N2 P2 -Ag2 -O4_e P2 -Ag2 -O4 P2 -Ag2 -N2 O4 -Ag2 -N2 O4 -Ag2 -O4_e

Conclusions

Six new silver(I) phosphine mixed ligand complexes, and one pseudo polymorph of 4,4′-bipyridine (4,4′-bipy) complex of silver(I) perchlorate, solvated by acetonitrile, have been synthesized and fully characterized. They include

$[Ag_2(4,4'\text{-bipy})(P1)_2(NO_3)_2]_n$ (**1**),

$[Ag_2(4,4'\text{-bipy})(P2)_2(NO_3)_2]_n$ (**2**),

$[Ag_2(4,4'\text{-bipy})(P3)_2(NO_3)_2]_n$ (**3**),

$[Ag_2(4,4'\text{-bipy})(P4)_2(NO_3)_2]_n$ (**4**),

$\{[Ag(4,4'\text{-bipy})(P2)](ClO_4)\}_n$ (**5**),

$\{[(CH_3CN)Ag(4,4'\text{-bipy})][Ag(4,4'\text{-bipy})]_3\cdot(ClO_4)_4\cdot 5CH_3CN\}_n$ **(6)**

and $[Ag_2(4,4'\text{-bipy})(P5)_2(NO_3)_2]_n$ (**7**)

[where P1 = Diphenylcyclohexyl phosphine, P2 = Dicyclohexylphenyl phosphine, P3 = Diphenyl(p-tolyl) phosphine, P4 = Tricyclohexyl phosphine, and P5 = 1,2-Bis(diphenyl-phosphino)ethane].

In the crystal structures of complexes **1-4** and **7** the 4,4′-bipy ligand molecule is essentially planar with a good fit of the Ag^I ion in the ''cavity'' between the tertiary phosphine phosphorous, the counter ion oxygen and 4,4′-bipy nitrogen donor atoms. In the case of complex **5** the ligand 4,4′-bipy is slightly twisted with a fairly good fit of the Ag^I ion in the ''cavity'' between the phosphorous donor atom of the monodetate tertiary phosphine ligand and the 4,4′-bipy nitrogen donor atoms of two individual ligand molecules. In the case of complex **6**, one-dimensional multi-layered network is obtained with acetonitrile lattice molecules. Single crystal analysis of the silver(I) complex **7,** containing the biphosphine ligand **P5**, revealed a two-dimensional polymeric network. In complexes **1-4** and **7** the silver(I) atoms are bridged by an oxygen atom of the nitrate anions, this type of bridging results in the formation of one-dimensional polymeric chains in the case of complexes **1**-**4**, and a 2D network in the case of **7**. In complex **5**, which is unexpectedly chiral (monoclinic, space group $P2_1$), the silver(I) atom is coordinated by the nitrogen donor atoms of two individual 4,4′-bipy ligand molecules and results in the formation of a one-dimensional zigzag polymeric chain. In the case of complex **6** the resulting product proved to be a complicated series of four independent silver-4,4′-

bipyridine chains, in one of which an acetonitrile molecule coordinates to the silver(I) atom.

It has been shown that it is possible to form silver(I) phosphine mixed-ligand complexes using the exo-dentate ligand 4,4′-bipyridine. Using various tertiary phosphines both one- and two-dimensional coordination polymers were synthesized. The nitrate anion is shown to be particularly useful to bridge two silver(I) atoms. In the case of the silver(I) perchlorate complexes the anion does not coordinate to the metal atom.

References

(1) Cote, A. P.; Shimizu, G. K. H. *Inorg. Chem.* **2004**, 43, 6663.

(2) Bosch, E.; Barnes, C. L. *Inorg. Chem.* **2001**, 40, 3097.

(3) Bi, W.; Sun, D.; Cao, R.; Hong, M. *Acta Crystallogr.* **2002**, E58, m324.

(4) Tong, M.-L. ; Chen, X-M. ; Ng, S. W.; *Inorg. Chem. Commun*. **2000**, 3, 436.

(5) Thaler, A.; Bergter, R.; Ossowski, T.; Cox, B. G.; Schneider, H.; *Inorg. Chim. Acta.* **1999**, 285, 1.

(6) Janiak, C. *Angew. Chem. Int.Ed.Engl.***1997**, 36, 1431.

(7) Robson, R.; Btten, S. *Angew.Chem., Int. Ed.* **1998**, 37, 1460.

(8) Connor, T. A.; Charlton, M.;Cupertino, D. C.; Liemke, A.; Mcpartlin, M.; Scowen, I. J.; Tasker, P. A. *J . Chem. Soc., Dalton Trans.* **1996**, 2835.

(9) Blake, A. J.; Baum, G.; Champness, N. R.; Chung, S. S. M.; Cooke, P. A.; Fenske, D.;Khlobystov, A. N.; Lemenovskii, D. A.; Li, W-S.; Schroder, M. *J. Chem. Soc., Dalton Trans.* **2000**, 4285.

(10) Lehn, J. M. *Angew. Chem., Int. Ed. Engl.* **1990**, 1304.

(11) Eddaoudi, M.; Moler, D. B.; Li, H.; Chen, B.;Reineke, T. M.; Keeffe, M. O.; Yaghi, O. M. *Acc. Chem. Res.***2001**, 34, 319.

(12) Blake, J. A.; Champness, N. R.; Crew, M.; Parsons, S. *New. J. Chem.; Letters.***1999**, 13.

(13) Robson, R. *J. .Chem. Soc., Dalton Trans.* **2000**, 3735.

(14) Yaghi, O. M:, Li, H. *J. Am. Chem. Soc.* **1996**, 118, 295.

(15) Abrahams, B. F.; Batten, S. R.; Hoskins, B. F.; Robson, R.; *Inorg. Chem.* **2003**, 42, 26.

(16) Cunha-Silva, L.; Ahmad, R.; Hardie, M. J.*Aust. J. Chem.* **2006**, 59, 40.

(17) Mantero, D. G.; Neels, A.; Stoeckli-Evans, H. *Acta Crystallogr., Sect. E. Struct. Rep. Online.* **2006**, 62, m1381.

(18) Robinson, F.; Zaworotko, M. *J. Chem. Commun.* **1995**, 2413.

(19) Sampanthar, J. T. ; Vittal, J. J. *Crystal Engineering* . **2000**, 3, 117.

(20) Wang, L.-S.; Zhang, J.-F.; Yang, S.-P. *Acta Crystallogr., Sect. E. Struct. Rep. Online.* **2004**, 60, m1484.

Chapter 6:

Coin Metal Tertiary Phosphine Precursors

Part A:

Silver(I) tertiary phosphine precursors for mixed-ligand silver(I) tertiary phosphine complexes: Structural and spectroscopic studies

Abstract

One-, two-, three- and four-coordinate silver(I) complexes, AgX (X = NO_3^-, CN^-, PF_6^-, and SbF_6^-), with triphenyl phosphine, tricyclohexyl phosphine, diphenylcyclohexyl phosphine, and dicyclohexylphenyl phosphine have been synthesized and characterized by single crystal X-ray diffraction, elemental analysis, infrared spectroscopy and ^{13}C & ^{31}P NMR spectroscopy. The 1:1 (metal salt to ligand ratio) compound crystallizes as $[Ag(PCy_3)_2(NO_3)]_2$ (**1**) a centrosymmetric dimer, whereas the 1:2, 1:3, and 1:4 compounds $[Ag(PPhCy_2)_2(NO_3)]$ (**2**), $[Ag(PPh_2Cy)_3(CN)].5H_2O$ (**3**), $[Ag(PCy_3)_2].PF_6$ (**4**), $[Ag(PPh_3)_4)].SbF_6.CHCl_3$ (**5**), $[Ag(PCy_3)_2].SbF_6$ (**6**), $[Ag(PPh_2Cy)_2(0.75C_3H_6O)].SbF_6$ (**7**), and $[Ag(PPhCy_2)_2].SbF_6.CHCl_3$ (**8**) crystallize as monomers, with a wide variety of geometries around the central silver(I) atom. The compounds **2** and **7** have distorted trigonal planar geometry and compounds **3** and **5** have slightly distorted tetrahedral geometry around the silver(I) atom. The compounds **4**, **6**, and **8** show linear geometry around the metal centre. The elemental analysis and NMR spectroscopy results are consistent with the single crystal structural results.

Introduction

Silver(I) exhibits a remarkable diversity in its structural chemistry. This is illustrated by a wide variety of structural types that are encountered in complexes of silver(I) salts. In silver(I) mononuclear and multinuclear complexes with neutral phosphine and amine ligands the silver(I) atom exhibits variable coordination numbers.[1-5] Reactions of AgX (X = NO_3^-, ClO_4^-, $C_2H_3O_2^-$, CN^-, SCN^-, PF_6^-, SbF_6^-, Cl^-, Br^-, and I^- etc.,) with monodentate tertiary phosphine and multidentate nitrogen donor bases yielded a diverse array of two-, three- and four- coordinate complexes with structural and spectroscopic properties that are determined by, specific choices of the phosphine and the other ligands, the stoichiometry and to a lesser extent by the choice of the anion.[6-10] Tertiary phosphine complexes of silver(I) of the type $[AgXL_n]$, where L = tertiary phosphine; n = 1-4; X = coordinating or non-coordinating anion, were first prepared in 1937.[11] The general method of preparation involves the reaction of stoichiometric amounts of the phosphine ligand with the appropriate silver(I) salt. The reaction of silver(I) salts with monodentate tertiary phosphines in a 1:2 stoichiometric ratio generally results in the formation of either monomeric $[AgX(PR_3)_2]$ / $[Ag(PR_3)2].X$[12-24] or dimeric complexes $[\{AgX(PR_3)_2\}_2]$,[24-27] depending on the donor properties of the phosphine ligand, the bulkiness of the ligand, the substituents and the donor properties of the anion. These complexes show a diversity of structural types and several reviews on this topic has been published.[28-31] The metal centre in the majority of the neutral $[AgX(PR_3)_2]$ and $[\{AgX(PR_3)_2\}_2]$ complexes are predominantly four coordinate with the anion acting as either a bidentate chelating ligand or as a bridging ligand, with two or three coordination found only in circumstances where the anion is a week donor or the substituents on the phosphine ligand are bulky.[16,19-24]

Our interest in silver(I) complexes with tertiary phosphine is based on the attempted synthesis of mixed ligand complexes with a variety of N, O, S, P, and carbon donor ligands. Initially, we prepared coinage metal complexes with monodentate tertiary phosphine ligands and later we used these silver(I) phosphine precursors for the preparation of mixed ligand complexes with pre-designed structure and properties.

There is great interest to know about how the molecular properties of the ligands affect the evolving structures of the complexes and their physical, chemical and biological properties.[32-33] Much efforts have been devoted to the design and syntheses of pre-organized ligands that are able to control the structure and properties of complexes.[34-37] Silver(I) complexes with various N, S, O, P and C donor ligands are of growing interest owing to their wide variation in structural format and rich physical, photo-physical, biological and chemical properties.[38-42]

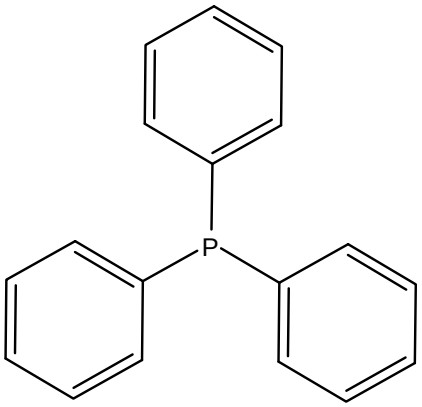

triphenyl phosphine

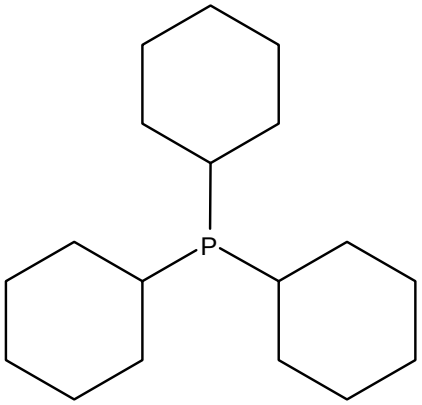

tricyclohexyl phosphine

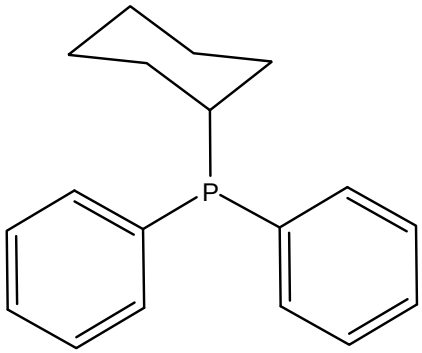

cyclohexyldiphenyl phosphine

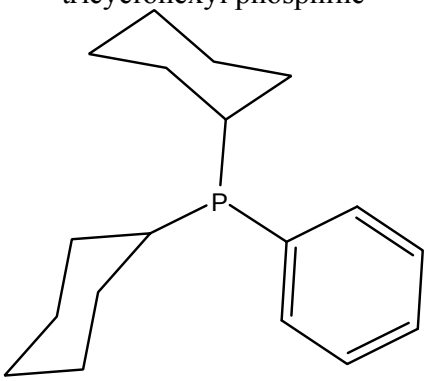

dicyclohexyl(phenyl) phosphine

Scheme 1.

In our current investigations into the dependence of the structural and spectroscopic properties of these compounds on the choice of monodentate tertiary phosphine and

coordinating and non-coordination anions, we have sought to extend the array of available data for two-, three-, and four-coordinate complexes of silver(I) with triphenyl phosphine, tricyclohexyl phosphine, diphenylcyclohexyl phosphine, and dicyclohexylphenyl phosphine (Scheme 1). Single crystal X-ray structures have been determined for 1:1 to 1:4 adducts for X = NO_3^-, CN^-, PF_6^-, and SbF_6^-. Spectroscopic data has been obtained from low frequency infrared spectroscopy and ^{13}C & ^{31}P NMR spectroscopy.

Along with X-ray diffraction techniques, there are several potentially useful spectroscopic techniques for characterizing compounds in the solid state and solution. Thus IR, FAR-IR, UV-Visible and NMR spectroscopy have proved to be useful techniques for the determination of the structures of silver(I) complexes.[43-46] Silver(I)-phosphine complexes and their single crystal X-ray structures, IR absorption spectra and NMR spectroscopic properties are discussed here. The single crystal X-ray diffraction analysis has been carried out at low temperature (-100ºC).

Experimental

All the reactions were carried out in air. All the reactants and solvents were commercial products of Aldrich and ACROS and were used with out further purification. In all cases, the crystalline products were obtained by slow evaporation method. Microanalysis was done by Mr. D. Mooser (Ecole d'ingénieurs de Fribourg, Filière de chimie). The IR spectra were recorded as KBr plates on a PerkinElmer Spectrum One FTIR instrument. ^{13}C and ^{31}P NMR spectra were recorded on Bruker AMX 400 MHz using d_2-CD_2Cl_2, d_3-CD_3Cl and d_4-CD_3OD as solvents. The TMS was used as the internal standard.

Synthesis

$[Ag(PCy_3)_2(NO_3)]_2$ (1)

To a solution of $AgNO_3$ (0.017 g, 0.1 mmol) in distilled water (5 mL) was added tricyclohexyl phosphine (0.028 g, 0.1 mmol) in acetone (15 mL). After the reaction

mixture was stirred for 1h at room temperature. The colourless solution obtained was filtered to avoid any impurity and left undisturbed for slow evaporation. After three days colourless block crystals were obtained. A suitable crystal was chosen for X-ray diffraction studies. The rest of the crystalline product was collected by filtration and air dried. Yield was found 78%. Anal. Calc. for $C_{36}H_{66}Ag_2N_2O_6P_2$: C, 47.96; H, 7.32; N, 3.10. Found: C, 48.67; H, 7.46; N, 3.13%. IR (υ, cm^{-1}): 3551m, 3412m, 2918s, 2828s, 1638m, 1616s, 1446vs, 1297m, 1174s, 1005s, 839vs, 557s.

$[Ag(PPhCy_2)_2(NO_3)]$ (2)

To a solution of $AgNO_3$ (0.017 g, 0.1 mmol) in distilled water (5 mL) was added dicyclohexylphenyl phosphine (0.055 g, 0.2 mmol) in acetone/acetonitrile (1:1) (20 mL). After mixing the reaction mixture was stirred for 2h at room temperature. The clear solution obtained was filtered and kept at room temperature for slow evaporation. After few days colourless plate like crystals were obtained. A suitable crystal was used for X-ray diffraction analysis and rest of the crystalline product was collected by filtration. The yield was found 68%. Anal. Calc. for $C_{36}H_{54}AgNO_3P_2$: C, 60.11; H, 7.51; N, 1.95. Found: C, 60.43; H, 7.62; N, 2.28%. IR (υ, cm^{-1}): 3551m, 3478s, 3412s, 3075w, 3052w, 2928vs, 2858s, 1638m, 1617s, 1447vs, 1277m, 1175s, 1003s, 847m, 658vs, 533m.

$[Ag(PPh_2Cy)_3(CN)].5H_2O$ (3)

The same procedure was followed for the synthesis of compound **3** as described for compound **1** & **2**. To the solution of AgCN (0.014 g, 0.1 mmol) in MeOH/distilled water (3:2) (10 mL) was added diphenylcyclohexyl phosphine (0.086 g, 0.3 mmol) in acetonitrile (15 mL). The reaction mixture was stirred for overnight at 50˚C. The colourless solution obtained was filtered to avoid any impurity and cool down to room temperature and evaporated slowly. After 5 days colourless plate like crystals were obtained. A suitable crystal was chosen for X-ray diffraction analysis. The rest of the product was collected by decantation of solvent and yield was found 62%. Anal. Calc. for $C_{55}H_{67}AgNO_2P_3$: C, 67.70; H, 6.87; N, 1.43. Found: C, 67.66; H, 6.60; N, 1.76%. IR (υ, cm^{-1}): 3412s, 3070m, 3050m, 2926vs, 2849s, 2344w, 2151w, 2107m, 1638m, 1617s, 1434vs, 1265m, 1183s, 998s, 847m, 743m, 617m, 510m.

$[Ag(PCy_3)_2].PF_6$ (4)

To the solution of $AgPF_6$ (0.025 g, 0.1 mmol) in acetonitrile (5 mL) was added tricyclohexyl phosphine (0.057 g, 0.2 mmol) in CH_2Cl_2 (10 mL). The reaction mixture was stirred for 30 minutes at room temperature. The colourless solution obtained was filtered to avoid any impurity and left undisturbed for slow evaporation. After two days colourless plate like crystals were obtained. A suitable crystal was used for X-ray diffraction analysis. The crystalline product was collected from the evaporation dish and yield was found 83%. Anal. Calc. for $C_{36}H_{66}AgF_6P_3$: C, 53.09; H, 8.11. Found: C, 54.10; H, 8.46%. IR (υ, cm^{-1}): 3549m, 3409m, 2922s, 2825s, 1633m, 1618s, 1451vs, 1293m, 1171s, 1015s, 834vs, 622m, 557s.

$[Ag(PPh_3)_4)].SbF_6.CHCl_3$ (5)

To the solution of $AgSbF_6$ (0.035 g, 0.1 mmol) in acetonitrile (5 mL) was added 2-mercapto thiazoline (0.018 g, 0.2 mmol) in MeOH (5 mL) and triphenyl phosphine (0.027 g, 0.1 mmol) in $CHCl_3$ (10 mL). The reaction mixture was stirred overnight at 50˚C. The colourless solution obtained was cool down to room temperature and filtered to avoid any impurity. The resultant solution was evaporated slowly at room temperature. After three days colourless block crystals of unexpected product was obtained. A suitable crystal was chosen for X-ray diffraction studies. The crystalline product was collected by filtration and yield was found 17%. Anal. Calc. for $C_{73}H_{61}AgCl_3F_6P_4Sb$: C, 57.93; H, 4.03. Found: C, 57.13; H, 4.56%. IR (υ, cm^{-1}): 3551m, 3478s, 3412s, 3075m, 3052m, 1633m, 1615s, 1437vs, 1257m, 1155s, 1013s, 750m, 843m, 646vs, 503m.

$[Ag(PCy_3)_2].SbF_6$ (6)

To the solution of $AgSbF_6$ (0.035 g, 0.1 mmol) in acetonitrile (5 mL) was added tricyclohexyl phosphine (0.057 g, 0.2 mmol) in CH_2Cl_2 (10 mL). The reaction mixture was stirred for 30 minutes at room temperature. The colourless solution obtained was filtered to avoid any impurity and left undisturbed for slow evaporation. After three days colourless rod like crystals were obtained. A suitable crystal was used for X-ray diffraction analysis and rest of the product was collected and weighed. The yield was found 74%. Anal. Calc. for $C_{36}H_{66}AgF_6P_2Sb$: C, 47.76; H, 7.29. Found: C, 47.95; H,

7.25%. IR (υ, cm^{-1}): 3553m, 3412m, 2929s, 2823s, 1634m, 1617s, 1447vs, 1291m, 1168s, 1003s, 837vs, 628m, 555s.

$[Ag(PPh_2Cy)_2(C_3H_6O)].SbF_6$ (7)

The same procedure was followed for the synthesis of compound **7** as described for compound **6**. To the solution of $AgSbF_6$ (0.035 g, 0.1 mmol) in acetonitrile (5 mL) was added to a solution of diphenylcyclohexyl phosphine (0.057 g, 0.2 mmol) in CH_2Cl_2 (10 mL). The reaction mixture was stirred for 30 minutes and colourless solution obtained was filtered to avoid any impurity and left undisturbed for crystallization. After the evaporation of solvent a transparent solid product was obtained. The resultant product was re-dissolved in CH_2Cl_2/acetone (1:2) (15 mL) and kept for slow evaporation; after 3 days colourless block crystals were obtained. The crystalline product was carefully collected and weighed. The yield was found 56%. Anal. Calc. for $C_{39}H_{48}AgF_6OP_2Sb$: C, 49.87; H, 5.11. Found: C, 50.29; H, 5.24%. IR (υ, cm^{-1}): 3550m, 3413s, 3007m, 3069m, 2931s, 2889m, 2859m, 2837m, 1695s,1637m, 1617s, 1436vs, 1229m, 1176m, 1097s, 885m, 749s, 668m, 505s.

$[Ag(PPhCy_2)_2].SbF_6.CHCl_3$ (8)

The synthesis of compound **8** was done by following the same procedure as described for compound **6** & **7**. To the solution of $AgSbF_6$ (0.035 g, 0.1 mmol) in acetonitrile (5 mL) was added to a solution of dicyclohexylphenyl phosphine (0.055 g, 0.2 mmol) in CH_2Cl_2 (10 mL). The reaction mixture was stirred for 30 minutes and colourless solution obtained was filtered to avoid any impurity and left undisturbed for crystallization. After 5 days colourless crystals were obtained. A suitable crystal was chosen for single crystal X-ray diffraction studies. The crystalline product was collected carefully and weighed. The yield was found 83%. Anal. Calc. for $C_{37}H_{55}AgCl_3F_6P_2Sb$: C, 43.88; H, 5.43. Found: C, 43.95; H, 5.21%. IR (υ, cm^{-1}): 3550m, 3478s, 3412s, 3071w, 3051w, 2930vs, 2851s, 1637m, 1617s, 1449vs, 1270m, 1179s, 1001s, 847m, 747m, 659vs, 531m.

X-ray Crystallography.

The intensity data were collected at 173K on either, a one circle (ϕ scans)[1], or a two circle (ω and ϕ scans)[2] Stoe Image Plate Diffraction System, using MoKα graphite monochromated radiation. The structures were solved by Direct methods using the program SHELXS-97[3]. The refinement and all further calculations were carried out using SHELXL-97[3]. The H-atoms were either located from Fourier difference maps and freely refined or included in calculated positions and treated as riding atoms using SHELXL default parameters. The non-H atoms were refined anisotropically, using weighted full-matrix least-squares on F^2. In most cases multi-scan absorption corrections were applied using the MULscanABS routine in PLATON[4]. A summary of crystal data and refinement details for compounds **1**-**8** are given in Table 1, and selected bond lengths and angles are listed in Table 2.

1) Stoe & Cie (2000) IPDS-I Bedienungshandbuch. Stoe & Cie GmbH, Darmstadt, Germany.

2) Stoe & Cie. (2006) *X-Area V1.35 & X-RED32 V1.31 Software*. Stoe & Cie GmbH, Darmstadt, Germany.

3) G. M. Sheldrick (2008). Acta Crystallgr. A64, 112-122.

4) A. L. Spek (2003). J.Appl.Cryst. 36, 7-13

Table 1. Summery of crystal data and structure refinement details for compounds **1-8.**

$\{^{a}\ \mathbf{R1} = \Sigma||F_O| - |F_C||/\Sigma|F_O|.\ ^{b}\ \mathbf{wR2} = [\Sigma w(F_O^2 - F_C^2)^2/\Sigma wF_O^4]^{1/2}\}$

	1	**2**
Formula	$C_{36}H_{66}Ag_2N_2O_6P_2$	$C_{36}H_{54}AgNO_3P_2$
M	900.59	718.61
Wavelength/Å	0.71073	0.71073
Temperature/K	173	173
Crystal symmetry	Triclinic	Monoclinic
Space group	P -1	P 2_1
a/Å	9.1676(7)	10.9551(7)
b/Å	9.1338(7)	13.7042(6)
c/Å	13.3139(10)	12.2536(8)
α/°	91.077(6)	90
β/°	97.359(6)	107.158(5)
γ/°	116.098(6)	90
V/ $Å^3$	989.39(13)	1757.77(18)
Z	1	2
D_c/Mg m^{-3}	1.512	1.358
μ(Mo-Kα)/mm^{-1}	1.115	0.699
F(000)	468	756
Crystal size/mm	0.50 x 0.50 x 0.29	0.37 x 0.37 x 0.16
θ Limits/°	1.55 - 29.72	1.73 - 29.43
Measured reflections	14354	27426
Unique reflections(R_{int})	5332(0.0229)	9005(0.0669)
Observed reflections[$F_o > 2\sigma(F_o)$]	5057	7682
Goodness of fit on F^2	1.085	0.976
$R_1(F)$,[a][$I > 2\sigma(I)$]	0.0234	0.0374
w$R_2(F^2)$,[b][$I > 2\sigma(I)$]	0.0592	0.0865

Table 1cont,d

	3	**4**
Formula	$C_{55}H_{73}AgNO_5P_3$	$C_{36}H_{66}AgF_6P_3$
M	1028.92	813.67
Wavelength/Å	0.71073	0.71073
Temperature/K	173	173
Crystal symmetry	Orthorhombic	Triclinic
Space group	P n a 2_1	C 2/m
a/Å	21.5982(15)	24.145(2)
b/Å	18.7015(13)	17.8524(10)
c/Å	13.2231(8)	9.7455(8)
α/°	90	90
β/°	90	105.671(9)
γ/°	90	90
V/ $Å^3$	5341.1(6)	4044.6(5)
Z	4	4
D_c/Mg m^{-3}	1.280	1.336
μ(Mo-Kα)/mm^{-1}	0.513	0.668
F(000)	2168	1712
Crystal size/mm	0.38 x 0.35 x 0.20	0.30 x 0.27 x 0.11
θ Limits/°	1.44 - 25.48	2.10-25.85
Measured reflections	27065	16060
Unique reflections(R_{int})	9418(0.0723)	4065(0.0664)
Observed reflections	6498	2533
Goodness of fit on F^2	0.896	0.869
$R_1(F)$,[a] $[I > 2\sigma(I)]$	0.0476	0.0426
w$R_2(F^2)$,[b] $[I > 2\sigma(I)]$	0.1028	0.1032

Table 1cont,d

	5	**6**
Formula	$C_{73}H_{61}AgCl_3F_6P_4Sb$	$C_{36}H_{66}AgF_6P_2Sb$
M	1512.07	904.45
Wavelength/Å	0.71073	0.71073
Temperature/K	173	173
Crystal symmetry	Monoclinic	Monoclinic
Space group	P 2_1/c	P 2_1/n
a/Å	12.0120(5)	14.3626(5)
b/Å	23.0780(6)	19.1856(10)
c/Å	23.4887(10)	15.9332(6)
α/°	90	90
β/°	90.499(3)	114.936(3)
γ/°	90	90
V/ $Å^3$	6511.1(4)	3981.2(3)
Z	4	4
D_c/Mg m^{-3}	1.542	1.509
μ(Mo-Kα)/mm^{-1}	0.998	1.303
F(000)	3048	1856
Crystal size/mm	0.46 x 0.32 x 0.21	0.50 x 0.27 x 0.23
θ Limits/°	1.70-29.28	1.61-29.63
Measured reflections	88111	54225
Unique reflections(R_{int})	17605(0.0627)	10766(0.07)
Observed reflections	12913	8572
Goodness of fit on F^2	0.989	1.043
$R_1(F)$,[a] $[I > 2\sigma(I)]$	0.0375	0.0417
w$R_2(F^2)$,[b] $[I > 2\sigma(I)]$	0.0811	0.1028

Table 1cont,d

	7	**8**
Formula	$C_{39}H_{48}AgF_6OP_2Sb$	$C_{37}H_{55}AgCl_3F_6P_2Sb$
M	938.33	1011.72
Wavelength/Å	0.71073	0.71073
Temperature/K	173	173
Crystal symmetry	Triclinic	Orthorhombic
Space group	P -1	P b c a
a/Å	12.9403(15)	16.3557(14)
b/Å	13.6997(17)	29.989(3)
c/Å	14.0354(17)	17.548(2)
α/°	114.286(13)	90
β/°	96.745(14)	90
γ/°	111.183(13)	90
V/ $Å^3$	2008.4(4)	8607.1(15)
Z	2	8
D_c/Mg m^{-3}	1.552	1.561
μ(Mo-Kα)/mm^{-1}	1.297	1.394
F(000)	944	4080
Crystal size/mm	0.38 x 0.34 x 0.23	0.35 x 0.15 x 0.08
θ Limits/°	1.95 - 26.40	2.10 - 26.00
Measured reflections	15848	39451
Unique reflections(R_{int})	7346(0.0)	8329(0.0598)
Observed reflections	5004	4648
Goodness of fit on F^2	0.898	0.811
$R_1(F)$,[a] $[I > 2\sigma(I)]$	0.0390	0.0357
w$R_2(F^2)$,[b] $[I > 2\sigma(I)]$	0.0944	0.0781

Crystal structure of $[Ag(PCy_3)_2(NO_3)]_2$ (1): The molecular structure of the complex **1** is depicted in Fig. **1a**, with complete atom labelling Scheme. Compound **1** is a centrosymmetric dimer. The $PAg(ONO_2)_2AgP$ unit is planar with experimental error (oxygen atoms bonded to silver atoms are in the plane and rest of NO_2 part of nitrate is out of plane).

The two phosphine ligand molecules coordinated with silver(I) atom are staggered and adopt disposition of opposite chirality. The P-C(7) bond rotates out of the $Ag(O)_2Ag$ plane and this rotation results in an unsymmetrical interactions between oxygen atom of the nitrate anion and neighbouring cyclohexyl group hydrogen atoms such as Ag-O1 is smaller than Ag-O′1 and P-Ag-O1 bond angle is greater than P-Ag-O′1 bond angle (table **2**). This distortion is accommodated by dislocation of the two Cy_3PAgO fragments within the $PAg(ONO_2)_2AgP$ plane. In this dimer compound rest of the nitrate group is out of the plane.

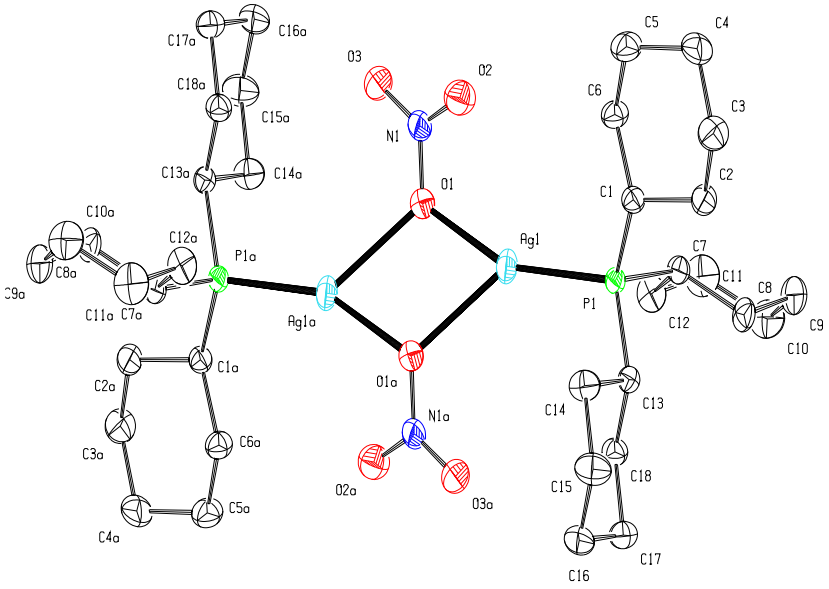

Figure 1a. Ortep view of the molecular structure of $[Ag(PCy_3)_2(NO_3)]_2$ with complete atom labelling Scheme and projected normal to the central $Ag_2O_2P_2$ plane.

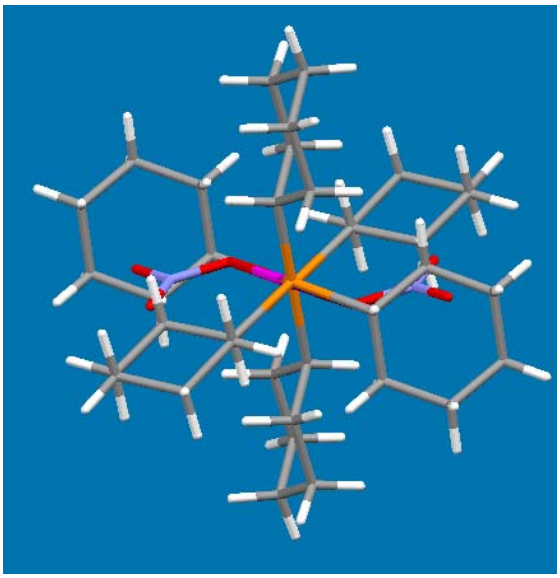

Figure 1b. Pattern showing the staggered conformation of the two tricyclohexyl phosphine molecules coordinated with the silver(I) atom in compound **1**.

The compound **1** shows that Ag-P bond length is 2.3374(11) Å and Ag-O bond distances are 2.2475(12) and 2.4210(12) Å. Whereas the Ag…Ag distance is ca. 3.813 Å. The O-Ag-P bond angles are 155.78(3) and 133.60(3)˚ respectively. The O-Ag-O bond angle is 70.55(5)˚. The Ag…Ag bond length observed in this complex does not show any metal-metal interaction. The values of bond angles around the silver(I) atom describe the presence of distorted trigonal planar geometry.

Crystal structure of $[Ag(PPhCy_2)_2(NO_3)]$ (2): The single crystal structure of complex **2** is shown in Fig. **2a**, with complete atom labelling Scheme. Compound **2** possesses a chiral structure as described by the space group P 2_1, hence complex **2** could eventually be very useful for catalytic reactions.

In compound **2**, the geometrical environment around silver(I) atom is pseudo trigonal planar, the silver(I) atom is coordinated with two phosphorous atoms of monodentate tertiary phosphine molecules and one oxygen atom of the nitrate counter ion as shown in the ORTEP drawing of the molecule in Fig. **2a.** The Ag-P bond distances are 2.4044(8) and 2.4261(8) Å respectively. The Ag-O1 and Ag-O3 bond distances are ca. 2.606 and 2.688 Å. These bond lengths values are longer than that found in dimer complex **1**. These

bond lengths values describe the presence of weaker Ag-O coordination bond in complex **2**. The Ag-P bond distances found in complex **2** are also longer than that found in complex **1**. The two phosphine ligands are present in partially eclipsed conformation in compound **2**. The O-Ag-P bond angles are ca. 89.74 & 115.46˚ and P-Ag-P bond angle is 154.25(3)˚. The bond angles values around silver(I) atom show greater deviation from ideal trigonal planar angle of 120˚. The crystallographic environment found around central metal atom in complex **2** is comparable as that found in compound **1**.

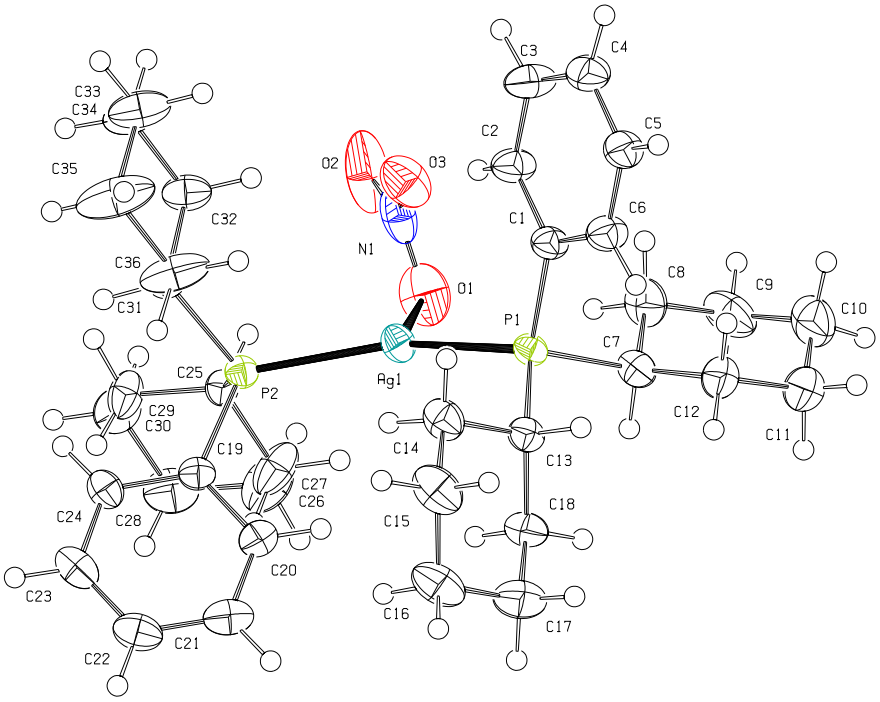

Figure 2a. Ortep drawing of the molecular structure of **2** with complete atom labelling Scheme and displacement ellipsoids are shown at 50% probability.

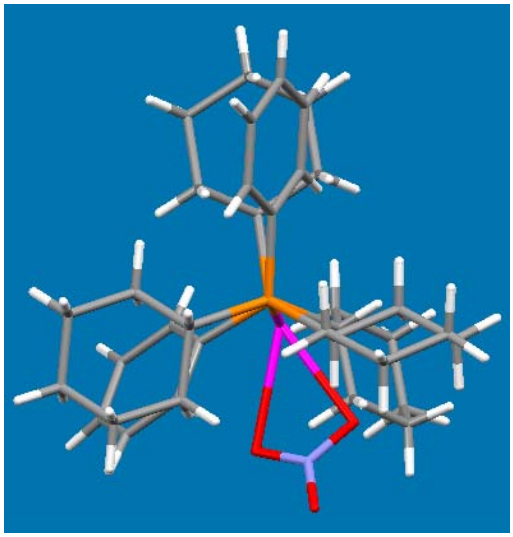

Figure 2b. Pattern showing the two tertiary phosphine ligand molecules coordinated with the silver(I) atom are partially eclipsed in compound **2**.

Crystal structure of $[Ag(PPh_2Cy)_3(CN)].5H_2O$ (3): The crystal structure of compound **3** is depicted in Fig. **3a**, with atom labelling Scheme. The complex is isostructural with a considerable family of $[Ag(PR_3)_3(X)]$[5,40] arrays; the anion being modelled as C-bonded in this complex. In compound **3** the geometry around the silver(I) atom is distorted tetrahedral. Silver(I) atom is coordinated with three phosphorous atoms of monodentate tertiary phosphine ligand molecules and one carbon atom of cyanide counter ion. The molecular structure of compound **3** also shows that complex molecule is solvated by five water molecules as well. The Ag-C bond distance is 2.176(6) Å and is longer than that found in similar type of silver(I) cyanide phosphine complexes.[5,40] The Ag-P bond distances are 2.5183(18), 2.5246(13), and 2.5223(14) Å respectively. The Ag-P bond lengths found in complex **3** are longer than that found in compounds **1** & **2**. The Ag-P bond length difference found in compounds **1-3** are normal and are attributed to the presence of different geometrical environment, counter ions and chemical composition of the tertiary phosphine ligands as well. The P-Ag-P bond angles range from 107.00(5) to 107.81(5)˚ and P-Ag-C bond angles vary from 109.7(2) to 112.74(15)˚. These bond angles values around silver(I) atom describe the presence of distorted tetrahedral geometry. In compound **3** bond angles values are close to ideal tetrahedral angle 109.5˚.

In compound **3**, cyclohexyl rings are present in chair conformation, as found in the compound **1** & **2**.

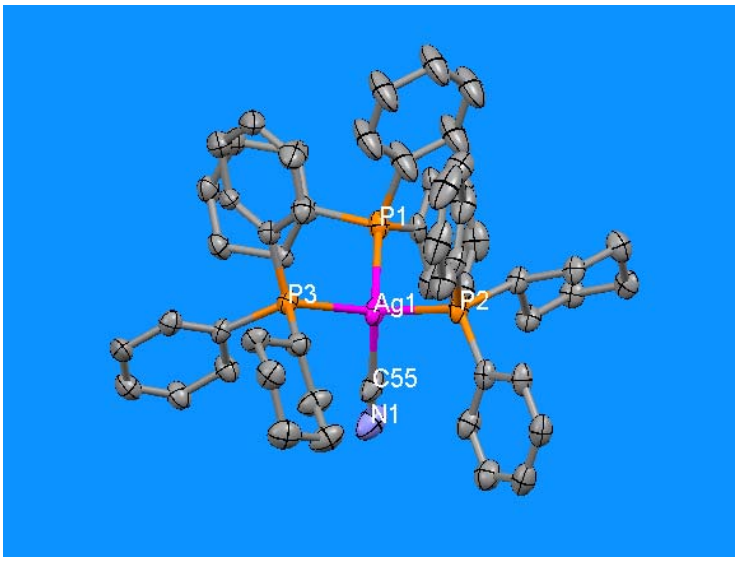

Figure 3a. View of the molecular structure of **3** with atom labelling Scheme and displacement ellipsoids are shown at 50% probability.

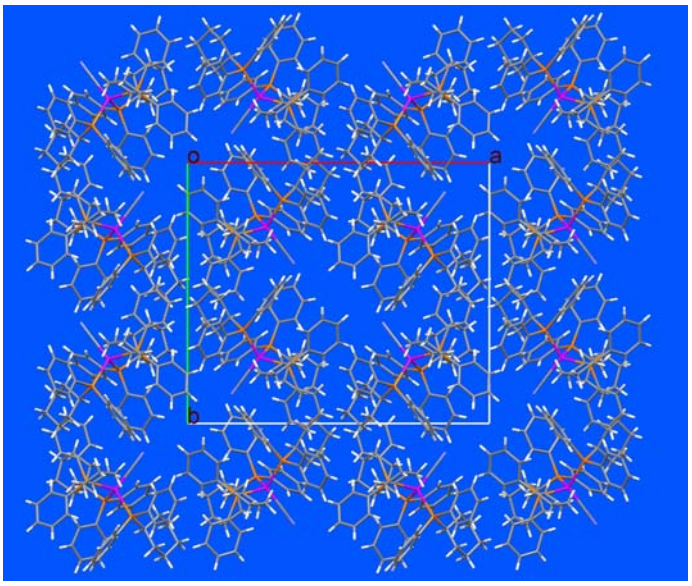

Figure 3b. View of packing diagram of molecular structure of complex **3**.

Crystal structure of $[Ag(PCy_3)_2].PF_6$ (4): The molecular structure of compound **4** is illustrated in Fig. **4a**, with complete atom labelling Scheme. In compound **4**, the

geometry around central silver(I) atom is linear. Silver(I) atom is coordinated with two phosphorous atoms of monodentate tertiary phosphine ligand molecules. PF_6^- is well separated from the metal centre and does not show any coordination. The phosphorous atom of the counter ion is hexa-coordinated and ideal octahedron is observed around phosphorous atom. The PAgP unit is planar, two phosphine ligand molecules are eclipsed and cyclohexyl rings are present in chair conformation.

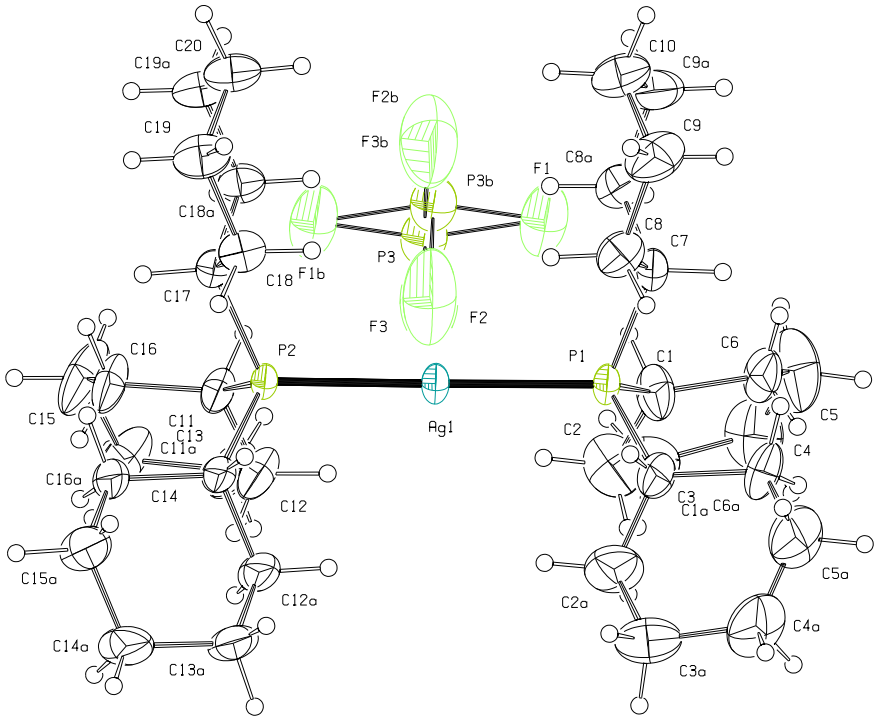

Figure 4a. Representative view of the molecular structure of complex **4** with complete atom labelling Scheme and displacement ellipsoids are shown at 50% probability.

The molecular structure of compound **4** is highly symmetric and C_2 symmetry is observed here. The phosphorous atom of the counter ion is found to be disordered about the C_2 axis. The Ag-P bond distances are 2.379(13) and 2.378(12) Å. These bond length values are shorter than that found in compound **2** & **3** and longer than that found in compound **1**. The P-Ag-P bond angle is 179.41(5)˚, it is very close to ideal linear angle of 180˚. Whereas, the linearity around central silver(I) atoms found in complexes **6** & **8** is not as much as found in complex **4**.

The Ag-P bond length differences found in complex **4** and other silver(I) complexes reported here are attributed to different crystallographic environment around central atom, chemical composition of the tertiary phosphine ligands and to some extent counter ions as well.

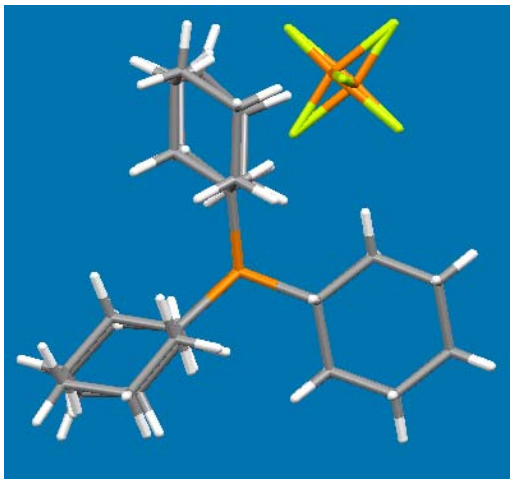

Figure 4b. Panel is showing two tertiary phosphine molecules coordinated with silver(I) centre in compound **4** are present in eclipsed form.

Crystal structure of $[Ag(PPh_3)_4)].SbF_6.CHCl_3$ (5): The representative view of the crystal structure of complex **5** is shown in Fig. **5**, with complete atom labelling Scheme. The compound **5** is pseudo polymorph of the complex $[Ag(PPh_3)_4)].SbF_6$.[49] In compound **5** the geometrical environment around Ag(I) atom is distorted tetrahedral. Silver(I) atom is coordinated with four phosphorous atoms of monodentate tertiary phosphine ligand molecules. The compound **5** is solvated by one chloroform molecule as well. The SbF_6^- counter ion is not coordinated with the metal centre. The Sb atom is hexa-coordinated by six fluorine atoms and an octahedral geometrical environment is observed around Sb(V) atom of the counter ion.

The Ag-P bond distances vary from 2.6197(6) to 2.6281(6) Å. These Ag-P bond distances are longer than that found in compounds **1-4** & **6-8** and are shorter than that found in its polymorphic form $[Ag(PPh_3)_4)].SbF_6$.[49] The P-Ag-P bond angles range from 108.01(2) to 110.62(2)˚. These bong angles values around silver(I) atom are close to ideal tetrahedral angle and comparable with its polymorphic form. The P-Ag-P bond angles

values are considerably different than that found in complex $[Ag(PPh_3)_4)].SbF_6$ with same geometrical environment around silver(I) atom. The geometry around silver(I) atom in compound **5** is close to ideal tetrahedral.

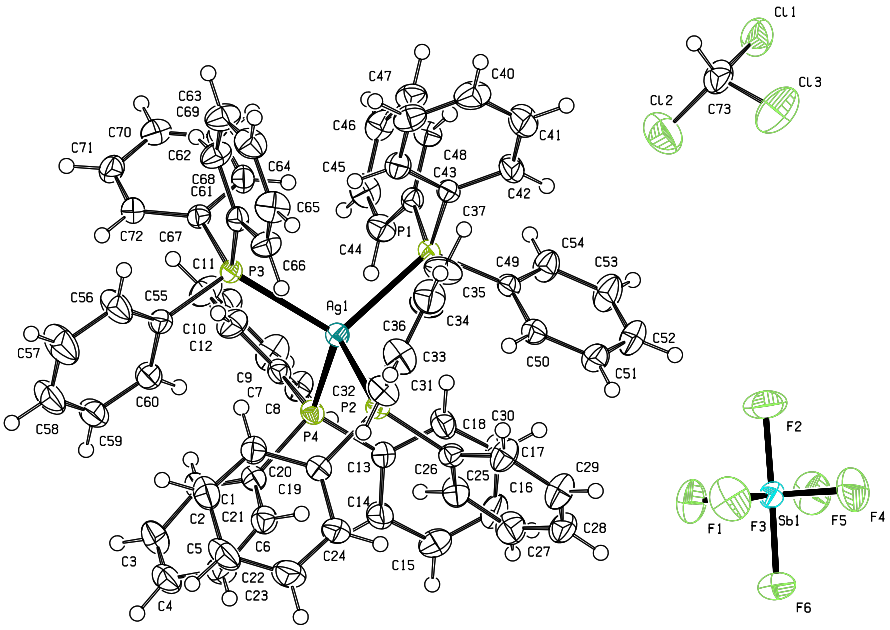

Figure 5. Ortep view of the single crystal structure of **5** with complete atom labelling Scheme and displacement ellipsoids are shown at 50% probability.

Crystal structure of $[Ag(PCy_3)_2].SbF_6$ (6): The single crystal structure of the monomer complex **6** is illustrated in Fig. **6a**, with complete atom labelling Scheme.

In compound **6**, the geometrical environment around silver(I) atom is linear and the central metal atom is coordinated with two phosphorous atoms of monodentate tertiary phosphine ligand molecules. The SbF_6^- is well separated from the central metal atom and does not show any coordination with central Ag(I) atom. The molecular structure of compound **6** does not show any C_2-symmetry unlike compound **4**. However, Sb atom has octahedral geometry as that found in compound **5** and is coordinated with six fluorine atoms. The PAgP unit is linear with experimental error but linearity found in compound **6** is much less than that found in complex **4**. The tertiary phosphine ligand molecules are

eclipsed and cyclohexyl rings are present in chair conformation like complex **4**. The Ag-P bond distances are 2.3775(7) and 2.3766(7) Å respectively.

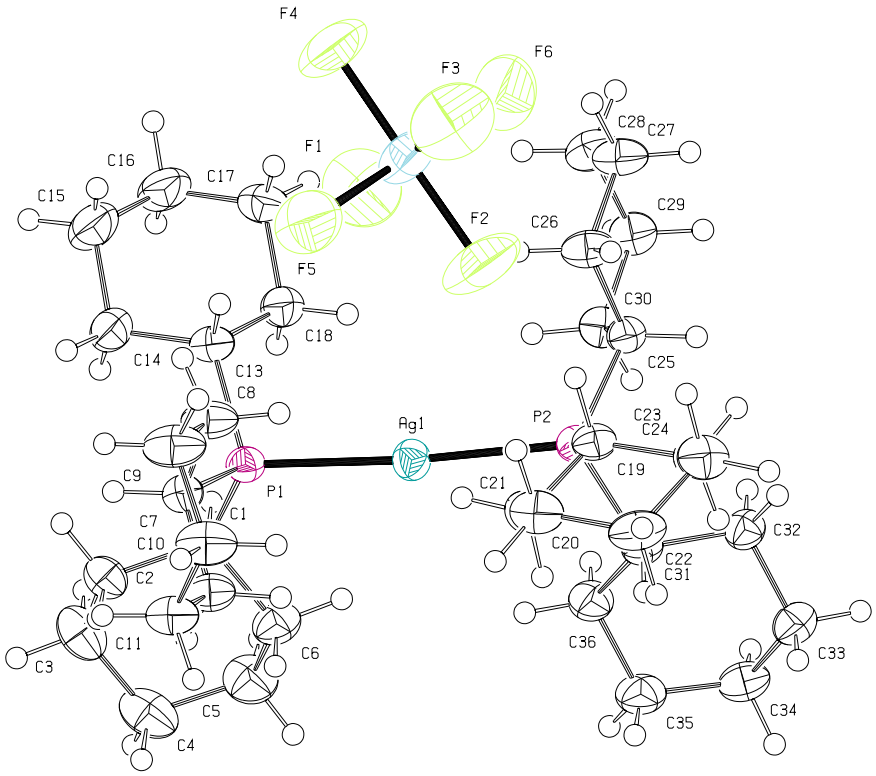

Figure 6a. Ortep view of the molecular structure of **6** with complete atom labelling Scheme and displacement ellipsoids are shown at 50% probability.

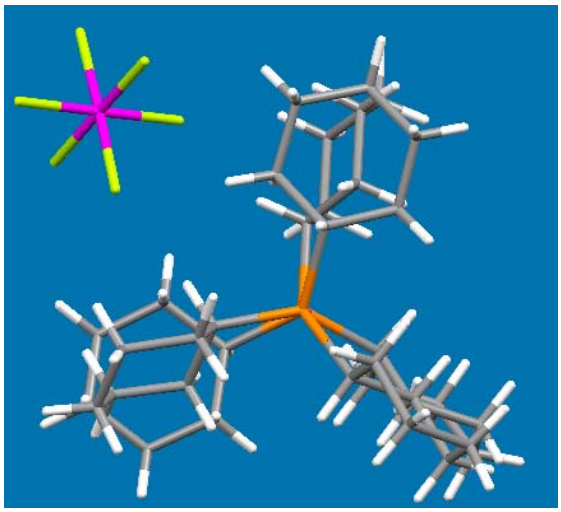

Figure 6b. Pattern is showing two tertiary phosphine ligand molecules are present in partially eclipsed form in compound **6**.

The P-Ag-P bond angle 175.37(2)˚ around silver(I) atom is smaller than that found in compound **4** and show much deviation from the ideal linear angle of 180˚. The Ag-P bond distances values found here are comparatively similar as that found in compound **4** and longer than those compounds **2** & **3**. These bond lengths differences are attributed to several reasons as described before.

Crystal structure of $[Ag(PPh_2Cy)_2(C_3H_6O)].SbF_6$ (7): The molecular structure of compound **7** is illustrated in Fig. **7a**, with complete atom labelling Scheme. Fig. **7a**, illustrates how the highly disordered acetone molecule of crystallization coordinates to the silver(I) atom. On the basis of this evidence, we suggest a distorted trigonal planar geometry around the silver(I) atom in this complex. The central silver(I) atom is further coordinated with two phosphorous atoms of monodentate tertiary phosphine ligand molecules. The SbF_6^- is well separated from the central metal atom and does not show any coordination with central metal atom. However, the Sb(V) atom has an octahedral geometry as in compounds **5** & **6** and is coordinated with six fluorine atoms. The Ag-P bond distances are 2.4129(13) and 2.4167(13) Å, respectively. These bond lengths values are greater than those found in compounds **4** & **6,** and shorter than those in compounds **3** & **5**. The Ag-P bond distances found in compound **7** are comparatively similar to those found in compound **2**. The Ag-O bond distance is 2.677 Å is long and shows weak coordination of this disordered oxygen atom of the solvated molecule. The P-Ag-P bond angle is 158.92(13)˚ and O-Ag-P bond angle values are ca. 95.37 & 105.36˚.

The P-Ag-P bond angle 158.94(5)˚ shows much deviation from ideal linear angle of 180˚ and ideal tigonal planar angle of 120˚. These bond angles values provide an additional evidence of the week coordination of acetone molecule with silver(I) metal centre in **7**; which is not obvious from the Ortep drawing of the molecular structure of compound **7** (Fig. **7a**). The cyclohexyl rings of the tertiary phosphine molecules are present in chair conformation as that found in compounds **1-4** & **6**.

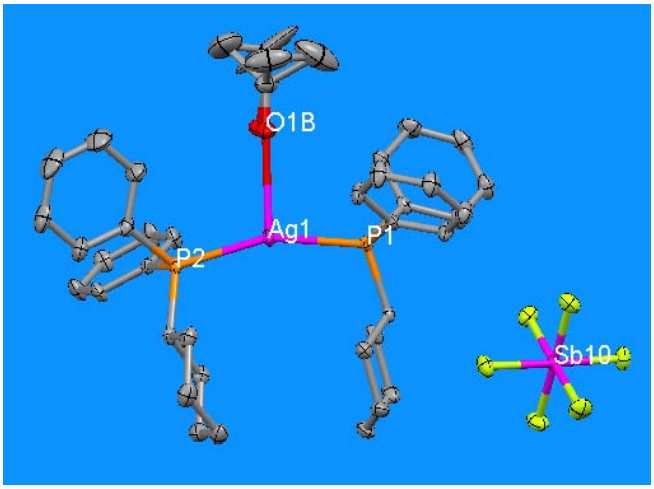

Figure 7a. Panel is showing the coordination of the highly disordered acetone molecule through the oxygen atom with metal centre in compound **7**.

Crystal structure of $[Ag(PPhCy_2)_2].SbF_6.CHCl_3$ (8): The perspective view of the molecular structure of compound **8** is shown in Fig. **8a**, with complete atom labelling Scheme. The compound **8** crystallizes in orthorhombic space group 'P b c a'. Selected bond lengths and angles are tabulated in table **2**.

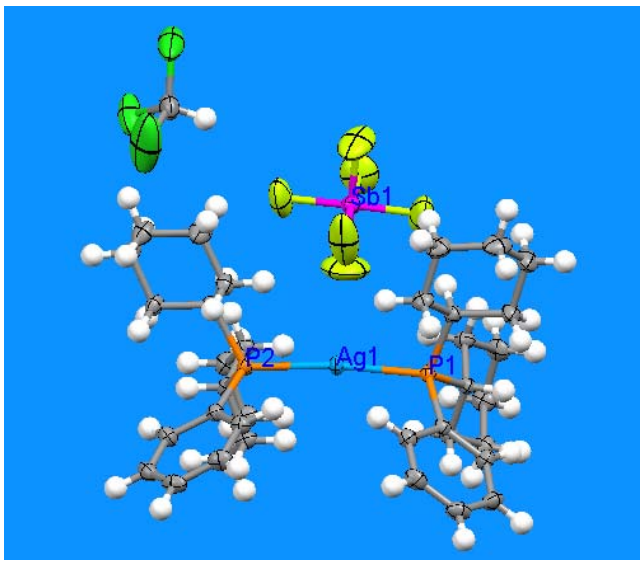

Figure 8a. Representative view of molecular structure of compound **8** with selected atom labelling Scheme and displacement ellipsoids are shown at 50% probability.

In compound **8**, the geometrical environment around silver(I) is linear with experimental error. Silver(I) atom is coordinated with two phosphorous atoms of monodentate tertiary phosphine ligand molecules. The SbF_6^- counter ion is well separated from the central metal atom and does not show any coordination with central metal atom. The complex **8** is also solvated with one unit of chloroform solvent molecule. The Ag-P bond distances are 2.3886(11) and 2.3867(12) Å respectively. These bond distances are more or less comparable as that found in compound **4** & **6**. These bond distances are shorter than that found in compounds **2**, **3** & **7** and longer than that found in compound **1**. The P-Ag-P bond angle is 173.42(4)˚ smaller than that found in compound **4** & **6**. The bond angle found around silver(I) atom in compound **8** show much deviation from ideal linear angle of 180˚. The differences in bond length and bond angle values found in compounds **4**, **6** & **8** are attributed to different chemical composition of the compounds and to some extent to counter ions as well.

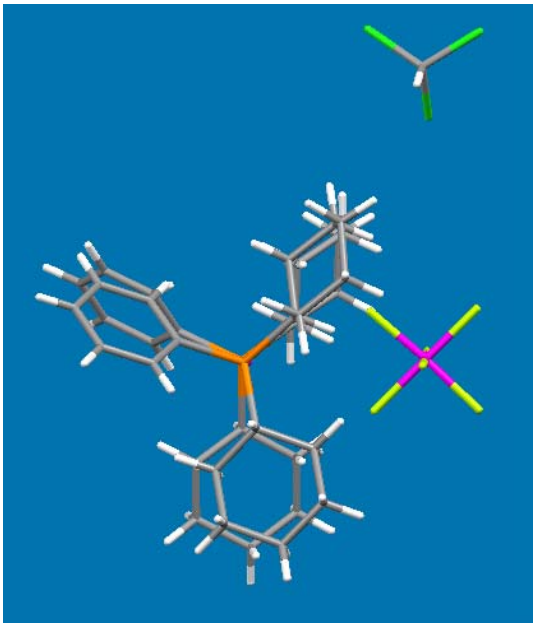

Figure 8b. Tertiary phosphine molecules coordinated with silver(I) atom in compound **8** are partially eclipsed.

Table 2. Selected bond lengths (Å) and bond angles (˚) for compounds **1-8**

Bond lengths (Å)		Bond angles (˚)	
1			
Ag(1)-O(1)	2.2475(12)	O(1)-Ag(1)-P(1)	155.78(3)
Ag(1)-P(1)	2.3374(4)	O(1)-Ag(1)-O(1)#1	70.55(5)
Ag(1)-O(1)#1	2.4210(12)	P(1)-Ag(1)-O(1)#1	133.60(3)
Symmetry operations;		N(1)-O(1)-Ag(1)	112.07(10)
#1 -x+1, -y, -z+1		N(1)-O(1)-Ag(1)#1	123.06(10)
		Ag(1)-O(1)-Ag(1)#1	109.45(5)
2		P(1)-Ag(1)-P(2)	154.25(3)
Ag(1)-P(1)	2.4044(8)	C(1)-P(1)-C(13)	105.01(14)
Ag(1)-P(2)	2.4261(8)	C(1)-P(1)-Ag(1)	111.27(11)
P(1)-C(1)	1.835(3)	C(13)-P(1)-Ag(1)	114.46(11
3			
Ag(1)-C(55)	2.176(6)	C(55)-Ag(1)-P(1)	109.7(2)
Ag(1)-P(1)	2.5183(18)	C(55)-Ag(1)-P(3)	111.66(17)
Ag(1)-P(3)	2.5223(14)	P(1)-Ag(1)-P(3)	107.00(5)
Ag(1)-P(2)	2.5246(13)	C(55)-Ag(1)-P(2)	112.74(15)
		P(1)-Ag(1)-P(2)	107.68(5)
		P(3)-Ag(1)-P(2)	107.81(5)
4			
Ag(1)-P(2)	2.3785(12)	P(2)-Ag(1)-P(1)	179.41(5)
Ag(1)-P(1)	2.3793(13)	C(7)-P(1)-Ag(1)	109.98(17)
5			
Ag(1)-P(3)	2.6197(6)	P(3)-Ag(1)-P(1)	109.38(2)
Ag(1)-P(1)	2.6236(6)	P(3)-Ag(1)-P(2)	110.62(2)
Ag(1)-P(2)	2.6261(6)	P(1)-Ag(1)-P(2)	109.16(2)
Ag(1)-P(4)	2.6281(6)	P(3)-Ag(1)-P(4)	109.40(2)
		P(1)-Ag(1)-P(4)	110.25(2)
		P(2)-Ag(1)-P(4)	108.01(2)

6			
Ag(1)-P(2)	2.3766(7)	P(2)-Ag(1)-P(1)	175.37(2)
Ag(1)-P(1)	2.3775(7)	C(13)-P(1)-C(7)	107.66(13)
Sb(1)-F(2)	1.851(3)	F(1)-Sb(1)-F(2)	91.8(2)
Sb(1)-F(6)	1.852(3)	F(1)-Sb(1)-F(5)	90.74(19)
		F(2)-Sb(1)-F(5)	90.27(15)
7			
Ag(1)-P(2)	2.4129(13)	P(2)-Ag(1)-P(1)	158.92(5)
Ag(1)-P(1)	2.4167(13)	F(2)-Sb(10)-F(6)	90.80(15)
Sb(10)-F(2)	1.865(3)	F(2)-Sb(10)-F(4)	90.43(16)
Sb(10)-F(6)	1.867(3)	F(6)-Sb(10)-F(4)	92.02(16)
Sb(10)-F(4)	1.870(3)		
8			
Ag(1)-P(2)	2.3867(11)	P(2)-Ag(1)-P(1)	173.42(4)
Ag(1)-P(1)	2.3886(11)	C(13)-P(1)-C(7)	105.1(2)
Sb(1)-F(1)	1.800(5)	F(5)-Sb(1)-F(2)	90.7(3)
Sb(1)-F(5)	1.815(5)	F(3)-Sb(1)-F(6)	91.1(2)
		F(1)-Sb(1)-F(6)	90.2(2)

^{13}C and ^{31}P NMR spectroscopic studies

^{31}P NMR spectra of silver(I) complexes **1-4** & **6-8** were recorded at room temperature. Naturally occurring isotopes of silver (^{107}Ag, 51.82% natural abundance; ^{109}Ag, 48.18%) and their magnetogyric ratios are similar in magnitude [$\gamma(^{109}Ag)/\gamma(^{107}Ag) = 1.15$]. The ^{31}P NMR spectra of complexes of silver(I) with phosphrous-donor ligand may show splitting due to ^{1}J(P-Ag) coupling. At room temperature in dichloromethane solution; the complexes **2**, **4** & **6-8** gave ^{31}P NMR spectra doublet peaks. ^{31}P NMR spectra of complex **1** in methanol solution gave a well defined doublet at 42 ppm at room temperature. At room temperature ^{31}P NMR spectra of complex **3** in dichloromethane solution gave single line at 11.92 ppm and it is because of rapid intermolecular exchange of phosphine

between different silver atoms and free phosphine as well.[48] ^{31}P NMR spectrum of complex **2** show peaks at 24 and 27 ppm. ^{31}P NMR spectra of complexes **4**, **6-8** gave well defined doublet peaks at 37 & 40, 39 & 42, 26, 34 & 37 ppm respectively. Silver(I) complexes with (1:2 stoichiometric ratio) show well resolved pairs of doublets , the resolution of signals for 1:2 species is due to ^{1}J(P-Ag) coupling. These results are consistent with the previously reported results.[22-44] The differences observed in ^{31}P NMR spectra of silver(I) complexes are attributed; to the presence of different geometries around silver(I) atom and coordination angle (P-Ag-P) in solution form.

^{13}C NMR spectra of silver(I) complexes **1-4** & **6-8** were recorded at room temperature in dichloromethane solution. ^{13}C NMR spectra of complexes **1**, **4** & **6** are almost similar and a set of peaks is observed between 26-32ppm as ligand used for the synthesis of these complexes is same (tricyclohexyl phosphine). ^{13}C NMR spectrum of complex **3** show two sets of peaks between 24 to 35 ppm (cyclohexyl group) and 128 to 134 ppm (phenyl group) and a small peak is observed at 118 ppm for CN^- group (carbon atom) for complex **3** only. The complexes **2** & **8** show two sets of peaks (for cyclohexyl and phenyl groups) at 25 to 33 ppm and 128 to 135 ppm respectively. Whereas no peak for chloroform carbon atom is observed as the complexes (**2** & **8**), either lose solvated molecule of chloroform at ambient condition or due to very low concentration of the solvated chloroform molecule. The ^{13}C NMR spectrum of complex **7** is comparatively similar to complexes **2** & **8** and show two sets of peaks between 26-35 and 127-133 ppm for cyclohexyl and phenyl groups respectively. No extra signals were observed for solvated acetone molecule as described by structural results. The complexes usually loose the solvated molecule of solvent with low boiling points at ambient conditions. These results are according to the expectations and consistent with the described structures.

Conclusions

The synthesis of silver(I) tertiary phosphine precursors reveals that geometry around silver(I) atom is highly dependent on type of tertiary phosphine and molar ratio of the reactants to some extents. The tertiary phosphine having bulky groups like cyclohexyl group impose linear geometry around the silver(I) atom with silver(I) salts containing

non-coordinating counter ions (SbF_6^- and PF_6^-) and trigonal planar to tetrahedral geometry in case of silver(I) salts with coordinating anions (NO_3^- and CN^-). Triphenyl phosphine reaction with silver(I) salts containing coordinating or non-coordinating anions impose tetrahedral geometry around central metal atoms.

References

1. D. E. Hibbs, M. B. Hursthouse, K. M. Abdul Malik, M. A. Becket and P. W. Jones, *Acta Crystallogr., Sect. C.*, 1996, **C52**, 884.
2. M. Camalli and F. Caruso, *Inorg. Chim. Acta.*, 1988, **144**, 205.
3. M. M. Olmstead, M. Sheffrin and F. Jiang, *Acta Crystallogr., Sect. E.*, 2004, **E60**, m1142.
4. S. W. Ng and A. H. Othman, *Acta Crystallogr., Sect. C.*, 1997, **C53**, 1396.
5. G. A. Bowmaker, Effendy, P. J. Harvey, P. C. Healy, B. W. Skelton and A. H. White, *J. Chem. Soc., Dalton Ttrans.*, 1996, 2449.
6. G. Zhang, G. Yang, Q. Chen and J. S. Ma, *Cryst. Growth Des.*, 2005, **5**, 661.
7. P. Aslanidis, P. Karagiannidis, P. D. Akrivos, B. Krebs and M. Läge, *Inorg. Chim. Acta.*, 1997, **254**, 277.
8. Effendy, G. G. Lobbia, M. Pellei, C. Pettinari, C. Santini, B. W. Skelton and A. H. White, *J. Chem. Soc., Dalton Ttrans.*, 2001, 528.
9. A. Cingolani, Effendy, M. Pellei, C. Pettinari, C. Santini, B. W. Skelton and A. H. White, *Inorg. Chem.*, 2002, **41**, 6633.
10. K. Nomiya, K.-I. Onoue, Y. Kondoh, N. C. Kasuga, H. Nagano, M. Oda and S. Sakuma, *Polyhedron.*, 1995, **14**, 1359.
11. F. G. Mann, A. F. Wells and D. Purdie, *J. Chem. Soc.*, 1937, 1828.
12. P. F. Barron, J. C. Dyason, P. C. Healy, L. M. Engelhardt , B. W. Skelton and A. H. White, *J. Chem. Soc., Dalton Ttrans.*, 1986, 1965.
13. G. A. Bowmaker, Effendy, J. V. Hanna, P. C. Healy, G. J. Millar, B. W. Skelton and A. H. White, *J. Phys. Chem.*, 1995, **99**, 3909.
14. M. I. Bruce, M. L. Williams, B. W. Skelton and A. H. White, J. Chem. Soc., *Dalton Ttrans.*, 1983, 799.

15. C. S. W. Harker, E. R .T. Tieknik, *Acta Crystallogr., Sect. C.*, 1989, **45**, 1815.
16. W. Lin, T. H . Warren, R. G. Nuzzu and G. S. Girolami, *J. Am. Chem. Soc.*, 1993, **115**, 11644.
17. S. M. Socol, R. A. Jacobson and J. G. Verkade, *Inorg. Chem.*, 1984, **23**, 88.
18. E. R .T. Tieknik, *J. Coord. Chem.*, 1988, **17**, 239.
19. E. C. Alyea, G. Ferguson and A. Somogyvari, *Inorg. Chem.*, 1982, **21**, 1369.
20. A. Baiada, F. H. Jardine and R. D. Willett, *Inorg. Chem.*, 1990, **29**, 3042.
21. L. J.Baker, G. A. Bowmaker, Effendy, B. W. Skelton and A. H. White, *Aust. J. Chem.*, 1992, **45**, 1909.
22. M. Camali and F. Caruso, *Inorg. Chim. Acta.*, 1988, **144**, 205.
23. G. Wulfsberg, D. Jackson, W. Ilsley, S. Dou and A. Weiss, *Z. Naturforsch., Teil. A*, 1992, **47**, 75.
24. G. A. Bowmaker, Effendy, J. V. Hanna, P. C. Healy, B. W. Skelton and A. H. White, *J. Chem. Soc., Dalton Trans.*, 1993, 1387.
25. A. Cassel, *Acta Crystallogr., Sect. B.*, 1979, **35**, 174.
26. J. Howatson and B. Morosin, *Cryst. Struct. Commun.*, 1973, **2**, 51.
27. P. G. Jones, *Acta Crystallogr., Sect. C.*, 1993, **49**, 1148.
28. G. Booth, Adv.Inorg. Chem. Radiochem., 1964, **6**, 1; G. Booth, inorganic Phosphorus Compounds, eds. G. M. Kosolapoff and L. Maier, Wiley-Interscience, New York, 1972, vol. 1, PP. 433-545.
29. C. A. McAuliffe, Phosphine, Arsine and Stibine Complexes of the transition Elements, Elsevier, Amsterdam, 1979; Transition Metal Complexes of Phosphorus, Arsenic and Antimony Ligands, Halstead, New York, 1973.
30. W. E. Smith, *Coord. Chem. Rev.*, 1981, **35**, 253; 1982, **45**, 307; 1985, **67**, 297.
31. R. J. Lancashire, Comprehensive Coordination Chemistry, ed. G. Wilkinson, Pergamon, Oxford, 1987, **vol. 5**, p. 775.
32. K. Nomiya, K. Tsuda and N. C. Kasuga, *J. Chem. Soc., Dalton Ttrans.*, 1998, 1653.
33. Y.-Y. Lin, S.-W. Lai, C.-M. Che, W.-F. Fu, Z.-Y. Zhou and N. Zhu, *Inorg. Chem.*, 2005, **44**, 1511.
34. J. K. Kim, M. K. Hang, J. H. Ahn and M. Lee, *Angew. Chem. Int. Ed.*, 2005, **44**, 328.

35. W. L. Jia, T. McCormick, Y. Tao, J.-P. Lu and S. Wang, *Inorg. Chem.*, 2005, **44**, 5706.
36. P. Diaz, J. Benet-Buchholz, R. Vilar and A. J. P. White, *Inorg. Chem.*, 2006, **45**, 1617.
37. H. Rudmann, S. Shimada and M.F. Rubner, *J. Am. Chem. Soc.*, 2002, **124**, 4918.
38. Effendy, F. Marchetti, C. Pettinari, B. W. Skelton and A. H. White, *Inorg. Chim. Acta.*, 2007, **360**, 1424.
39. P. Karagiannidis, P. Aslanidis, S. Kokkou and C. J. Cheer, *Inorg. Chim. Acta.*, 1990, **172**, 247.
40. G. A. Bowmaker, Effendy, J. C. Reid, C. E. F. Rickard, B. W. Skelton and A. H. White, *J. Chem. Soc., Dalton Trans.*, 1998, 2139.
41. Q.-F. Zhang, J. Ding, Z. Yu, Y. Song, A. Rothenberger, D. Fenske and W.-H. Leung, *Inorg. Chem.*, 2006, **45**, 8638.
42. Q.-X. Liu, F.-B. Xu, Q.-S. Li, X.-S. Zeng, X.-B. Leng, Y. L. Chou and Z.-Z. Zhang, *Organometallics.*, 2003, **22**, 309.
43. P. F. Barron, J. C. Dyson, P. C. Heally, L. M. Englehardt, C. Pakawatchi, V. A. Patrick, and A. H. White, *J. Chem. Soc., Dalton Ttrans.*, 1987,1099.
44. G. A. Bowmaker, Effendy, P. J. Harvey, P. C. Healy, B. W. Skelton and A. H. White, *J. Chem. Soc., Dalton Ttrans.*, 1996, 2449.
45 J. C. Dyason, P. C. Healy, L. M. Engelhardt, C. Pakawatchai, V. A. Patrick, C. L. Raston and A. H. White, *J. Chem. Soc., Dalton Trans*, 1985, 831.
46. G. A. Bowmaker, A. Camus, P. C. Healy and B. W. Skelton, *Inorg. Chem*, 1989, **28**, 3823.
47. G. A. Bowmaker, Effendy, J. D. Kildea, E. N. de Silva and A. H. White, *Aust. J. Chem*, 1997, **50**, 627.
48. W. McFarlane, P. D. Akrivos, P. Aslanidis, P. Karagiannidis, C. Hatzisymeon, M. Numan and S. Kokkou, *Inorg. Chim. Acta,* 1998, **281,** 121.
49. Z. Ma, Y. Lin and Z.-H. Chen, *Jiegou Huaxue (Chin. J. Struct.Chem).*, 2004, **23**, 1277.

Part B:

Copper(I) halide tertiary phosphines complexes and an example of a mixed ligand CuI halide phosphine complex

Abstract

The complexes $[Cu_4I_4(PPh_2Cy)_4].2H_2O$ (**1**), $[CuI(PPhCy_2)_2]$ (**2**), $[CuCl(PPhCy_2)_2]$ (**3**), $[Cu_2I_2\{PPh_2(p\text{-tolyl})\}_3]$ (**4**), and $[CuBr(PPh_3)_3].CH_3CN$ (**5**) [where Ph = phenyl, Cy = cyclohexyl], have been synthesized and structurally characterized by X-ray diffraction, IR absorption spectra and NMR spectroscopic studies (where the solubility of samples was good). The X-ray diffraction analysis of complex (**1**) reveals a pseudo cubane like structure. Here the four corners of the cube are occupied by copper(I) atoms and four I atoms are present at the alternative corners of the cube, further more the copper(I) atoms are coordinated to monodentate tertiary phosphine. The complexes (**2**) and (**3**) are isostructural and isomorphous with trigonal planar geometry around the copper(I) atom. Complex (**4**) is a dimer in which the crystallographic environment around the two copper(I) atoms is pseudo tetrahedral and trigonal planar, respectively. The crystal structure of complex (**5**) is a pseudo polymorph of complex $[CuBr(PPh_3)_3]$ and the

geometrical environment around the copper(I) centre is distorted tetrahedral. The IR and NMR spectroscopic results are consistent with the single crystal X-ray diffraction analysis results.

Introduction

Reaction of copper(I) halides with monodentate tertiary phosphine bases yielded a diverse array of two, three, and four coordinated complexes with diverse structural properties that are determined by the specific choice of the phosphine ligand and to a lesser extent, by the choice of halide anions [1]. Neutral phosphine and amine ligands form mono- or multi-nuclear complexes with copper(I) and copper(II) salts, in which the coordination number ranges from two to four [2-10]. The greatest range of structural types has been found for the case of tertiary phosphines, of which the most extensively studied is triphenyl phosphine and to a lesser extent tricyclohexyl phosphine [11-15].

The geometry around the copper(I) atom in complexes with tertiary phosphine ligands depends on the stoichiometric ratio of the metal salt and ligand used, as well as the solvent of crystallization. Thus for a compound of 1:1 stoichiometry monomer, dimer and tetramer complexes are possible with general formulae of $[MX(PR_3)_3]$, $[M_2X_2(PR_3)_2]$ and $[M_4X_4(PR_3)_4]$ (where M = Au, Ag, & Cu. R = phenyl, alkyl, aryl or cyclohexyl group) [1,16-18]. Whereas, the compound with stoichiometry 1:1.5 is a dimer with formula $[Cu_2I_2\{P(o\text{-}tolyl)_3\}_3]$ [15], and compounds with stoichiometry 1:2 and 1:3 are monomers and dimers with tetrahedral and trigonal planar geometries, respectively, around metal centre [19-20]. The complexes of general formula $[M_4X_4(PR_3)_4]$ (X=Cl, Br or I) have pseudo cubane like structures [10, 21-22]. These types of structures can be described as two interpenetrating tetrahedra of four metals (M) and four triply bridging halides (anions) situated on alternative corners of a distorted cube with each metal atom being further coordinated to one terminal monodentate ligand [16]. Frequently a non-systematic deviation of the cubane core from the idealized tetrahedral geometry is observed for cubane like metal clusters [23-25].

Our interest in copper(I) complexes with tertiary phosphine is based on mixed ligand complexes with a variety of N, O, S, P, and halide donor ligands. Initially, we prepared coinage metal complexes with monodentate tertiary phosphine ligands and later we will use these metal phosphine precursors for the preparation of pre-designed products.

It is of great interest to learn about how the molecular properties of the ligands affect the evolving structures of the complexes and their physical properties [26-27]. Much effort has been devoted to the design and synthesis of pre-organized ligands that are able to control the structure and properties of complexes [27-30]. Copper(I) and copper(II) complexes with various N, S, O, and P donor ligands are of growing interest owing to their wide variation in structural format and rich physical, photo-physical, biological and chemical properties [31-33].

Although a huge number of copper(I) complexes with monodentate tertiary phosphine have been reported [1, 11-15], such complexes with neutral phosphines are consider as good starting material for the synthesis and crystal engineering of metal organic frameworks of pre-designed architectures and properties [6-8, 14, 30-31, 34-35]. Herein, we report the synthesis and structural characterization of five neutral copper(I) halide complexes with tertiary phosphines (Scheme 1). The single crystal X-ray structures, IR absorption spectra and NMR spectroscopic properties are discussed here. The single crystal X-ray diffraction analysis has been carried out at low temperature (-100 Cº).

Experimental

Material and physical measurements

All the reactions were carried out in air at rt. All chemical and solvents used were of analytical grade and were used without further purification. All chemicals were purchased from Aldrich and ACROS. Microanalysis was done by Mr. D. Mooser (Ecole d'ingénieurs de Fribourg, Filière de chimie). The IR spectra were recorded as KBr pellets

on a PerkinElmer Spectrum One FTIR instrument. ^{1}H, ^{13}C, and ^{31}P NMR spectra were recorded on a Bruker AMX 400 MHz using CD_2Cl_2 as solvent. TMS was used as the internal standard.

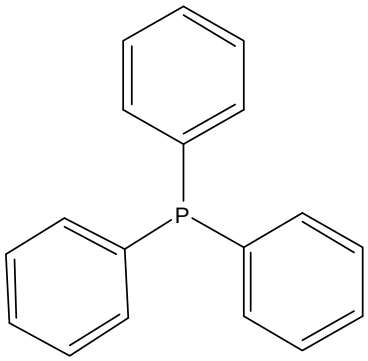

triphenyl phosphine

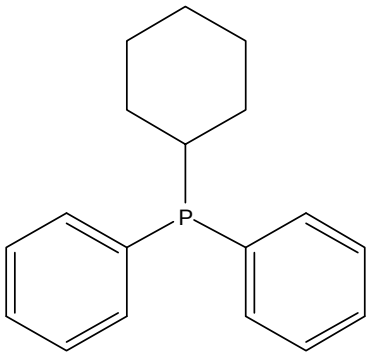

cyclohexyldiphenyl phosphine

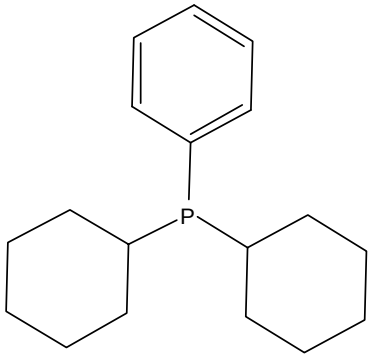

dicyclohexylphenyl phosphine

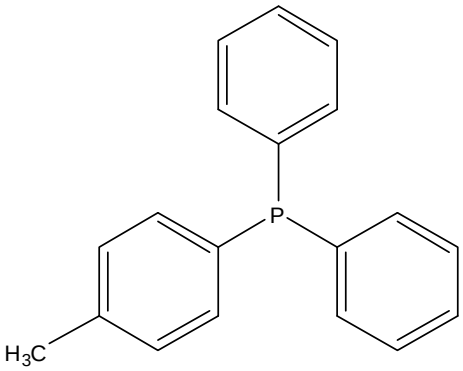

diphenyl(*p*-tolyl) phosphine

Scheme 1.

Preparation of $[Cu_4I_4(PPh_2Cy)_4].2H_2O$ (1)

For the synthesis of complex (**1**) CuI (0.19 g, 0.1 mmol) and PPh_2Cy (0.268 g, 0.1 mmol) were dissolved in 20 ml of CH_2Cl_2/MeOH (2:1). The reaction mixture was stirred for 10 minutes at room temperature. The clear solution obtained was filtered to avoid any impurity and kept at room temperature for slow evaporation. After two days colourless

block crystals were obtained. A suitable crystal was chosen for X-ray diffraction analysis. Yield: (75%). IR (υ, cm^{-1}): 3523b, 3414m, 3051w, 2924vs, 2847s, 1618vw, 1480m, 1432vs, 1331m, 1271m, 1169m, 1000m, 887m, 742vs, 527s. ^{1}H NMR (CD_2Cl_2; ppm): 1.6 to 2.00 (m, cyclohexyl CH_2), 2.5 (q, cyclohexyl CH), and 7.3 to 7.7 (m, phenyl H). ^{13}C NMR (CD_2Cl_2; ppm): 26.02 to 36.02 (cyclohexyl C), and 128.21 to 134.02 (phenyl C). ^{31}P NMR (CD_2Cl_2; ppm): -9.25 and small satellites are also observed.

Preparation of [CuI(PPhCy$_2$)$_2$] (2)

CuI (0.19 g, 0.1 mmol) and $PPhCy_2$ (0.55 g, 0.2 mmol) in 20 ml of MeCN were dissolved by continuous stirring with moderate heating. A small amount of $CHCl_3$ was added as solvent of crystallization. The colourless clear solution obtained was filtered to avoid any impurity and kept undisturbed for crystallization. After three days colourless plate-like crystals were obtained. A suitable crystal was chosen for X-ray diffraction studies. Yield: (67%). IR (υ, cm^{-1}): 3417m, 3045w, 2922vs, 2842s, 1619vw, 1483m, 1412vs, 1323m, 1275m, 1173m, 997m, 883m, 752vs, 526s. ^{1}H NMR (CD_2Cl_2; ppm): 1.2 to 2.4 (four multiplets for cyclohexyl 2H & 1H), and 7.3 to 7.6 (m, phenyl H). ^{13}C NMR (CD_2Cl_2; ppm): 26.06 to 32.45 (cyclohexyl C), and 127.93 to 134.67 (phenyl C). ^{31}P NMR (CD_2Cl_2; ppm): 6.26.

Preparation of [CuCl(PPhCy$_2$)$_2$] (3)

$CuCl_2$ (0.135 g, 0.1 mmol) and $PPhCy_2$ (0.55 g, 0.2 mmol) were dissolved by gentle heating and continuous stirring for 20 minutes in 20 ml of MeOH/H_2O (3:1), 10 ml of MeCN was added to the above reaction mixture to get a transparent solution. The clear solution obtained was filtered to avoid any impurity and kept at room temperature for slow evaporation. After five days plate like crystals were obtained. The crystalline product was collected by filtration and air dried. During this reaction Cu(II) is reduced to Cu(I) in the presence of strong reducing agents like tertiary phosphines. A suitable crystal was chosen for X-ray diffraction analysis. Yield: (78%). IR (υ, cm^{-1}): 3413m, 3053w, 2929vs, 2837s, 1613vw, 1471m, 1410vs, 1343m, 1259m, 1165m, 1008m, 873m, 755vs,

499s. ^{1}H NMR (CD_2Cl_2; ppm): 1.2 to 2.4 (four multiplets for cyclohexyl 2H & 1H), and 7.1 to 7.4 (m, phenyl H). ^{13}C NMR (CD_2Cl_2; ppm): 26.19 to 32.35 (cyclohexyl C), and 127.88 to 134.53 (phenyl C). ^{31}P NMR (CD_2Cl_2; ppm): 6.34.

Preparation of $[Cu_2I_2\{PPh_2(p\text{-tolyl})\}_3]$ (4)

CuI (0.19 g, 0.1 mmol) PPh_2(p-tolyl) (0.553 g, 0.2 mmol) were dissolved in 20 ml of MeCN by moderate heating and continuous stirring for 20 minutes. The resultant clear solution obtained was filtered to avoid any impurity and kept at room temperature to evaporate slowly. After three days colourless block crystals were obtained. The crystalline product was air dried. A suitable crystal was chosen for X-ray diffraction analysis. Yield: (82%). IR (υ, cm^{-1}): 3415m, 3068m, 3016m, 2917w, 1638w, 1617w, 1570m, 1433s, 1308w, 1155m, 1026s, 806s, 741vs, 626m, 506vs. ^{1}H NMR (CD_2Cl_2; ppm): 2.4 (s, 3H), and 7.1 to 7.5 (m, phenyl H). ^{13}C NMR (CD_2Cl_2; ppm): 21.10 (methyl C), and 128.33 to 140.18 (phenyl C). ^{31}P NMR (CD_2Cl_2; ppm): -9.21, and 27.58.

Preparation of $[CuBr(PPh_3)_3].CH_3CN$ (5)

$CuBr_2$ (0.224 g, 0.1 mmol) and PPh_3 (0.525 g, 0.2 mmol) in 15 ml CH_2Cl_2 were dissolved by continuous heating and mechanical stirring at 30ºC for twenty minutes. The resultant reaction mixture was further treated with thiosemicarbazide (0.091 g, 0.1 mmol) in 10 ml of MeCN/MeOH (1:1) solution. The reaction mixture was stirred for twenty minutes again. The resultant clear solution was filtered to avoid any impurity and kept undisturbed at room temperature for slow evaporation. During this reaction process, according to expectations, Cu(II) was reduced to Cu(I) in the presence of the strong reducing agent, triphenyl phosphine. After seven days colourless block crystals of unexpected product were obtained. A suitable crystal was chosen for X-ray diffraction analysis. Yield: (70%). IR (υ, cm^{-1}): 3413m, 3049s, 2223w, 1616w, 1584m, 1478vs, 1308m, 1154s, 997m, 741vs, 693s, 507vs. No NMR spectroscopic studies were done due to the poor solubility of the complex in the available solvents.

Preparation of $[Cu_2I_2(PPh_2Cy)_2(4,4'\text{-biep})]_n.2nCH_3CN$

Compound **1** 0.188 g (0.01 mmol) was dissolved in 15 ml of chloroform at room temperature and (E)-1,2-di(pyridine-4-yl)ethane (4,4′-biep) 0.07 g (0.04 mmol) in 10 ml acetonitrile was dissolved and added to copper-phosphine solution slowly drop by drop with continuous stirring for 20 minutes. The colourless transparent solution obtained was filtered to avoid any impurity and kept undisturbed at room temperature for crystallization. After one day lozenge shape orange/yellow crystals were obtained in the solvent. A suitable crystal was chosen for X-ray diffraction analysis and rest of the crystalline product was collected by decantation of the solvent and air dried.

X-ray Crystallography.

The intensity data were collected at 173K on either, a one circle (ϕ scans)[1], or a two circle (ω and ϕ scans)[2] Stoe Image Plate Diffraction System, using MoKα graphite monochromated radiation. The structures were solved by Direct methods using the program SHELXS-97[3]. The refinement and all further calculations were carried out using SHELXL-97[3]. The H-atoms were either located from Fourier difference maps and freely refined or included in calculated positions and treated as riding atoms using SHELXL default parameters. The non-H atoms were refined anisotropically, using weighted full-matrix least-squares on F^2. In most cases multi-scan absorption corrections were applied using the MULscanABS routine in PLATON[4]. A summary of crystal data and refinement details for compounds **1-5** are given in Table 1, and selected bond lengths and angles are listed in Tables 2-6.

1) Stoe & Cie (2000) IPDS-I Bedienungshandbuch. Stoe & Cie GmbH, Darmstadt, Germany.

2) Stoe & Cie. (2006) *X-Area V1.35 & X-RED32 V1.31 Software*. Stoe & Cie GmbH, Darmstadt, Germany.

3) G. M. Sheldrick (2008). Acta Crystallgr. A64, 112-122.

4) A. L. Spek (2003). J.Appl.Cryst. 36, 7-13

Table 1. Summary of crystal data and structure refinement details for compounds **1- 6**

$\{^{a}\ \mathbf{R1} = \Sigma||F_O| - |F_C||/\Sigma|F_O|.\ ^{b}\ \mathbf{wR2} = [\Sigma w(F_O^2 - F_C^2)^2/\Sigma wF_O^4]^{1/2}\}$

	1	**2**
Empirical formula	$C_{72}H_{88}Cu_4I_4O_2P_4$	$C_{36}H_{54}CuIP_2$
Formula weight	1871.06	739.17
Crystal size/mm	0.38 x 0.34 x 0.30	0.45 x 0.45 x 0.40
Wavelength/Å	0.71073	0.71073
Temperature/K	173	173
Crystal symmetry	Triclinic	Monoclinic
Space group	P -1	P 2_1/n
a/Å	13.6424(13)	10.4500(3)
b/Å	14.1754(14)	23.4853(10)
c/Å	21.583(2)	14.6356(5)
α/°	101.305(12)	90
β/°	96.666(12)	9.586(3)
γ/°	111.047(11)	90
V/ Å^3	3739.7(6)	3541.7(2)
Z	2	4
D_c/Mg m^{-3}	1.662	1.386
μ(Mo-Kα)/mm^{-1}	2.900	1.601
F(000)	1848	1528
θ Limits/°	2.07-26.04	1.65-29.55
Measured reflections	29409	68504
Unique reflections(R_{int})	13628(0.0459)	9593(0.0734)
Observed reflections	8896	8361
Goodness of fit on F^2	0.824	1.186
$R_1(F)$,[a][$I > 2\sigma(I)$]	0.0331	0.0438
w$R_2(F^2)$,[b][$I > 2\sigma(I)$]	0.0702	0.0990
Largest diff.peak, hole/e Å^{-3}	1.019, -1.013	0.813, -0.749

Table 1 cont,d

	3	**4**
Empirical formula	$C_{36}H_{54}ClCuP_2$	$C_{57}H_{51}Cu_2I_2P_3$
Formula weight	647.72	1209.77
Crystal size/mm	0.30 x 0.19 x 0.08	0.40 x 0.40 x 0.31
Wavelength/Å	0.71073	0.71073
Temperature/K	173	173
Crystal symmetry	Monoclinic	Triclinic
Space group	P 2_1/n	P -1
a/Å	10.2513(9)	14.067(2)
b/Å	24.433(2)	14.077(2)
c/Å	13.9602(12)	16.329(3)
α/°	90	101.39(2)
β/°	99.929(10)	104.24(2)
γ/°	90	117.895(17)
V/ Å^3	3444.2(5)	2579.0(7)
Z	4	2
D_c/Mg m^{-3}	1.249	1.558
μ(Mo-Kα)/mm^{-1}	0.828	2.151
F(000)	1384	1204
θ Limits/°	2.1-22.80	2.15- 25.85
Measured reflections	25811	20073
Unique reflections(R_{int})	6761(0.2323)	9354(0.1862)
Observed reflections	1925	4713
Goodness of fit on F^2	0.710	0.879
$R_1(F)$,[a] $[I > 2\sigma(I)]$	0.0661	0.0866
w$R_2(F^2)$,[b] $[I > 2\sigma(I)]$	0.1506	0.2195
Largest diff.peak, hole/e Å^{-3}	0.585, -1.108	1.443, -1.893

Table 1 cont,d

	5	**6**
Empirical formula	$C_{56}H_{48}BrCuNP_3$	$C_{52}H_{58}Cu_2I_2N_4P_2$
Formula weight	971.31	1181.84
Crystal size/mm	0.30 x 0.19 x 0.11	0.23 x 0.20 x 0.15
Wavelength/Å	0.71073	0.71073
Temperature/K	173	173
Crystal symmetry	Triclinic	Triclinic
Space group	P -1	P -1
a/Å	11.5329(10)	9.0585(10)
b/Å	13.0973(11)	10.4699(12)
c/Å	15.7012(14)	14.1284(16)
α/°	88.859(10)	107.274(9)
β/°	83.677(10)	90.693(9)
γ/°	84.956(10)	99.146(9)
V/ $Å^3$	2348.0(4)	1260.8(2)
Z	2	2
D_c/Mg m^{-3}	1.374	1.557
μ(Mo-Kα)/mm^{-1}	1.457	2.170
F(000)	1000	592
θ Limits/°	1.90-25.90	1.51-26.13
Measured reflections	18563	11412
Unique reflections(R_{int})	8580(0.0606)	4722(0.0260)
Observed reflections	4743	4132
Goodness of fit on F^2	0.760	0.985
$R_1(F)$,[a] $[I > 2\sigma(I)]$	0.0319	0.0221
wR_2 (F^2),[b] $[I > 2\sigma(I)]$	0.0516	0.0500
Largest diff.peak, hole/e $Å^{-3}$	0.466, -0.521	0.431, -0.479

Results and Discussions

Crystal structures

$[Cu_4I_4(PPh_2Cy)_4].2H_2O$ (1)

The crystal structure of $[Cu_4I_4(PPh_2Cy)_4].2H_2O$ (**1**) has been determined at low temperature and the molecular structure is given in Fig. **1**. Selected bond lengths and angles are tabulated in Table **2**. The asymmetric unit of complex **1** consists of one molecule of $[Cu_4I_4(PPh_2Cy)_4]$ and two water molecules of crystallization. It is isostructural with molecular complexes of general formula $[Cu_4X_4(PPh_3)_4]$ [23-25].

The central unit of the complex **1** can be described as a strongly distorted cube in which four corners are occupied by four I atoms and on alternative corners of the cube there are four Cu(I) atoms. The Cu(I) atoms are coordinated with a monodentate tertiary phosphine as a terminal ligand. The molecular structure of the complex adopts a cubane-like configuration with two interpenetrating tetrahedra of complex; the copper and iodine atoms form a markedly distorted cube (as shown in Fig. **1**), each copper atom being further coordinated to a diphenylcyclohexyl phosphine ligand.

The most notable structural feature of complex **1** is that both the bonding and nonbonding distances of Cu_4I_4 core deviate greatly from the idealized cubic tetrahedral geometry expected from bonding considerations. In this distorted cubane like structure the Cu...Cu distance is ca. 2.9657(9) Å; I…I inter atomic distances vary from ca. 4.184 to 4.301 Å. The Cu-I distances range from 2.6402(8) to 2.7252(7) Å. These inter-cubane distances indicate that there is no metal-metal interaction (d^{10}-d^{10} interaction) in the solid state structure of complex **1**. Inter atomic distances found in complex **1** are comparable with those found in the previous studies [10].

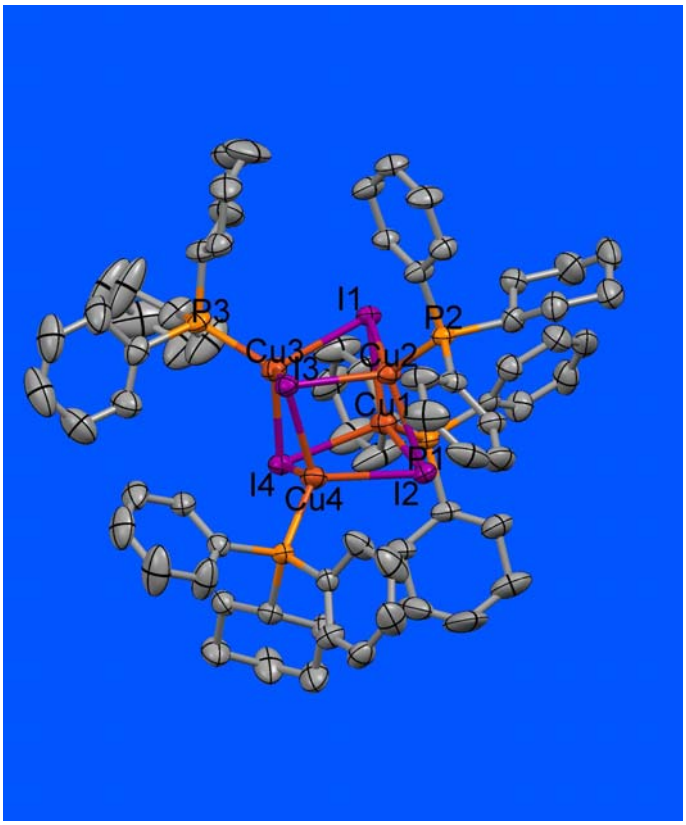

Figure 1. View of the molecular structure of complex **1** with selected atom labelling Scheme.

Table 2. Selected bond distances (Å) and bond angles (˚) for complex **1**

Bond lengths (Å)		Bond angles (˚)	
I(1)-Cu(1)	2.6850(8)	Cu(1)-I(1)-Cu(2)	67.19(3)
I(1)-Cu(2)	2.6748(8)	Cu(1)-I(1)-Cu(3)	71.63(2)
I(1)-Cu(3)	2.7140(8)	Cu(2)-I(1)-Cu(3)	73.72(2)
I(2)-Cu(1)	2.6625(8)	Cu(1)-I(2)-Cu(2)	67.65(3)
I(2)-Cu(2)	2.6650(8)	Cu(1)-I(2)-Cu(4)	73.41(2)
I(2)-Cu(4)	2.7252(7)	Cu(2)-I(2)-Cu(4)	71.63(2)
I(3)-Cu(2)	2.7004(8)	Cu(2)-I(3)-Cu(3)	73.35(2)
I(3)-Cu(3)	2.7122(8)	Cu(2)-I(3)-Cu(4)	71.38(2)
I(3)-Cu(4)	2.7063(8)	Cu(3)-I(3)-Cu(4)	70.36(3)
I(4)-Cu(1)	2.7188(8)	Cu(1)-I(4)-Cu(3)	72.24(2)
I(4)-Cu(3)	2.6402(8)	Cu(1)-I(4)-Cu(4)	72.96(2)

I(4)-Cu(4)	2.6979(8)	Cu(3)-I(4)-Cu(4)	71.57(3)
Cu(1)-P(1)	2.2419(15)	I(1)-Cu(1)-I(2)	111.06(3)
Cu(2)-P(2)	2.2435(15)	I(1)-Cu(1)-I(4)	104.50(3)
Cu(3)-P(3)	2.2429(16)	I(1)-Cu(3)-P(3)	114.38(5)
Cu(4)-P(4)	2.2508(16)	I(1)-Cu(2)-I(2)	111.30(3)
		I(3)-Cu(3)-I(4)	108.64(3)
		I(3)-Cu(3)-P(3)	112.09(5)
		I(1)-Cu(3)-I(3)	100.90(3)
		I(4)-Cu(3)-P(3)	113.96(5)
		I(2)-Cu(4)-I(3)	104.72(3)
		I(3)-Cu(4)-P(4)	112.29(5)
		I(4)-Cu(4)-P(4)	115.35(5)

The evidence concerning the large deformation of the Cu_4I_4 core is given by the Cu-I-Cu angles which range from 67.19(3) to 73.72(2)º and the I-Cu-I angles which vary from 100.90(2) to 111.30(3)º. These bond angles describe well the deviation from ideal cubane like structures.

[CuI(PPhCy$_2$)$_2$] (2)

A perspective view of the molecular structure of complex **2** is shown in Fig. **2**, with the atom labelling Scheme. The crystal structure of complex **2** is isostructural to the complexes with general formulae [CuX(PCy$_3$)$_2$] (X= Cl, Br, I) [1]. The geometry around the copper(I) centre is trigonal planar. The Cu-P average distance 2.2395(8) Å, this is shorter than that found in other Cu(I) complexes [1]. Whereas, the Cu-I distance 2.536(4) Å is also shorter than that found in complex [CuI(PCy$_3$)$_2$] [1]. The bond angles around Cu(I) centre are 133.04(3), 111.55(3) and 115.37(2)º for P-Cu-P and I-Cu-P respectively. The bond angles values show considerable deviation from the ideal trigonal planar angle of 120˚.

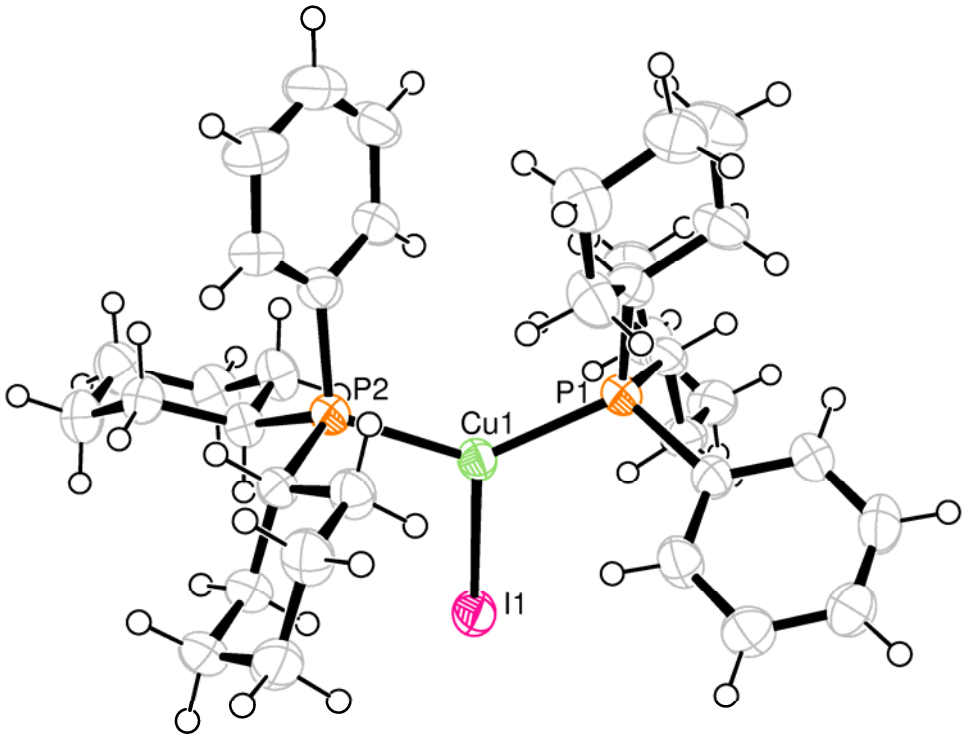

Figure 2. View of the crystal structure of complex **2** with atom labelling Scheme.

Table 3 Selected bond distances (Å) and bond angles (˚) for complex **2**

Bond distances (Å)		Bond angles (˚)	
I(1)-Cu(1)	2.5359(5)	I(1)-Cu(1)-P(1)	115.37(2)
Cu(1)-P(1)	2.2392(8)	I(1)-Cu(1)-P(2)	111.55(3)
Cu(1)-P(2)	2.2399(8)	P(1)-Cu(1)-P(2)	133.04(3)

[CuCl(PPhCy$_2$)$_2$] (3)

The molecular structure of complex **3** is isostructural and isomorphous to complex **2**. Both complexes crystallize in monoclinic unit cell space group P2$_1$/n. The perspective view of the molecular structure of complex **3** is shown in Fig. **3**, with selected atom labelling Scheme. The geometrical environment around Cu(I) centre in complex **3** is distorted trigonal planar, as found in complex **2**. The Cu-Cl bond distance 2.241(2) Å is

shorter than Cu-I bond distance found in complex **2** and this difference is attributed to the different atomic sizes of chlorine and iodine atoms. The Cu-P bond distances 2.250(2) and 2.257(2) Å are longer than that found in complex **2**. The P-Cu-Cl bond angles are 113.33(9) and 116.51(8)º, whereas the P-Cu-P bond angle is 130.10(9)º. These bond angles values show considerable deviation from ideal trigonal planar angle of 120˚.

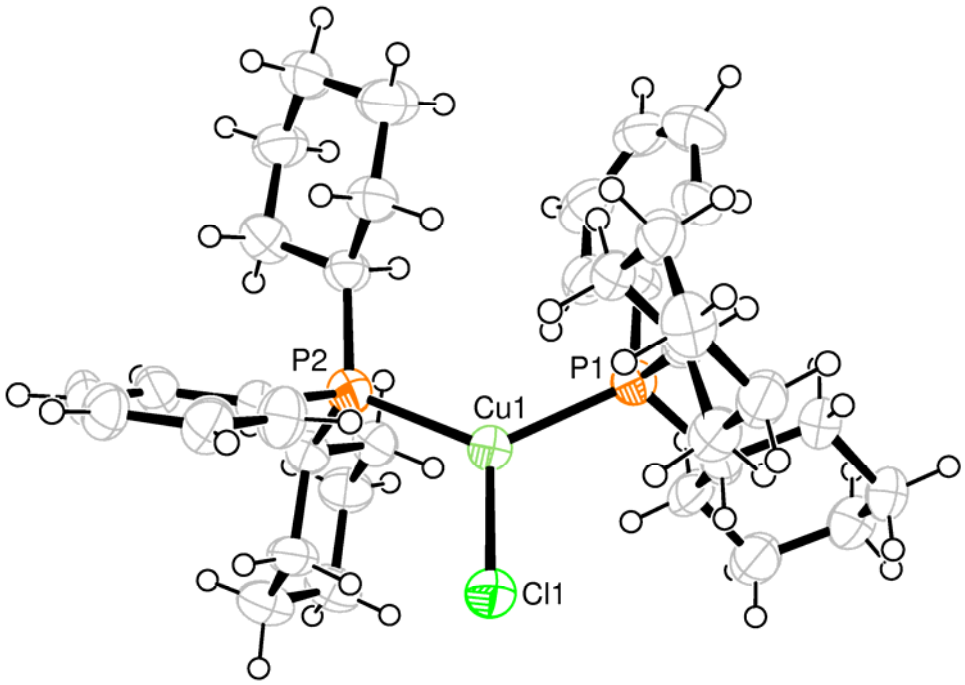

Figure 3. View of the molecular structure of complex **3** with selected atom labelling Scheme and ellipsoids are drawn at 50% probability level.

Table 4. Selected bond distances (Å) and bond angles (˚) for complex **3**

Bond distances (Å)		Bond angles (˚)	
Cu(1)-Cl(1)	2.241(2)	Cl(1)-Cu(1)-P(1)	113.33(9)
Cu(1)-P(1)	2.250(2)	Cl(1)-Cu(1)-P(2)	116.51(8)
Cu(1)-P(2)	2.257(2)	P(1)-Cu(1)-P(2)	130.10(9)

$[Cu_2I_2\{PPh_2(p\text{-tolyl})\}_3]$ (4)

The molecular structure of complex **4** is illustrated in Fig. **4**, with slected atom labelling Scheme. The complex **4** is binuclear molecule. Two copper(I) atoms are bridged by two iodine atoms. The atom Cu1 is further coordinated with two monodentate diphenyl(p-tolyl) phosphine ligand molecules and the geometrical environment around atom Cu1 is distorted tetrahedral. Whereas, atom Cu2 is coordinated with one phosphine ligand molecule and geometrical environment around atom Cu2 is trigonal planar, as shown in Fig. **4**.

Table 5 Selected bond distances (Å) and bond angles (˚) for complex **4**

Bond distances (Å)		Bond angles (˚)	
I(1)-Cu(2)	2.5506(17)	Cu(2)-I(1)-Cu(1)	64.38(5)
I(1)-Cu(1)	2.7392(19)	Cu(2)-I(2)-Cu(1)	64.95(5)
I(2)-Cu(2)	2.5344(18)	P(2)-Cu(1)-P(1)	122.64(11)
I(2)-Cu(1)	2.7147(17)	P(2)-Cu(1)-I(2)	102.89(9)
Cu(1)-P(2)	2.264(3)	P(1)-Cu(1)-I(2)	108.54(9)
Cu(1)-P(1)	2.276(3)	P(2)-Cu(1)-I(1)	106.82(9)
Cu(1)-Cu(2)	2.822(2)	P(1)-Cu(1)-I(1)	107.94(9)
Cu(2)-P(3)	2.209(3)	I(2)-Cu(1)-I(1)	107.07(5)
P(1)-C(20)	1.819(13)	P(2)-Cu(1)-Cu(2)	127.84(9)

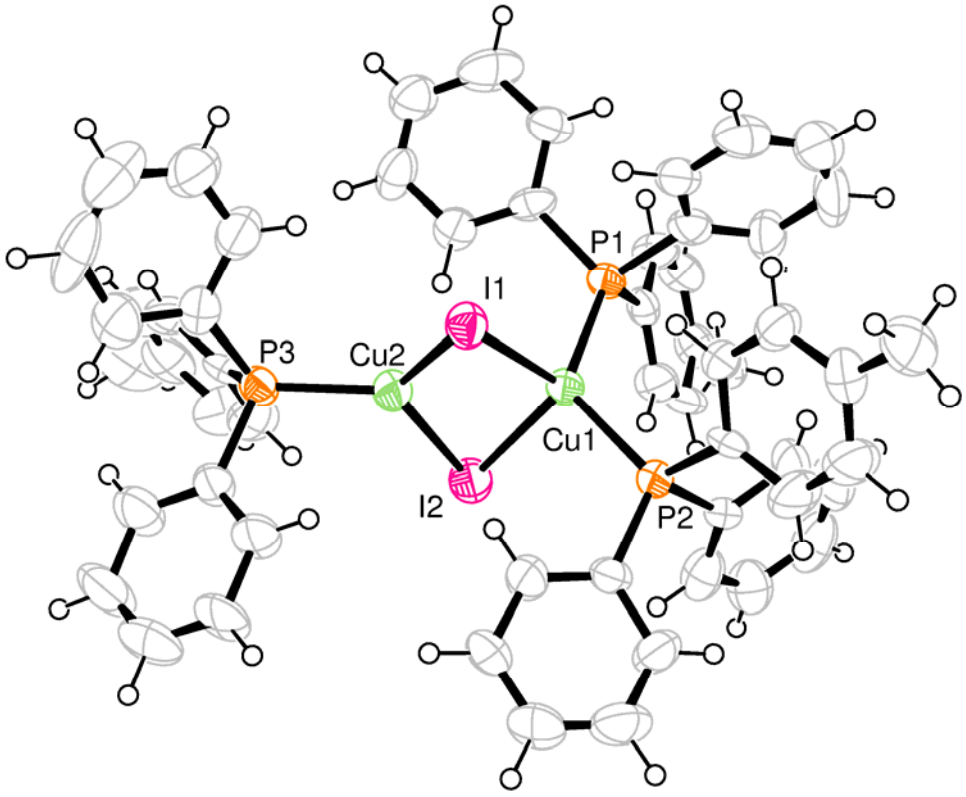

Figure 4. View of the single crystal structure of complex **4** with partial atom labelling and displacement ellipsoids are drawn at 50% probability level.

The Cu…Cu inter atomic distance is ca. 2.822(2) Å and shorter than that found in the reported structure of complex $[Cu_2I_2\{P(o\text{-}tolyl)_3\}_3]$. This distance indicates the presence of metal-metal interaction in this binuclear complex **4** [15]. The Cu-I distances range from 2.5344(18) to 2.7392(19) Å. The Cu1-I bond distances are longer than the Cu2-I bond distances. The difference in Cu-I bond distances is attributed to the presence of different geometrical environmental around both copper(I) atoms in this binuclear dimer complex molecule. The Cu-I-Cu bond angles are 64.38(5) and 64.95(5)º. The P-Cu1-P bond angle is 122.64(11)º and the P-Cu1-I bond angles vary from 102.89(9) to 108.54(9)º. The I-Cu1-I bond angle is 109.46(9)º. The bond angles values around atom Cu1 show considerable deviation from the ideal tetrahedral angle of 109.5˚. Whereas, the P-Cu2-I bond angles values are 117.12(11) and 122.69(11)º. The I-Cu2-I bond angle is 119.21(6)º. The bond angles values around atom Cu2 show little deviation from the ideal trigonal planar angle of 120º.

[CuBr(PPh$_3$)$_3$].CH$_3$CN (5)

View of molecular structure of complex **5** is shown in Fig. **5**, with selected atom labelling Scheme. The molecular structure of the complex is a pseudo-polymorph of the complex [CuBr(PPh$_3$)$_3$], [CuBr(PPh$_3$)$_3$].THF, and [CuBr(PPh$_3$)$_3$].(CH$_3$)$_2$CO [5,36]. The crystallographic environment around Cu(I) atom is distorted tetrahedral, as found in the other polymorphic forms [5,36]. The asymmetric unit contains one acetonitrile molecule as well. The solvent molecule does not show any coordination with the metal centre and is well separated.

Table 6. Selected bond distances (Å) and bond angles (˚) for complex **5**

Bond distances (Å)		Bond angles (˚)	
Br(1)-Cu(1)	2.4826(6)	P(2)-Cu(1)-P(1)	112.69(3)
Cu(1)-P(2)	2.3046(10)	P(2)-Cu(1)-P(3)	120.08(3)
Cu(1)-P(1)	2.3111(9)	P(1)-Cu(1)-P(3)	114.56(4)
Cu(1)-P(3)	2.3137(9)	P(2)-Cu(1)-Br(1)	99.05(3)
		P(1)-Cu(1)-Br(1)	105.53(3)
		P(3)-Cu(1)-Br(1)	101.63(3)

This observation is similar to the other pseudo-polymorphic forms of the complex [5,36]. The copper(I) centre is coordinated with three monodentate triphenyl phosphine ligand molecules and one bromine atom. The Cu-P bond distances range from 2.3046(10) to 2.3137(9) Å, and the Cu-Br bond distance is 2.4826(6) Å. The Cu-P bond distances are shorter than those found in the polymorphic forms [5,36] and the Cu-Br bond distance is longer than that found in [CuBr(PPh$_3$)$_3$].THF [36] and shorter than that found in [CuBr(PPh$_3$)$_3$] and [CuBr(PPh$_3$)$_3$].(CH$_3$)$_2$CO [5]. The bond angles values around Cu(I) atom vary from 99.05(3) to 120.08(3)º. These bond angle values describe the presence of a distorted tetrahedral geometry around the copper(I) atom in this complex **5**. The deviation from ideal tetrahedral geometry around the central metal atom is similar to that found in its polymorphic forms.

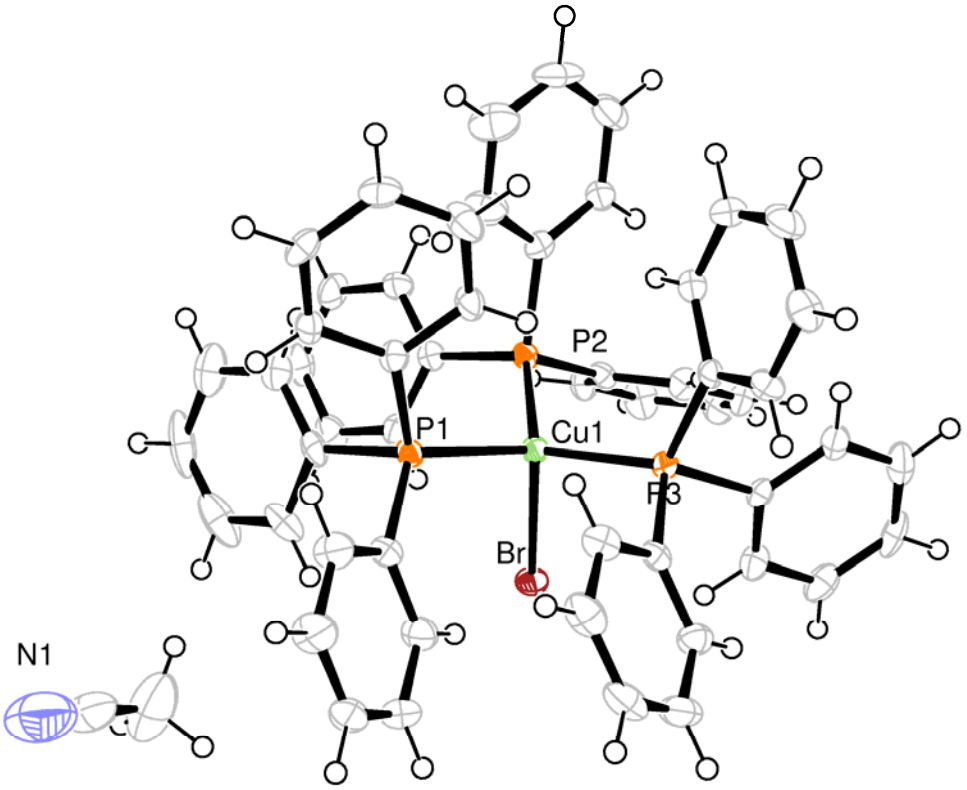

Figure 5. Ortep view of the molecular structure of complex **5** and displacement ellipsoids are shown at 50% probability.

$\{[Cu_2I_2(PPh_2Cy)_2(4,4'\text{-biep})].2CH_3CN\}_n$ (6)

4,4′-biep =

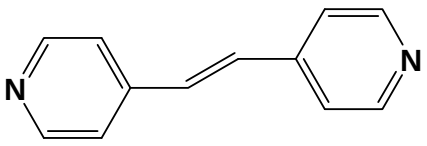

(*E*)-1,2-di(pyridin-4-yl)ethene

The molecular structure of the copper(I)-mixed ligand complex **6** is shown in the Fig. **6**, with complete atom labelling Scheme. The molecular structure is a one-dimensional stair or step-like polymeric chain structure. The geometry around the copper(I) centre is distorted tetrahedral. The Cu-N and Cu-P bond lengths are 2.055(2) and 2.2288(7) Å. The Cu-I bond distances are 2.7025(4) and 2.7089(5) Å. The I-Cu-N, I-Cu-P and N-Cu-P bond angles values are 111.89(2), 101.33(6), and 121.72(6)˚, respectively. The I-Cu-I and Cu-I-Cu bond angle values are 108.11(1) and 71.89(1)˚, respectively. These bond angles values show considerable deviation from the ideal tetrahedral angle of 109.5˚. The Cu…Cu distance is ca. 3.176 Å, which shows a strong metal-metal interaction.

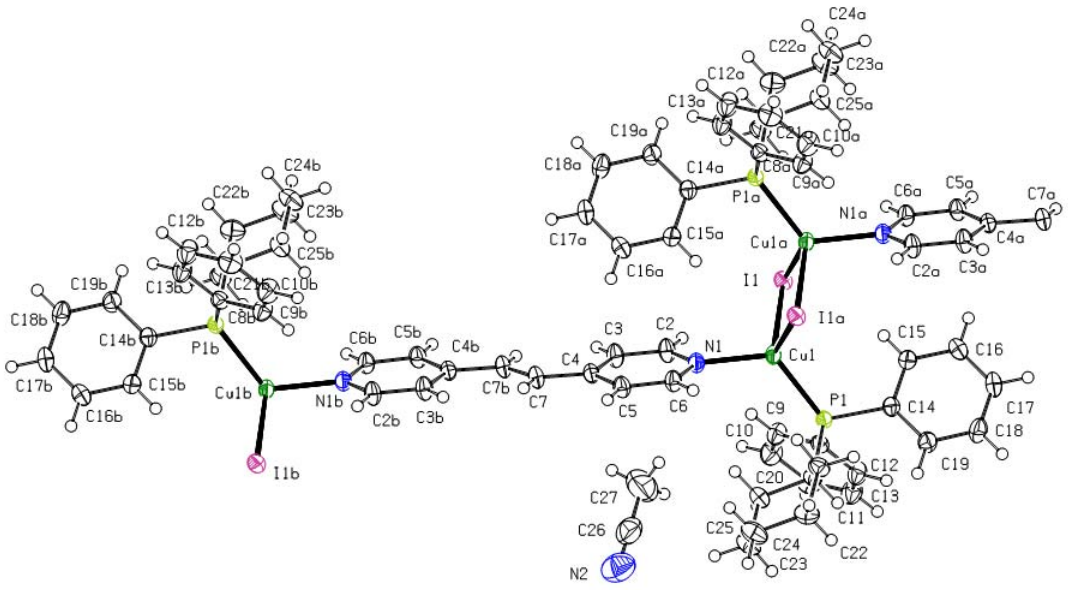

Figure 6. View of the molecular structure of complex **6**, a mixed ligand CuI phosphine complex, with complete atom labelling Scheme. Displacement ellipsoids are shown at 50% probability level.

Spectroscopic studies

The IR spectra of compounds **1**-**5** have been recorded in the range of 4000 to 450 cm^{-1} and are characterized by many absorption bands of the coordinated tertiary phosphine

ligands, apart from the characteristic bands for aromatic and non-aromatic hydrogen 2900 to 3100 cm^{-1} for all complexes. For complexes **1** and **5**, several stretching bands are also observed in these spectra.

At room temperature complexes **1-3** in dichloromethane solution gave ^{31}P NMR spectra consisting of a single line. This is the result of rapid intermolecular exchange of the phosphine between the different copper atoms and with the free phosphines, as a tertiary phosphine in these complexes is present in the same type of electronic and magnetic environment. This type of behaviour of phosphine is well documented [37]. ^{1}H NMR spectra for complexes **1-4** are consistence with the structure. For complex **1** two sets of multiplet peaks in the range of 1.5 to 2.5 ppm and 7.1 to 7.8 ppm are observed for hydrogen atoms bonded to cyclohexyl and phenyl carbons, respectively. The ^{13}C NMR spectrum of the complex **1** also shows the same trend and two different set of peaks are observed for the cyclohexyl and phenyl carbons. The same trend is observed for ^{13}C NMR spectra of complexes **2** and **3**. Although in the ^{31}P NMR spectrum of complex **4** two peaks are observed at -9.21, and 27.58 ppm, the presence of these two peaks is attributed to the different crystallographic, electronic and magnetic environment for the tertiary phosphine. In this dimer molecule the geometrical environment around one of the copper(I) atom is trigonal planar and around the other atom; it is tetrahedral. The ^{1}H & ^{13}C NMR spectral results are consistent with the molecular structure of the complex **4**.

Conclusions

Using complex **1** as a precursor and the bridging ligand (E)-1,2-di(pyridine-4-yl)ethane; it is shown here that it is possible to synthesize a mixed ligand CuI phospine complex. The resultant compound was shown by X-ray crystallographic analysis to be a one-dimensional coordination polymer with the ligand bridging a Cu_2I_2 unit.

References

[1] G.A. Bowmaker, S.E. Boyd, J.V. Hanna, R.D. Hart, P.C. Healy, B.W. Skelton, A.H. White, J. Chem. Soc., Dalton Trans. (2002) 2722.

[2] B. Murphy, G. Roberts, S. Tyagi, B.J. Hathaway, Journal of Molecular Structure. 698 (2004) 25.

[3] D. Choquesillo-Lazarte, B. Covelo, J. M. Gonàlez-Pérez, A. Castineiras, J. Niclos-Gutiérrez, Polyhedron. 21 (2002) 1485.

[4] D.B. Leznoff, N.D. Draper, R.J. Batchelor, Polyhedron. 22 (2003) 1735.

[5] C. Näther, I. Jeß, Monatshefte für Chemie. 132 (2001) 897.

[6] J.M. Knaust, S.W. Keller, Inorg. Chem. 41 (2002) 5650.

[7] R.-Z. Li, D. Li, X.-C. Huang, Z.-Y. Qi, Z.-M. Chen, Inorg. Chem. Commun. 6 (2003) 1017.

[8] J. Lu, G. Crisci, T. Niu, A.J. Jacobson, Inorg. Chem. 36 (1997) 5140.

[9] J. Mo, H.-Y. Qian, H.-D. Du, W. Chen, Acta Cryst. E62 (2006) m726.

[10] J.C. Dyason, P.C. Healy, L.M. Engelhardt, C. Pakawatchai, V.A. Patrick, C.L. Raston, A.H. White, J. Chem. Soc., Dalton Trans. (1985) 831.

[11] T. Kräuther, B. Neumüller, Polyhedron. 15 (1996) 2851.

[12] P. Aslanidas, S.K. Hadjikakou, P. Karagiannidis, M. Gdaniec, Z. Kosturkiewicz, Polyhedron. 12 (1993) 2221.

[13] W.R. Clayton, S.G. Shore, Cryst. Struct. Comm. 2 (1973) 605.

[14] G.A. Bowmaker, A. Camus, P.C. Healy, B.W. Skelton, Inorg. Chem. 28 (1989) 3823.

[15] G.M. Golzar Hossain, A. Banu, Z. S. Seddigi, Acta Cryst. E61 (2005) m2629.

[16] B.-K. Teo, J.C. Calabbrese, Inorg. Chem. 15 (1976) 2467.

[17] I.R. Whittall, M.G. Humphrey, M. Samoc, B. Luther-Davies, D.C.R. Hockless, J. Organomet. Chem. 544 (1997) 189.

[18] M.R. Churchill, F.T. Rotella, Inorg. Chem. 18 (1979) 166.

[19] P.F. Barron, J.C. Dyason, P.C. Healy, L.M. Engelhardt, C. Pakwatchai, V.A. Patrick, A.H. White, J. Chem. Soc., Dalton Trans. (1987)1099.

[20] G.A. Bowmaker, J.C. Dyason, P.C. Healy, L.M. Engelhardt, C. Pakwatchai,

A.H. White, J. Chem. Soc., Dalton Trans. (1987) 1089.

[21] M.R. Churchill, K.L. Kalra, Inorg. Chem. 13 (1974) 1065.

[22] B.-K. Teo, J.C. Calabbrese, Chem. Commun. (1976) 185.

[23] P.F. Barron, J.C. Dyason, L.M. Engelhardt, P.C. Healy, A.H. White, Inorg. Chem. 23 (1984) 3766.

[24] B.-K. Teo, J.C. Calabbrese, J. Am. Chem. Soc. 97 (1975) 1256.

[25] G.A. Bowmaker, Effendy, R.D. Hart, J.D. Kildea, A.H. White, Aust. J. Chem. 50 (1997) 653.

[26] X.M. Zhang, R.Q. Fang, Inorg. Chem. 44 (2005) 3955.

[27] J.K. Kim, M.K. Hang, J.H. Ahn, M. Lee, Angew. Chem. Int. Ed. 44 (2005) 328.

[28] H. Rudmann, S. Shimada, M.F. Rubner, J. Am. Chem. Soc. 124 (2002) 4918.

[29] P. Diaz, J. Benet-Buchholz, R. Vilar, A.J.P. White, Inorg. Chem. 45 (2006) 1617.

[30] W.L. Jia, T. McCormick, Y. Tao, J.-P. Lu, S. Wang, Inorg. Chem. 44 (2005) 5706.

[31] X.-H. Zhou, T. Wu, D. Li, Inorg. Chim. Acta. 359 (2006) 1442.

[32] A. Tadsanaprasittipol, H.-B. Kraatz, G.D. Enright, Inorg. Chim. Acta. 278 (1998) 143.

[33] T.S. Lobana, S.Khanna, R.J. Butcher, A.D. Hunter, M. Zeller, Polyhedron. 25 (2006) 2755.

[34] L.M. Engelhardt, P.C. Healy, J.D. Kildea, A.H. White, Aust. J. Chem., 42 (1989) 895.

[35] A. Müller, H. Bögge, U. Schimanski, Inorg. Chim. Acta. 69 (1983) 5.

[36] H. Eriksson, M. Ortendahl, M. Ha°kansson, Organomet. 15 (1996) 4823.

[37] P.F. Barron, J.C. Dyason, P.C. Healy, L.M. Engelhardt, B.W. Skelton, A.H. White, J. Chem. Soc., Dalton Trans. (1986) 1965.

Part C:

Gold(I) halide tertiary phosphines complexes

Abstract

Reactions of equimolar amounts of $KAuCl_4$ and diphenyl(*p*-tolyl) phosphine, and diphenylcyclohexyl phosphine gave monomer complexes [Au(Cl)(PPh_2(p-tolyl))] (**1**), [Au(Cl)(PPh_2Cy)] (**2**), respectively. These gold(I)-tertiary phosphine complexes are isostructural and the crystallographic environment around the Au(I) atom in these complexes is typically linear. Complex **1** crystallizes in triclinic space group 'P -1' and complex **2** crystallizes in monoclinic space group 'P 2_1/n'. Elemental analysis and IR spectra of the gold(I) complexes were recorded.

Introduction

The study of coinage metal complexes, bearing different functional ligands and therefore exhibiting interesting physical, chemical, biological and pharmacological properties has attracted much attention [1-5]. There is considerable interest in the coordination chemistry of coinage metals such as silver(I), gold(I) & gold(III), and copper(II) with biological and potential applications in various fields of life [6-10]. The studies of gold(I) complexes have mostly been focused on their antiarthritic, antitumor, and antimicrobial activities. Gold(III) complexes have been a long-standing biological interest because of the prospect of inorganic drug design and their use in studying biochemical reaction mechanisms [11-15]. It has been found that gold(I)-phosphine complexes with AuNP, AuSP, AuPP, and AuSS coordination environments show marked medicinal and biological activities against bacteria and yeast [16-17].

Transition metal complexes of common ligands with group 15 donor atoms are widely investigated in various fields of bioinorganic chemistry, electrochemistry and organometallic chemistry. We have decided to investigate systematically coinage metal complexes containing ligands with group 15 donor atoms as we are interested in the synthesis, crystal engineering, molecular design, and single crystal determination of coinage metal complexes with common ligands. Here we report the structures of two such compounds, [Au(Cl)(P(*p*-tolyl)Ph_2)] (**1**) and [Au(Cl)(PPh_2Cy)] (**2**). The geometrical environment around the gold(I) atom in complexes **1** & **2** is linear , which is typical for gold(I) complexes with bulky tertiary phosphine ligands, such as those used here (Scheme 1). The gold(I) phosphine complexes are known to exhibit promising antitumor properties [11, 18-20]. The single crystal X-ray structures and IR absorption spectra of complexes **1** and **2** are discussed here. The single crystal X-ray diffraction analyses were carried out at low temperature (-100ºC).

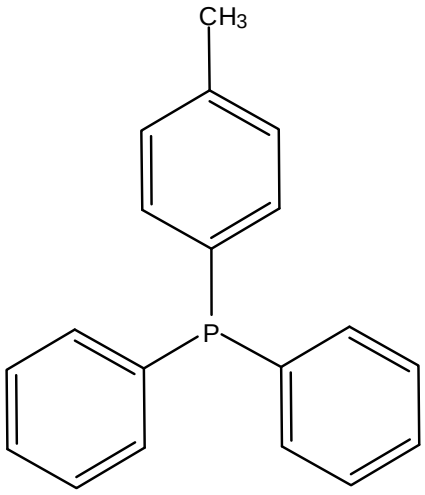

diphenyl(*p*-tolyl) phosphine

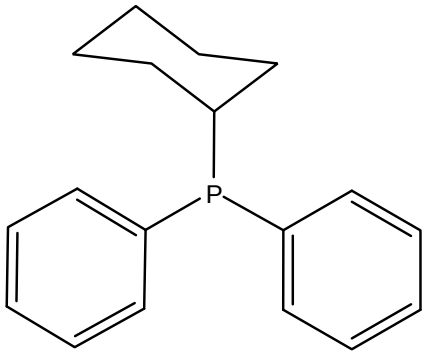

cyclohexyldiphenyl phosphine

Scheme 1

Experimental

Material and physical measurement

All the reactions were carried out under normal conditions. All chemicals and solvents used in the synthesis were of analytical grade and were used without further purification. All chemicals were purchased from Aldrich and ACROS. Microanalysis was done by Mr. D. Mooser (Ecole d'ingénieurs de Fribourg, Filière de chimie). The IR spectra were recorded as KBr pellets on a PerkinElmer Spectrum One FTIR instrument.

Preparation of [Au(Cl)(PPh_2(p-tolyl))] (1)

To a solution of diphenyl(p-tolyl) phosphine (0.275 g, 1.0 mmol) in 10 ml of dichloromethane was added $KAuCl_4$ (0.378 g, 1.0 mmol) in 15 ml of ethanol at room temperature with continuous stirring for 3h. The colourless solution obtained was filtered to avoid any impurity and kept undisturbed for slow evaporation. After three days colourless block crystals were obtained. A suitable crystal was chosen for X-ray diffraction analysis. Yield 58%. Anal. Calc. for $C_{19}H_{17}AuClP$: C, 44.81; H, 3.34. Found: C, 44.68; H, 3.27%. IR (υ, cm^{-1}): 3417m, 3055w, 2928vs, 2837s, 1613vw, 1471m, 1415vs, 1346m, 1258m, 1155m, 1008m, 873m, 759vs, 500s.

Preparation of [Au(Cl)($PCyPh_2$)] (2)

To a solution of cyclohexyldiphenyl phosphine (0.287 g, 1.0 mmol) in 10 ml of dichloromethane was added vigorously $KAuCl_4$ (0.378 g, 1.0 mmol) in 15 ml of ethanol. The reaction mixture was stirred mechanically for 30 minutes at room temperature. The colourless solution obtained was filtered to avoid any impurity and kept for crystallization by slow evaporation. After three days a colourless product was obtained. The transparent material was re-dissolved in dichloromethane and small amount of acetonitrile was added as solvent of crystallization. The resultant solution was kept for slow evaporation. After three days colourless block-like crystals were obtained. A suitable crystal was used for X-ray diffraction studies. Yield 47%. Anal. Calc. for

$C_{18}H_{21}AuClP$: C, 43.13; H, 4.19. Found: C, 43.07; H, 4.13%. IR (υ, cm^{-1}): 3402s, 3078m, 3034m, 2922vs, 2839s, 2346w, 2141w, 2117m, 1632m, 1615s, 1434vs, 1265m, 1183s, 998s, 847m, 743m, 617m, 510m.

X-ray Crystallography.

Suitable crystals of complexes **1** & **2** were grown by slow evaporation of their concentrated reaction solutions at room temperature. The intensity data were collected at 173K on a two circle (ω and ϕ scans)[1] Stoe Image Plate Diffraction System, using MoKα graphite monochromated radiation. The structures were solved by Direct methods using the program SHELXS-97[2]. The refinement and all further calculations were carried out using SHELXL-97[3]. The H-atoms were either located from Fourier difference maps and freely refined or included in calculated positions and treated as riding atoms using SHELXL default parameters. The non-H atoms were refined anisotropically, using weighted full-matrix least-squares on F^2. In most cases multi-scan absorption corrections were applied using the MULscanABS routine in PLATON[3]. A summary of crystal data and refinement details for compounds **1**-**2** are given in Table 1, and selected bond lengths and angles are listed in Table 2.

1) Stoe & Cie. (2006) *X-Area V1.35 & X-RED32 V1.31 Software*. Stoe & Cie GmbH, Darmstadt, Germany.

3) G. M. Sheldrick (2008). Acta Crystallgr. A64, 112-122.

3) A. L. Spek (2003). J. Appl. Cryst. 36, 7-13

Table 1. Summary of crystal data and refinement details for compounds **1** and **2**

$\{^{a}\ \mathbf{R1} = \Sigma||F_O| - |F_C||/\Sigma|F_O|.\ ^{b}\ \mathbf{wR2} = [\Sigma w(F_O^2 - F_C^2)^2/\Sigma wF_O^4]^{1/2}\}$

	1	**2**
Empirical formula	$C_{19}H_{17}AuClP$	$C_{18}H_{21}AuClP$
Formula weight	508.71	500.73
Crystal size/mm	0.34 x 0.32 x 0.14	0.43 x 0.40 x 0.20
Wavelength/Å	0.71073	0.71073
Temperature/K	173(2)	173(2)
Crystal symmetry	Triclinic	Monoclinic
Space group	P -1	P 2_1/n
a/Å	8.8622(16)	9.0181(10)
b/Å	10.4933(19)	17.3886(17)
c/Å	11.058(2)	11.1016(11)
α/°	61.086(13)	90
β/°	77.278(15)	91.441(8)
γ/°	78.063(14)	90
V/ $Å^3$	872.0(3)	1740.3(3)
Z	2	4
D_c/Mg m^{-3}	1.938	1.911
μ(Mo-Kα)/mm^{-1}	8.672	8.690
F(000)	484	960
θ Limits/°	2.12-29.58	1.83-29.62
Measured reflections	8465	5558
Unique reflections/(R_{int})	4346/0.	3330/0.
Observed reflections	3732	2947
Goodness of fit on F^2	1.067	1.127
$R_1(F)$,[a] $[I > 2\sigma(I)]$	0.0550	0.0548
wR_2 (F^2),[b] $[I > 2\sigma(I)]$	0.1439	0.1553
Largest diff.peak, hole/e $Å^{-3}$	3.945, -4.795	3.200, -2.296

Table 2. Selected bond lengths and bond angles (Å,˚) for complexes **1**-**2**

Bond lengths (Å)		Bond angles (˚)	
1			
Au(1)-P(1)	2.233(2)	P(1)-Au(1)-Cl(1)	176.68(8)
Au(1)-Cl(1)	2.287(2)	C(1)-P(1)-Au(1)	114.6(3)
		C(7)-P(1)-Au(1)	110.8(3)
		C(13)-P(1)-Au(1)	114.5(3)
2			
Au(1)-P(1)	2.238(2)	P(1)-Au(1)-Cl(1)	177.70(9)
Au(1)-Cl(1)	2.283(2)	C(7)-P(1)-Au(1)	114.6(3)
		C(1)-P(1)-Au(1)	111.5(3)
		C(13)-P(1)-Au(1)	111.2(3)

Results and Discussions

In both compounds the oxidation state of gold(III) has been reduced to gold(I) and the coordination geometry around the gold(I) atom is linear with central metal atom coordinated with one chlorine atom and one phosphorous donor atom of the mono-dentate tertiary phosphine ligand. The perspective views of the molecular structures of complexes **1** and **2** are shown in Figs. **1** & **2**.

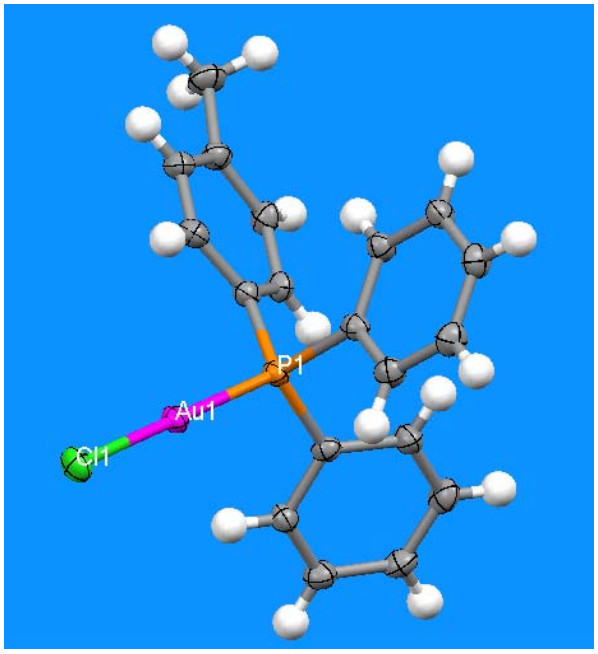

Figure 1. A view of the molecular structure of complex **1**.

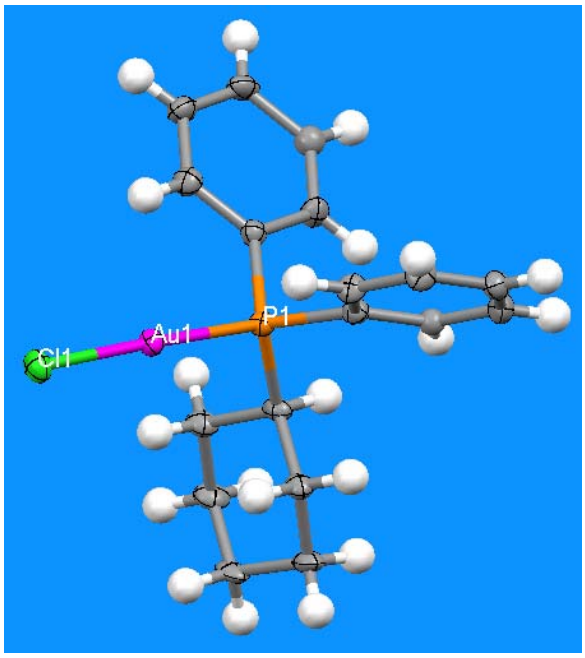

Figure 2. A view of the molecular structure of complex **2**.

In complexes **1** and **2** the Au-Cl bond distances are 2.287(2) and 2.283(2) Å, respectively, and the Au-P bond distances are 2.233(2) & 2.238(2) Å, respectively. These bond distances are similar to those found in [AuCl(PPh_3)], and related gold(I) complexes [21-

23]. The P-Au-Cl bond angles are 176.68(8) & 177.70(9)º for complexes **1** and **2**, respectively. These bond angles values show considerable deviation from ideal linear angle of 180º. The remaining bond lengths and bond angles in complexes **1** and **2** are similar and close to the values reported for related gold(I) complexes [21-23, 24].

Conclusions

While the two compounds have a very similar geometry, because of the different phosphine ligands the compounds crystallize in different crystal systems and the packing in the solid state is quite different.

In compound **1**, which crystallizes in the triclinic space group P-1, molecules related by the centre of symmetry are linked via C-H…Cl hydrogen bonds to form centrosymmetric dimers (Figure **3**).

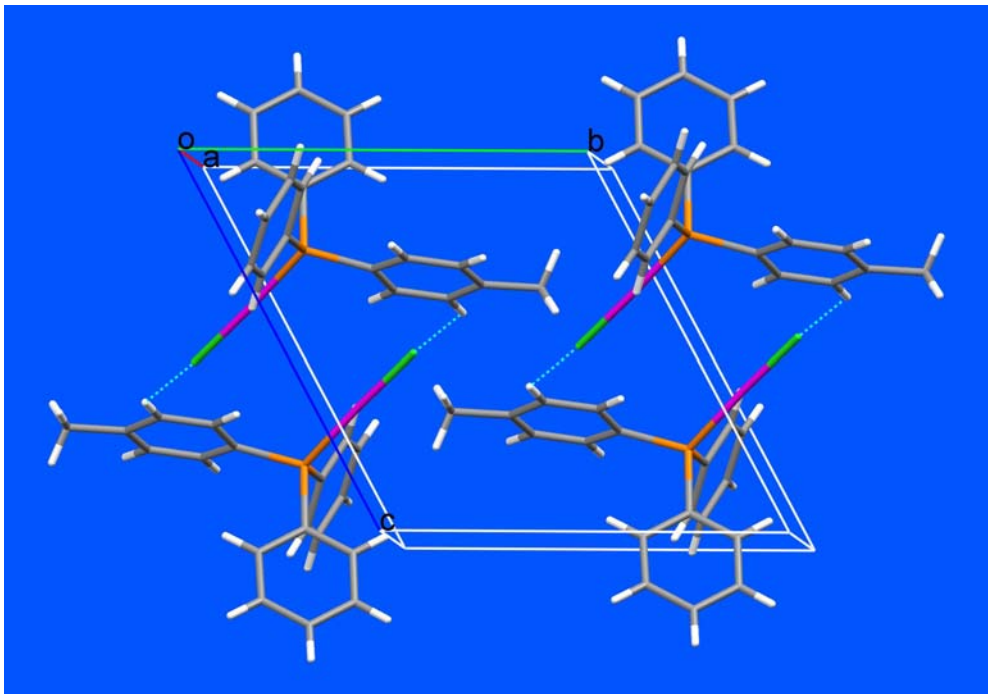

Figure 3. A view along the *a* axis of the crystal packing of compound **1**, showing the formation of centrosymmetric C-H…Cl hydrogen bonded dimers (Hydrogen bonds are shown as blue dotted lines).

In the case of compound **2**, which crystallizes in the monoclinic space group $P2_1/n$, C-H…Cl hydrogen bonding is also important and leads to the formation of a two-dimensional network parallel to the *ac* plane (Figure **4**).

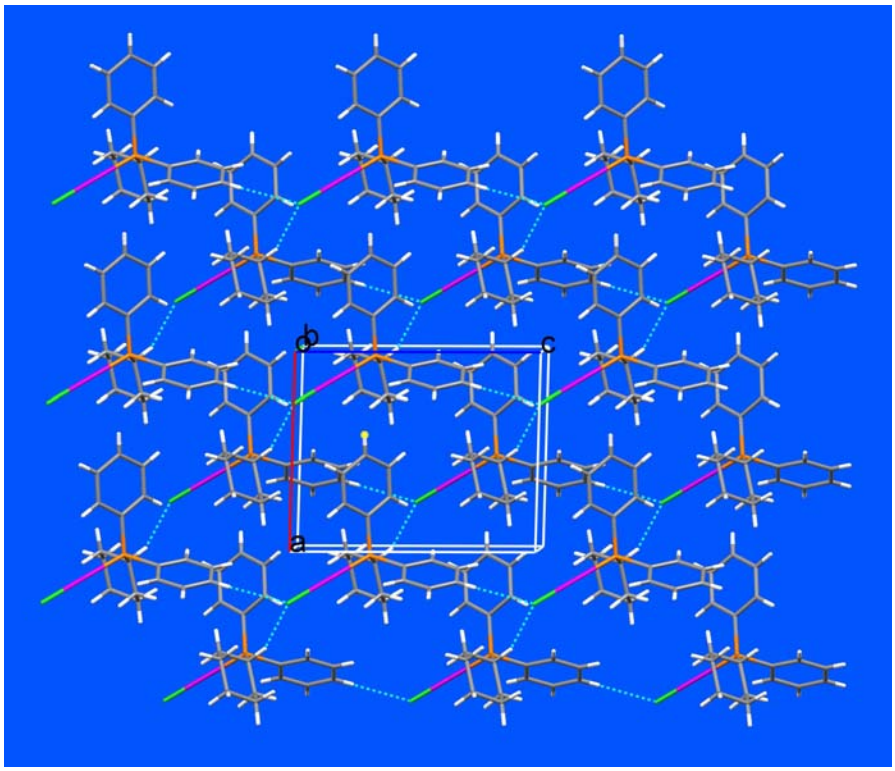

Figure 4. A view along the *b* axis of the crystal packing in compound **2**, showing the formation of the two-dimensional C-H…Cl hydrogen bonded network (Hydrogen bonds are shown as blue dotted lines).

Attempts to use these compounds as precursors for the formation of mixed-ligand gold(I) phosphine complexes has not been successful for the moment.

Reference

[1] W. Huang, H.Qian, Transition Metal Chemistry. 31 (2006) 621.

[2] P. Sharrock, M. Melnik, F. Berlanger-Gariepy, A.L. Beauchamp, Can. J. Chem. 63 (1985) 2564.

[3] T. McCormick, W.-L. Jia, S. Wang, Inorg. Chem. 45 (2006) 147.

[4] D. Ghoshal, T.K. Maji, G. Mostafa, S. Sain, T.-H. Lu, J. Ribas, E. Zangrando and N.R. Chaudhruri, *Dalton Trans.,* 1687 (2004).

[5] K. Sancak, M. Er, Y. ünver, M. Yildrim and I. Degirmencioglu, *Transitional Metal Chem.,* 32, 16 (2007).

[6] R. Rowan, T. Tallon, A.M. Sheahan, R. Curran, M. MacCann, K. Kavanagh, M. Devereux and V. McKee, *Polyhedron,* 25, 1771 (2006).

[7] R. Noghuchi, A. Hara, A. Sugie, K. Nmiya, Inorg. Chem. Commun. 9 (2006) 355.

[8] K. Nmiya, R. Noghuchi, K. Osawa, K. Suda, M. Oda, J. Inorg. Biochem. 78 (2000) 363.

[9] B.P. Howe, Metal Based Drugs. 4 (1997) 273.

[10] V.J. Ctalano, A.O. Etogo, J. Organomet. Chem. 690 (2005) 6041.

[11] O. Crespo, V.V. Brusko, M.C. Giameno, M.L. Tornil, A. Laguna, N.G. Zabirov, Eur. J. Inorg. Chem. (2004) 423.

[12] K. Nmiya, R. Noghuchi, M. Oda, Inorg. Chim. Acta. 298 (2000) 24.

[13] H.-Q. Liu, T.-C. Cheung, S.-M. Peng, C.-M. Che, J. Chem. Soc., Chem. Commun. (1995) 1787.

[14] C.J. O'Connor, E. Sinn, Inorg. Chem. 17 (1978) 2067.

[15] M.A. Cinellu, G. Minghetti, M.V. Pinna, S. Stoccoro, A. Zucca, M. Manassero, M. Sansoni, J. Chem. Soc., Dalton Trans. (1998) 1735.

[16] K. Nmiya, S. Takahashi, R. Noghuchi, J. Chem. Soc., Dalton Trans. (2000) 2091.

[17] R.C. Elder, K. Ludwig, J.N. Cooper, M.K. Eidsness, J. Am. Chem. Soc. 107 (1985) 5024.

[18] P.J. Sadler, R.E. Suc, Met. Based Drugs. 1 (1994) 107.

[19] S.J. Berners-Price, P.J. Sadler, Struct. Bond. 70 (1988) 27.

[20] T.M. Sunon, D.H. Kunishima, G.J. Vibert, A. Lorber, Cancer Res. 41 (1981) 94.

[21] N.C. Baenziger, W.E. Bennett, D.M. Soboroff, Acta Crystallogr. Sect.

32 (B1976) 962.

[22] P. Schwerdtfeger, H.L. Hermann, H. Schmidbaur, Inorg. Chem. 42 (2003) 1334.

[23] F. Bachechi, A. Burini, R. Galassi, B.R. Pietroni, J. Chem. Crystallogr. 34 (2004) 743.

[24] E. Herrero-Go′mez, C. Nieto-Oberhuber, S. Lo′pez, J. Bennet-Buchholz, A.M. Echavarren, Angew. Chem. Int. Ed. 45 (2006) 5455.

Chapter 7:
Conclusions and Perspectives

In this report, various structural and biological aspects of coin metal complexes have been reported. The knowledge of molecular structure is fundamental in order to understand and to take full advantage of the chemical and biological properties of these coin metal complexes. A series of silver(I)-mixed ligand complexes have been tested against bacteria, fungi and a human ovarian cancer cell line. Nine silver(I) compounds and one commercial silver(I)-sulfadiazine (SSD) were tested against *M. Tuberculosis* under the same experimental conditions and their minimal inhibitory concentration (MIC μg/mL) values were determined. For the silver(I)-mixed ligand compounds MIC values range from 7-15 μg/mL and for SSD 7.8 μg/mL. These values show that at least one of the silver(I) compounds has a better inhibition of *M. Tuberculosis* than the commercial drug. This series of silver(I) compounds merits more attention for further anti-tubercular tests against other strains of the bacteria.

As we know, Tuberculosis (TB) is a fatal disease and despite the availability of effective chemotherapies at the present time, TB causes nearly 3 million deaths annually worldwide. The estimated 8.8 million of new cases every year corresponds to 52,000 deaths per week and more than 7,000 deaths each day. It is because many drugs are loosing their effectiveness against Tuberculosis due to the emergence of multi-drug resistance strains of *M. Tuberculosis*. To overcome this problem there is an exponential growing interest of the pharmaceutical industry, academic research and public health care to find new and more effective drugs. So further investigation of this series of silver(I) compounds against more strains of Tuberculosis bacteria in vitro and vivo could make them a useful addition as anti-tuberculosis drugs.

We have also tested the same series of silver(I) compounds against four strains of gram-negative, one strain of gram-positive bacteria and one strain of fungus, and their minimum inhibitory concentration (MIC μg/mL) values were determined. The MIC values for this series of compounds are very encouraging and they show relatively high selectivity for these particular strains of bacteria. Further biological tests of this series of silver(I) compounds against more pathogenic bacterial strains may make them approved pathogenic agents for the future.

Anticancer tests of this series of compounds were carried out on KGN (human ovarian cancer cell line) and their MIC values were determined. All the compounds of this series were found to be active against this cancer cell line; compound **7** being the best with an IC50 (50% inhibitory concentration) value of 70 ng/mL (115nM) in 10 hour duration in vitro. It is well known that cancer is one of the worst killer diseases even in the 21st century and there exists many different forms in all parts of the world. There is a high level of research work going on to develop new anti-cancer drugs, for example about 3,000 cisplatin analogues have been synthesized over the past thirty years but only half a dozen are presently in the clinical use. Cisplatin is one of most expensive and most widely used metallo-drugs for solid tumours. Despite its success, clinical use of cisplatin is limited due to the acquired and intrinsic resistance of the cancer cells to the drug and its high toxicity to some normal cells. In this regard, further anticancer tests against more cancer cell lines for this series of silver compounds are required to take the advantages of our present work. To the best of our knowledge no work has been reported on silver(I) mixed ligand compounds in the domain of anti cancer drugs. Silver(I) is much less toxic than platinum(II) and human body friendly. Initially these compounds could be tested against solid tumours and further investigations in vivo may be useful to introduce much cheaper and useful drugs to help the suffering humanity in third world countries.

In short, this series of compounds has shown their broad spectrum of anticancer, anti-tubercular, antimicrobial and antifungal activities, together with a relatively high selectivity for the inhibition of particular bacterial and fungal strains. In the future, this series of silver(I) compounds may be classified as reference antibiotics since their MIC

values are in the μg/mL range. This series of compounds has shown marked activity against several pathogenic strains of gram-negative and gram-positive bacteria, which is rare for antibiotics.

According to literature reports, the major factor in the spectra of the biological activity of silver-compounds is the nature of the donor atom coordinated to the silver(I) ion and its properties, such as solubility and degree of polymerization. In our recent studies to develop new coin metal drugs; we have synthesized a series of silver(I)-biotin complexes. X-ray diffraction analysis of this series of complexes has revealed that biotin has three possible bonding sites. This property of biotin helped us to synthesize silver(I)-biotin coordination polymers with different (AgS_2O_2 and AgS_2O) metal cores and different geometries around the central metal atom. Biotin (vitamin H) like vitamin B_{12}, has no toxic effects on human body cells. We hope to test these silver(I)-biotin complexes against pathogenic bacterial strains. The antimicrobial studies of this series of compounds may be useful to develop new metallo-drugs with more selective inhibition of particular strains and less toxicity to the normal body cells.

The fascinating properties of silver(I) coordination polymers in all fields of life encouraged us to design and synthesize silver(I)-coordination polymers having silver(I)-N, silver(I)-O bonds, as this type of silver(I)-compounds show potential antimicrobial activity against many micro-organisms. The effective antimicrobial activities of silver(I)-O/N bonding complexes are due to the weak silver(I)-O/N bonds; they are easily replaced by biological molecules especially those having a thiol group. As this series of silver(I)-coordination polymers possess silver(I)-O/N bonds. Antimicrobial tests of this series of compounds could be useful for developing new drugs in the field of pharmacy in future.

A series of one-, and two-dimensional silver(I)-phosphine mixed ligand complexes of 4,4′-bipyridine were also prepared and structurally characterized. Silver(I)-tertiary phosphine with 4,4′-bipy results in the formation of only one-dimensional (undulating step-like and zigzag) polymeric chain structures and in one a two-dimensional polymer network was obtained. Again the presence of Ag-N/O and Ag-P coordination bonds in

this series of coordination polymers could make them useful antibacterial agents for the future.

A series of silver(I)-, copper(I)-, and gold(I)-phosphine complexes were also synthesized and structurally characterized. The main purpose of these syntheses was to explore their structural properties and to use them as precursors for the synthesis of mixed ligand coin metal complexes with versatile metal-cores and geometries around the metal centres. These coin metal-phosphine complexes are easy to crystallize and can be used easily for the synthesis of mixed ligand complexes with different chemical compositions and geometries around the metal centre. We were successful in synthesizing silver(I)-phosphine mixed ligand complexes (Chapters **2** & **5**) and to some extent with copper(I)-phosphine complexes. Our efforts to crystallize gold(I)-phosphine mixed ligand complexes were unfortunately unsuccessful.

Appendix: Supplementary Information for Chapter 2

Part 1

Test antibacterium and antifungal

Activité antibactérienne contre des gram- et gram+
Activité antifongique contre le *fusarium oxysporum f.sp. Albedinis.*

Introduction :

Les composés synthétisés ont été évalués *in vitro* pour leur activité antifongique contre un champignon filamenteux (*Fusarium oxysporum f.sp. albedinis* ***FOX***) et leur activité antibactérienne contre quatre souches gram négatif (*Pseudomonas aeroge* ***PAG***, *Proteus vulgaris* ***PRV,*** *Escherichia coli ATCC* ***ECC*** *et Klebsiella pneumoniae* ***KLP***) et une souche gram positif (*Staphyloccocus aureus* ***STA)***.

Tableau 1. Structure des composés testés

produit	MM g/mol	Structure Nom
L1	**91.13** CN_3SH_5	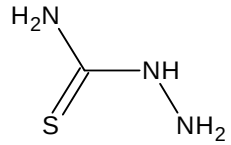 hydrazinecarbothioamide

L3	**119.21** $C_3H_5NS_2$	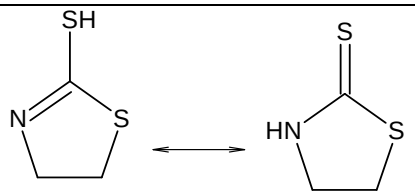 4,5-dihydro-1,3-thiazole-2-thiol
Complex		
A1 **or** **Hel-01**	**614.41** $C_{20}H_{25}N_7O_3S_2P_1Ag_1$	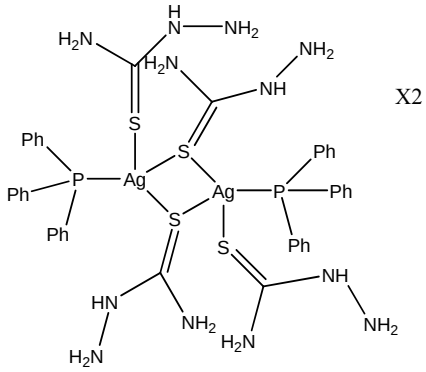 X2 X = NO_3^-
A2 **or** **Hel-02**	**606.45** $C_{24}H_{25}O_3N_3S_2P_1Ag_1$	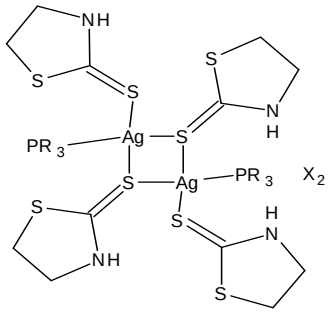 X_2 X = NO_3^- & R = Ph

A3 **or** **Hel-03**	**624.59** $C_{24}H_{43}O_3N_3S_2P_1Ag_1$	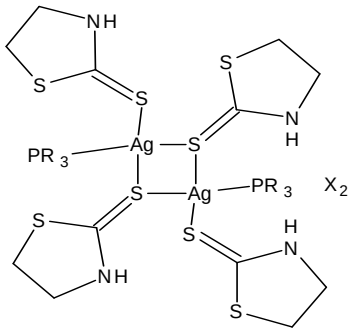 X = NO_3^- & R = Cy
A4 **or** **Hel-04**	**715.53** $C_{20}H_{43}N_6S_2P_2F_6Ag_1$	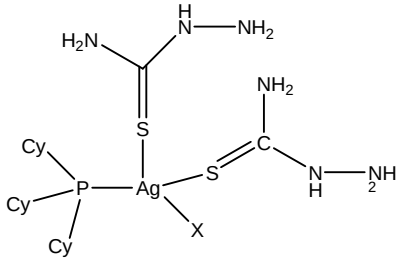 X = PF_6^-
A5 **or** **Hel-05**	**849.83** $C_{40}H_{63}N_4O_3S_1P_2Ag_1$	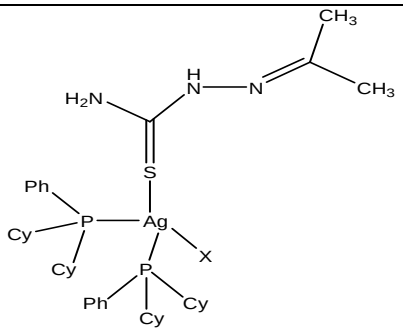 X = NO_3^-
A6 **or** **Hel-06**	**620.40** $C_{21}H_{38}N_1S_1P_2F_6Ag_1$	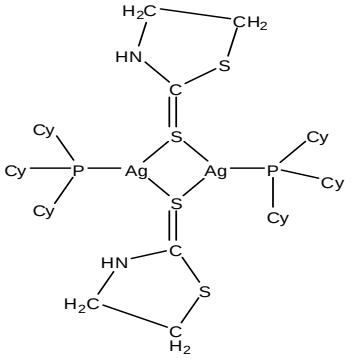 X_2 X = PF6$^-$ & R = Cy

A7 **or** **Hel-07**	**606.85** $C_{22}H_{30}N_3S_1O_4C_{l1}P_1Ag_1$	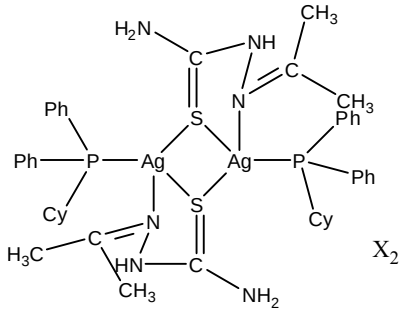 X_2 $X = ClO_4^-$
A8 **Or** **Hel-08**	**871.093** $C_{42}H_{43}N_3S_1P_2Br_1Ag_1$	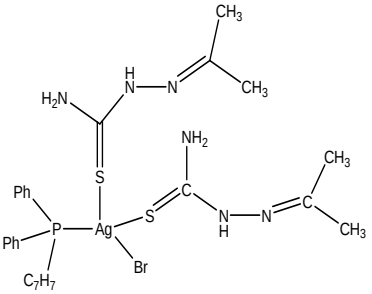
A9 **or** **Hel-09**	**563.35** $C_{22}H_{25}N_4O_3S_1P_1Ag_1$	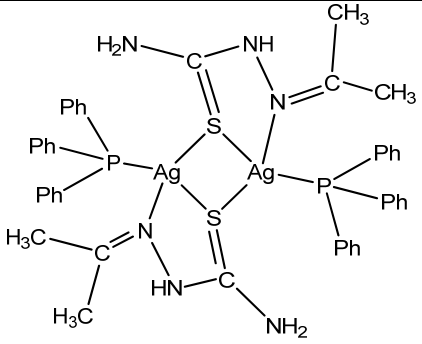 $X = NO_3^-$
A11 **or** **Hel-11**	**837.83** $C_{40}H_{51}N_4O_3S_1P_2Ag_1$	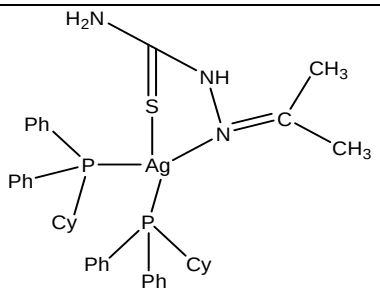 $X = NO_3^-$

1. Tests antibactériens

A partir des composés sous forme de poudre, des solutions de stockage ont été préparées dans le Dimethyle Sulfoxyde (DMSO) avec une concentration d'environ 6 g/L et 12 g/L. Pour éviter l'interférence du solvant, les solutions mères ont été diluées au préalable dans de l'eau distillée stérile, de façon à garder un pourcentage du solvant ne dépassant pas les 0,5 % dans les solutions finales.

Test de diffusion sur milieu solide

Un test préliminaire de criblage est indispensable pour déterminer la sensibilité des produits avant de passer à la détermination de leurs CMI. Le criblage a été réalisé par la méthode de diffusion sur gélose, effectuée en milieu solide de Mueller-Hinton (BIOKAR DIAGNOSTICS-Beauvais-France ; pH : 7,4 ± 0,2).

Les disques stériles en papier Whatman 3 Chr, d'épaisseur moyenne 0,36 mm et de diamètre 5 mm, sont imprégnés de 10 µL de composé et laissés sécher à l'air libre. Ces disques sont déposés par la suite à la surface d'un milieu gélosé Mueller-Hinton, préalablement inoculées avec une culture pure de la souche à étudier.

Ce test est réalisé sur ***Proteus vulgaris (PRV),*** une souche bactérienne à gram négatif qui a montré une bonne activité bactérienne lors de la culture d'activation. Après incubation pendant 20 heures à 37°C, les boites de gélose sont examinées pour vérifier la présence de zones d'inhibition de croissance. Un résultat est considéré positif si les zones d'inhibition de croissance, produite par la souche bactérienne, sont d'au moins 2 mm de diamètre.

Tableau 2. Résultats du test de Diffusion sur milieu solide (24 h Incubation à 37°C)*

Composés	Diamètre d'inhibition de croissance en mm	Sensibilité
Hel-L1	1	-
A1 or Hel-01	4,5	++++
A2 or Hel-02	1,5	-
A3 or Hel-03	1,5	-
A4 or Hel-04	4	+++
A5 or Hel-05	ND	ND
A6 or Hel-06	2	+
A7 or Hel-07	3	++
A8 Or Hel-08	1,5	-
A9 or Hel-09	4,5	++++
A11 or Hel-11	ND	ND
L3	1	-

(++++) : Zone d'inhibition de croissance ≥ 4,5 mm ;
(+++) : Zone d'inhibition de croissance 3,5 ~ 4 mm ;
(++) : Zone d'inhibition de croissance 2,5 ~ 3 mm ;
(+) : zone d'inhibition de croissance 2 mm ;
(-) : zone d'inhibition de croissance ≤ 2 mm.

Test de CMI sur milieu liquide :

La CMI a été déterminée par la méthode de microdilution, effectuée en milieu liquide de Mueller-Hinton (BIOKAR DIAGNOSTICS-Beauvais-France ; pH : 7,4 ± 0,2). Dans le BMH distribué dans les cupules d'une plaque de microtitration stérile, les composés en solution sont incorporés à des concentrations croissantes, selon une progression géométrique de raison 2 (0,97 à 125 µg/mL). Chaque dilution a été placée en contact d'un inoculum bactérien en phase de croissance exponentielle avec une

concentration d'environ de 10^4 à 10^5 µg/mL, obtenu à partir d'une culture en bouillon de 20 heures à 37 ºC et diluée au 1/10. Une culture témoin sans composé a été également réalisée. L'incubation est réalisée à 37 ºC pendant 18 à 24 heures en atmosphère ordinaire. La CMI est définie comme la plus faible concentration de composé ne permettant pas de culture visible.

Tableau 3 : Valeurs des CMI des composés contre les souches gram – ***(PRV, PAG, ECC, KLP)*** et gram + ***(STA).***

Souches	**Gram -**				**Gram +**
	PRV	***PAG***	***ECC***	***KLP***	***STA***
Composés	**CMI µg/mL**				
Hel-L1	500	125	125	125	31,3
A1 (Hel-01)	125	31,3	15,6	**31,3**	15,6
A2 (Hel-02)	15,6	125	62,5	125	31,3
A3 (Hel-03)	31,3	31,3	15,6	**31,3**	**7,8**
A4 (Hel-04)	62,5	125	62,5	125	**7,8**
A5 (Hel-05)	> 125	**15,6**	**3,9**	62,5	31,2
A6 (Hel-06)	**7,8**	**15,6**	**3,9**	62,5	15,6
A7 (Hel-07)	15,6	125	125	125	**7,8**
A8 (Hel-08)	> 125	125	62,5	> 125	31,2
A9 (Hel-09)	15,6	62,5	31,3	62,5	**7,8**
A11 (Hel-11)	> 125	> 125	> 125	> 125	15,6
L3	> 125	> 125	125	> 125	125

PRV : *Proteus vulgaris*; ***PAG*** *: Pseudomonas aeroge;* ***ECC :*** *Escherichia coli ATCC.*

KLP : *Klebsiella pneumoniae*; ***STA :*** *Staphyloccocus aureus.*

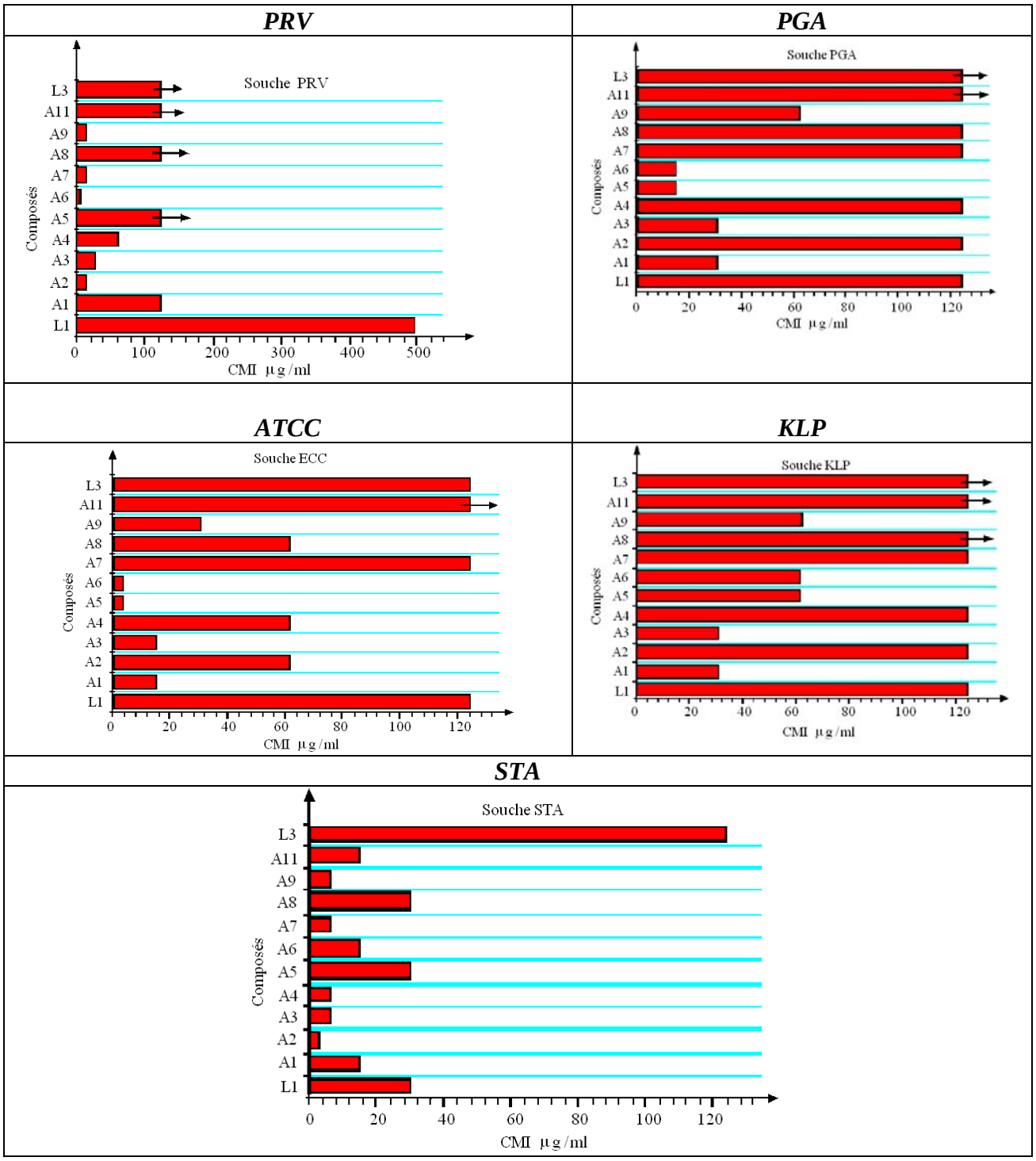

Remarques

On remarque que les meilleurs acitivités sont trouvés contre les souches PRV et STA. En general, les ligands libres sont moins actifs que ceux compléxés, sauf pour (L3 PRV et L1, STA).

Pour chaque souche nous avons une selectivité marquée pour un composé bien défini. Pour la souche PRV c'est (A6, A2, A3,A7 et A9); pour PGA c'est (A1, A3, A5 et A6); pour ATTC c'est (A5, A6); pour KLP c'est (A1, A3); pour STA (A2, A3, A4, A7, A9).

2. Tests antifongiques

Pour les tests antifongiques, la CMI a été déterminée par la méthode de diffusion sur milieu solide. Le milieu utilisé pour cette étude est le PDA : Potato Dextrose Agar (BIOKAR DIAGNOSTICS-Beauvais-France) spécifique pour culture du champignon. Les solutions de stockage des produits à tester ont été distribuées - à différents volumes - directement dans 10 mL de milieu de culture maintenu à une température de 45 ºC, après agitation rigoureuse (afin d'assurer l'homogénéité de la dilution finale) chaque tube est versé dans une boite de pétri (de diamètre 50 mm et une hauteur de 20mm) préalablement stérilisée. Après solidification de la gélose, les boites sont ensemencées par des pastilles du champignon obtenues à partir d'une culture de six jours à 27ºC. Une culture témoin sans composé a été également réalisée. L'incubation est réalisée à 27 ºC pendant environ une semaine en atmosphère ordinaire. La CMI est déterminée après calcul des pourcentages d'inhibition de l'activité du champignon.

Tableau 4 : Valeurs des CMI des composés contre *le fusarium oxysporum f.sp. Albedinis*

Composés	*CMI en µg/mL*
Hel-L1	85
A1 (Hel-01)	64
A2 (Hel-02)	48
A3 (Hel-03)	24
A4 (Hel-04)	24
A5 (Hel-05)	**CMI < 26**
A6 (Hel-06)	**26**
A7 (Hel-07)	40
A8 (Hel-08)	64
A9 (Hel-09)	35
A11 (Hel-11)	43
L3	CMI > 85

FOX : *Fusarium oxysporum f.sp. albedinis.*

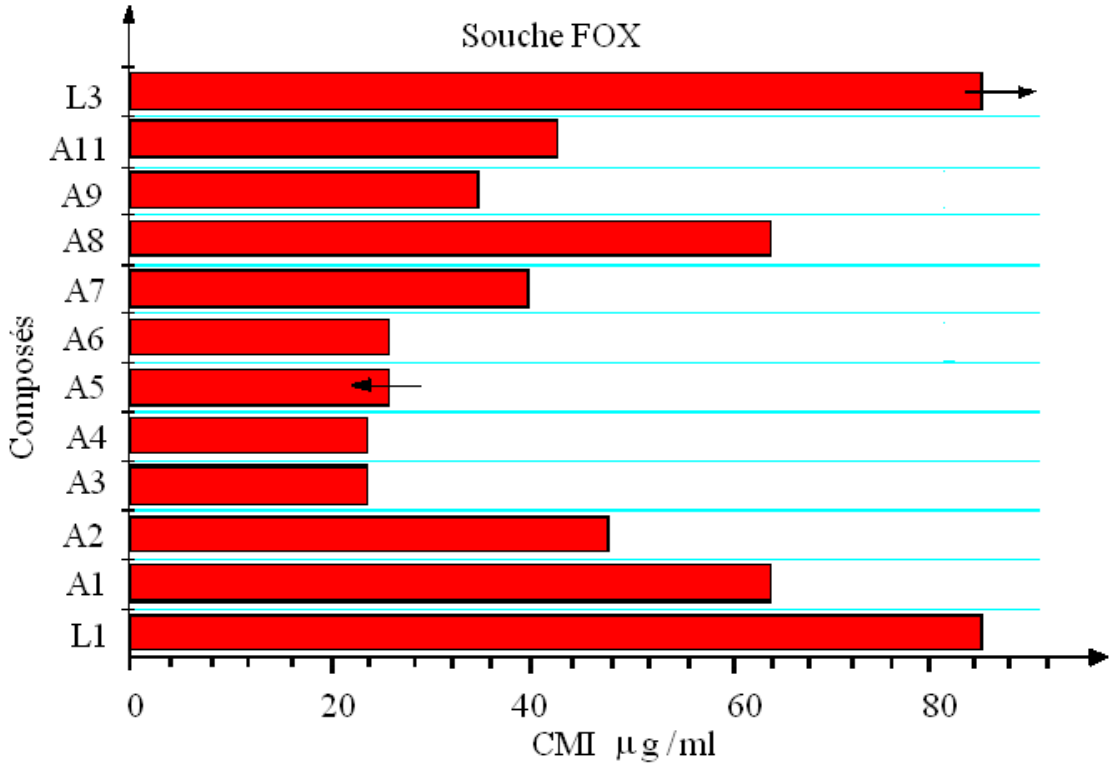

Ici les meilleures activités sont soulignées pour quatre composés A3, A4, A5 et A6; les ligands libres ne sont pas actifs.

Note: Compound 1-9= A1-A9 and compound 10= A11.

Part 2

Anti-cancer tests

Effet des différents produits sur la prolifération des cellules KGN

partie réalisée dans le Laboratoire de Biochimie (EA 2608-*USC INRA Université de Caen, France*.
En collaboration avec l'équipe du Pr P.J. Bonnamy
Et les Pr A.Hakkou et M. Bouakka du Laboratoire de Biochimie de la faculté des sciences d'Oujda

Produits obtenus par le Département de Chimie, Université Mohamed I^{er}, Faculté des sciences Oujda MAROC

Les produits (A1,A2,A3,A4,A5,A7,A8,A9,A11, L1 et L2),.sur des cultures KGN, une lignée cellulaire

Matériels :

- Cellules KGN
- Boites de cultures
- filtres à seringues de 0,2 μM
- pipettes stériles
- Salle équipé pour la culture cellulaire (Hot, étuve, …….)

Produits :

- Milieux de culture : Ham F12 et DEM (H/D)
- Antibiotiques et antifongiques
- Enzymes utilisés pour obtention des cellules
- Tampon PBS
- Produits A1à A11 Oujda

- Crystal-violet : 0,1% dans du PBS
- Acide acétique et autres
- lecture des densités Optique sur micro-plaques 96 puits METERTESH 960

I) Appareils de Protocole expérimental.

1. Culture des cellules

Après décongélation d'un tube de KGN à un million de cellules par ml, les cellules sont mises en culture dans une boîte de 75 puit. Une semaine après la boîte est à confluence.

Une trypsination de la boîte (cf Protocole). Après une culture de quatre jours les cellules sont

Les boîtes de 48 puits sont ensemencées à raison de 10 000 cellules/puit sous un volume de 500 µl. Les cellules sont mises en culture pendant 4 jours, placées dans une étuve 37°C et 5% de CO_2 avant la confluence.

Changement du milieu et incubation en présence de différentes concentrations des produits étudiés (A1 à A11, L1 et L3).

2. Préparation des solutions de traitements :

Les produits sont solubilisés dans de DMSO 10 mg/ml, puis une dilution de 10 fois est réalisée dans le milieu de culture pour chaque produit (1 mg/ml). Autres dilution sont réalisées dans le milieu de culture.

Le traitement et fait de sorte à ajouter 100 µl de la solution contenant le produit pour faire des concentrations finales choisis au départ. La durée d'incubation en présence de différents produits est de 48 heures.

4- Traitement au Crystal Violet

Le Crystal violet est un produit qui se fixe au niveau des cellules, permet d'évaluer la prolifération cellulaire par lecture de la densité Optique à 600 nm. (voir Protocole)

Protocole de traitement au Crystal-Violet

Après 48 heures d'incubation, le milieu de culture est éliminé. 200 µl de la solution de Crystal-violet préparé dans du PBS sont ajoutés dans chaque puit. La coloration des cellules se fait à température ambiante pendant 30 minutes.
Le réactif est éliminé, puis les cellules sont rincées par du PBS 600 µl deux fois 7 minutes. Le tapis cellulaire est solubilisé par 200 µl d'acide acétique 20%. Après 10 minutes d'agitation, 100 µl de cette sont placés dans des plaques de lecture 96 puits / plaque. La Densité Optique est proportionnelle à la concentration du Crystal-Violet, qui lui est en fonction de la quantité des cellules présentes dans les puits de culture.

Différentes concentrations de ces produits sont nécessaires pour déterminer la concentration minimale qui inhibe de 50% la prolifération cellulaire.

II) Résultats

Nous avons traité 6 séries de 3 puits par différentes concentrations de DMSO qui est la même pour chaque concentration de l'échantillon, en finale le % de DMSO dans le milieu de culture est de 0,5% à 0,03%. Nous n'avons pas observé de changement de morphologie ni d'inhibition de la prolifération des KGN suite aux traitements par ce solvant puissant des produits.

Par contre le traitement des cellules par les produits à forte concentrations allant de50 à 12 µg/ml provoque une destruction et la mort des cellules après 5 heures d'incubation, observation sous microscope inverse.

Pour des concentrations inférieures, une inhibition de prolifération est doses dépendantes. (voir Fig 1,2 ../). La CMI est différente pour chaque produit (voir résultats).

A des faibles concentrations, de 3 à 1 µg/ml, tous les produits restent sans effets. (voir courbes)

Par contre les produits L1 et L3 à des concentrations allant de 50 µg/ml à 1 µg/ml n'ont aucun effet sur la prolifération des KGN

Tableaux I : Densité Optique à 600 nm

B est la densité Optique de obtenue en dehors des cellules.

Traitement des KGN plaques de 48 puits par différents produits pendant 48 heures le 20.04.2007

DO x 1000 à 600nm

% DMSO				DO-B			Moyen	Ecart
0,5	1156	1357	1420	1121	1322	1385	**1276**	138
0,25	1459	1435	1297	1424	1400	1262	**1362**	87
0,125	1335	1527	1573	1300	1492	1538	**1443**	126
0,06	1557	1406	1444	1522	1371	1409	**1434**	79
0,03	1282	1415	1395	1247	1380	1360	**1329**	72
0,015	1509	1469	1478	1474	1434	1443	**1450**	21
A1 en ug/ml								
50	69	81	83	34	46	48	**43**	8
25	87	74	74	52	39	39	**43**	8
12,5	73	84	90	38	49	55	**47**	9
6,25	425	429	485	390	394	450	**411**	34
3,125	941	1123	1174	906	1088	1139	**1044**	122
1,562	1495	1557	1450	1460	1522	1415	**1466**	54
A2 en ug/ml								
50	74	78	80	39	43	45	**42**	3
25	74	99	84	39	64	49	**51**	13
12,5	125	101	88	90	66	53	**70**	19
6,25	1100	831	852	1065	796	817	**893**	150
3,125	1266	1469	1516	1231	1434	1481	**1382**	133
1,562	1512	1569	1469	1477	1534	1434	**1482**	50
A3 en ug/ml								
50	81	83	95	46	48	60	**51**	8
25	77	72	88	42	37	53	**44**	8
12,5	105	114	88	70	79	53	**67**	13
6,25	229	243	263	194	208	228	**210**	17
3,125	572	600	570	537	565	535	**546**	17
1,562	1094	1134	1063	1059	1099	1028	**1062**	36
A4 en ug/ml								
50	68	70	72	33	35	37	**35**	2
25	72	79	80	37	44	45	**42**	4

12,5	72	77	84	37	42	49	**43**	6
6,25	610	603	670	575	568	635	**593**	37
3,125	1310	143	1498	1275	108	1463	**949**	734
1,562	1721	1721	1624	1686	1686	1589	**1654**	56
A5 en ug/ml								
50	72	80	70	37	45	35	**39**	5
25	73	84	76	38	49	41	**43**	6
12,5	149	159	213	114	124	178	**139**	34
6,25	1423	1502	1240	1388	1467	1205	**1353**	134
3,125	1362	1519	1573	1327	1484	1538	**1450**	110
1,562	1704	1673	1598	1669	1638	1563	**1623**	55
A6 en ug/ml								
50	76	78	75	41	43	40	**41**	2
25	74	71	75	39	36	40	**38**	2
12,5	82	76	79	47	41	44	**44**	3
6,25	93	85	88	58	50	53	**54**	4
3,125	425	419	427	390	384	392	**389**	4
1,562	792	915	756	757	880	721	**786**	83
A7 en ug/ml								
50	78	76	75	43	41	40	**41**	2
25	70	77	77	35	42	42	**40**	4
12,5	79	99	87	44	64	52	**53**	10
6,25	382	414	420	347	379	385	**370**	20
3,125	957	1340	1364	922	1305	1329	**1185**	228
1,562	1450	1523	1357	1415	1488	1322	**1408**	83
A8 en ug/ml								
50	83	77	93	48	42	58	**49**	8
25	89	90	87	54	55	52	**54**	2
12,5	144	170	203	109	135	168	**137**	30
6,25	1085	1093	1032	1050	1058	997	**1035**	33
3,125	1237	1322	1299	1202	1287	1264	**1251**	44
1,562	1330	1398	1268	1295	1363	1233	**1297**	65
A9 en ug/ml								
50	87	88	85	52	53	50	**52**	2
25	94	101	94	59	66	59	**61**	4
12,5	94	101	114	59	66	79	**68**	10

6,25	921	979	857	886	944	822	**884**	61
3,125	1299	1491	1541	1264	1456	1506	**1409**	128
1,562	1561	1602	1462	1526	1567	1427	**1507**	72

A11 en ug/ml

50	96	94	95	61	59	60	**60**	1
25	84	78	84	49	43	49	**47**	3
12,5	88	98	97	53	63	62	**59**	6
6,25	355	337	324	320	302	289	**304**	16
3,125	529	784	1021	494	749	986	**743**	246
1,562	1495	1456	1176	1460	1421	1141	**1341**	174

L1 en ug/ml

50	1086	1224	1229	1051	1189	1194	**1145**	81
25	1360	1438	1417	1325	1403	1382	**1370**	40
12,5	1284	1395	1435	1249	1360	1400	**1336**	78
6,25	1462	1456	1367	1427	1421	1332	**1393**	53
3,125	1115	1342	1282	1080	1307	1247	**1211**	118
1,562	1398	1301	1140	1363	1266	1105	**1245**	130

L3 en ug/ml

50	1220	1280	1323	1185	1245	1288	**1239**	52
25	1344	1412	1288	1309	1377	1253	**1313**	62
12,5	1262	1417	1465	1227	1382	1430	**1346**	106
6,25	1512	1535	1398	1477	1500	1363	**1447**	73
3,125	1387	1593	1634	1352	1558	1599	**1503**	132
1,562	1599	1545	1438	1564	1510	1403	**1492**	82

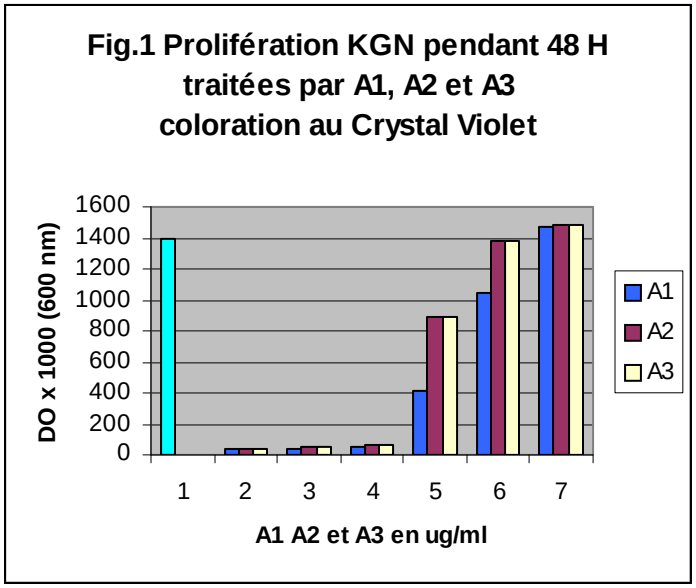
Fig.1 Prolifération KGN pendant 48 H
traitées par A1, A2 et A3
coloration au Crystal Violet
DO x 1000 (600 nm)
1600
1400
1200
1000
800
600
400
200
0
1
2
3
4
5
6
7
A1 A2 et A3 en ug/ml
A1
A2
A3

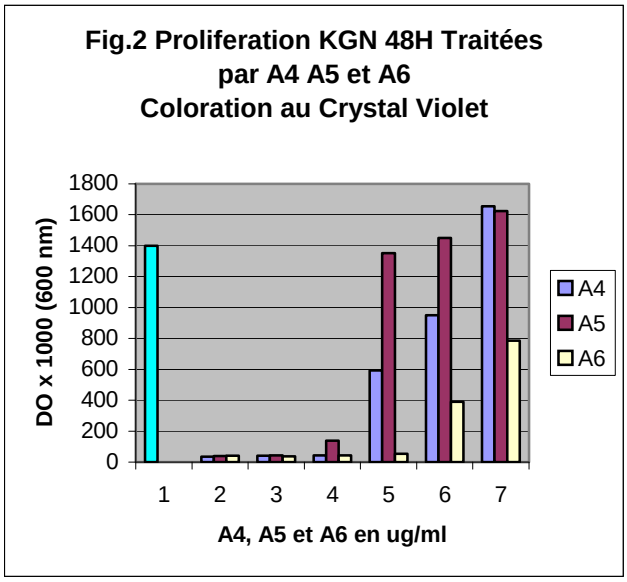
Fig.2 Proliferation KGN 48H Traitées
par A4 A5 et A6
Coloration au Crystal Violet
DO x 1000 (600 nm)
1800
1600
1400
1200
1000
800
600
400
200
0
1
2
3
4
5
6
7
A4, A5 et A6 en ug/ml
A4
A5
A6

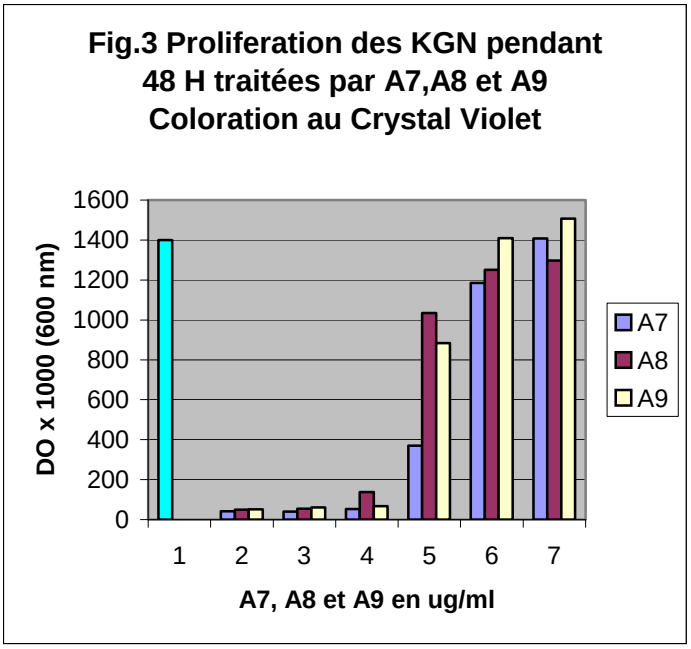
Fig.3 Proliferation des KGN pendant
48 H traitées par A7,A8 et A9
Coloration au Crystal Violet
DO x 1000 (600 nm)
1600
1400
1200
1000
800
600
400
200
0
1
2
3
4
5
6
7
A7, A8 et A9 en ug/ml
A7
A8
A9

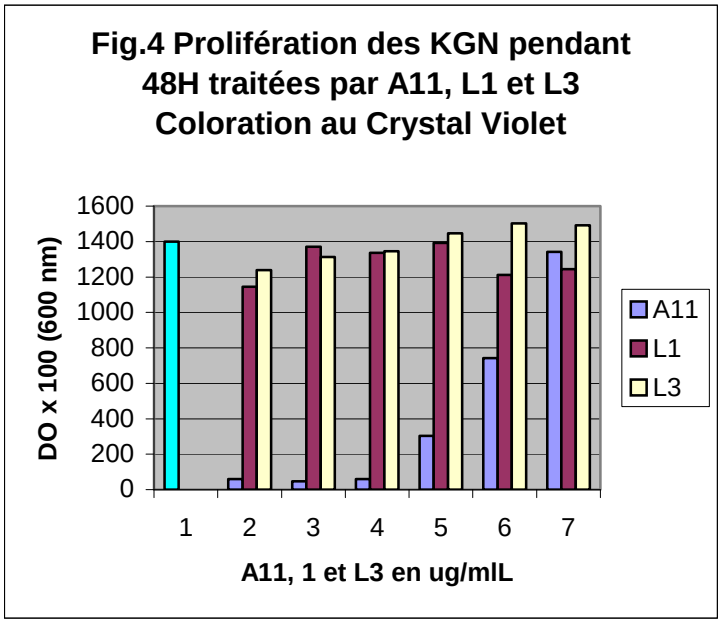
Fig.4 Prolifération des KGN pendant
48H traitées par A11, L1 et L3
Coloration au Crystal Violet
DO x 100 (600 nm)
1600
1400
1200
1000
800
600
400
200
0
1
2
3
4
5
6
7
A11, 1 et L3 en ug/mlL
A11
L1
L3

Résultats des tests de culture cellulaire

produit	Structure Nom	Formule poids moléculaire	CMI µg / mL
Hel-L1	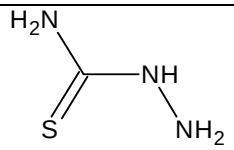 hydrazinecarbothioamide	CN_3SH_5 91.13	**> 50**
L3	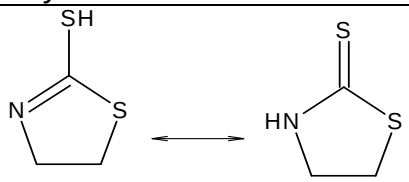 4,5-dihydro-1,3-thiazole-2-thiol	$C_3H_5NS_2$ 119.21	**> 50**
Complex			
A1 **or** **Hel-01**	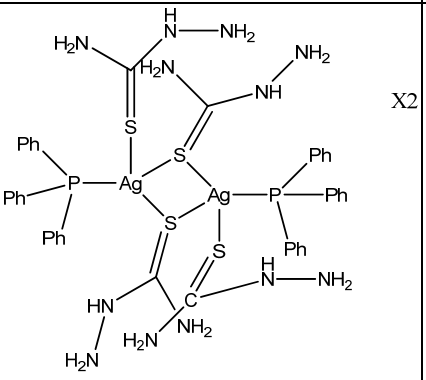 X2 $X = NO_3^-$	$C_{20}H_{25}N_7O_3S_2P_1Ag_1$ 614.41	**4,9**

A2 **or** **Hel-02**	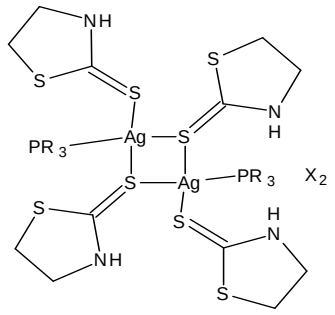 X = NO_3^- & R = Ph	$C_{24}H_{25}O_3N_3S_2P_1Ag_1$ 606.45	**7,6**
A3 **or** **Hel-03**	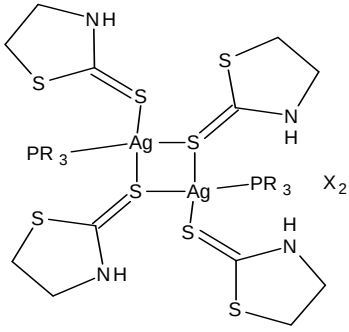 X = NO_3^- & R = Cy	$C_{24}H_{43}O_3N_3S_2P_1Ag_1$ 624.59	**2,7**
A4 **or** **Hel-04**	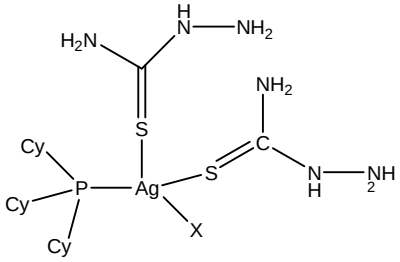 X = PF_6^-	$C_{20}H_{43}N_6S_2P_2F_6Ag_1$ 715.53	**4,3**
A5 **or** **Hel-05**	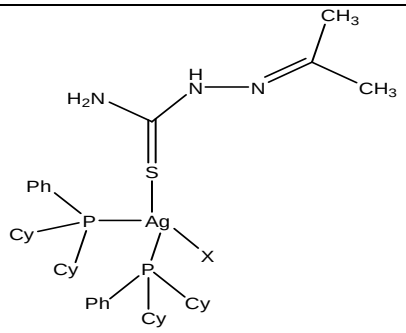 X = NO_3^-	$C_{40}H_{63}N_4O_3S_1P_2Ag_1$ 849.83	**9,5**

A6 **or** **Hel-06**	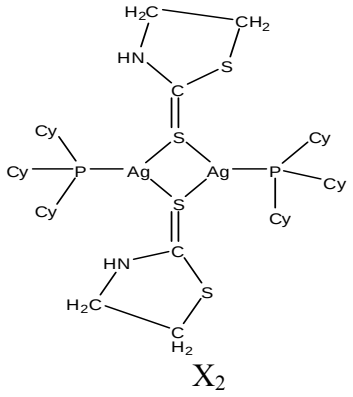 X_2 X = $PF6^-$ & R = Cy	$C_{21}H_{38}N_1S_1P_2F_6Ag_1$ 620.40	**1,8**
A7 **or** **Hel-07**	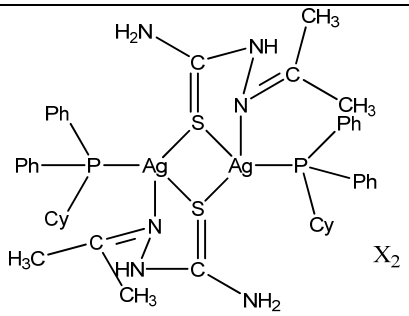 X_2 X = ClO_4^-	$C_{22}H_{30}N_3S_1O_4C_{l1}P_1Ag_1$ 606.85	**5**
A8 **Or** **Hel-08**	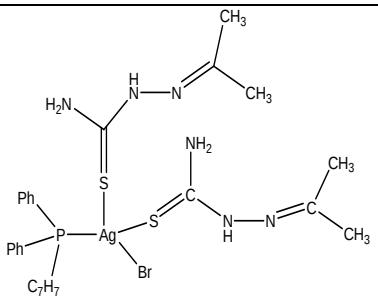	$C_{42}H_{43}N_3S_1P_2Br_1Ag_1$ 871.093	**8,5**
A9 **or** **Hel-09**	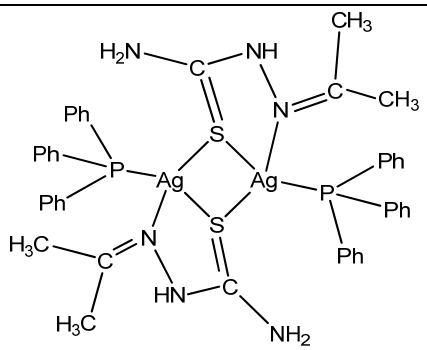 X = NO_3^-	$C_{22}H_{25}N_4O_3S_1P_1Ag_1$ 563.35	**7,5**

A11 **or** **Hel-11**	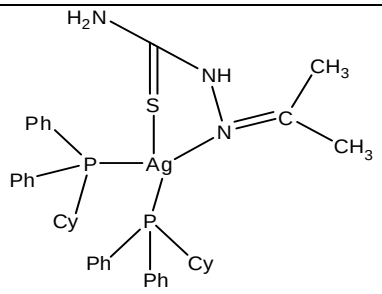 X = NO_3^-	$C_{40}H_{51}N_4O_3S_1P_2Ag_1$ 837.83	**3,6**

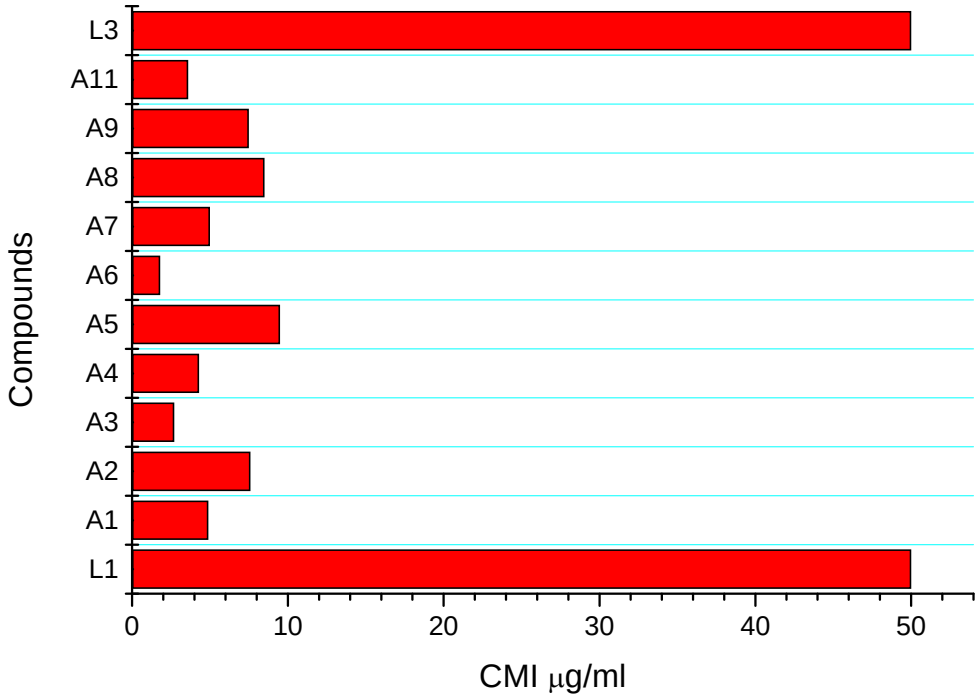

Results of the treatment of KGN cell lines with different concentrations of the free ligand L3, and of silver complexes A1, A2 and A5.

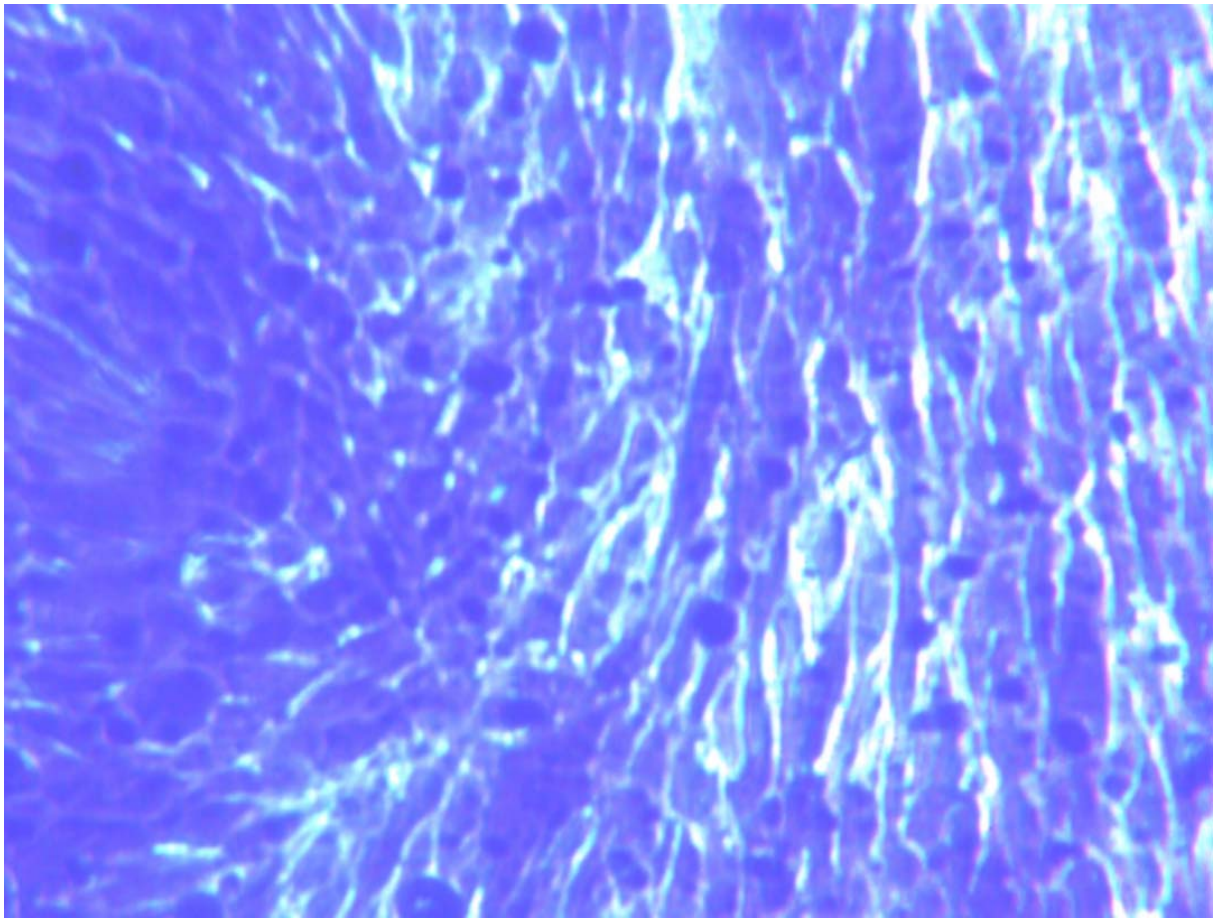

Treatment of KGN with 3 µg/mL of L3

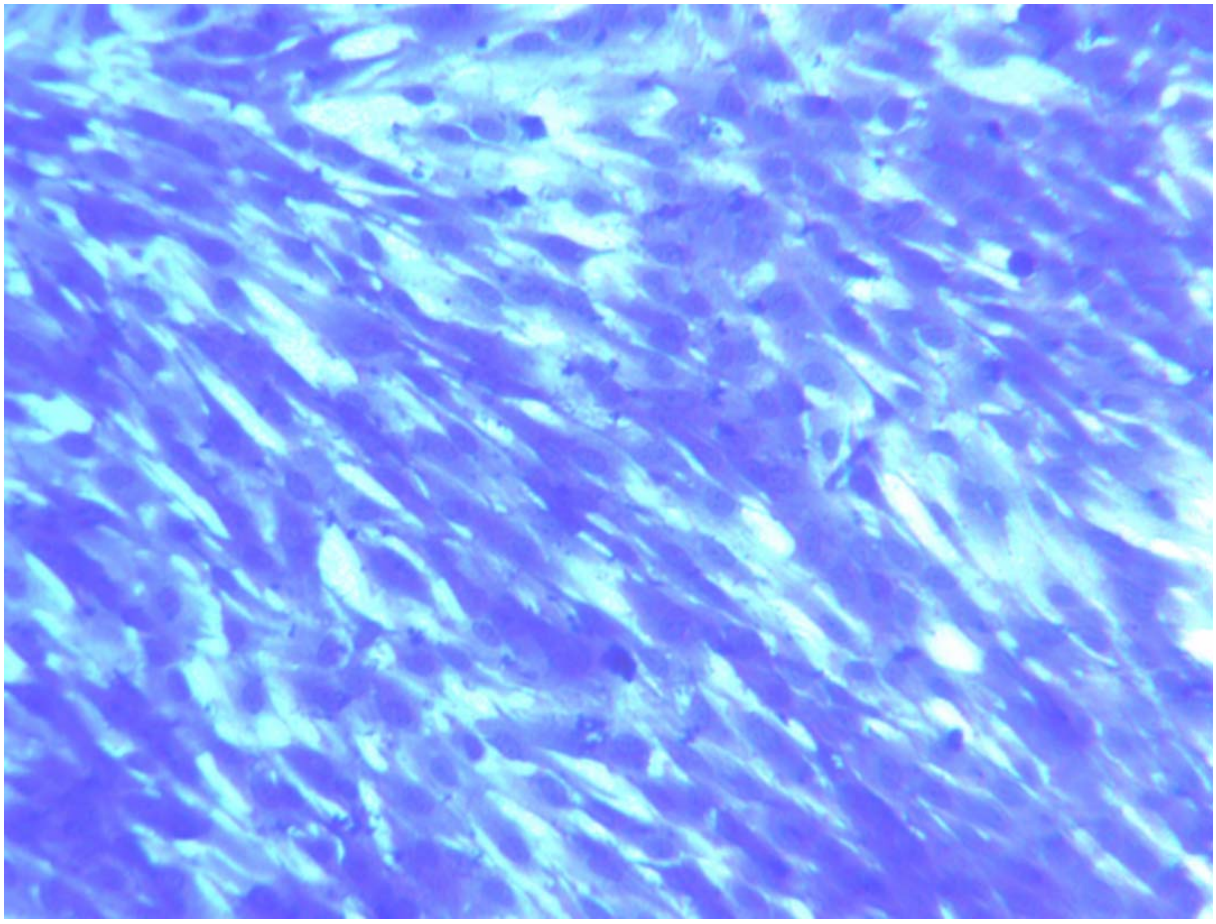

Treatment of KGN with 25 µg/mL of L3

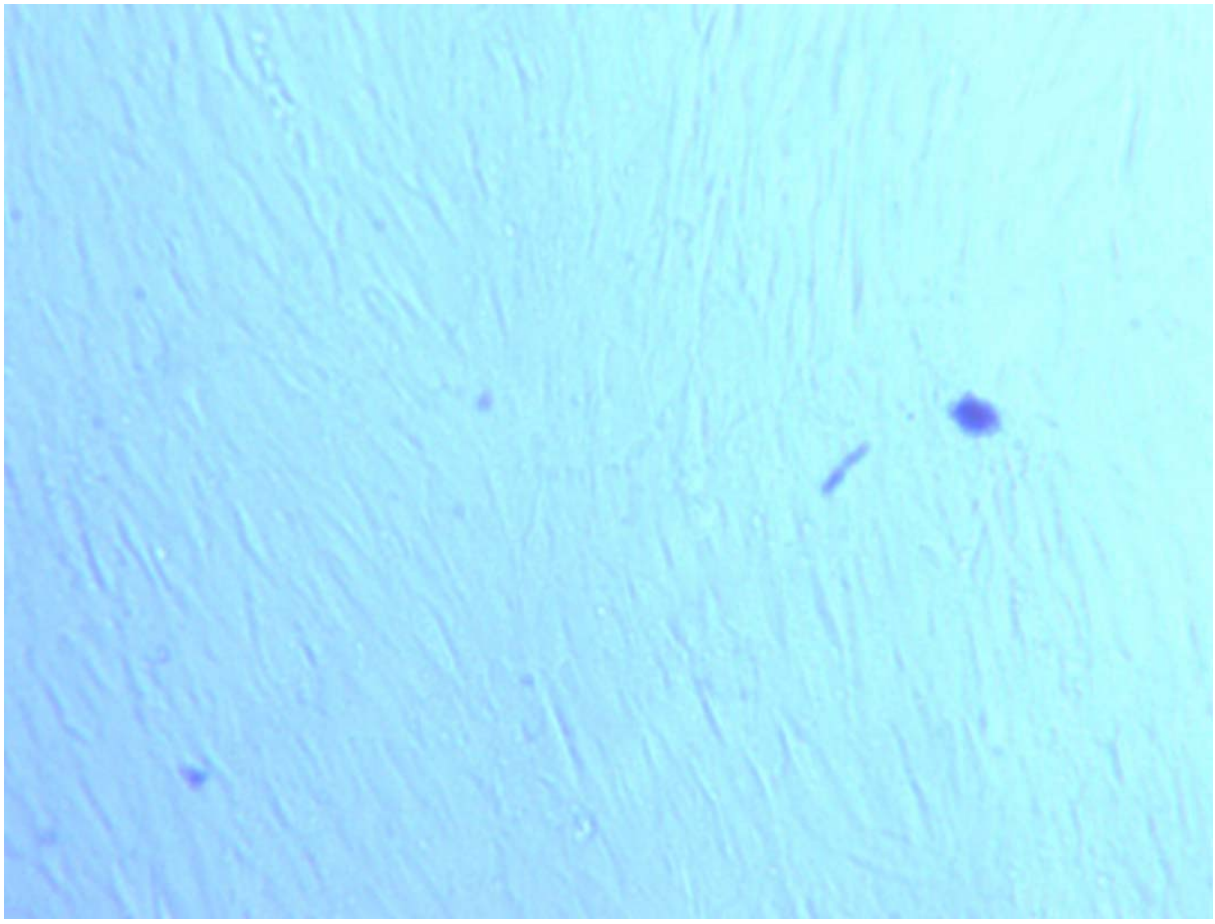

Treatment of KGN with 3 μg/mL of A1

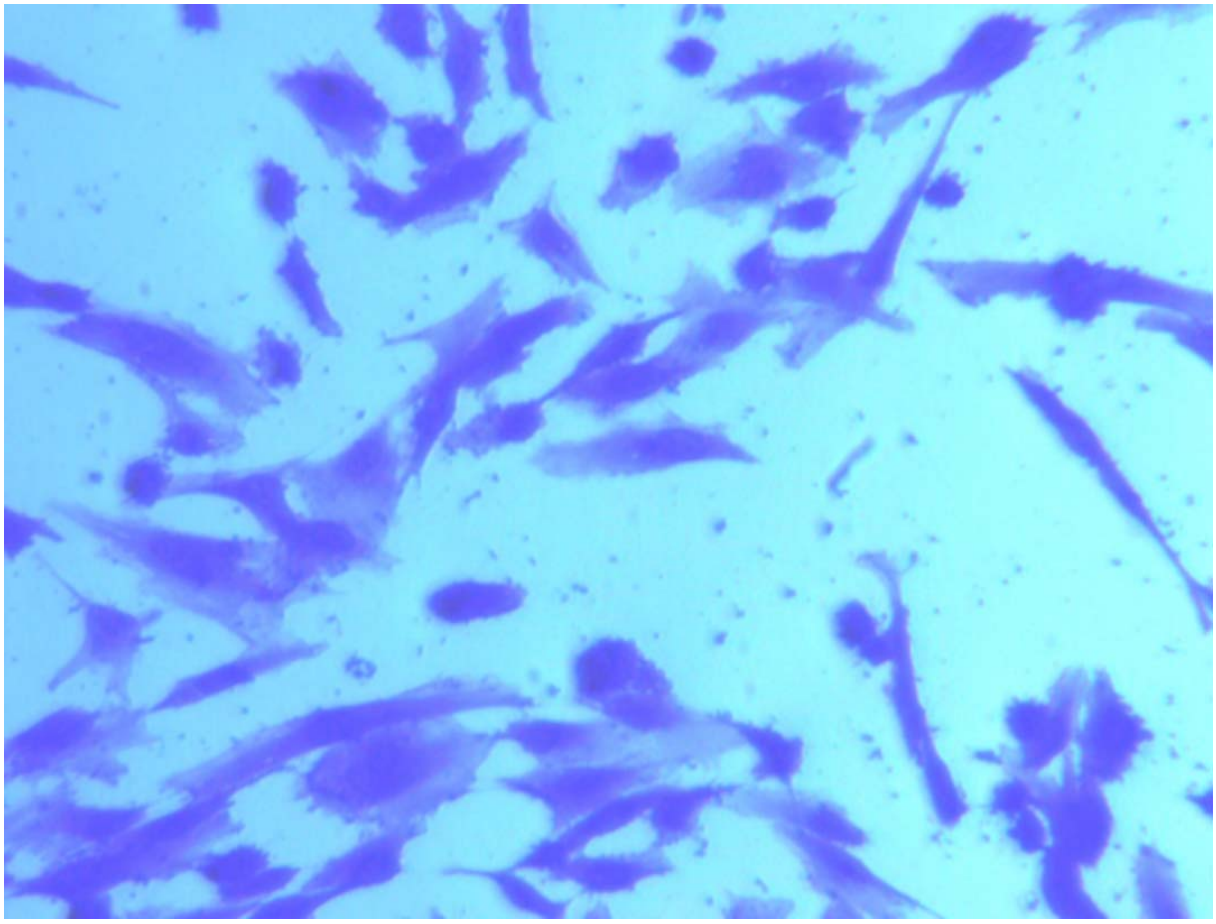

Treatment of KGN with 6 μg/mL of A1

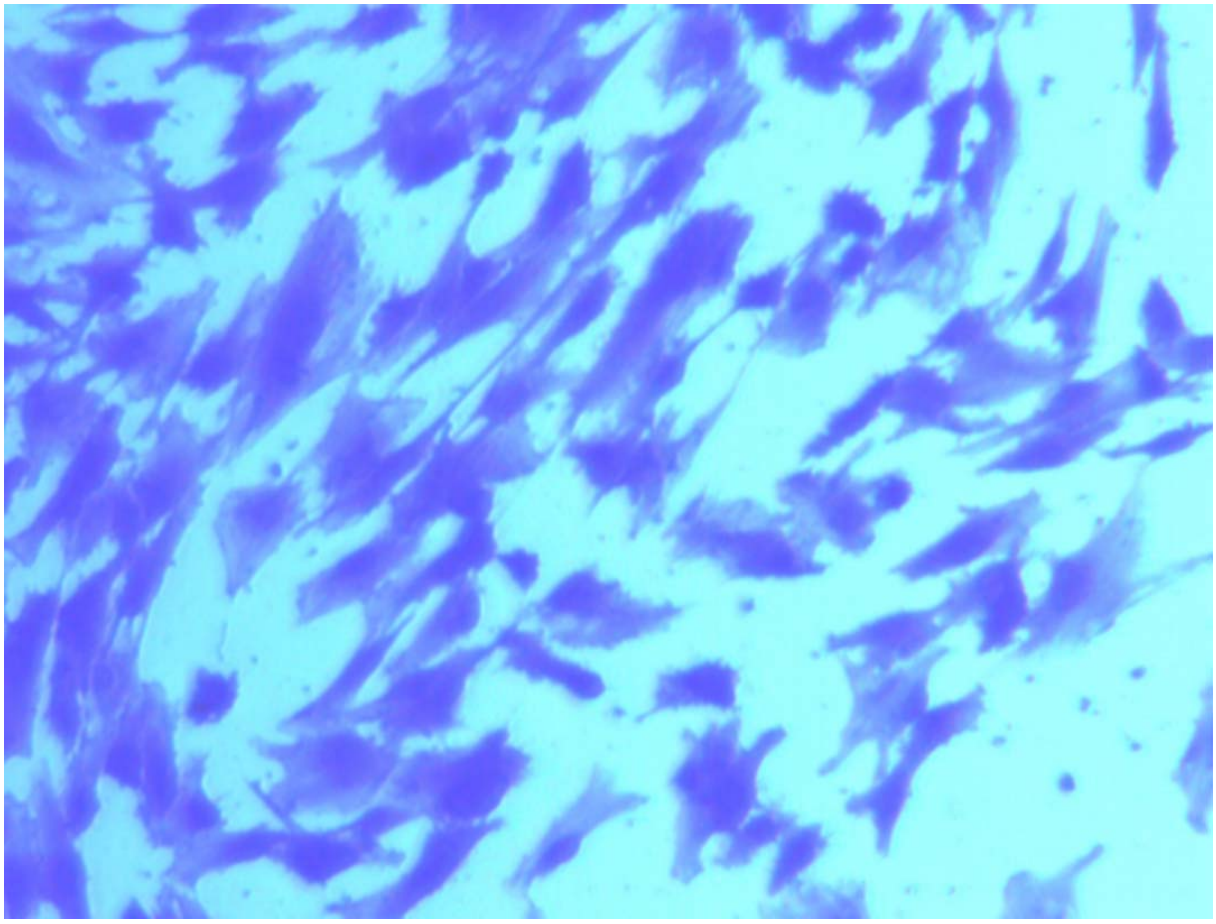

Treatment of KGN with 3 μg/mL of A2

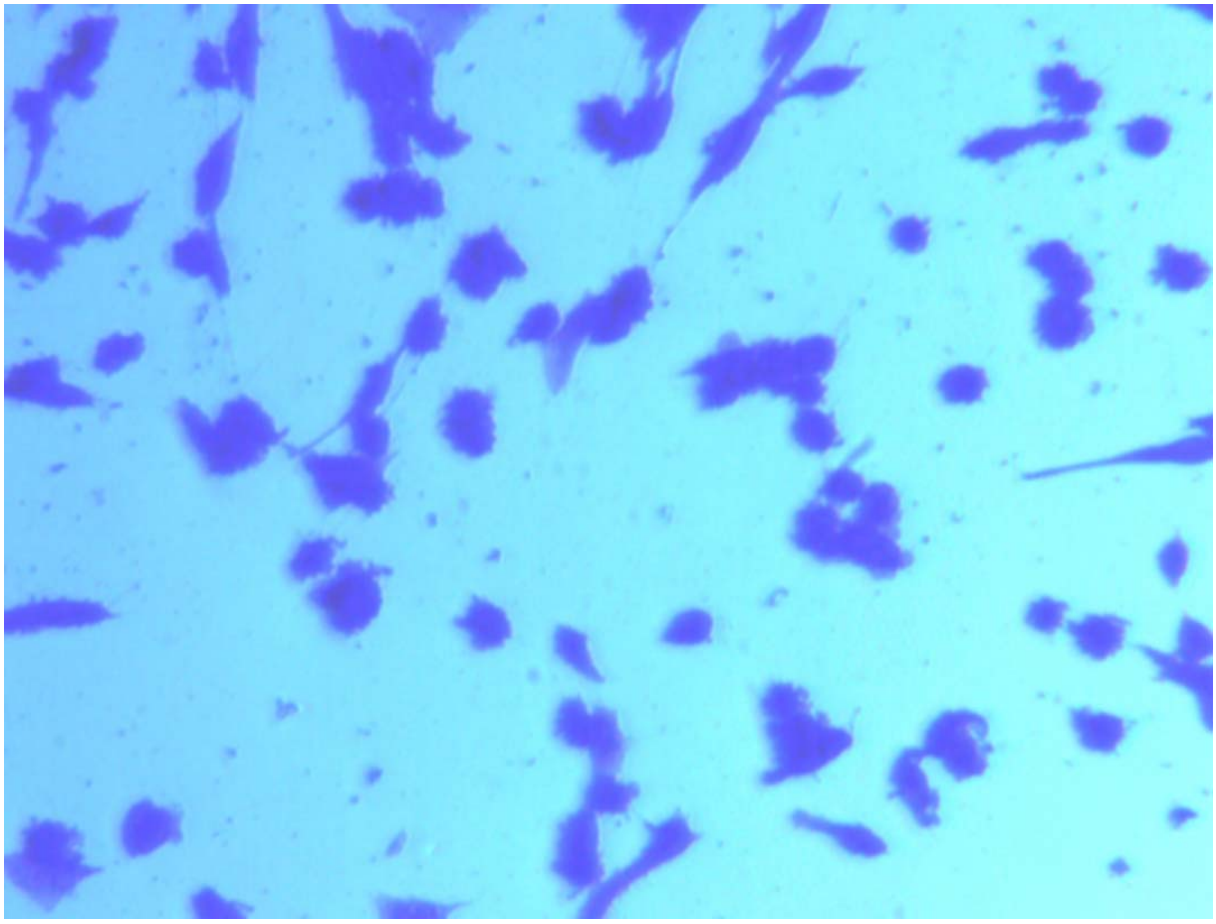

Treatment of KGN with 6 μg/mL of A2

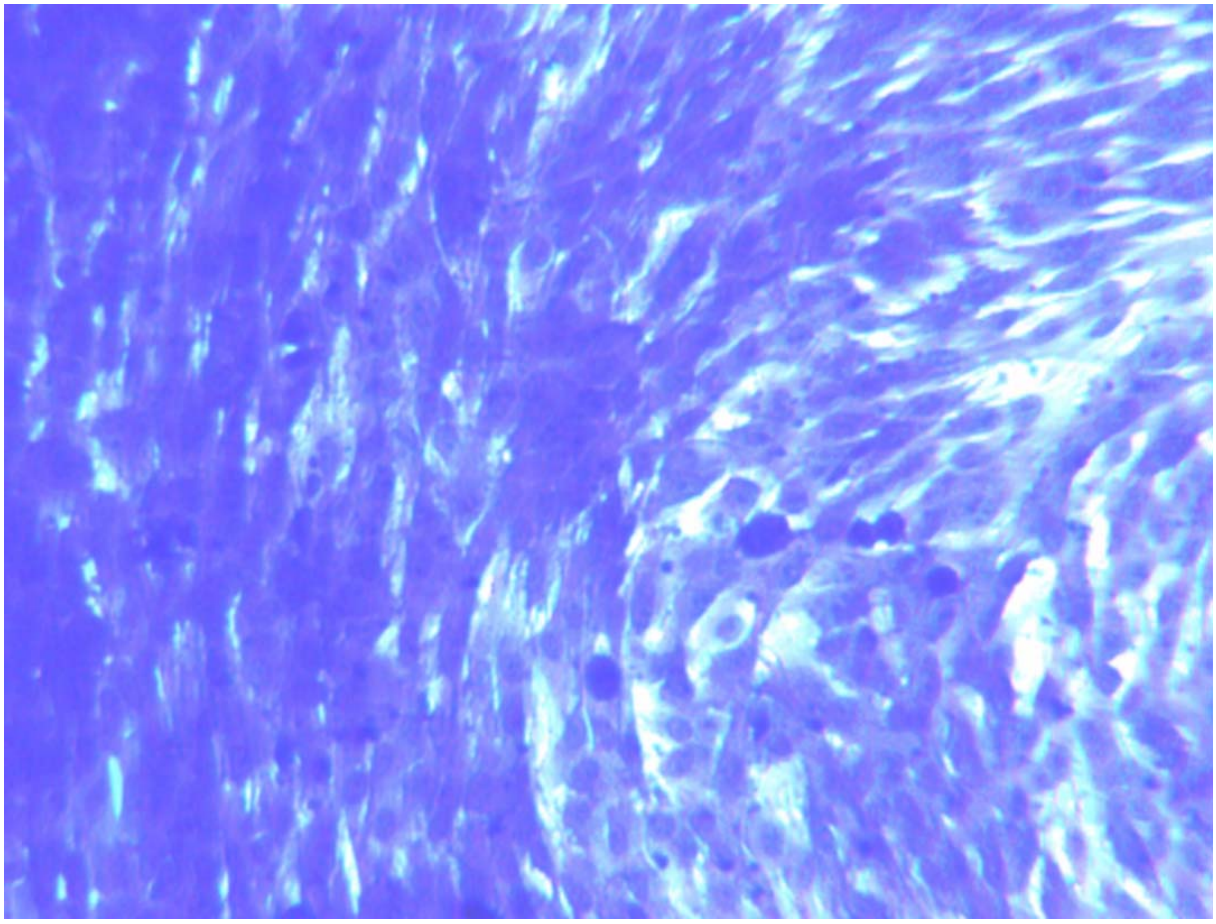

Treatment of KGN with 1.5 μg/mL of A5

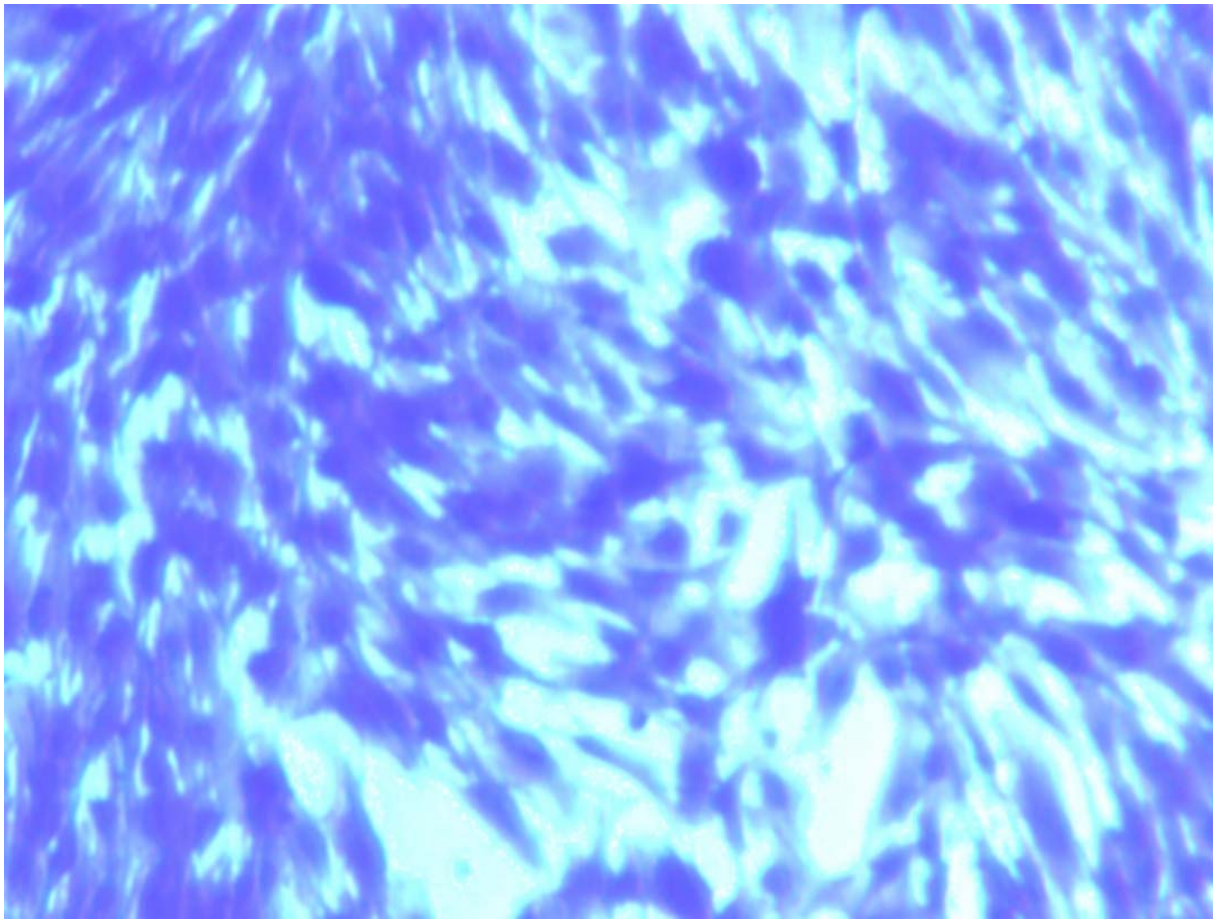

Treatment of KGN with 3 μg/mL of A5

Muhammad ALTAF

Faculty of Sciences, Institute of Physics
Department of Physical Chemistry
University of Neuchâtel
http://www2.unine.ch/lcp
E-mail: Muhammad.altaf@unine.ch

PhD Thesis: **Silver(I) and Other Coin Metal Complexes of N, O, S and P Containing Ligands: Structures and Biological Properties**

MPhil Thesis: **Synthesis and Kinetic Studies of Organo-Tin(IV) Complexes of Non-Steroidal Anti-Inflammatory Drugs (NSAIDS)**

MSc Thesis **Trace metal analysis in Himalayan rock samples by Atomic Absorption spectroscopy and UV-Visible spectroscopy**

Education

Since March 2005 PhD student in the group of Prof. Helen Stoeckli-Evans, University of Neuchâtel, Switzerland. Thesis subject: "Synthesis and Crystal Engineering of Coin Metal Complexes with Potential and Biological Applications"

2004-2005 Senior Research Assistant in the group of Prof. Saqib Ali, Department of Chemistry, Quaid-i-Azam University Islamabad, Pakistan.

2002-2004 M.Phil in Inorganic/Analytical Chemistry in the group of Prof. Saqib Ali, Department of Chemistry, Quaid-i-Azam University Islamabad, Pakistan.

2000-2002 Master of Science in Inorganic/Analytical Chemistry, Department of Chemistry, Quaid-i-Azam University Islamabad, Pakistan.

1998-2000 Junior Research Fellowship, Institute of Research and Development for Pesticide and veterinary Medicine Punjab, Pakistan.

1995-1997 Bachelor of Science (Medical Group), Bahauddin Zakariya University, Multan, Pakistan.

Research interests

- Synthesis, crystal engineering, and single crystal X-ray structure analysis
- Silver(I) and Gold(I) complexes of N, O, P, and S containing ligands: Anti-cancer, anti-bacterial, and Anti-fungal properties.

- Synthesis of multi-dimensional polymeric metal-organic frameworks with biological and potential applications.

Publications:

9. Poly[bis(μ2-cyanido)-κ2C:N;κ2N:C-(μ2-N,N,N',N'-tetramethylthiourea-κ2S:S)disilver(I)], M. Hanif, S. Ahmad, M. Altaf, H. Stoeckli-Evans, Acta Crystallogr. **2007**, E63 (10), m2594
8. Bis(cyanido-κC)(ethane-1,2-diamine-κ2N,N')silver(II), S. Ahmad, M. Monim-ul-Mehboob, M. Hanif, M. Altaf, H. Stoeckli-Evans, Acta Crystallogr. **2007**, E63 (10), m2548
7. Synthesis and Crystal Structure of a Cyano-Bridged Bimetallic Nickel(II)-Silver(I) Complex, [Ni(dmen)2{Ag(CN)2}2] · 0.5H2O, S. Ahmad, M. Monim-ul-Mehboob, M. Altaf, H. Stoeckli Evans, R. Mehmood, J. Chem. Crystallogr. **2007**, 37 (10), 685-689
6. (E)-3-(1, 3-Benzodioxol-4-yl)-2-(4-bromophenyl)acrylic acid, M. Hussain, A. Siddique, S. Ali, M. Altaf, H. Stoeckli-Evans, Acta Cryst. **2007**, E63 (1), o1-o3
5. 6-Nitro-1, 3-benzodioxole-4-carbaldehyde, M. Hussain, S. Ali, M. Altaf, H. Stoeckli-Evans, Acta Cryst. **2006**, E62 (11), o5323-o5325
4. Pyridin-4-ylmethanediol: the hydrated form of isonicotinaldehyde, D. G. Mantero, M. Altaf, A. Neels, H. Stoeckli-Evans, Acta Cryst. **2006**, E62 (11), o5204-o5206
3. (E)-3-(6-Nitrobenzo[d][1,3]dioxol-5-yl)-2-phenylacrylic acid, M. Hussain, M. Hanif, S. Ali, M. Altaf, H. Stoeckli-Evans, Acta Cryst. **2006**, E62 (11), o5020-o5021
2. A Kinetic Study of the Cleavage of Tin-Carbon Bond in Triphenyltin(IV)[2-(2,6-dichlorophenyl)aminophenyl acetate] by Ethyl Iodide, S. Ali, S. Ahmad, M. Altaf and S. Shahzadi. Jour.Chem.Soc.Pak. Vol.28, No. 4, **2006**
1. Kinetics and mechanism of the substitution reactions of triphenyltin(IV)[2-(2,6-dichlorophenyl)aminophenyl acetate] with iodine, S. Ali, S. Ahmad, M. Altaf, S. Shahzadi, A. Badshah, Inorg. React. Mech. **2006**, 6 (1), 49-58

ADDITIONAL PROFESSIONAL ACTIVITIES:

♣ Member of Swiss Chemical Society (SCS) and Active Member of Scientific Communities.
♣ Regular Visitor of Swiss Chemical Society (SCS) Spring and Autumn Meetings.
♣ **Poster presentation** in the inorganic chemistry section at the Fall Meeting of the Swiss Chemical Society, September **2006** at ETH (Zurich, Switzerland), title: Synthesis and single crystal analysis of "potentially" biologically important coinage metal complexes. Muhammad Altaf and Helen Stoeckli-Evans.
♣ **Summer School** on Fundamental of Kinetics and Thermodynamics in (Metallo)Supramolecular Assemblies. September 10-14, **2006**. Eurotel Victoria Villars, Villars-sur-Ollon, Switzerland.
♣ **Poster presentation** in the inorganic chemistry section at the Fall Meeting of the Swiss Chemical Society, September **2005** at EPFL (Lausanne, Switzerland), title: Metal halide complexes of thiolate ligands: Anions dependence. Muhammad Altaf and Helen Stoeckli-Evans.

♣ **Summer School** on Advance Materials: Magnetism, Light Emission and Charge Transport. September 18-22, **2005**. Eurotel Victoria Villars, Villars-sur-Ollon, Switzerland.

♣ Participated in 7 days workshop on **combinatorial Chemistry** held from 7th –13th of May **2004**.

Resource person was Prof. Dr. J. Rademann University of Berlin, Germany.

♣ Participated in **4th International &14thNational Chemistry conference** held from 15th –17th of May **2004** in Lahore, Pakistan.

HOBBIES:

Social work, Reading books, Football, Volleyball, Table tennis, Swimming, and Cricket

RESEARCH AWARD:

- Awarded **Doctoral Fellowship of the Swiss National Science Foundation** (August 2005-2008)
- Awarded **Land owner Organization Scholarship for Overseas Studies** (2005)
- Awarded **University Grant Commission (UGC)** Islamabad-Pakistan **r**esearch fellowship during
  M. Phil. studies at Quaid-i-Azam University Islamabad-Pakistan (2002-2004).
- Merit scholarship of Quaid-i -Azam Islamabad, Pakistan during M.Phil studies (2002-2004).

REFERENCE

1. **Prof. Helen Stoeckli-Evans**

Contact **office B19**
Phone **+41(0)32 718 24 26**
Fax **+41(0)32 718 25 11**
E-mail **Helen.Stoeckli-Evans@unine.ch**
University of Neuchatel,
Faculty of Sciences, Neuchâtel.
Switzerland

A series of zinc(II), cadmiun(II) and mercury(II) thiolate complexes, with general fomula MX_2L_2, where X = Cl, Br, I, and L = thiolate ligand, have been synthesized and charaterized crystallographically. The ligands include Tetramethyl-thiourea(L1), Thiazolidine-2-thione (L2),, 2-Amino-3-mercapto-3-methyl-butyric acid (or DL-penicillamine) (L3), and Thionicotinamide (L4). The structures of the ligands and their coordination modes are compared.

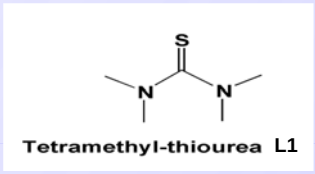

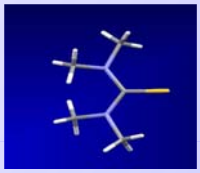

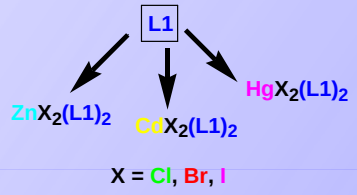

Zn

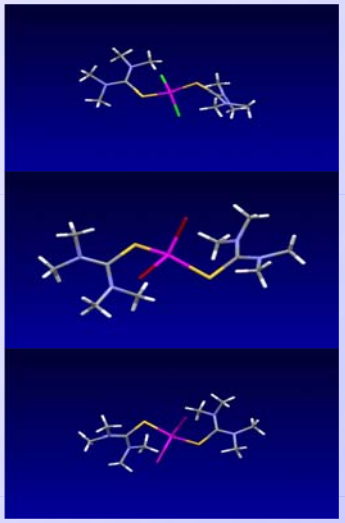

Cd

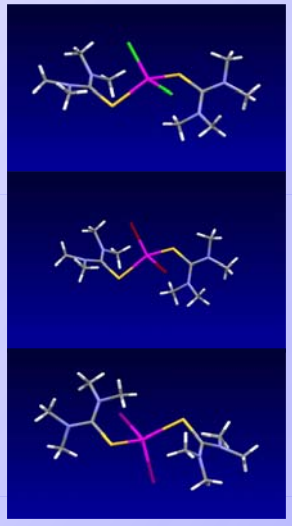

Hg

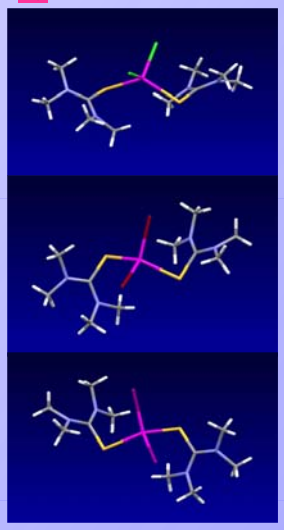

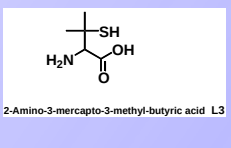

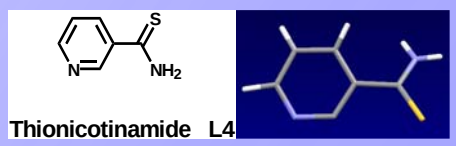

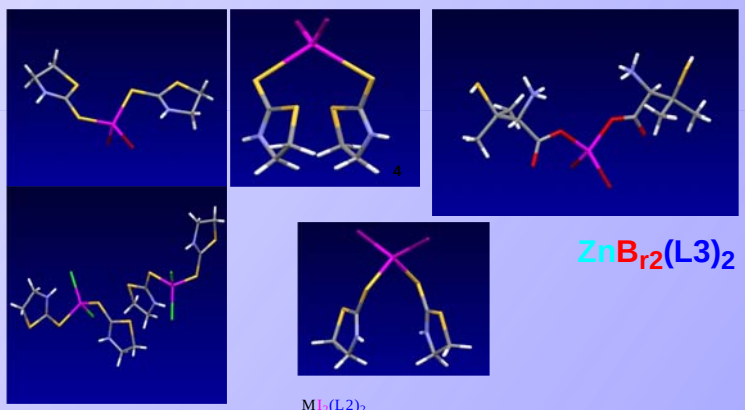

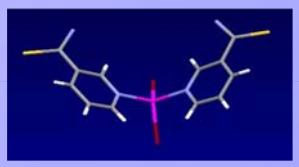

$ZnX_2(L4)_2$
X= Cl , Br

$ZnX_2(L2)_2$
X= Cl , Br

$ML_2(L2)_2$
M= Cd , Hg

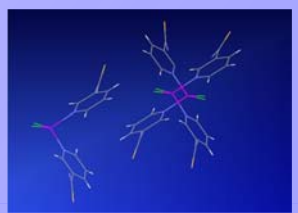

For L2 the cadmium and mercury iodide complexes have crystallographic C_2 symmetry. For L1 the zinc, cadmium and mercury bromide and iodide complexes have crystallographic C_2 symmetry. In the case of mercury, the chloride complex also has crystallographic C_2 symmetry. For ligand L3, which coordinates via the carboxylate group, the zinc bromide complex has crystallographic C_2 symmetry. For ligand L4, which coordinates via the pyridine N-atom, the zinc bromide complex crystallizes in the chiral space group $P2_12_12_1$, but as an inversion twin [X = 0.43(1)]. In complexes of L2 the average C=S bond distance is ca. 1.684 Å, while the same distance in complexes of ligand L1 is longer, ca. 1.727 Å. The average IR absorption frequencies are 1554 cm^{-1} and 1525 cm^{-1}, respectively, compared to the values observed in the free ligands [1503 cm-1 assigned to 89% ν_{asym} (CN) +11% δ (NCS) is shifted in complexes to higher energies][6].

1. E. S. Rapper, R. E. Oughtred, I. W. Nowell, Inorg. Chim. Acta., 77, 1983, L89
2. H. E. Howard-Lock, C. J. L. Lock, P. S. Smalley, J. Crystallogr. Spectrosc. Res., 13, 1983, 333
3. G. R. Form, E. S. Raper, T. C. Downie, Acta Crystallogr, Sec. B: Crystallogr. Cryst. Chem., 29, 1973, 776
4. S. K. Hadjikakou, M. N. Xanthopoulou, N. Hadjiliadis, M. Kubicki, Canadian J. Analytical Sci. Spectroscopy., 48, 2003, 38
5. N. A. Bell, W. Clegg, S. J. Coles, C. P. Constable, R. W. Harrington, M. B. Hursthouse, M. E. Light, E. S. Rapper, C. Sammon, M. R. Walker, Inorg. Chim. Acta., 357, 2004, 2091
6. R. K. Gosavi, U. Agarwala, C. N. R. Rao, J. Amer. Chem. Soc., 89, 1967, 235

Synthesis and single crystal analysis of "potentially" biologically important coinage metal complexes

Muhammad Altaf and Helen Stoeckli-Evans.

Institut de Microtechnique, Université de Neuchâtel, Rue Emile-Argand 11,CH-2009 Neuchâtel, Switzerland

E-mail:muhammad.altaf@unine.ch

The use of coinage metal complexes (silver and gold) as antitumour, antibacterial, antifungal and antiarthritic drugs have been well known for centuries[1-3]. Genetic hybridization of microbes is an ever increasing problem, as is their resistance to current antimicrobial drugs such as antibiotics. New compounds are constantly required to efficiently inhibit the growth of pathogenic micro organisms.

Silver(I) compounds are commonly prescribed today for their topical antibacterial effects, for example, silver sulfadiazine (Silvadene©, Flamzine©) for the treatment of burns, and dilute solutions of $AgNO_3$ are used prophylactically against bacterial conjunctivitis in infants[4-5].

In the past decades antimicrobial activities of Ag(I) and Au(I) complexes have been actively studied. The main aims of this research are the synthesis of compounds with Ag(I)— N, Ag(I)—S, Ag(I)—O and Ag(I)—P bonds, and in future work the establishment of structure-activity relationships of such complexes with respect to antimicrobial activities[6-7].

Silver(I) Complexes

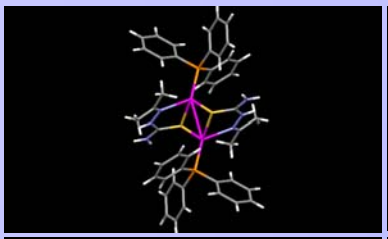

$[Ag(L1)_2(PPh_3)]_2(NO_3)_2$ & $[Ag(L1)(PCyPh_2)_2]NO_3$

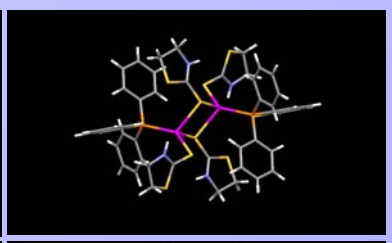

$[Ag(L2)_2(PPh_3)]_2(ClO_4)_2$ & $[Ag(L2)(PCy_3)]_2(PF_6)_2$

Our interest in mixed ligand silver(I) complexes with heterocyclic thiones and triaryl-phosphines stems from our current research on coordination compounds of coinage metals. Silver(I) phosphine complexes are growing in number after the discovery that such complexes participate in biological processes and attempts are being made to correlate the structure and reactivity of the biologically active species[8]. Ag(I) drugs are also marketed with different brand names and are used as hydrofibre dressings with acclaimed antimicrobial properties and are prescribed for use on various categories of open wounds (Squibb & Sons, 2003).

The knowledge of the coordination behaviour of heterocyclic thione ligands is useful for the study of the coordination of heavy metals to nucleotides and related compounds, such as nucleic acids, which may posses antitumour activity [9]. These studies encouraged our work on the synthesis of Ag(I) mononuclear and binuclear complexes, which have different configurations around the Ag atom.

Gold(I) & Gold(III) Complexes

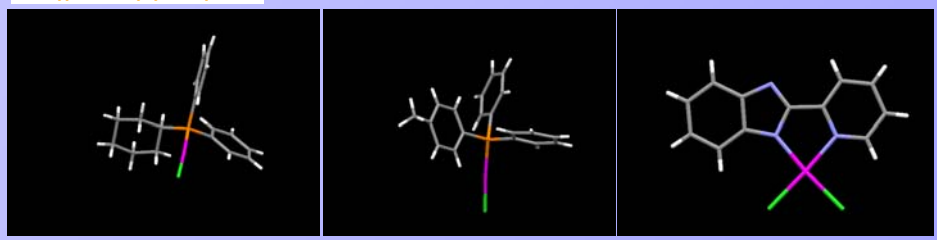

$[Au(PCyPh_2)Cl]$ $[Au(P(p\text{-tolyl})(Ph_2)Cl]$ $[Au(L3)Cl_2]CH_2Cl_2$

There is a considerable interest in the coordination chemistry of silver(I) and gold(I) complexes with biological and pharmacological activity [10]. Studies of gold(I) complexes have focused mainly on their anti-arthritic applications and anti-microbial activities. The molecular design and structure determination of such silver(I) and gold(I) complexes are an intriguing aspect of bioinorganic and metal-based drugs. A large number of gold(I) phosphine complexes are also known to exhibit promising antitumour properties [11].

Copper(II) Complexes

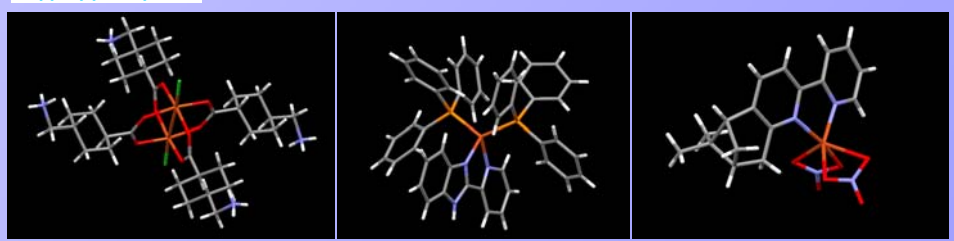

$[Cu(L4)_2Cl]_2.Cl_2.6H_2O$ $[Cu(L3)(PPh_3)_2]Cl_2.H_2O$ $[Cu(L5)(NO_3)_2]$

Copper(II) complexes are well known for their biological activity in pharmacological and bio-inorganic chemistry. The major purpose of this study is to compare the biological activity of copper complexes with silver and gold complexes.

L1 = 2-(propan-2-ylidene)hydrazinecarbothioamide
L2 = thiazolidine-2-thione
L3 = 2-(pyridin-2-yl)-1H-benzo[d]imidazole
L4 = 4-(aminomethyl)cyclohexanecarboxylic acid
L5 = (-)-5,6-Pinene-2,2'-bipyridine
Ph = phenyl
Cy = cyclohexyl

1. W. Kaim, B. Schwederski, Bioinorganic Chemistry: Inorganic Elements in the Chemistry of life; Jhon Wiley: New York,1994; p373.
2. K. Nomiya, K. Tsuda, N. C. Kasuga, J.Chem. Soc., Dalton Trans. 1998, 1653.
3. K. Nomiya, S. Takahashi, R. Noguchi, J.Chem. Soc., Dalton Trans. 2000, 2091
4. R. C. Elder, M. K. Eidsness, Chem. Rev. 1987, 87, 1027.
5. J. M. T. Hamilton-Miller, S. Shah, Int. J. Antimicrob. Agent. 1996, 7, 97.
6. H. J. Klasen, Burns. 2000, 26, 131.
7. K. Nomiya, Y. Kondoh, N. C. Kasugo, H. Nagano, M. Oda, T. Sudoh, S. Skuma, J. Inorg. Biochem. 1995, 58, 255.
8. E. L. Muetterties, C. W. Alegranti, J. Am. Chem. Soc. 1972, 94, 6386.
9. S. Fujieda, E. Tabata, A. Hatano, T. Osa, Hetrocycles. 1981, 15,743.
10. I. Tsyba, B. B. Mui, R. Bau, R. Noguchi, K. Nomia, Inorg. Chem. 2003, 42, 8028.
11. P. J. Sadler, R. E. Suc, Met. Based Drugs. 1994, 1, 107.